



Stacjonarne Studia Doktoranckie
Genetyki Molekularnej, Cytogenetyki
i Biofizyki Medycznej

Patrycja Marta Gralewska

Terapia celowana oparta na zwiększeniu wrażliwości komórek raka jajnika na olaparib poprzez zastosowanie inhibitorów białek regulujących stres replikacyjny wywołany pęknięciami nici DNA

Targeted therapy based on increasing the sensitivity of ovarian cancer cells to olaparib by using protein inhibitors that regulate replication stress caused by DNA strand breaks

Praca doktorska

wykonana w Katedrze Biofizyki Medycznej
Instytutu Biofizyki

Promotor:

- Dr hab. Aneta Rogalska,
prof. UŁ

Promotor pomocniczy:

- Dr Arkadiusz Gajek



Dziękuję moim promotorom - dr hab. Anecie Rogalskiej, prof. UŁ oraz dr. Arkadiuszowi Gajkowi, za wszelką pomoc, cierpliwość, opiekę merytoryczną, zaangażowanie oraz przekazaną mi przez te lata wiedzę.

Składam podziękowania dla

prof. dr hab. Agnieszki Marczak, Kierownika Katedry Biofizyki Medycznej UŁ

dr hab. n.med. Agnieszki Śliwińskiej, Kierownika Zakładu Biochemii Kwasów Nukleinowych UMED

oraz dr hab. Doroty Rybaczek, prof. UŁ, Katedra Cytofizjologii UŁ

za współpracę i pomoc w realizacji badań.

Dziękuję koleżankom i kolegom z Uczelni, oraz pracownikom Katedry Biofizyki Medycznej za stworzenie wspaniałej atmosfery.

Szczególne podziękowania pragnę złożyć moim najbliższym, Rodzicom oraz Patrycjuszowi, za cierpliwość, motywację oraz nieustanne wsparcie.

SPIS TREŚCI

Źródła finansowania	4
Dorobek naukowy	5
Publikacje wchodzące w skład rozprawy doktorskiej.....	5
Pozostały dorobek naukowy.....	6
Streszczenie	10
Abstract	13
Wykaz stosowanych skrótów	16
Wprowadzenie	18
Cel pracy	23
Materiały i metody badawcze	24
Omówienie wyników	26
Podsumowanie uzyskanych wyników oraz wnioski	36
Literatura	37
Kopie publikacji wchodzących w skład rozprawy doktorskiej	
Oświadczenia współautorów publikacji wchodzących w skład rozprawy doktorskiej	

ŹRÓDŁA FINANSOWANIA

Badania przeprowadzone w ramach niniejszej rozprawy doktorskiej zostały sfinansowane z następujących źródeł:

➔ Grant Narodowego Centrum Nauki przyznany w ramach konkursu SONATA BIS 9 nr 2019/34/E/NZ7/00056 pt. „Wykorzystanie olaparibu i inhibitorów kinazy ATR/CHK1 jako celowanej terapii przeciwnowotworowej opartej na syntetycznej letalności”; kierownik – dr hab. Aneta Rogalska, prof. UŁ



PUBLIKACJE WCHODZĄCE W SKŁAD ROZPRAWY DOKTORSKIEJ

Na niniejszą rozprawę doktorską składa się cykl trzech opublikowanych i powiązanych tematycznie artykułów naukowych – jedna praca przeglądowa oraz dwie prace doświadczalne.

Publikacja przeglądowa:

1. **Gralewska P.**, Gajek A., Marczak A., Rogalska A. Participation of the ATR/CHK1 pathway in replicative stress targeted therapy of high-grade ovarian cancer. *J Hematol Oncol.* 2020, 13, 39. <https://doi.org/10.1186/s13045-020-00874-6>
140 pkt MEiN; IF = 14,414; IF 5-letni = 17,520

Publikacje doświadczalne:

1. **Gralewska P.**, Gajek A., Marczak M., Mikuła M., Ostrowski J., Śliwińska A., Rogalska A. PARP inhibition increases the reliance on ATR/CHK1 checkpoint signaling leading to synthetic lethality-an alternative treatment strategy for epithelial ovarian cancer cells independent from HR effectiveness. *Int. J. Mol. Sci.* 2020, 21(24), 9715; <https://doi.org/10.3390/ijms2124971>
140 pkt MEiN; IF = 5,924; IF 5-letni = 6,628
2. **Gralewska P.**; Gajek A.; Rybaczek D.; Marczak A.; Rogalska A. The Influence of PARP, ATR, CHK1 Inhibitors on Premature Mitotic Entry and Genomic Instability in High-Grade Serous BRCA^{MUT} and BRCA^{WT} Ovarian Cancer Cells. *Cells* 2022, 11, 1889. <https://doi.org/10.3390/cells11121889>
140 pkt MEiN; IF = 7,666; IF 5-letni = 7,677

Suma **punktów** według listy czasopism punktowanych **MEiN wynosi 420**, sumaryczny współczynnik oddziaływania (**IF**, ang. *Impact Factor*) publikacji (w roku opublikowania) wynosi **28,004**; **IF 5-letni** wynosi **31,825**.

Publikacje:

1. **Gralewska P.**; Gajek A.; Marczak A.; Rogalska A. Metformin Affects Olaparib Sensitivity through Induction of Apoptosis in Epithelial Ovarian Cancer Cell Lines. *Int. J. Mol. Sci.* 2021, 22, 10557. [https://doi.org/ 10.3390/ijms221910557](https://doi.org/10.3390/ijms221910557)
140 pkt MEiN; IF = 6,208
2. Szelenberger R.; Dziedzic A.; Włuka A.; **Gralewska P.**; Janaszewska A. Editorial. VI PhD Students National Conference of Life Sciences "BioOpen". *Folia Biologica et Oecologica*, 2021, 17:5-6. <https://doi.org/10.18778/1730-2366.15.01>
20 pkt MEiN; IF = 0,906
3. Gajek A.; **Gralewska P.**; Marczak A.; Rogalska A. Current Implications of microRNAs in Genome Stability and Stress Responses of Ovarian Cancer. *Cancers* 2021, 13, 2690. [https://doi.org/ 10.3390/cancers13112690](https://doi.org/10.3390/cancers13112690)
140 pkt MEiN; IF = 6,575
4. Szymczak-Pajor I.; Fleszar K.; Kasznicki J.; **Gralewska P.**; Śliwińska A. A potential role of calpains in sulfonylureas (SUs) –mediated death of human pancreatic cancer cells (1.2B4). *Toxicology in Vitro*, 2021, 73,105128. <https://doi.org/10.1016/j.tiv.2021.105128>
100 pkt MEiN; IF = 3,685

Całkowity dorobek naukowy:

Sumaryczna liczba **punktów** dla całkowitego dorobku naukowego według listy czasopism punktowanych **MEiN wynosi 820**, sumaryczny **IF** publikacji (w roku opublikowania) wynosi **45,378**.

Doniesienia konferencyjne:

Prezentacje ustne:

1. **Gralewska P.**, Gajek A., Rybaczek D., Górna N., Marczak A., Rogalska A. „ATRI and CHK1i significantly increased chromosomal abnormalities caused by olaparib in HGSOC BRCA^{MUT} and BRCA^{WT} ovarian cancer cell lines”. *4th ISFMS – Biochemistry, Molecular Biology and Druggability of Proteins*, Florencja, Włochy, 06-09.09.2022 r.
2. **Gralewska P.**, Gajek A., Marczak A., Rogalska A. „ATR and CHK1 inhibition intensifies olaparib treatment effectiveness in HR-deficient and proficient ovarian cancer cell lines”. *8th Central European Congress of Life Sciences*, Kraków, 20-22.06.2022 r.
3. Górna N., **Gralewska P.**, Marczak A., Rogalska A. „Rola olaparibu i inhibitorów kinaz ATR i CHK1 w indukowaniu apoptozy w linii komórkowej raka jajnika SKOV-3 (p53^{NULL}, BRCA^{WT})”. *VII Ogólnopolska Konferencja Doktorantów Nauk o Życiu BIOOPEN*, Łódź, 07-08.04.2022 r.
4. **Gralewska P.**, Gajek A., Marczak A., Rogalska A. „DNA damaging effect of ATR and CHK1 inhibitors combined with olaparib in HR deficient and proficient high grade serous ovarian cancer cell lines”. *The 9th Intercollegiate Biotechnology Symposium SYMBIOZA*, Warszawa, 21-23.05.2021 r.
5. **Gralewska P.**, Gajek A., Marczak A., Rogalska A. „DNA damaging and cytotoxic effect of ATR and CHK1 inhibitors combined with olaparib on HR proficient HGSOC cell line SKOV3”. *International Young Scientists Conference on Molecular and Cell Biology 2021*, Warszawa, 25-26.02.2021 r.
6. Błasiak J., Barszczewska G., **Gralewska P.**, Kaarniranta K. „Oxidative stress induces mitochondrial dysfunction and autophagy in ARPE-19 cells”. *22nd EVER Congress*, Nicea, Francja, 17-19.10.2019 r. (abstrakt opublikowany w *Acta Ophthalmologica*, Abstracts from the 2019 European Association for Vision and Eye Research Conference, IF 3.761).

Postery:

1. Poczta A., **Gralewska P.**, Krzeczyński P., Tobiasz J., Marczak A. „New derivatives of melphalan as compounds with improved proapoptotic properties”. *8th Central European Congress of Life Sciences*, Kraków, 20-22.06.2022 r.
2. **Gralewska P.**, Gajek A., Górna N., Marczak A., Rogalska A. „ATR and CHK1 inhibition enhances genotoxic effect of olaparib in p53^{MUT} ovarian cancer cell line”. *25th Gliwice Scientific Meetings*. Gliwice, 18-20.11.2021 r.

3. Górna N., **Gralewska P.**, Marczak A., Rogalska A. „Combination of Olaparib with ATR or CHK1 inhibitors induces apoptosis in BRCA^{MUT} and BRCA^{WT} ovarian cancer”. *25th Gliwice Scientific Meetings. Gliwice, 18-20.11.2021 r.*
4. **Gralewska P.**, Gajek A., Marczak A., Rogalska A. „Increasing treatment effectiveness in BRCA^{MUT} and BRCA^{WT} ovarian cancer by targeting DNA repair-associated proteins”. *BACR Response and Resistance in Cancer Therapy, Leeds, Anglia, 06-08.09.2021 r.*
5. **Gralewska P.**, Gajek A., Marczak A., Rogalska A. „Zwiększenie wrażliwości komórek raka jajnika BRCAWT na olaparib za pomocą metforminy” *VI Ogólnopolska Konferencja Doktorantów Nauk o Życiu BIOOPEN, Łódź, 15-16.04.2021 r.*
6. **Gralewska P.**, Gajek A., Marczak A., Rogalska A. „Combination of olaparib and metformin in BRCA wild type ovarian cancer - cytotoxicity assessment”. *24th Gliwice Scientific Meetings. Gliwice, 21-22.11.2020 r.*
7. **Gralewska P.**, Gajek A., Marczak A., Rogalska A. „ Enhancing the cytotoxic effect of olaparib with ATR and CHK1 kinase inhibitors in HR deficient cell line”. *23rd Gliwice Scientific Meetings. Gliwice, 22-23.11.2019 r.*
8. **Gralewska P.**, Gajek A., Marczak A., Rogalska A. „Zwiększenie cytotoksycznego działania olaparibu przez inhibitory kinazy ATR i CHK1” *III Konferencja Doktorantów Nauk Przyrodniczych, Gdańsk, 25-28.06.2019 r.*

Pozostałe osiągnięcia:

- ➔ Opieka nad częścią eksperymentalną pracy magisterskiej P. Natalii Górnej, studentki kierunku Biologia na Wydziale BiOŚ UŁ, pt.: „Indukowanie apoptozy przez olaparib, MK8776 i AZD6738 w komórkach raka jajnika”

Organizacja konferencji naukowej:

- ➔ *VI Ogólnopolska Konferencja Doktorantów Nauk o Życiu BIOOPEN, Łódź, 15-16.04.2021 r* - członkini Komitetu Naukowego Sekcji Biologia Molekularna i Medyczna

Szkolenia Naukowe:

- ➔ „Znaczenie jakości wody w analizie białek. Dlaczego woda może stanowić zagrożenie”, szkolenie firmy Merck, 14.06.2021 r.
- ➔ „ZooMab® innowacyjne rekombinowane przeciwciała monoklonalne”, szkolenie firmy Merck, 11.06.2021 r.

- ➔ „Western blotting - wskazówki i porady dotyczące optymalizacji procesu”, szkolenie firmy Merck, 28.05.2021 r.
- ➔ „Hodowle komórek w 3D, szkolenie firmy Merck, 23.04.2021 r.
- ➔ „Zakażenia hodowli mykoplazmą - zapobieganie oraz detekcja”, szkolenie firmy Merck, 19.03.2021 r.
- ➔ Kurs dla osób uczestniczących w wykonywaniu procedur z udziałem zwierząt, Zwierzętarnia UŁ, 30.11-04.12.2020 r.
- ➔ “Western blotting tips and tricks”, szkolenie firmy Bio-Rad, 10.04.2020 r.
- ➔ “Normalization in western blotting with v3 workflow”, szkolenie firmy Bio-Rad, 09.04.2020 r.
- ➔ Panel Szkoleniowy firmy Animalab, 05.02.2020 r.
- ➔ Konferencja naukowa Łódzkiej Szkoły Diabetologii „Problemy terapeutyczne u chorych na cukrzycę typu 2 współistniejącą z innymi chorobami, Łódź, 04.12.2019 r.
- ➔ „10. Seminarium Open Access”, Warsztaty Zarządzania danymi badawczymi, Biblioteka Uniwersytetu Łódzkiego, 25.10.2019 r.

Członkostwo w Towarzystwach Naukowych:

- ➔ Polskie Towarzystwo Chorób Metabolicznych, od 07.2019 r.
- ➔ Polskie Towarzystwo Biochemiczne, od 12.2019 r.
- ➔ Polskie Towarzystwo Biofizyczne, od 12.2019 r.

Popularyzowanie nauki:

- ➔ Instytut Kreatywnej Biologii Wydziału Biologii i Ochrony Środowiska Uniwersytetu Łódzkiego – warsztaty: „Jak hodować komórki w warunkach in vitro?”, 06.2022 oraz 11.2019 r.
- ➔ XX Edycja Festiwalu Nauki Techniki i Sztuki w Łodzi – warsztaty: „Jak hodować komórki w warunkach in vitro?”, 10.2021 r.
- ➔ Noc Biologów – warsztaty: „Criminal Busters! – sposób na złodziejstwo”, 01.2020 r.
- ➔ Instytut Kreatywnej Biologii Wydziału Biologii i Ochrony Środowiska Uniwersytetu Łódzkiego – warsztaty: „CSI – Kryminalne Zagadki Hollywood – Złap mnie, jeśli potrafisz”, 11.2019 r.

STRESZCZENIE

Spośród wszystkich nowotworów ginekologicznych, rak jajnika charakteryzuje się najwyższą śmiertelnością, około 40%. Związane jest to z trudnościami w prawidłowym rozpoznaniu, gdyż w początkowych stadiach daje on niespecyficzne objawy. Standardowa procedura leczenia obejmuje usunięcie masy guza i tkanek mogących zawierać przerzuty. Jednak gdy, nowotwór jest wysoce zaawansowany, interwencja chirurgiczna nie zawsze jest możliwa. W takiej sytuacji leczenie jest głównie oparte na chemioterapii – karboplatynie i taksanach. Leki zwiększają przeżywalność pacjentek w IV, najwyższym stadium, jednakże 5-letni wskaźnik przeżycia ciągle pozostaje na bardzo niskim poziomie. Tak wysoka śmiertelność wymusza potrzebę poszukiwania nowych strategii leczenia.

Olaparib, PARPi, stanowi długo oczekiwany krok naprzód w leczeniu raka jajnika z mutacją BRCA1/2. Inhibitor polimerazy poli (ADP-rybozy) (PARPi) prowadzi do akumulacji pęknięć jednoniciowych. Sprzyja to powstawaniu pęknięć dwuniciowych, a w przypadku nowotworów z mutacją BRCA1/2 niemożnością ich efektywnej naprawy, skutkując śmiercią komórki na drodze tzw. syntetycznej letalności. Jest to zjawisko, w którym wyłączenie dwóch lub więcej szlaków naprawy DNA silniej indukuje śmierć komórkową niż wyłączenie każdego ze szlaków pojedynczo. Aktywacja szlaku odpowiedzi na uszkodzenia DNA prowadzi także do uruchomienia punktów kontroli cyklu komórkowego i zatrzymania podziałów, co uniemożliwia przekazanie uszkodzonego DNA do komórek potomnych. Pomimo to oporność na inhibitory PARP jest zjawiskiem często występującym. Z tego powodu m.in. bada się efektywność połączenia olaparibu z lekami przeciwnowotworowymi, które zakłócają szlak naprawy DNA poprzez rekombinację homologiczną (HR), wykorzystując inhibitory blokujące kinazę ATR (ataxia telangiectasia and Rad3-related protein) lub CHK1 (checkpoint kinase 1). Oczekuje się, że takie podejście może prowadzić do zwiększenia skuteczności terapii opartej o inhibicję PARP.

Celem niniejszej rozprawy doktorskiej była ocena cytotoksycznego działania inhibitorów kinazy ATR (AZD6738, ATRi, ceralasertib) i CHK1 (MK8776, CHK1i) w skojarzeniu z inhibitorem PARPi (AZD2281, PARPi, olaparib) w trzech liniach komórkowych raka jajnika o zróżnicowanym profilu genetycznym – SKOV-3 – model *BRCA*^{WT} oporny na cisplatynę – konwencjonalną terapię stosowaną w leczeniu raka jajnika, OV-90 – model raka jajnika niskozróżnicowanego *BRCA*^{WT}, z mutacją *TP53* oraz PEO-1 – model raka jajnika niskozróżnicowanego z mutacją w genie *BRCA2*, predysponowany do leczenia PARPi.

Wykazano, że po dłuższym czasie inkubacji (5 dni) obie testowane kombinacje – PARPi+ATRi, jak i PARPi+CHK1i, działają synergistycznie w komórkach raka jajnika, a najbardziej optymalnym stężeniem związków jest to, w którym stosunek obu stosowanych inhibitorów wynosi 1:1 (0,5 μ M: 0,5 μ M). Zastosowanie kombinacji PARPi+ATRi oraz PARPi+CHK1i, po 5 dniowej inkubacji, prowadziło do nasilonej śmierci komórek raka jajnika, na drodze syntetycznej letalności. Wyniki te uzyskano stosując subletalne dawki związków, co sugeruje, że koncepcja stosowania terapii skojarzonej PARPi+ATRi oraz PARPi+CHK1i może przynosić potencjalne korzyści terapeutyczne w zastosowaniu klinicznym. Stwierdzono, że PARPi zwiększył zależność komórek raka jajnika od szlaku ATR/CHK1, w celu utrzymania stabilności genomu w linii *BRCA^{MUT}*. Test kometowy potwierdził genotoksyczne działanie monoterapii, jak i skojarzonego podania związków. Wykazano, że ilość uszkodzeń DNA indukowana przez PARPi, ATRi czy CHK1i oraz ich kombinacje jest zależna od czasu inkubacji. Proapoptotyczne właściwości badanych inhibitorów oszacowano na podstawie analizy aktywności kaspaz wykonawczych – 3 oraz 7. Kombinacje leków po 48 godzinach inkubacji spowodowały ich wzrost, sugerując, że jednym z mechanizmów odpowiedzialnych za śmierć komórek raka jajnika poddanych działaniu badanych związków może być apoptoza.

Celem drugiej części badań było poznanie mechanizmu śmierci komórkowej indukowanej przez badane związki, w początkowej fazie odpowiedzi komórek na olaparib oraz inhibitory szlaku ATR/CHK (24 i 48 godzin). Stężenie związków zostało zwiększone do 4 μ M, przy jednoczesnym zachowaniu stosunku stężeń 1:1 w skojarzeniu. Kombinacje PARPi z ATRi/CHK1i nie były bardziej cytotoksyczne w porównaniu do odpowiednich monoterapii w badaniach prowadzonych do 48 godzin. Olaparib w krótkich czasach wykazywał działanie cytostatyczne w komórkach raka jajnika. Zdolność badanych inhibitorów do indukowania uszkodzeń DNA została potwierdzona, określając ekspresję markera uszkodzeń DNA, γ H2AX. W czasie 48 godzin i przy stężeniu 4 μ M olaparib okazał się niewystarczający do zwiększenia ekspresji tego białka, kombinacje leków natomiast prowadziły do większych zmian niż monoterapia PARPi. Ocenę właściwości proapoptotycznych przeprowadzono z wykorzystaniem następujących metod: szacując odsetek komórek apoptotycznych i nekrotycznych metodą podwójnego barwienia (Hoechst 33258/jodek propidyny), badając eksternalizację fosfatydyloseryny (wczesnego markera związanego z procesem apoptozy), mierząc kondensację chromatyny oraz ekspresję aktywnej formy efektorowej kaspazy-3. Wykazano, że po krótkim czasie działania, olaparib nie indukuje apoptozy w komórkach badanych linii. Nie wykazano zmian istotnych statystycznie pomiędzy kombinacjami leków PARPi+ATRi/PARPi+CHK1i a monoterapią ATRi/CHK1i. Na podstawie różnic w inkorporacji BrdU w linii PEO-1 stwierdzono zwiększenie liczby komórek we wczesnej fazie S, co może być oznaką stresu replikacyjnego. Terapia skojarzona nie wykazywała silniejszego wpływu na proliferację komórek niż monoterapia ATRi czy CHK1i. Uzyskane wyniki

sugerują, że uszkodzenia DNA, w tym DSB, nie prowadzą do natychmiastowej śmierci komórek raka jajnika traktowanych olaparibem, ATRi czy CHK1i. Komórki te, pomimo obecnych uszkodzeń DNA, mogą wejść przedwcześnie w mitozę, w wyniku czego dochodzi do powstania aberracji chromosomowych, co zostało potwierdzone podczas analizy mikrojąder czy płytki metafazowej. Niestabilność chromosomów może wywołać katastrofę mitotyczną, będącą jednym z etapów pośrednich, prowadzących do śmierci komórek raka jajnika.

Dodatkowym etapem badań była ocena wpływu PARPi, ATRi, CHK1i oraz ich skojarzonego działania na potencjalny wzrost ekspresji glikoproteiny P, białka związanego z występowaniem zjawiska oporności wielolekowej. Badane inhibitory, zarówno w monoterapii, jak i w kombinacjach nie zwiększyły ekspresji białka MDR1 po 24 i 48 godzinach inkubacji. Dokonano również oceny ekspresji cytochromu c w celu rozszerzenia badań nad programowaną śmiercią komórki, indukowaną przez badane związki. Kombinacje PARPi+ATRi/CHK1i prowadziły do istotnego statystycznie wzrostu ekspresji cytochromu c jedynie w linii SKOV-3 po 48 godzinach inkubacji.

Przeprowadzone eksperymenty, stanowiące podstawę tej rozprawy doktorskiej potwierdziły, że skojarzone działanie PARPi+ATRi lub PARPi+CHK1i prowadzi do nasilonej śmierci komórek raka jajnika na drodze syntetycznej letalności, a także, że badane kombinacje hamują, zależnie od czasu, proliferację komórek raka jajnika i działają niezależnie od obecności mutacji *BRCA*. Wyniki te sugerują, że koncepcja stosowania terapii skojarzonej PARPi+ATRi oraz PARPi+CHK1i może przynosić potencjalne korzyści terapeutyczne w leczeniu raka jajnika.

ABSTRACT

Ovarian cancer has the highest mortality rate among gynaecological malignancies, which is approximately 40%. This fact is partly attributed to the difficulties in diagnosis, because of the non-specific symptoms it may give in the initial stages. The standard treatment procedure involves the removal of the tumour and tissues that may have metastasized, but when the cancer is highly advanced, the surgical procedure is not always possible. In such a situation, the treatment is mainly based on chemotherapy, which involves carboplatin and taxanes. These drugs increase the survival rate of patients suffering from the stage IV of ovarian cancer, but the 5-year survival rate still remains very low. Such high mortality rates necessitate the search for new treatment strategies.

Olaparib, PARPi, represents a long-awaited step forward in the treatment of BRCA1/2 mutated ovarian cancer. Poly(ADP-ribose) polymerase inhibitor (PARPi) leads to the accumulation of single-strand breaks. This may cause double-strand breaks, which in BRCA1/2-mutated tumours cannot be repaired effectively, leading to tumour cell death by synthetic lethality. It is a concept in which a concurrent defects in two or more DNA repair pathways induce the cell death more strongly than each of the pathways separately. The activation of the DNA damage response pathway also triggers the activation of the cell cycle checkpoints and stops division and thus prevents the transmission of damaged DNA into daughter cells. Despite this fact the resistance to PARP inhibitors is a common phenomenon and because of that, the combination of olaparib with anticancer drugs that interfere with the homologous recombination (HR) DNA repair pathway through inhibitors that block ATR kinase (ataxia telangiectasia and Rad3-related protein) or CHK1 (checkpoint kinase 1) is being studied. It is expected that such an approach may lead to an increase in the effectiveness of the therapy based on the PARP inhibition.

This doctoral dissertation aimed to evaluate the cytotoxic effect of ATR kinase (AZD6738, ATRi, ceralasertib) and CHK1 (MK8776, CHK1i) inhibitors in combination with a PARPi inhibitor (AZD2281, PARPi, olaparib) in three ovarian cancer cell lines with a diverse genetic profile - SKOV-3 – *BRCA*^{WT} cisplatin-resistant – the conventional therapy used in the treatment of ovarian cancer, OV-90 – high-grade serous ovarian carcinoma *BRCA*^{WT} with *TP53* mutation and PEO-1 – high-grade serous ovarian carcinoma with a *BRCA2* mutation, predisposed to PARPi treatment.

It has been demonstrated that after a longer incubation time (5 days), both tested combinations - PARPi+ATRi and PARPi+CHK1i act synergistically in ovarian cancer cells, and the most effective concentration of compounds is the one in which the ratio of both inhibitors used is 1:1

(0.5 μ M: 0.5 μ M). PARPi+ATRi and PARPi+CHK1i combinations, after 5 days of incubation, led to the increased ovarian cancer cell death on the path of synthetic lethality. These results were obtained using sublethal doses of the compounds, which suggests that the concept of PARPi+ATRi and PARPi+CHK1i combined therapy may provide potential therapeutic benefits in a clinical use. PARPi was found to increase the reliance of ovarian cancer cells on the ATR/CHK1 pathway to maintain genome stability in the *BRCA^{MUT}* cell line. What is more, the comet assay confirmed the genotoxic effect of the monotherapy as well as the combined therapy of the compounds. It has been shown that the amount of DNA damage induced by PARPi, ATRi or CHK1i and their combinations is time-dependent. The proapoptotic properties of the tested inhibitors were estimated by the analysis of the activity of executive caspases - 3 and 7. The drug combinations after 48 hours of incubation caused an increase in caspase 3/7 ratio, suggesting that apoptosis may be one of the mechanisms responsible for the ovarian cancer cell death exposed to the tested compounds.

The second part of the study aimed to understand the mechanism of cell death induced by the tested compounds in the initial phase of the cell response to olaparib and ATR/CHK pathway inhibitors (24 and 48 hours). The concentration of compounds was increased to 4 μ M, while maintaining a 1:1 ratio of compound concentrations in the combination. The combinations of PARPi with ATRi/CHK1i were not more cytotoxic compared to the respective monotherapies, up to 48 hours. Olaparib showed a cytostatic activity in the ovarian cancer cells after a shorter incubation time. The ability of the tested inhibitors to induce DNA damage was confirmed by determining the expression of the DNA damage marker, γ H2AX. Within 48 hours and at a concentration of 4 μ M, olaparib was insufficient to increase the expression of this protein, while drug combinations led to greater changes than PARPi monotherapy. The assessment of the proapoptotic properties was carried out using the following methods: by estimating the percentage of the apoptotic and necrotic cells by double staining (Hoechst 33258/propidium iodide), by examining the externalization of phosphatidylserine (an early marker associated with the process of apoptosis), by measuring chromatin condensation and the expression of the active effector form of caspase-3. It has been shown that after a short incubation time, olaparib does not induce apoptosis in the tested cell lines. There were no statistically significant differences between PARPi+ATRi/PARPi+CHK1i drug combinations and ATRi/CHK1i monotherapy. An increase in the number of cells in the early S phase was found based on differences in BrdU incorporation in the PEO-1 line, which may be a sign of replication stress. The combination therapy showed no greater effect on cell proliferation than ATRi or CHK1i monotherapy. The obtained results suggest that DNA damage, including DSB, does not immediately lead to the death of ovarian cancer cells treated with olaparib, ATRi or CHK1i. These cells may progress into mitosis, despite the presence of DNA damage, resulting in chromosomal aberrations, which has

been confirmed by the analysis of the micronuclei or metaphase spread. Chromosomal instability may lead to mitotic catastrophe, which is one of the intermediate steps, leading to the death of ovarian cancer cells.

An additional stage of the research was to assess the effect of PARPi, ATRi, CHK1i and their combination on the potential increase in the expression of the P-glycoprotein, a protein associated with the occurrence of multidrug resistance. The tested inhibitors, both in monotherapy and in combination, did not increase MDR1 protein expression after 24 and 48 hours of incubation both in monotherapy and in combination. The cytochrome c expression was also assessed to extend the research into programmed cell death induced by the tested compounds. It has been observed that the PARPi+ATRi/CHK1i combinations led to a statistically significant increase in the cytochrome c expression only in the SKOV-3 cell line after 48 hours of incubation.

The experiments conducted in this doctoral dissertation have confirmed that the combined action of PARPi+ATRi or PARPi+CHK1i leads to the increased death of the ovarian cancer cells by synthetic lethality. The tested combinations inhibit the proliferation of ovarian cancer cells in a time-dependent manner and act independently of the presence of a *BRCA* mutation. These results suggest that the concept of PARPi+ATRi and PARPi+CHK1i combination therapy may have potential therapeutic benefits in the treatment of ovarian cancer.

WYKAZ STOSOWANYCH SKRÓTÓW

ABC (ang. <i>ATP-binding cassette</i>)	Kaseta wiążąca ATP
alt-NHEJ	Alternatywna naprawa DNA przez niehomologiczne łączenie końców
APOBEC (ang. <i>apolipoprotein B mRNA editing catalytic polypeptide-like</i>)	Apolipoproteina B, polipeptyd edytujący mRNA
ARid1A (ang. <i>AT-rich interaction domain 1A</i>)	Bogate w AT białko zawierające domenę interaktywną 1A
ATM (ang. <i>ataxia-telangiectasia mutated</i>)	Kinaza białkowa serynowo-treoninowa; zmutowane białko w zespole ataksja teleangiektazja
ATR (ang. <i>ataxia-telangiectasia and Rad3-related</i>)	Kinaza białkowa serynowo-treoninowa; ataksja teleangiektazja związana z białkiem Rad3
ATRI (ang. <i>ATR inhibitor</i>)	Inhibitor ATR
ATRIP (ang. <i>ATR-interacting protein</i>)	Białko oddziałujące z ATR
BASC (ang. <i>BRCA1-associated genome surveillance complex</i>)	Kompleks nadzorujący genom związany z BRCA1
BER (ang. <i>base excision repair</i>)	Naprawa DNA przez wycinanie zasad
BLM (ang. <i>RecQ-like DNA helicase</i>)	Helikaza DNA podobna do RecQ
BRCA^{MUT} (ang. <i>BRCA mutated</i>)	Mutacja genu <i>BRCA</i>
BRCA^{WT} (ang. <i>BRCA wild-type</i>)	Gen <i>BRCA</i> typu dzikiego
CCNE1 (ang. <i>G1/S-specific cyclin E1</i>)	Cyklina E1 G1/S specyficzna
CDC25 (ang. <i>cell division control protein 25</i>)	Białko kontrolujące cykl komórkowy
CDI (ang. <i>coefficient of drug interaction</i>)	Współczynnik oddziaływania leków
CDK (ang. <i>cyclin-dependent kinase</i>)	Kinaza zależna od cykliny
CHK1 (ang. <i>checkpoint kinase 1</i>)	Kinaza punktu kontrolnego 1
CHK1i (ang. <i>CHK1 inhibitor</i>)	Inhibitor CHK1
CHK2 (ang. <i>checkpoint kinase 2</i>)	Kinaza punktu kontrolnego 2
CHKs (ang. <i>checkpoint kinases</i>)	Kinazy punktu kontrolnego
DDR (ang. <i>DNA damage response</i>)	Szlak odpowiedzi na uszkodzenia DNA
DSB (ang. <i>double-strand break</i>)	Dwuniciowe pęknięcie DNA
EMA (ang. <i>European Medicines Agency</i>)	Europejska Agencja Leków
FDA (ang. <i>Food and Drug Administration</i>)	Agencja Żywności i Leków

HGSOC (ang. <i>high-grade serous ovarian cancer</i>)	Niskozróżnicowany surowiczy rak jajnika
HR (ang. <i>homologous recombination</i>)	Rekombinacja homologiczna
MC (ang. <i>mitotic catastrophe</i>)	Katastrofa mitotyczna
MCM2 (ang. <i>minichromosome maintenance protein 2 homolog</i>)	Białko utrzymujące minichromosomy, zaangażowane w inicjację replikacji genomu, składnik kompleksu przedreplikacyjnego (pre_RC)
MDR1 (ang. <i>multidrug resistance protein 1</i>)	Białko oporności wielolekowej 1
MMEJ (ang. <i>microhomology-mediated end joining</i>)	Mikrohomologiczne łączenie zasad
MRE11 (ang. <i>double-strand break repair protein MRE11</i>)	Białko naprawiające podwójne pęknięcia DNA MRE11
NBS1 (ang. <i>nibrin</i>)	Nibryna
NHEJ (ang. <i>non-homologous end joining</i>)	Naprawa DNA przez niehomologiczne łączenie końców
PALB2 (ang. <i>partner and localizer of BRCA2</i>)	Białko partnerujące dla białka BRCA2 w procesie naprawy DNA
PARP (ang. <i>poly(ADP-ribose)polymerase</i>)	Polimeraza poli(ADP-rybozy)
PARPi (ang. <i>PARP inhibitor</i>)	Inhibitor PARP
PCC (ang. <i>premature condensation of chromosomes</i>)	Przedwczesna kondensacja chromosomów
P-gp (ang. <i>P-glycoprotein</i>)	Glikoproteina P
PIKK (ang. <i>phosphatidylinositol 3-kinase-related kinase</i>)	Kinaza białkowa 3-fosfatydyloinozytolu
RAD51 (ang. <i>DNA repair protein RAD51 homolog 1</i>)	Białko odpowiedzialne za naprawę DNA RAD51 homolog 1
RPA (ang. <i>replication protein A</i>)	Białko replikacyjne A
RS (ang. <i>replication stress</i>)	Stres replikacyjny
RSR (ang. <i>replication stress response</i>)	Odpowiedź na stres replikacyjny
SSB (ang. <i>single-strand break</i>)	Pęknięcie pojedynczej nici DNA
VEGF (ang. <i>vascular endothelial growth factor</i>)	Czynnik wzrostu śródbłonna naczyń

WPROWADZENIE

Rak jajnika jest najczęstszą przyczyną śmierci spośród nowotworów ginekologicznych [1], częściowo dlatego, że około 80% pacjentek diagnozowanych jest w zaawansowanym stadium choroby (III lub IV), ze względu na brak badań przesiewowych oraz metod wczesnej detekcji tego typu nowotworu [2]. Najczęściej występującym i wykazującym najgorsze rokowanie typem nowotworu jest niskozróżnicowany surowiczy rak jajnika o wysokim stopniu złośliwości (HGSOC, ang. *high-grade serous ovarian carcinoma*). Pomimo nieustannego rozwoju ginekologii onkologicznej, 5-letni wskaźnik przeżycia pacjentek z HGSOC ciągle pozostaje na poziomie 35-40% [3].

Zwiększone ryzyko rozwoju raka jajnika związane jest z występowaniem spontanicznych bądź dziedzicznych mutacji w genach *BRCA1/2* (ang. *breast cancer gene*). Prawdopodobieństwo rozwoju tego typu nowotworu u kobiet, u których wykryto mutację w genie *BRCA2* wynosi 16-27%, natomiast u kobiet z mutacją *BRCA1* wynosi ono od 36 do aż 60% [4]. Ponadto, większość (96%) raków jajnika typu II, obejmujących głównie niskozróżnicowane guzy surowicze i charakteryzujących się złośliwym przebiegiem [5], posiada mutację w genie *TP53*. Dodatkowo, około połowa HGSOC wiąże się z mutacjami genów kodujących białka uczestniczące w naprawie dwuniciowych pęknięć DNA poprzez rekombinację homologiczną (HR, ang. *homologous recombination*). Najczęściej jest to *BRCA1/2* [6, 7].

Standardowa procedura leczenia, zgodnie z rekomendacjami Polskiego Towarzystwa Ginekologii Onkologicznej, obejmuje zabiegi chirurgiczne i chemioterapię. Operacje mają na celu usunięcie masy guza i tkanek mogących zawierać przerzuty. Jednak gdy, nowotwór jest wysoce zaawansowany, standardowe postępowanie chirurgiczne nie zawsze jest możliwe. Chemioterapia natomiast obejmuje pochodne platyny – karboplatynę i cisplatynę oraz taksany, przede wszystkim paklitaksel oraz docetaksel. Pochodne platyny powodują głównie powstawanie wiązań krzyżowych w DNA, a ich akumulacja prowadzi do powstawania dwuniciowych pęknięć DNA (DSB, ang. *double-strand breaks*) [8]. Coraz częściej wdraża się także chemioterapię neoadjuwantową, która dodatkowo, oprócz leków wymienionych wcześniej, uzupełniana jest o bewacyzumab, humanizowane przeciwciało monoklonalne, wiążące czynnik wzrostu śródbłonna naczyń (VEGF, ang. *vascular endothelial growth factor*) [9]. Chemioterapia zwiększa przeżywalność, jednak u 70% pacjentek dochodzi do nawrotów choroby. Jeśli progresję obserwuje się w czasie krótszym niż 6 miesięcy po leczeniu pochodnymi platyny, nowotwór uznaje się za oporny [10]. Z tego powodu poszukiwanie nowych strategii terapeutycznych ciągle pozostaje wyzwaniem dla naukowców. Białka związane z naprawą DNA mogą stać się obiecującym celem molekularnym w ukierunkowanej terapii nowotworów jajnika.

Pęknięcia pojedynczych nici DNA (SSB, ang. *single-strand breaks*) mogą zostać dokładnie naprawione przy użyciu drugiej nici jako matrycy, a w procesie tym bierze udział polimeraza poli(ADP-rybozy 1) (PARP1) [11]. Inhibitory PARP (PARPi) zaburzają możliwość naprawy SSB bezpośrednio lub pośrednio, poprzez upośledzenie funkcjonowania systemu naprawy związanego z wycinaniem zasad (BER, ang. *base-excision repair*) [12], powodując powstawanie dwuniciowych pęknięć DNA, których nie można efektywnie naprawić w nowotworach z mutacją *BRCA1/2* (*BRCA^{MUT}*, ang. *BRCA mutated*). Prowadzi to do śmierci komórek nowotworowych na drodze syntetycznej letalności - zjawiska, w którym wyłączenie jednocześnie dwóch lub więcej białek lub genów, silniej indukuje śmierć komórkową niż zahamowanie każdego z nich pojedynczo [13]. DSB są głównie naprawiane dwoma szlakami: HR i poprzez niehomologiczne łączenie końców (NHEJ, ang. *non-homologous end joining*) [14]. Istotną rolę w naprawie DNA odgrywają białka BRCA1 i BRCA2. Oba zaangażowane są w naprawę DSB poprzez HR w fazie S cyklu komórkowego. Białko BRCA1 uczestniczy w detekcji uszkodzeń DNA i regulacji cyklu komórkowego. W reakcji na uszkodzenie DNA białko BRCA1 jest fosforylowane przez kinazy ATM (ang. *ataxia telangiectasia mutated*) czy ATR (ang. *ataxia telangiectasia and Rad3-related protein*). Białko BRCA1 w miejscu uszkodzenia DNA tworzy kompleksy białkowe, odpowiedzialne za dalsze przekazanie informacji o uszkodzeniu DNA, w tym kompleks BASC (ang. *BRCA1-associated genome surveillance complex*), który wpływa na wybór drogi naprawy materiału genetycznego. Kompleks BASC to, poza BRCA1, białka uczestniczące w szlaku naprawy DNA błędnie sparowanych zasad (MSH2, MSH6, MLH1), kompleks MRN (MRE11 (ang. *double-strand break repair protein MRE11*)-RAD51 (ang. *DNA repair protein RAD51 homolog 1*)-NBS1 (ang. *nibrin*)), czynnik replikacyjny C, helikaza BLM (ang. *RecQ-like DNA helicase*), biorąca udział w rekombinacji [15]. Białko BRCA2 natomiast ułatwia utworzenie i przyłączenie filamentów RAD51 do uszkodzonej nici. Białko RAD51 z kolei odpowiada za reakcję wymiany nici DNA między homologicznymi sekwencjami [16].

DSB mogą także być usuwane poprzez mikrohomologiczne łączenie zasad (MMEJ, ang. *microhomology end-joining*), znane również jako alternatywny NHEJ (alt-NHEJ). W mechanizmie tym istotną rolę pełni polimeraza DNA θ (POLQ), której aktywacja również zależna jest od PARP1 [17, 18]. W komórkach nowotworowych z niesprawnym systemem HR i z mutacjami w genach *BRCA1/2*, próba naprawy DSB odbywa się z wykorzystaniem podatnych na błędy mechanizmów naprawy (m.in. NHEJ, MMEJ), co może skutkować akumulacją mutacji i śmiercią komórki [19]. Linie komórkowe raka jajnika ze zmutowanym *BRCA1/2* i w konsekwencji niefunkcyjnym systemem HR, charakteryzuje zatem wyższa wrażliwość na PARPi, w porównaniu z liniami *BRCA* typu dzikiego (*BRCA^{WT}*, ang. *BRCA wild-type*) [20]. Pacjenci z *BRCA^{MUT}* także są bardziej podatni na chemioterapię opartą o inhibicję PARP [4]. Z tego względu analiza mutacji *BRCA* ma kluczowe znaczenie dla wyboru rodzaju terapii [21]. Kolejny mechanizm działania PARPi opiera się na zablokowaniu PARP na chromatynie (ang.

PARP trapping). Talazoparib, jeden z PARPi, zwiększa wychwytywanie PARP1 przyłączonego do DSB, prowadząc do zmniejszenia aktywności systemu NHEJ, co w konsekwencji prowadzi do śmierci komórki [22, 23].

PARPi stanowią długo oczekiwany krok naprzód w leczeniu raka jajnika [24-26]. Pierwszym inhibitorem PARP zatwierdzonym przez Agencję Żywności i Leków (FDA, ang. *Food and Drug Administration*) do leczenia pacjentek z rakiem jajnika z *BRCA^{MUT}* był olaparib [27]. Jak dotąd cztery PARPi zostały zatwierdzone przez Europejską Agencję Leków (EMA, ang. *European Medicines Agency*) oraz FDA do leczenia raka jajnika - olaparib, rucaparib, niraparib oraz talazoparib. Różnica pomiędzy stosowanymi klinicznie PARPi polega na odmiennej zdolności do wychwytywania PARP1. Talazoparib, ma zdolność wychwytywania PARP1 około 100 razy skuteczniej niż niraparib, który jest z kolei silniejszy niż olaparib i rucaparib [28]. Obecnie są one stosowane jako leczenie pierwszego lub drugiego rzutu oraz leczenie podtrzymujące po odpowiedzi na terapię opartą na platynie [29, 30]. W Polsce monoterapia olaparibem stosowana jest w przypadku pacjentek z *BRCA^{MUT}* HGSOc w zaawansowanym stadium, które na pierwszą linię chemioterapii opartej na pochodnych platyny wykazały całkowitą lub częściową odpowiedź [9]. Od 1 stycznia 2022 roku refundowana jest także monoterapia niraparibem, w leczeniu podtrzymującym pacjentek z rakiem jajnika, niezależnie od statusu mutacji *BRCA* [31].

Badania kliniczne wykazały, że odsetek odpowiedzi na leczenie PARPi u kobiet chorujących na raka jajnika, które są nosicielkami mutacji genu *BRCA1/2* wynosi około 40% (ICEBERG2, NCT00494442). Udowodniono także, że PARPi prowadzą do supresji nowotworów, jednak nie do ich całkowitej regresji [32]. Rzadka jest również kompletna odpowiedź na leczenie przy stosowaniu wyłącznie monoterapii PARPi [33]. Dodatkowo, niestety, często występującym zjawiskiem jest oporność na inhibitory PARP. W odpowiedzi na leczenie PARPi komórki nowotworowe *BRCA^{MUT}* mogą przywrócić naprawę HR i/lub stabilizację widełek replikacyjnych, np. poprzez zwiększenie ekspresji RAD51, promowanie alt-NHEJ, mutację wtórną *BRCA* (przywracającą funkcjonalność tego białka) [34-36]. W komórce nowotworowej może również nastąpić zwiększenie ekspresji glikoproteiny P (P-gp, ang. *P-Glycoprotein*), nazywanej także białkiem oporności wielolekowej (MDR1, ang. *multidrug resistance protein 1*) [37].

W odpowiedzi na zaburzenia biosyntezy DNA, komórki uruchamiają szereg reakcji biochemicznych określanych mianem stresu replikacyjnego (RS, ang. *replication stress*). Jednym ze źródeł RS są czynniki genotoksyczne. Mogą one prowadzić do zaburzenia procesu replikacji, zablokowania możliwości wejścia komórki w mitozę do czasu aktywacji genów naprawczych. RS aktywuje zatem szlaki odpowiedzi na uszkodzenia DNA (DDR, ang. *DNA damage response*).

Konsekwencją zablokowania białek uczestniczących w DDR mogą być uszkodzenia DNA, niestabilność genomowa i śmierć komórki [38].

Kinazy ATM i ATR uczestniczą w aktywacji szlaku odpowiedzi na uszkodzenia DNA. ATR, kinaza serynowo-treoninowa należąca do rodziny kinaz białkowych 3-fosfatydyloinozytolu (PIKK, ang. *phosphatidylinositol 3-kinase-related kinase*) jest głównym białkiem odpowiedzialnym za regulację odpowiedzi na stres replikacyjny (RSR, ang. *replication stress response*). Zaburzenia funkcjonowania widełek replikacyjnych aktywują szlaki podległe kinazie ATR. Aktywowana jest ona m.in. poprzez uszkodzenia DNA takie jak SSB, DSB, addukty DNA. Kinaza ta zatrzymuje działanie polimerazy DNA. Kinaza ATM natomiast jest głównie aktywowana na skutek wykrycia DSB. Ponadto, do bezpośrednich substratów kinazy ATR zalicza się m. in. białko replikacyjne A (RPA, ang. *replication protein A*), MCM2 (ang. *minichromosome maintenance protein 2 homolog*) czy p53, które odpowiedzialne są za postęp widełek replikacyjnych, kontrolę cyklu komórkowego oraz naprawę DNA [39, 40]. Rola ATR polega na zatrzymaniu cyklu komórkowego od fazy S do G2, a także na utrzymaniu prawidłowego funkcjonowania punktu kontrolnego G2/M [41].

W warunkach stresu replikacyjnego BRCA1/2 wiąże się z zatrzymanymi widełkami replikacyjnymi, chroniąc komórkę przed niestabilnością genomową. Proces ten kontrolowany jest przez szlak ATR/CHK1, który stabilizując widełki replikacyjne zapobiega powstawaniu DSB. Początkowo kompleks ATR i białka oddziałującego z ATR (ATRIP, ang. *ATR-interacting protein*) przyłącza się do SSB. Następnie ATR aktywuje CHK1 przez fosforylację białka w pozycji Ser345 [42, 43]. Fosforylowane CHK1 stabilizuje widełki replikacyjne, uczestniczy w naprawie DNA poprzez fosforylację białek BRCA2 i RAD51, zaangażowanych w szlak naprawy HR [44]. W komórkach z mutacją *BRCA1* jego aktywność jest niezbędna do prawidłowej naprawy uszkodzeń DNA. CHK1 poprzez inaktywację fosfataz CDC25A oraz CDC25C (ang. *cell division control protein 25*), które w dalszej kolejności odpowiedzialne są za aktywację kinaz CDK (ang. *cyclin-dependent kinase*), może prowadzić do zatrzymania cyklu komórkowego w fazie G2/M [45]. Z tego powodu połączenie olaparibu ze związkami przeciwnowotworowymi, które zakłócają szlak naprawy HR, poprzez np. blokowanie kinazy ATR lub CHK1, może uwrażliwić komórki raka jajnika na olaparib. Inhibicja ATR/CHK1 przeciwdziała zatrzymaniu cyklu komórkowego wywołanego uszkodzeniem DNA, skutkując nieprawidłowym wejściem komórki nowotworowej w mitozę, aberracjami chromosomowymi i apoptozą [46]. Zahamowanie ATR w komórkach z mutacjami w genach *RAS*, *MYC*, *CCNE1* (ang. *G1/S-specific cyclin E1*), *TP53*, a także w genach związanych z naprawą DNA (*BRCA1/2*, *PALB2* (ang. *partner and localizer of BRCA2*), *ATM*) może prowadzić do śmierci komórkowej [47-49]. Kinaza CHK1 natomiast może ulegać autofosforylacji i przez to być aktywowana niezależnie od ATR [50].

Obecnie, szereg badań klinicznych sprawdza efektywność terapii inhibitorami ATR (ATRi) czy CHK1 (CHK1i) w połączeniu z olaparibem. Cztery ATRi są aktualnie testowane w badaniach klinicznych I i II fazy - AZD6738 (ceralasertib), M6620 (berzosertib), M4344 (VX-803) i BAY1895344, jednak AZD6738 jest z nich najbardziej selektywny w stosunku do kinazy ATR [51].

Pierwszym poznanym inhibitorem CHK1 był UCN-01, jednakże wykazywał on niską specyficzność substratową. Kolejnym badanym CHK1 był LY2606368 (preksasertib), który zapobiegał autofosforylacji zarówno CHK1 jak i CHK2 (ang. *checkpoint kinase 2*). Za wysoce selektywny inhibitor CHK1 uznano natomiast MK8776 [52].

CAPRI (NCT03462342), badanie kliniczne drugiej fazy skupia się na określeniu skuteczności terapii skojarzonej olaparibu i ATRi (AZD6738) w nawracającym raku jajnika opornym na pochodne platyny i PARPi, a także w raku jajnika z mutacją *BRCA1/2* lub innymi mutacjami w genach szlaku HR. Inne badanie kliniczne wykorzystujące takie samo połączenie j. w. – ATARI (NCT04065269) – zostało rozszerzone o inne nowotwory ginekologiczne z mutacją lub jej brakiem w genie *ARid1A* (ang. *AT-rich interaction domain 1A*), kodującym białko rodziny SWI/SNF, które reguluje transkrypcję genów poprzez zmianę struktury chromatyny. Badanie OLAPCO (NCT02576444) zostało z kolei rozszerzone na wszystkie typy nowotworów z mutacjami w genach szlaku HR – *ATM*, *CHK2*, *APOBEC* (ang. *Apolipoprotein B mRNA Editing Catalytic Polypeptide-like*) oraz *MRE11*. Badanie NCT04267939 wykorzystuje natomiast inny ATRi niż badany w niniejszej rozprawie (BAY1895344) oraz niraparib (PARPi) w guzach litych i raku jajnika. Efektywność terapii niraparibem razem z M4344 (ATRi) w raku jajnika opornym na PARPi jest także sprawdzana w badaniu klinicznym nr NCT04149145. Badanie NCT03057145 określa efektywność terapii preksasertibu (CHK1i) w połączeniu z olaparibem w zaawansowanych guzach litych, włączając raka jajnika *BRCA^{MUT}* HGSOc. Badania te rozszerzają nieznacznie docelową grupę pacjentek dedykowaną do leczenia PARPi.

Inhibitory szlaku ATR/CHK1, w kombinacji z już stosowanym klinicznie lekiem przeciwnowotworowym (olaparibem), mogą poprawić jego skuteczność w terapii raka jajnika. Pomimo trwających badań klinicznych, molekularne mechanizmy działania monoterapii PARPi, ATRi czy CHK1i jak i terapii skojarzonej ATRi/CHK1i z olaparibem pozostają niejasne. W rozprawie doktorskiej stosowano linie komórkowe o zróżnicowanym profilu genetycznym – model HGSOc z mutacją w genie *BRCA2*, predysponowany do leczenia PARPi, model HGSOc *BRCA^{WT}*, z mutacją *TP53* oraz model *BRCA^{WT}* oporny na cisplatynę – konwencjonalną terapię stosowaną w leczeniu raka jajnika. Podjęta tematyka rozprawy doktorskiej znajduje się w głównym nurcie badań podstawowych. Wyniki uzyskane przy zastosowaniu zróżnicowanych modeli badawczych raka jajnika pozwolą na ocenę możliwości stosowania terapii skojarzonej PARPi+ATRi lub PARPi+CHK1i w nowych grupach docelowych pacjentek, w tym *BRCA^{WT}*.

CEL PRACY

Celem niniejszej rozprawy doktorskiej była ocena cytotoksycznego efektu działania inhibitorów kinazy ATR (AZD6738, ATRi, ceralasertib) i CHK1 (MK8776, CHK1i) w skojarzeniu z inhibitorem polimerazy poli(ADP-rybozy) (AZD2281, PARPi, olaparib) w trzech liniach komórkowych raka jajnika – SKOV-3, OV-90 oraz PEO-1 – ze sprawnym jak i uszkodzonym systemem rekombinacji homologicznej.

Cele szczegółowe obejmowały analizę wpływu badanych związków na aktywację szlaku ATR/CHK1 oraz ocenę ich działania genotoksycznego i w konsekwencji określenie czy terapia PARPi+ATRi i PARPi+CHK1i doprowadzi do śmierci komórek raka jajnika, na drodze syntetycznej letalności.

Materiał badawczy:

Materiał badawczy stanowiły trzy linie komórkowe raka jajnika:

- ➔ SKOV-3 (human ovarian adenocarcinoma), ATCC HTB-77, odporne na cisplatynę i doksorubicynę, $P53^{NULL}$, $BRCA^{WT}$
- ➔ OV-90 (human ovarian papillary serous adenocarcinoma), ATCC CRL-11732, HGSOC, $p53^{MUT}$, $BRCA^{WT}$
- ➔ PEO-1 (human ovarian cancer; oestrogen receptor positive), ECACC cat. 10032308, HGSOC, $p53^{MUT}$, $BRCA2^{MUT}$

Badane związki:

- ➔ Inhibitor polimerazy poli (ADP-rybozy), PARPi, AZD2281, olaparib
- ➔ Inhibitor białka ATR, ATRi, AZD6738, ceralasertib
- ➔ Inhibitor białka CHK1, CHK1i, MK8776

Metody badawcze:

- ➔ Ocena cytotoksyczności badanych związków oraz rodzaju oddziaływań między związkami za pomocą testu metabolicznego z MTT.
- ➔ Określenie przeżywalności komórek za pomocą testu wzrostu klonalnego.
- ➔ Określenie poziomu ekspresji białek – PARP, ATR, pATR, CHK1, pCHK1, kaspazy-3, γ H2AX, cytochromu c oraz MDR1 za pomocą techniki western blot.
- ➔ Ocena poziomu uszkodzeń jedno- i dwuniciowych DNA za pomocą metody kometowej w wersji alkalicznej.
- ➔ Określenie poziomu uszkodzeń dwuniciowych DNA za pomocą metody kometowej w wersji neutralnej.
- ➔ Analiza cytofluorymetryczna aktywności kaspazy 3/7.
- ➔ Ilościowa analiza aberracji chromosomowych za pomocą testu płytki metafazowej.
- ➔ Ocena aberracji chromosomowych za pomocą testu mikrojądrowego.
- ➔ Określenie tempa proliferacji komórek.

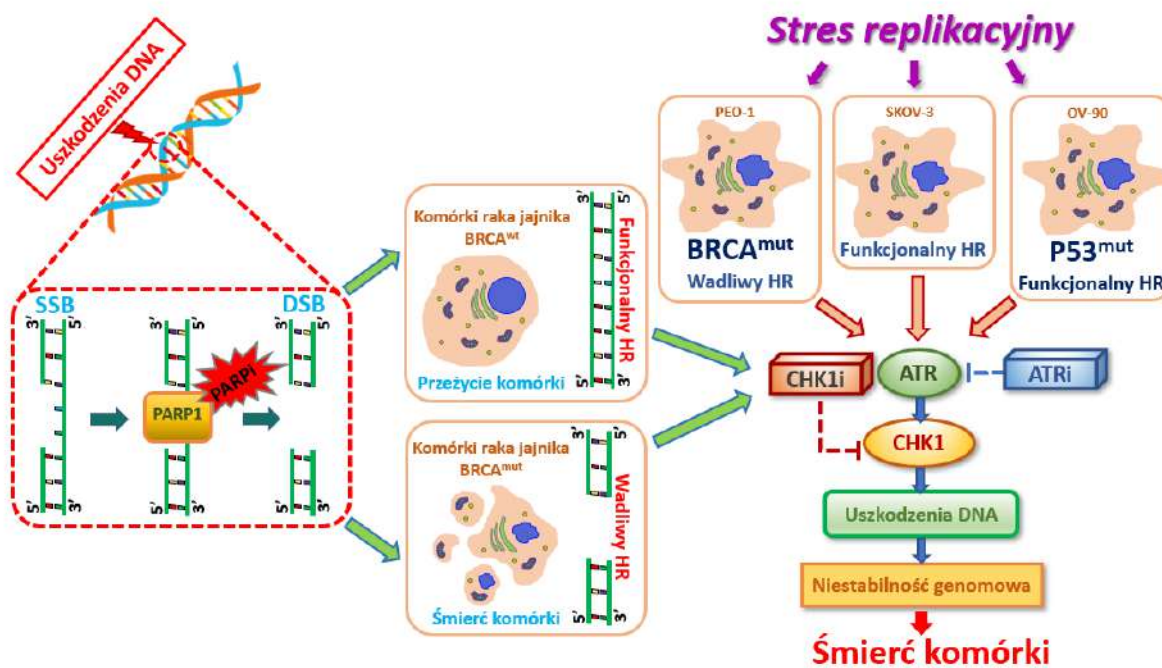
- ➔ Analiza rozkładu faz cyklu komórkowego za pomocą cytometrii przepływowej z wykorzystaniem inkorporacji BrdU.
- ➔ Immunofluorescencyjna detekcja kaspazy-3 i γ H2AX.
- ➔ Ilościowa analiza zmian apoptotycznych poprzez cytofluorymetryczne oznaczenie kondensacji chromatyny.
- ➔ Detekcja progresji fazy S cyklu komórkowego za pomocą testu wbudowywania 5-etynilo-2'-deoksyurydyny (EdU).
- ➔ Pomiar eksternalizacji fosfatydyloseryny.
- ➔ Ocena zmian morfologicznych – apoptozy i nekrozy poprzez zastosowanie podwójnego barwienia metodą Hoechst 33342/jodek propidyny przy zastosowaniu mikroskopii fluorescencyjnej.
- ➔ Analiza statystyczna wyników.

OMÓWIENIE WYNIKÓW



Cykl artykułów wchodzących w skład niniejszej rozprawy doktorskiej otwiera publikacja przeglądowa pt.: „**Participation of the ATR/CHK1 pathway in replicative stress targeted therapy of high-grade ovarian cancer**” [53], stanowiąca podsumowanie najnowszych doniesień literaturowych związanych z tematyką pracy doktorskiej.

Publikacja ta skupia się na wyjaśnieniu roli mechanizmów naprawy DNA w leczeniu raka jajnika. Szlaki odpowiedzi na uszkodzenia DNA uczestniczą w rozpoznaniu i naprawie wszystkich typów zaburzeń struktury DNA. Regulacja tych odpowiedzi komórkowych poprzez liczne inhibitory kinaz może prowadzić do zwiększenia niestabilności genomowej i w konsekwencji śmierci komórkowej. Z tego powodu stres replikacyjny i zaburzenia cyklu komórkowego mogą być potencjalnym celem w terapii raka jajnika. W pracy przeglądowej omówiono rolę białka PARP w naprawie DNA oraz uzasadniono stosowanie jego inhibitorów w nowotworach *BRCA^{MUT}*. Wymieniono także aktualne badania kliniczne, w których stosowane są wymienione w pracy inhibitory. Następnie przedstawiono działanie kinaz ATR, CHK1 oraz ich znaczenie jako celów terapeutycznych w terapii raka jajnika. Badania kliniczne sprawdzające skuteczność ATRi, CHK1i oraz PARPi zostały zebrane w Tabeli 1 [53]. W kolejnym rozdziale skupiono się na potencjalnym synergizmie skojarzonego działania PARPi+ATRi oraz PARPi+CHK1i. Ostatni rozdział pracy przeglądowej opisuje nowe modele badawcze wykorzystywane do optymalizacji terapii raka jajnika w warunkach przedklinicznych. Praca ta ponadto podkreśla rolę szlaków naprawy DNA w poszukiwaniu nowatorskich celi terapeutycznych. W pracy wyraźnie podkreślono koncepcję umożliwiającą zwiększenie efektywności terapeutycznej olaparibu poprzez połączenie go z ATRi lub CHK1i, co może stanowić nowy schemat leczenia raka jajnika. Proponowany model odpowiedzi komórki nowotworowej na opisane inhibitory przedstawiony został na rysunku nr 1.



Rys. 1. Proponowany model odpowiedzi komórek raka jajnika na inhibitory stresu replikacyjnego oraz ich skojarzone działanie z PARPi. Szlak ATR/CHK1 stabilizuje widełki replikacyjne i zapobiega powstawaniu DSB. SSB mogą być dokładnie naprawiane, przy użyciu nieuszkodzonej nici DNA jako matrycy, a proces ten wymaga enzymu PARP. Białka BRCA1/2 zaangażowane są w bezbłędną naprawę DSB poprzez system naprawy HR. ATRi lub CHK1i w monoterapii jak i w leczeniu skojarzonym z PARPi prowadzą do niestabilności genomowej komórek raka jajnika, na drodze syntetycznej letalności [54].



Praca oryginalna pt. „**PARP inhibition increases the reliance on ATR/CHK1 checkpoint signaling leading to synthetic lethality- an alternative treatment strategy for epithelial ovarian cancer cells independent from HR effectiveness**” [54] obejmuje pierwszy etap badań.

Celem badań było wykazanie, że cytotoksyczne działanie inhibitora PARP można zwiększyć poprzez równoczesną inhibicję białek zaangażowanych w regulację punktów kontrolnych cyklu komórkowego.

W pracy oceniono potencjał cyto- i genotoksyczny inhibitorów PARP, ATR i CHK1 w trzech liniach komórkowych raka jajnika – SKOV-3, OV-90 i PEO-1. Ocena przeżywalności komórek po 5-dniowej inkubacji ze związkami pozwoliła wyznaczyć efektywne stężenia związków pod kątem ich cytotoksycznego działania w kombinacjach (PARPi+ATRi i PARPi+CHK1i) oraz określić rodzaj oddziaływań między związkami. Na podstawie krzywych zależności dawka-efekt dla badanych linii komórkowych raka jajnika po pięciu dniach inkubacji z rosnącymi stężeniami olaparibu, ATRi oraz CHK1i (0,1-30 μ M) wyznaczono wartości parametrów IC50, które pozwoliły określić wrażliwość badanych linii komórkowych wobec zastosowanych inhibitorów. Najbardziej wrażliwą na działanie

związków linią okazała się linia $BRCA^{MUT}$, PEO-1. Monoterapia PARPi zmniejszyła przeżywalność komórek linii PEO-1 do 29%, linii OV-90 do 60% i linii SKOV-3 do 48%. Inhibitor CHK1 był bardziej cytotoksyczny dla linii komórkowych $BRCA^{WT}$, niż dla linii $BRCA^{MUT}$, natomiast efekt cytotoksyczny ATRi, podobnie jak PARPi był najsilniejszy w linii PEO-1. Następnie wybrane stężenia związków (0,5; 1; 5 μ M) przebadano pod kątem ich cytotoksycznego działania zarówno w monoterapii, jak i w kombinacjach wobec komórek linii SKOV-3, OV-90 i PEO-1. Umożliwiło to oszacowanie wartości współczynnika interakcji leków (CDI, ang. *coefficient of drug interaction*) i pozwoliło następnie określić jaki rodzaj oddziaływań występuje między badanymi związkami stosowanymi w podaniu skojarzonym (synergizm, działanie addytywne lub antagonizm). Na podstawie obliczonego CDI wybrano stosunek 1:1 (0,5:0,5 μ M – PARPi+ATRi; PARPi+CHK1i) jako najniższe, biologicznie aktywne stężenie mające jednocześnie oddziaływanie synergistyczne. Skojarzone działanie PARPi+CHK1i jak i PARPi+ATRi miało znacznie silniejsze działanie cytotoksyczne niż monoterapia, Fig. 2A-B [54]. ATRi w skojarzeniu z PARPi był równie cytotoksyczny zarówno w komórkach raka jajnika z niedoborem BRCA2, jak i w komórkach $BRCA^{WT}$. Kombinacja PARPi+ATRi wykazała synergizm we wszystkich badanych liniach komórkowych, natomiast kombinacja PARPi+CHK1i wykazywała działanie synergistyczne tylko w komórkach $BRCA^{MUT}$.

Następnie, aby sprawdzić długoterminowy efekt działania leków wykonano test wzrostu klonalnego, który pozwala określić przeżywalność komórek na podstawie zdolności do tworzenia kolonii. Skuteczność przeciwnowotworowego działania związków w kombinacji w porównaniu z monoterapią oceniono również na podstawie współczynnika CDI. Monoterapia olaparibem okazała się mniej skuteczna niż kombinacje związków w redukowaniu zdolności komórek do tworzenia kolonii. ATRi zahamował zdolność komórek do tworzenia kolonii w dwóch liniach komórkowych – PEO-1 oraz OV-90 i znacząco, do 28%, zmniejszył liczbę kolonii w linii SKOV-3. CHK1i natomiast zmniejszył liczbę kolonii do około 98% w linii SKOV-3, do 4% w linii OV-90 i do >1% w linii PEO-1. Kombinacja PARPi+ATRi okazała się bardziej cytotoksyczna niż kombinacja PARPi+CHK1i we wszystkich badanych liniach komórkowych. Dodatkowo, po upływie pierwszej doby inkubacji z kombinacjami związków zaobserwowano wyraźne zmiany w morfologii komórek, które obkurczyły się, przyjmując wrzecionowaty bądź owalny kształt. Zaobserwowano również znaczny udział frakcji komórek martwych (opalizujących), które oddzieliły się od dna naczynia hodowlanego.

W dalszej kolejności zbadano poziom białka PARP1 po działaniu badanych związków oraz wpływ olaparibu na aktywację szlaku ATR/CHK1. Po zablokowaniu PARP, najwyższy poziom aktywnych form białek ATR/CHK1 obserwowany był w linii komórkowej $BRCA^{MUT}$. Monoterapia olaparibem prowadziła do wzrostu ekspresji ufosforylowanej formy białka ATR w linii PEO1, w celu utrzymania stabilności genomu. We wszystkich badanych liniach komórkowych kombinacja PARPi+ATRi wywołała spadek indukowanej przez olaparib, zwiększonej ekspresji pATR.

Uszkodzenia DNA są kluczowymi zmianami prowadzącymi do powstawania strukturalnych aberracji chromosomalnych i niestabilności genomowej związanej z zaburzoną naprawą HR w raku jajnika. Stąd poziom uszkodzeń DNA w odniesieniu do SSB i DSB analizowano testem kometowym w wersji alkalicznej (wykrywającej zarówno SSB jak i DSB) i neutralnej (wykrywającej bezpośrednio DSB). Wykazano, że ilość uszkodzeń DNA indukowana przez PARPi, ATRi oraz CHK1i jest zależna od czasu inkubacji z tymi związkami. Największe zmiany obserwowano po 48 godzinach inkubacji i po działaniu kombinacji związków, które wywoływały większe zmiany w poziomie uszkodzeń DNA niż monoterapie, a najwyższą liczbę DSB obserwowano w linii komórkowej *BRCA^{MUT}*. Zważywszy na to, że uszkodzenia DNA mogą wywoływać apoptozę komórek, określono zatem poziom aktywnych form kaspaz wykonawczych (3 oraz 7) po działaniu badanych inhibitorów. Kombinacje leków po 48 godzinach inkubacji spowodowały nieznaczny wzrost aktywności kaspazy 3/7, sugerując, że jednym z mechanizmów odpowiedzialnych za śmierć komórek raka jajnika poddanych działaniu inhibitorów stresu replikacyjnego może być apoptoza.

Podsumowanie pierwszej części badań:

1. Monoterapia PARPi zwiększyła ekspresję białek szlaku ATR/CHK1 w linii *BRCA^{MUT}*, co może sugerować zależność skuteczności terapii olaparibem od sprawności tego szlaku.
2. Terapia skojarzona PARP+ATRi lub PARPi+CHK1i jest bardziej cytotoksyczna niż monoterapia w komórkach raka jajnika w dawkach subletalnych po dłuższym czasie inkubacji (5 dni).
3. Terapia skojarzona działa synergistycznie w komórkach raka jajnika, a najefektywniejszym połączeniem jest to, w którym stosunek molowy stężeń związków wynosi 1:1.
4. Terapia skojarzona indukuje wzrost poziomu uszkodzeń DNA.
5. Kombinacja PARP+ATRi oraz PARPi+CHK1i jest cytotoksyczna i genotoksyczna dla komórek raka jajnika niezależnie od obecności mutacji genu *BRCA*.



W drugiej pracy doświadczalnej, pt.: „**The Influence of PARP, ATR, CHK1 Inhibitors on Premature Mitotic Entry and Genomic Instability in High-Grade Serous *BRCA^{MUT}* and *BRCA^{WT}* Ovarian Cancer Cells**” [55] celem badań było poznanie mechanizmu śmierci komórkowej indukowanej przez badane związki, w początkowej fazie odpowiedzi komórek na olaparib oraz inhibitory szlaku ATR/CHK. W pracy skupiono się na wczesnym etapie działania związków (24 i 48 godzin) oraz zwiększono ich stężenie do 4 μ M, zachowując stosunek stężeń związków 1:1. W badanym stężeniu po 24 godzinach związki nie wpłynęły znacząco na żywotność komórek. Po 48 godzinach ATRi był najbardziej cytotoksyczny dla linii *BRCA^{MUT}*, natomiast inhibitor CHK1 był nieznacznie bardziej cytotoksyczny dla linii *BRCA^{WT}*, co pozostaje w zgodzie z wynikami osiągniętymi po 5 dniach inkubacji dla niższych stężeń związków.

Połączenie ATRi/CHK1i z PARPi nie wykazywało większej cytotoksyczności niż monoterapia ATRi i CHK1i.

Zdolność badanych związków do wywoływania uszkodzeń DNA została potwierdzona ponownie, dodatkowymi badaniami określającymi ekspresję markera uszkodzeń DNA, γ H2AX. W czasie 48 godzin i przy stężeniu 4 μ M olaparib okazał się niewystarczający do zwiększenia ekspresji fosforylowanego histonu H2AX. Kombinacje leków natomiast prowadziły do większych zmian niż monoterapia PARPi. Największe zmiany ekspresji histonu γ H2AX obserwowano w linii komórkowej SKOV-3, pomimo tego, że linia ta wykazywała najniższy poziom ekspresji histonu γ H2AX w komórkach kontrolnych w porównaniu do kontroli w liniach OV-90 i PEO-1 [Supplementary Fig. S5], [55].

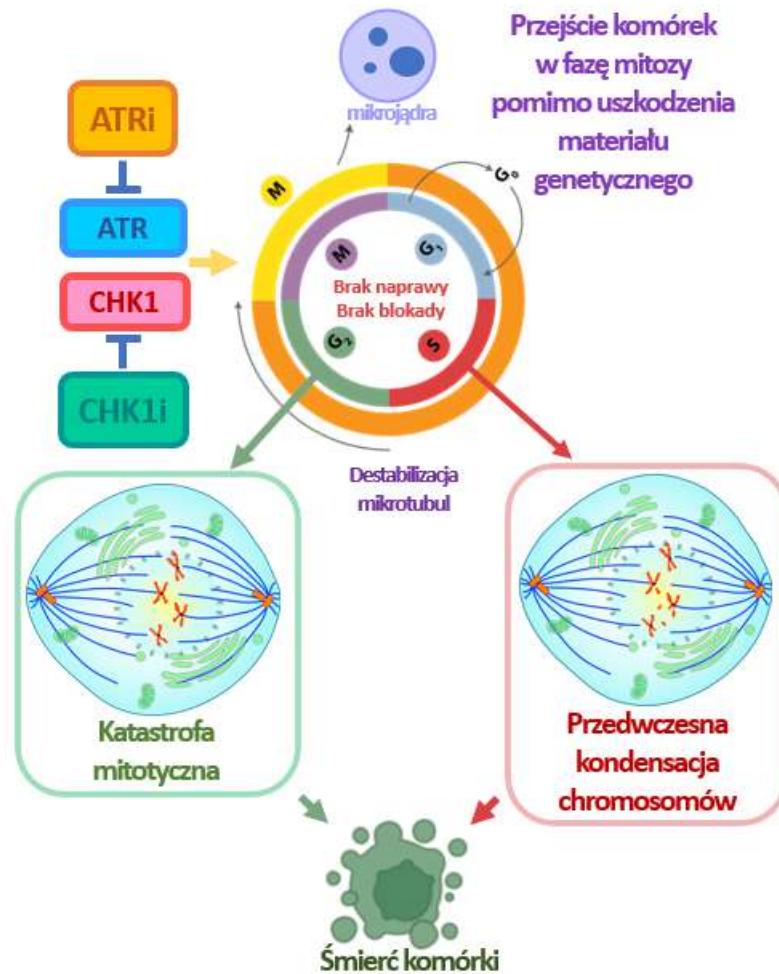
Ocenę właściwości proapoptotycznych przeprowadzono szacując odsetek komórek apoptotycznych i nekrotycznych metodą podwójnego barwienia (Hoechst 33258/jodek propidyny), badając eksternalizację fosfatydyloseryny (wczesnego markera związanego z procesem apoptozy), mierząc kondensację chromatyny oraz ekspresję aktywnej formy efektorowej kaspazy-3. Wszystkie wymienione metody wykazały, że po krótkim czasie działania olaparib nie indukuje apoptozy w komórkach badanych linii. Natomiast badane kombinacje związków okazały się skuteczne w indukowaniu apoptozy (kondensacja, fragmentacja i marginalizacja chromatyny powstawanie ciałek apoptotycznych), jednakże, pomimo tendencji wzrostowych, nie wykazano zmian istotnych statystycznie pomiędzy kombinacjami leków PARPi+ATRi/PARPi+CHK1i a monoterapią ATRi/CHK1i.

Biorąc pod uwagę fakt, iż szlak ATR/CHK1 uczestniczy w regulacji cyklu komórkowego, zbadano rozkład faz cyklu komórkowego, ze szczególnym uwzględnieniem odsetka komórek znajdujących się w fazie G2/M. Aberracje chromosomowe w komórkach traktowanych PARPi+ATRi lub PARPi+CHK1i prawdopodobnie wynikały z niewłaściwej naprawy DSB przed wejściem w mitozę, zwiększonego zapadania się widełek replikacyjnych i zniesienia punktów kontrolnych fazy G2/M w komórkach PEO-1 i SKOV-3. Tylko w komórkach OV-90 stwierdzono, że ATRi i CHK1i wzmacniają efekt olaparibu i promują niewielki wzrost liczby komórek w fazie G2/M. Linia OV-90 była także najbardziej wrażliwa na działanie skojarzone PARPi+ATRi i PARPi+CHK1i.

W warunkach stresu replikacyjnego, wejście w mitozę jest zablokowane do czasu aktywacji odpowiedzi na uszkodzenia DNA - DDR. Uszkodzenia DNA aktywują punkt kontrolny fazy S cyklu i jednocześnie spowalniają ruch widełek replikacyjnych [56]. Aby zbadać wpływ ATRi oraz CHK1i w połączeniu z olaparibem na proliferację komórek i monitorowanie fazy S, zastosowano inkorporację 5'-bromo-2'-deoksyurydyny (BrdU) oraz 5-etynylo-2'-deoksyurydyny (EdU) do DNA. Na podstawie różnic w inkorporacji BrdU w linii PEO-1 stwierdzono zwiększenie liczby komórek we wczesnej fazie S, co może być oznaką stresu replikacyjnego. Terapia skojarzona nie wykazywała silniejszego wpływu na

proliferację komórek niż monoterapia ATRi czy CHK1i. Z kolei inkorporację EdU zastosowano do zilustrowania wpływu inhibitorów na trzy etapy fazy S (wczesna, późna i środkowa). W komórkach obserwowano charakterystyczne znakowanie prawidłowej fazy S: znakowanie jednorodne, typowe dla wczesnej fazy S (jednolita fluorescencja w jądrze); silne znakowanie jednorodne, specyficzne dla środkowej fazy S oraz znakowanie heterogenne w późniejszej fazie S (ryc. 7C). Aktywacja szlaku ATR/CHK1 wydaje się konieczna we wczesnej fazie S, aby ograniczyć replikację w obecności uszkodzonego DNA. Obserwowano ponadto niewielki spadek indeksu mitotycznego (procentowy udział komórek dzielących się w stosunku do całej populacji) w komórkach linii OV-90 po traktowaniu ATRi, CHK1i oraz ich kombinacjami z olaparibem, a także w komórkach linii SKOV-3 po PARPi+CHK1i. Dodatkowo w komórkach linii SKOV-3 i PEO-1 po leczeniu skojarzonym doszło do wzrostu indeksu aberracji chromosomowych (procentowy stosunek liczby komórek wykazujących aberracje chromosomowe do wszystkich komórek mitotycznych). W linii OV-90 wzrost indeksu aberracji obserwowano tylko po działaniu kombinacji PARPi+CHK1i.

Kombinacja PARPi+ATRi znacząco zwiększyła ilość mikrojąder w linii PEO-1, w porównaniu do leków stosowanych pojedynczo. Katastrofa mitotyczna (MC, ang. *mitotic catastrophe*) nie jest oddzielnym trybem śmierci komórki, ale raczej procesem poprzedzającym śmierć komórki, która może nastąpić poprzez martwicę lub apoptozę [57]. Uzyskane wyniki sugerują, że uszkodzenia DNA, w tym DSB, nie prowadzą do natychmiastowej śmierci komórek raka jajnika traktowanych olaparibem, ATRi czy CHK1i. Komórki te mogą wejść przedwcześnie w mitozę, mimo obecnych uszkodzeń DNA, w wyniku czego dochodzi do powstania aberracji chromosomowych, co zostało potwierdzone podczas analizy mikrojąder czy płytki metafazowej. Niestabilność chromosomów może spowodować śmierć komórki przez MC. Graficzna ilustracja wyników została przedstawiona na Rys. 2.



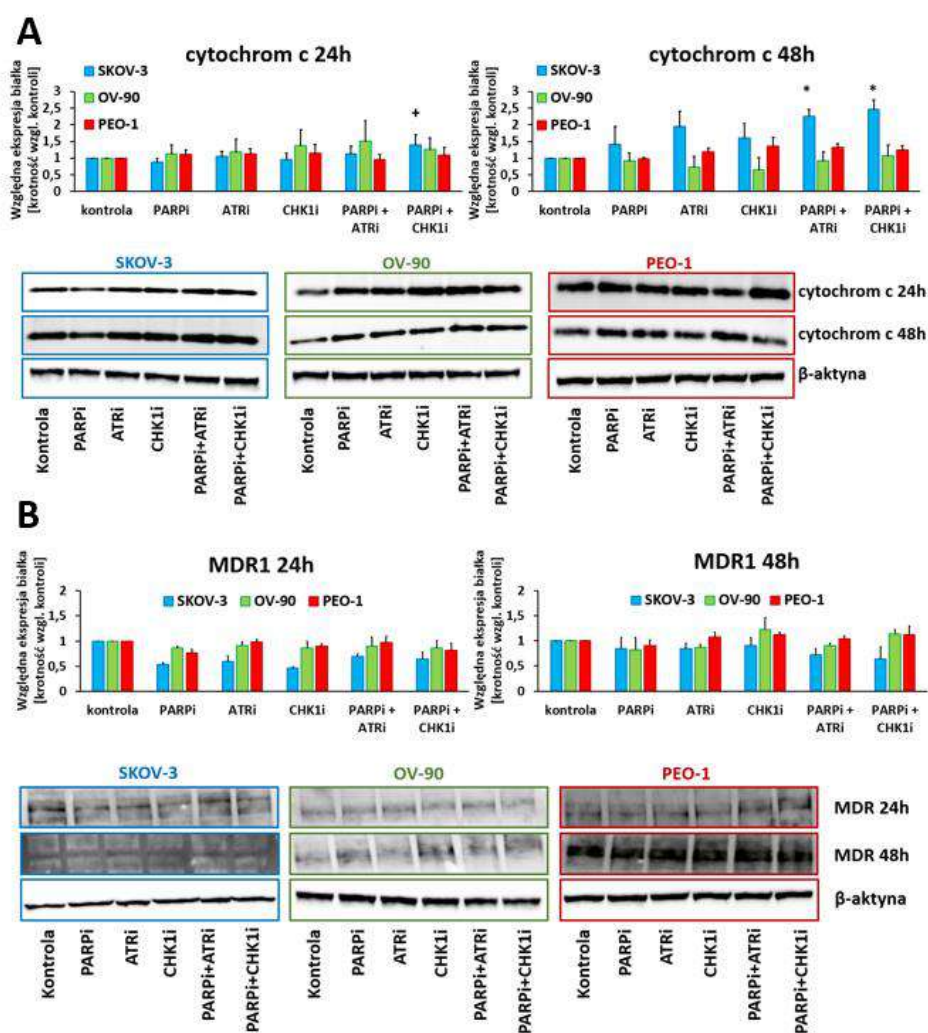
Rys. 2. Po zablokowaniu szlaku ATR/CHK1 komórki przechodzą do fazy M cyklu komórkowego bez zatrzymania w punkcie kontrolnym G2/M. ATRi/CHK1i indukują przedwczesną kondensację chromosomów (PCC, ang. *premature condensation of chromosomes*) omijając wewnętrzny mechanizm punktu kontrolnego fazy S. Nienaprawione podwójne pęknięcia DNA w konsekwencji powodują powstawanie mikrojąder i MC [55].

Podsumowanie drugiej części badań:

1. Terapie skojarzone PARPi z ATRi/CHK1i nie są bardziej cytotoksyczne w porównaniu do odpowiednich monoterapii w badaniach prowadzonych do 48 godzin. Olaparib w krótkich czasach wykazuje działanie cytostatyczne w komórkach raka jajnika.
2. Zarówno ATRi jak i CHK1i oraz ich kombinacje z olaparibem powodują wejście komórek raka jajnika w mitozę z uszkodzonym DNA, niezależnie od statusu $BRCA^{MUT}$, prowadząc do akumulacji aberracji chromosomowych, niestabilności genomu i apoptozy.



Ostatnim etapem badań, dotychczas nie opublikowanych, była ocena wpływu PARPi, ATRi, CHK1i oraz ich skojarzonego działania na potencjalny wzrost ekspresji glikoproteiny P, białka związanego z występowaniem oporności wielolekowej. Dokonano również oceny ekspresji cytochromu c w celu rozszerzenia badań nad programowaną śmiercią komórki, indukowaną przez badane związki. Oznaczenia w badanych liniach komórkowych raka jajnika wykonano metodą western blot po 24 i 48 godzinach inkubacji ze związkami w stosunku 1:1, w stężeniu 4 μ M. Doświadczenia te zostały przeprowadzone tak jak opisano poprzednio [58], używając króliczego przeciwciała I-rzędowego monoklonalnego przeciw glikoproteinie P (P-Glycoprotein Recombinant Rabbit Monoclonal Antibody (SN06-4) cat. # MA5-32282, Thermo Fisher Scientific (Waltham, MA, USA)) oraz króliczego przeciwciała I-rzędowego monoklonalnego przeciw cytochromowi c (Cytochrome c (D18C7) Rabbit mAb cat. #11940 Cell Signaling Technology, Inc. (Danvers, MA, USA)). Wyniki zostały przedstawione na rysunku nr 3.



Rys. 3. Względna ekspresja cytochromu c (A) oraz MDR1 (B) w komórkach raka jajnika po działaniu badanych związków. * różnice istotne statystycznie między komórkami traktowanymi związkiem a komórkami kontrolnymi

($p < 0,05$); + różnice istotne statycznie pomiędzy komórkami inkubowanymi z PARPi w stosunku do kombinacji (PARPi+ATRi, PARPi+CHK1i) ($p < 0,05$); (B) Reprezentatywne zdjęcia western blot.

MDR1 jest jednym z najbardziej znanych transporterów błonowych, należących do rodziny białek ABC (ang. *ATP-binding cassette*). P-gp ma bardzo szeroką specyficzność substratową, co umożliwia interakcje z wieloma związkami. Nadekspresja tego białka ma miejsce w przypadku wielu nowotworów w tym raka jajnika [59]. Niektóre badania wykazały także zależność pomiędzy opornością na olaparib, a zwiększoną ekspresją MDR1 [37, 60, 61]. Analiza wyników western blot wykazała, że stosowane inhibitory nie zwiększają ekspresji białka MDR1 po 24, jak i 48 godzinach inkubacji w zastosowanych warunkach badawczych, a potencjalna oporność na te inhibitory, na wczesnym etapie ich działania, nie jest związana ze wzrostem ekspresji P-gp w komórkach raka jajnika o zróżnicowanym profilu genetycznym.

Zaburzenie integralności błony mitochondrialnej, a pośrednio uwolnienie cytochromu c, jest kluczowe w procesie apoptozy. Po 24 godzinach inkubacji nie zaobserwowano znaczących zmian w poziomie ekspresji cytochromu c w liniach SKOV-3 oraz PEO-1. Po 48 godzinach inkubacji obie kombinacje zastosowanych związków zwiększyły ekspresję białka około 2,5-krotnie w linii SKOV-3, w porównaniu do około 1,5-krotnego wzrostu po PARPi i CHK1i oraz około 2-krotnego po inkubacji z ATRi. W linii PEO-1 po 48 godzinach obserwowano 1,3-krotny wzrost poziomu białka po działaniu kombinacji PARPi+ATRi. Podobnie jak w linii OV-90 po 24 godzinach inkubacji obserwowano około 1,5-krotny wzrost ekspresji badanego białka po działaniu kombinacji PARPi+ATRi. Natomiast zmiany obserwowane po 48-godzinnej inkubacji w tej linii komórkowej były nieznaczne. Wykazano, że badane związki indukują uszkodzenia DNA, co może dodatkowo powodować stres mitochondrialny i apoptozę poprzez fosforylację białek mitochondrialnych zaangażowanych w uwalnianie cytochromu c [62]. ATR natomiast w odpowiedzi na uszkodzenia DNA spowodowane promieniowaniem UV wykazuje aktywność antyapoptotyczną, hamując uwalnianie cytochromu c [63]. W poprzedniej pracy [64] obserwowano 1,2-krotny wzrost poziomu ekspresji cytochromu c w linii SKOV-3 i 3,8-krotny wzrost w linii OV-90, po 24 godzinnej inkubacji z olaparibem, w dawce 5-krotnie wyższej, niż zastosowana w opisywanych badaniach (20 μM). Monoterapia olaparibem w stężeniu 4 μM nie była zatem wystarczająca do znaczącego zwiększenia ekspresji cytochromu c. Po 48 godzinach natomiast obie kombinacje zwiększyły istotnie statystycznie uwalnianie cytochromu c jedynie w linii SKOV-3. Zmiany ekspresji cytochromu c wydają się być wystarczające do zainicjowania apoptozy, o czym świadczy wzrost eksternalizacji fosfatydyloseryny, obserwowane zmiany w morfologii komórek po barwieniu H/PI oraz wzrost ekspresji ciętej kaspazy-3.

Podsumowanie:

1. Kombinacje PARPi+ATRI/CHK1i prowadzą do wzrostu ekspresji cytochromu c w linii SKOV-3 po 48 godzinach.
2. Inhibitory nie zwiększają ekspresji białka MDR1 zarówno w monoterapii, jak i w terapii skojarzonej.

PODSUMOWANIE UZYSKANYCH WYNIKÓW ORAZ WNIOSKI

Pierwsza opisywana praca oryginalna [54] potwierdziła, że PARPi zwiększył zależność komórek raka jajnika od szlaku ATR/CHK1, w celu utrzymania stabilności genomu. Kombinacja PARPi+ATRi całkowicie zahamowała zdolność komórek do tworzenia kolonii, niezależnie od statusu HR linii komórkowej. Obie testowane kombinacje natomiast zwiększyły ilość DSB, w efekcie indukując apoptozę komórek linii raka jajnika. Badania te potwierdziły wrażliwość stosowanych linii komórkowych na inhibitory ATR oraz CHK1. Zastosowanie kombinacji PARPi+ATRi oraz PARPi+CHK1i uwrażliwiło komórki na olaparib, poprzez zablokowanie możliwości naprawy DNA, na drodze syntetycznej letalności. Wyniki te uzyskano stosując subletalne dawki związków, co sugeruje, że koncepcja stosowania terapii skojarzonej PARPi+ATRi oraz PARPi+CHK1i może przynosić potencjalne korzyści terapeutyczne.

W drugiej pracy doświadczalnej [55] uzyskane wyniki pozwoliły stwierdzić, że monoterapia olaparibem w krótkich czasach inkubacji wykazuje aktywność cytostatyczną. Stosowane kombinacje nie były z kolei bardziej cytotoksyczne niż monoterapie inhibitorami ATRi oraz CHK1i. Efekt cytotoksyczny badanych związków zależny był od czasu inkubacji. Ponadto w publikacji wykazano, że ATRi i CHK1i prowadziły do nieprawidłowego przebiegu podziałów mitotycznych, aberracji chromosomowych, niestabilności genomowej i w konsekwencji śmierci komórki.

Wnioski:

- ➔ **Terapia olaparibem spowodowała aktywację szlaku ATR/CHK1 w linii *BRCA^{MUT}*.**
- ➔ **Skojarzone działanie PARPi+ATRi lub PARPi+CHK1i prowadzi do nasilonej śmierci komórek raka jajnika na drodze syntetycznej letalności.**
- ➔ **Kombinacje PARPi+ATRi/PARPi+CHK1i hamują, zależnie od czasu, proliferację komórek raka jajnika i działają niezależnie od obecności mutacji *BRCA*.**
- ➔ **Monoterapia ATRi oraz CHK1i działa genotoksycznie w badanych liniach komórkowych, indukując DSB, które prowadzą do powstania aberracji chromosomowych, niestabilności genomowej i w konsekwencji śmierci komórki.**

LITERATURA

1. Ahmed, N., et al., Ovarian Cancer, Cancer Stem Cells and Current Treatment Strategies: A Potential Role of Magmas in the Current Treatment Methods. *Cells*, 2020. 9(3).
2. Budiana, I.N.G., M. Angelina, and T.G.A. Pelayun, Ovarian cancer: Pathogenesis and current recommendations for prophylactic surgery. *J Turk Ger Gynecol Assoc*, 2019. 20(1): p. 47-54.
3. McGee, J., et al., Direct Genetics Referral Pathway for High-Grade Serous Ovarian Cancer Patients: The "Opt-Out" Process. *Journal of Oncology*, 2019. 2019: p. 1-7.
4. Huang, Y.-W., Association of BRCA1/2 mutations with ovarian cancer prognosis. *Medicine*, 2018. 97(2).
5. Wu, R., et al., Type I to Type II Ovarian Carcinoma Progression. *The American Journal of Pathology*, 2013. 182(4): p. 1391-1399.
6. Konstantinopoulos, P.A., et al., Homologous Recombination Deficiency: Exploiting the Fundamental Vulnerability of Ovarian Cancer. *Cancer Discovery*, 2015. 5(11): p. 1137-1154.
7. da Cunha Colombo Bonadio, R.R., et al., Homologous recombination deficiency in ovarian cancer: a review of its epidemiology and management. *Clinics*, 2018. 73.
8. Damia, G. and M. Broggin, Platinum Resistance in Ovarian Cancer: Role of DNA Repair. *Cancers*, 2019. 11(1).
9. Basta, P., et al., Zasady postępowania z chorymi z podejrzeniem i rozpoznaniem raka jajnika — rekomendacje Polskiego Towarzystwa Ginekologicznego. *Ginekologia i Perinatologia Praktyczna*, 2016. 1(3): p. 127-129.
10. Lokadasan, R., et al., Targeted agents in epithelial ovarian cancer: review on emerging therapies and future developments. *ecancermedicalscience*, 2016. 10.
11. Martí, J.M., et al., The Multifactorial Role of PARP-1 in Tumor Microenvironment. *Cancers*, 2020. 12(3).
12. Ronson, G.E., et al., PARP1 and PARP2 stabilise replication forks at base excision repair intermediates through Fbh1-dependent Rad51 regulation. *Nature Communications*, 2018. 9(1).
13. Kaelin, W.G., The Concept of Synthetic Lethality in the Context of Anticancer Therapy. *Nature Reviews Cancer*, 2005. 5(9): p. 689-698.
14. Bohrer, R.C., et al., Double-strand DNA breaks are mainly repaired by the homologous recombination pathway in early developing swine embryos. *FASEB J*, 2018. 32(4): p. 1818-1829.
15. Wang, Y., et al., BASC, a super complex of BRCA1-associated proteins involved in the recognition and repair of aberrant DNA structures. *Genes Dev*, 2000. 14(8): p. 927-39.
16. Carver, A. and X. Zhang, Rad51 filament dynamics and its antagonistic modulators. *Seminars in Cell & Developmental Biology*, 2021. 113: p. 3-13.
17. Gourley, C., et al., Moving From Poly (ADP-Ribose) Polymerase Inhibition to Targeting DNA Repair and DNA Damage Response in Cancer Therapy. *Journal of Clinical Oncology*, 2019. 37(25): p. 2257-2269.
18. Dai, C.-H., et al., Co-inhibition of pol θ and HR genes efficiently synergize with cisplatin to suppress cisplatin-resistant lung cancer cells survival. *Oncotarget*, 2016. 7(40): p. 65157-65170.

19. Spriggs, D.R. and D.L. Longo, Progress in BRCA-Mutated Ovarian Cancer. *New England Journal of Medicine*, 2018. 379(26): p. 2567-2568.
20. Baloch, T., et al., Sequential therapeutic targeting of ovarian Cancer harboring dysfunctional BRCA1. *BMC Cancer*, 2019. 19(1).
21. Gadducci, A., et al., Current strategies for the targeted treatment of high-grade serous epithelial ovarian cancer and relevance of BRCA mutational status. *Journal of Ovarian Research*, 2019. 12(1).
22. Valdez, B.C., et al., Combination of a hypomethylating agent and inhibitors of PARP and HDAC traps PARP1 and DNMT1 to chromatin, acetylates DNA repair proteins, down-regulates NuRD and induces apoptosis in human leukemia and lymphoma cells. *Oncotarget*, 2017. 9(3): p. 3908-3921.
23. Robert, C., et al., Histone deacetylase inhibitors decrease NHEJ both by acetylation of repair factors and trapping of PARP1 at DNA double-strand breaks in chromatin. *Leukemia Research*, 2016. 45: p. 14-23.
24. Matulonis, U.A., et al., Olaparib maintenance therapy in patients with platinum-sensitive, relapsed serous ovarian cancer and a BRCA mutation: Overall survival adjusted for postprogression poly(adenosine diphosphate ribose) polymerase inhibitor therapy. *Cancer*, 2016. 122(12): p. 1844-1852.
25. Pujade-Lauraine, E., et al., Olaparib tablets as maintenance therapy in patients with platinum-sensitive, relapsed ovarian cancer and a BRCA1/2 mutation (SOLO2/ENGOT-Ov21): a double-blind, randomised, placebo-controlled, phase 3 trial. *The Lancet Oncology*, 2017. 18(9): p. 1274-1284.
26. Cortez, A.J., et al., Advances in ovarian cancer therapy. *Cancer Chemotherapy and Pharmacology*, 2017. 81(1): p. 17-38.
27. Kim, G., et al., FDA Approval Summary: Olaparib Monotherapy in Patients with Deleterious Germline BRCA-Mutated Advanced Ovarian Cancer Treated with Three or More Lines of Chemotherapy. *Clinical Cancer Research*, 2015. 21(19): p. 4257-4261.
28. Valabrega, G., et al., Differences in PARP Inhibitors for the Treatment of Ovarian Cancer: Mechanisms of Action, Pharmacology, Safety, and Efficacy. *International Journal of Molecular Sciences*, 2021. 22(8).
29. Tew, W.P., et al., PARP Inhibitors in the Management of Ovarian Cancer: ASCO Guideline. *Journal of Clinical Oncology*, 2020. 38(30): p. 3468-3493.
30. Mirza, M.R., et al., The forefront of ovarian cancer therapy: update on PARP inhibitors. *Annals of Oncology*, 2020. 31(9): p. 1148-1159.
31. Onkologicznej, P.T.G. Zmiana wykazu leków nie podlegających refundacji w ramach RDTL. 2022 [21.11.2022]; Available from: <https://ptgo.pl/zmiana-wykazu-lekow-nie-podlegajacych-refundacji-w-ramach-rdtl/>.
32. George, E., et al., A patient-derived-xenograft platform to study BRCA-deficient ovarian cancers. *JCI Insight*, 2017. 2(1).
33. Morgan, R.D., et al., PARP inhibitors in platinum-sensitive high-grade serous ovarian cancer. *Cancer Chemotherapy and Pharmacology*, 2018. 81(4): p. 647-658.
34. D'Andrea, A.D., Mechanisms of PARP inhibitor sensitivity and resistance. *DNA Repair*, 2018. 71: p. 172-176.

35. Bitler, B.G., et al., PARP inhibitors: Clinical utility and possibilities of overcoming resistance. *Gynecologic Oncology*, 2017. 147(3): p. 695-704.
36. Sakai, W., et al., Functional Restoration of BRCA2 Protein by Secondary BRCA2 Mutations in BRCA2-Mutated Ovarian Carcinoma. *Cancer Research*, 2009. 69(16): p. 6381-6386.
37. Rottenberg, S., et al., High sensitivity of BRCA1-deficient mammary tumors to the PARP inhibitor AZD2281 alone and in combination with platinum drugs. *Proceedings of the National Academy of Sciences*, 2008. 105(44): p. 17079-17084.
38. Zeman, M.K. and K.A. Cimprich, Causes and consequences of replication stress. *Nature Cell Biology*, 2013. 16(1): p. 2-9.
39. Shibata, A. and P.A. Jeggo, ATM's Role in the Repair of DNA Double-Strand Breaks. *Genes*, 2021. 12(9).
40. Cimprich, K.A. and D. Cortez, ATR: an essential regulator of genome integrity. *Nature Reviews Molecular Cell Biology*, 2008. 9(8): p. 616-627.
41. Min, A., et al., AZD6738, A Novel Oral Inhibitor of ATR, Induces Synthetic Lethality with ATM Deficiency in Gastric Cancer Cells. *Molecular Cancer Therapeutics*, 2017. 16(4): p. 566-577.
42. Blackford, A.N. and S.P. Jackson, ATM, ATR, and DNA-PK: The Trinity at the Heart of the DNA Damage Response. *Molecular Cell*, 2017. 66(6): p. 801-817.
43. Wang, J., et al., Repression of ATR pathway by miR-185 enhances radiation-induced apoptosis and proliferation inhibition. *Cell Death & Disease*, 2013. 4(6): p. e699-e699.
44. Brill, E., et al., Prexasertib, a cell cycle checkpoint kinases 1 and 2 inhibitor, increases in vitro toxicity of PARP inhibition by preventing Rad51 foci formation in BRCA wild type high-grade serous ovarian cancer. *Oncotarget*, 2017. 8(67): p. 111026-111040.
45. Niida, H., et al., Specific Role of Chk1 Phosphorylations in Cell Survival and Checkpoint Activation. *Molecular and Cellular Biology*, 2007. 27(7): p. 2572-2581.
46. Menolfi, D. and S. Zha, ATM, ATR and DNA-PKcs kinases—the lessons from the mouse models: inhibition ≠ deletion. *Cell & Bioscience*, 2020. 10(1).
47. Pabla, N., et al., ATR-Chk2 Signaling in p53 Activation and DNA Damage Response during Cisplatin-induced Apoptosis. *Journal of Biological Chemistry*, 2008. 283(10): p. 6572-6583.
48. Reaper, P.M., et al., Selective killing of ATM- or p53-deficient cancer cells through inhibition of ATR. *Nature Chemical Biology*, 2011. 7(7): p. 428-430.
49. Kawahara, N., et al., Candidate synthetic lethality partners to PARP inhibitors in the treatment of ovarian clear cell cancer. *Biomedical Reports*, 2017. 7(5): p. 391-399.
50. Buisson, R., et al., Distinct but Concerted Roles of ATR, DNA-PK, and Chk1 in Countering Replication Stress during S Phase. *Molecular Cell*, 2015. 59(6): p. 1011-1024.
51. Barnieh, F.M., P.M. Loadman, and R.A. Falconer, Progress towards a clinically-successful ATR inhibitor for cancer therapy. *Current Research in Pharmacology and Drug Discovery*, 2021. 2.
52. Qiu, Z., N.L. Oleinick, and J. Zhang, ATR/CHK1 inhibitors and cancer therapy. *Radiotherapy and Oncology*, 2018. 126(3): p. 450-464.

53. Gralewska, P., et al., Participation of the ATR/CHK1 pathway in replicative stress targeted therapy of high-grade ovarian cancer. *Journal of Hematology & Oncology*, 2020. 13(1).
54. Gralewska, P., et al., PARP Inhibition Increases the Reliance on ATR/CHK1 Checkpoint Signaling Leading to Synthetic Lethality—An Alternative Treatment Strategy for Epithelial Ovarian Cancer Cells Independent from HR Effectiveness. *International Journal of Molecular Sciences*, 2020. 21(24).
55. Gralewska, P., et al., The Influence of PARP, ATR, CHK1 Inhibitors on Premature Mitotic Entry and Genomic Instability in High-Grade Serous BRCAMUT and BRCAWT Ovarian Cancer Cells. *Cells*, 2022. 11(12).
56. Kukulj, E., et al., PARP inhibition causes premature loss of cohesion in cancer cells. *Oncotarget*, 2017. 8(61): p. 103931-103951.
57. Lloyd, R.L., et al., Combined PARP and ATR inhibition potentiates genome instability and cell death in ATM-deficient cancer cells. *Oncogene*, 2020. 39(25): p. 4869-4883.
58. Gralewska, P., et al., PARP Inhibition Increases the Reliance on ATR/CHK1 Checkpoint Signaling Leading to Synthetic Lethality-An Alternative Treatment Strategy for Epithelial Ovarian Cancer Cells Independent from HR Effectiveness. *Int J Mol Sci*, 2020. 21(24).
59. Jaramillo, A.C., et al., How to overcome ATP-binding cassette drug efflux transporter-mediated drug resistance? *Cancer Drug Resistance*, 2018. 1(1): p. 6-29.
60. Lawlor, D., et al., PARP Inhibitors as P-glycoprotein Substrates. *Journal of Pharmaceutical Sciences*, 2014. 103(6): p. 1913-1920.
61. Kim, H., et al., Combining PARP with ATR inhibition overcomes PARP inhibitor and platinum resistance in ovarian cancer models. *Nature Communications*, 2020. 11(1).
62. Valdez, B.C., et al., The PARP inhibitor olaparib enhances the cytotoxicity of combined gemcitabine, busulfan and melphalan in lymphoma cells. *Leukemia & Lymphoma*, 2017. 58(11): p. 2705-2716.
63. Hilton, Benjamin A., et al., ATR Plays a Direct Antiapoptotic Role at Mitochondria, which Is Regulated by Prolyl Isomerase Pin1. *Molecular Cell*, 2015. 60(1): p. 35-46.
64. Gralewska, P., et al., Metformin Affects Olaparib Sensitivity through Induction of Apoptosis in Epithelial Ovarian Cancer Cell Lines. *International Journal of Molecular Sciences*, 2021. 22(19).

KOPIE PUBLIKACJI WCHODZĄCYCH W SKŁAD ROZPRAWY DOKTORSKIEJ

REVIEW

Open Access



Participation of the ATR/CHK1 pathway in replicative stress targeted therapy of high-grade ovarian cancer

Patrycja Gralewska, Arkadiusz Gajek, Agnieszka Marczak and Aneta Rogalska*

Abstract

Ovarian cancer is one of the most lethal gynecologic malignancies reported throughout the world. The initial, standard-of-care, adjuvant chemotherapy in epithelial ovarian cancer is usually a platinum drug, such as cisplatin or carboplatin, combined with a taxane. However, despite surgical removal of the tumor and initial high response rates to first-line chemotherapy, around 80% of women will develop cancer recurrence. Effective strategies, including chemotherapy and new research models, are necessary to improve the prognosis. The replication stress response (RSR) is characteristic of the development of tumors, including ovarian cancer. Hence, RSR pathway and DNA repair proteins have emerged as a new area for anticancer drug development. Although clinical trials have shown poly (ADP-ribose) polymerase inhibitors (PARPi) response rates of around 40% in women who carry a mutation in the BRCA1/2 genes, PARPi is responsible for tumor suppression, but not for complete tumor regression. Recent reports suggest that cells with impaired homologous recombination (HR) activities due to mutations in TP53 gene or specific DNA repair proteins are specifically sensitive to ataxia telangiectasia and Rad3-related protein (ATR) inhibitors. Replication stress activates DNA repair checkpoint proteins (ATR, CHK1), which prevent further DNA damage. This review describes the use of DNA repair checkpoint inhibitors as single agents and strategies combining these inhibitors with DNA-damaging compounds for ovarian cancer therapy, as well as the new platforms used for optimizing ovarian cancer therapy.

Keywords: ATR kinase, CHK1, ovarian cancer, PARP, replication stress, targeted therapy

Introduction

Ovarian cancer is considered to be one of the most lethal gynaecologic malignancies worldwide. It is the seventh most common cancer and the fifth leading cause of cancer-related deaths [1]. As a result of the absence of formal screening and the continued lack of early detection methods, the majority (around 80%) of patients are diagnosed at an advanced stage (III/IV) [2]. The 5-year survival rate of patients with high-grade serous ovarian carcinomas (HGSOCs) still ranges between 35 and 40%

[3]. In 2019 in the USA, an estimated 22,530 women were diagnosed with ovarian cancer and 13,980 died from the disease [4].

Ovarian tumors can be divided into two types: type I ovarian cancers are composed of mucinous, endometrioid and low-grade serous carcinomas, while type II tend to grow more aggressively and include carcinosarcomas, undifferentiated carcinomas and high-grade serous carcinomas [5]. Moreover, almost all of the type II carcinomas, i.e. 96%, have TP53 mutation [6] and around half of HGSOCs carry an alteration in homologous recombination (HR) pathway genes, most commonly in breast cancer gene (BRCA) 1/2 [7]. Women carrying mutations in these genes have a lifetime risk of

* Correspondence: aneta.rogalska@biol.uni.lodz.pl

Department of Medical Biophysics, Faculty of Biology and Environmental Protection, Institute of Biophysics, University of Lodz, Pomorska 141/143, 90-236, Lodz, Poland



© The Author(s). 2020 **Open Access** This article is licensed under a Creative Commons Attribution 4.0 International License, which permits use, sharing, adaptation, distribution and reproduction in any medium or format, as long as you give appropriate credit to the original author(s) and the source, provide a link to the Creative Commons licence, and indicate if changes were made. The images or other third party material in this article are included in the article's Creative Commons licence, unless indicated otherwise in a credit line to the material. If material is not included in the article's Creative Commons licence and your intended use is not permitted by statutory regulation or exceeds the permitted use, you will need to obtain permission directly from the copyright holder. To view a copy of this licence, visit <http://creativecommons.org/licenses/by/4.0/>. The Creative Commons Public Domain Dedication waiver (<http://creativecommons.org/publicdomain/zero/1.0/>) applies to the data made available in this article, unless otherwise stated in a credit line to the data.

developing ovarian cancer of 36 to 60% for BRCA1 and 16 to 27% for BRCA2 [8].

The initial, standard-of-care, adjuvant chemotherapy in epithelial ovarian cancer (EOC) is usually a platinum drug, such as cisplatin or carboplatin, combined with a taxane, usually paclitaxel [9]. Cisplatin interferes with the DNA repair mechanism by crosslinking the purine bases of the DNA, and thus inducing apoptosis of cancer cells [10]. The standard regimen for advanced ovarian cancer has been expanded with bevacizumab, a recombinant humanized monoclonal antibody directed against vascular endothelial growth factor (VEGF) [11]. Other promising angiogenesis inhibitors are sorafenib and sunitinib [12, 13]. Since the addition of bevacizumab to the combination of standard chemotherapeutics, many other targeted anticancer agents have been studied in the hope of increasing the effectiveness of ovarian cancer treatment. Ovarian cancer cells often acquire resistance to common chemotherapy drugs such as cisplatin. If a tumor recurs within 6 months of cisplatin treatment, it is considered to be platinum-resistant [14, 15].

The aim of this article is to review the current knowledge of the targeting of DNA repair pathways in ovarian cancer. This review describes the use of DNA repair checkpoint inhibitors, especially poly (ADP-ribose) polymerase inhibitors (PARPi), ataxia telangiectasia and Rad3-related protein inhibitors (ATRi) and checkpoint kinase 1 inhibitors (CHK1i), as monotherapy/single agents, and their role in the treatment of patients with BRCA^{mut} ovarian cancer. It also briefly characterizes the rationale of therapies combining these inhibitors, as well as recent updates/advances in those therapies *in vitro* and in clinical trials.

Replication stress and cell cycle disturbances in ovarian cancer

Increased understanding of the tumor repair pathways has revealed their significance in the sensitivity of cells to chemotherapeutic agents. DNA damage signalling pathways have a central role in detecting DNA damage and regulating its repair. Regulation of cellular responses to interference in these pathways by numerous extrinsic and intrinsic genotoxic agents leads to genomic instability and thus to cell death [16]. Replication stress is defined as perturbations in cell replication. In defence against disorders in the course of DNA biosynthesis, cells have developed a network of biochemical reactions that can be described as a response to replicative stress. Under conditions of replicative stress, the rate of DNA biosynthesis is decreased and the possibility of entering into mitosis is blocked until the expression of specific genes and activation of repair factors occurs. Ataxia telangiectasia mutated (ATM) and ataxia telangiectasia and RAD3-related (ATR) proteins share some phosphorylation targets, but their precise role

in the intra-S phase checkpoint pathway may differ depending on the nature of stress involved [17]. The action of ATR/ATM kinases induces cascade signal transmission to effector proteins (e.g. checkpoint kinase 1/2 (CHK1/CHK2)). Both biochemical pathways function according to the following event patterns: DNA breaks–ATM–CHK2 and DNA breaks–ATR–replication block–CHK1.

In each of these pathways, the target substrate is CDC25 phosphatase. ATR also activates Dbp4-dependent kinases (DDK). The other checkpoint protein, WEE1 kinase, also keeps cyclin-dependent kinases (CDK) muted. Inactivation of CDK/DDK is pivotal for the inhibition of origin firings under replication stress [18]. WEE1, which belongs to the large Ser/Thr family of protein kinases, is known as one of the most essential molecules in executing cell cycle arrest at the G2/M checkpoint, which is pivotal for premitotic DNA repair [19]. WEE1 kinase coordinates the initiation of mitosis by antagonistic regulation of Cdk1/Cdk2. In a comparable manner to ATR and CHK1, it operates during regular undisturbed cell division and is involved in the preservation of genome integrity [20].

Cyclin A-Cdk1 and cyclin B-Cdk1 complexes play a major role in the regulation of mitosis. They are inactive until the late G2 phase, due to two separate processes: inactivation of Cdk1 kinase and inhibition of its activators—Cdc25A, Cdc25B and Cdc25C phosphatases. The WEE1 kinase family—nuclear (WEE1) and membrane (Myt1)—are responsible for inhibiting Cdk1 activity. WEE1 and Myt1 start to work when the cell goes from mitosis to the G1 phase of the new cycle. At this time, reduction of the new cyclin B-Cdk1 complex is required for cyclin B degradation [21]. In addition, their activity may be increased in the case of DNA damage and expression of CHK1 and CHK2 kinases, which phosphorylate a specific WEE1 serine (Ser642) and induce attachment of 14-3-3 protein [22]. Autophosphorylation of WEE1 proteins is also possible, which contributes to their positive regulation (Fig. 1). To allow mitosis to occur, WEE1 is phosphorylated by Polo-like Kinase 1 (PLK1), which triggers WEE1 degradation [23].

Cancer cells, due to mutations in the p53/pRb pathway, frequently exhibit a deficient G1-arrest and mostly depend on G2-arrest [24]. WEE1 inhibitors appear to have potential high efficiency in p53-deficient ovarian cancers, generating a condition of synthetic lethality among p53 mutant tumors. Inhibition of WEE1 has demonstrated its effectiveness in DNA damage as a consequence of unregulated replication and strengthened the effectiveness of DNA-damaging agents [25]. Until now, only one (the most potent and selective) WEE1 inhibitor (Adavosertib, also under the names AZD1775 and MK1775) was found to be useful in clinical trials (in both phases I and II). WEE1i is able to stimulate origin

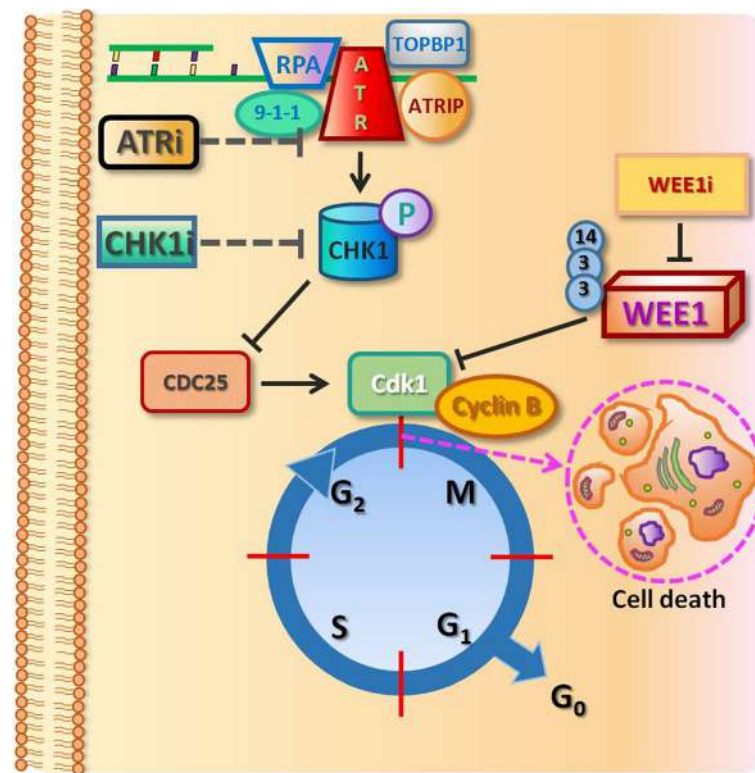


Fig. 1 Participation of WEE1 kinases (Cdk1 inhibitors) and CDC25 phosphatases (Cdk1 activators) in the regulation of the activity of Cdk1 kinase during G₂ and M phases. The binding of WEE1 kinases to 14-3-3 protein, which activates WEE1 kinases, may be carried out in two different ways—via the phosphorylation of ser642 (with participation of CHK1) or autophosphorylation. WEE1 inhibitor abrogates the G₂/M checkpoint, resulting in cancer cell death

firing, with dynamics of action comparable to ATR and CHK1 inhibitors. However, the mechanism of its action is not fully understood and requires a more detailed investigation [26]. MK1775 increased the cytotoxicity of numerous DNA-damaging drugs (such as antimetabolites, topoisomerase inhibitors and DNA crosslinking agents) towards various cancer cells. WEE1i was highly effective in p53-deficient cells and cells with defects in DNA damage repair pathways [27]. MK1775 was also combined with carboplatin treatment and paclitaxel in platinum-sensitive recurrent ovarian cancer [25]. The first report to present clinical evidence of MK1775 enhancing the efficacy of carboplatin in TP53-mutated tumors was published by Leijen et al. in 2016, NCT01164995 [28]. It was shown that it was active in a wide variety of human tumor xenografts, including models of ovarian cancer, with limited single-agent clinical activity [29].

ATR participates in the response to single-stranded (ssDNA) and double-stranded DNA breaks (DSBs) and to a variety of DNA lesions that interfere with replication [30]. ATR promotes cell cycle arrest and repair of DNA or induces apoptosis if the repair systems are overwhelmed. As a consequence, CHK1 is

activated. Proteins that are part of the DNA damage response (DDR) pathway are phosphorylated, including histone H2AX, breast cancer type 1/2 susceptibility protein (BRCA1/2), RAD51 and p53. In addition, inactivation of p53 leads to loss of activity of the G₁ checkpoint, which favours G₁–S transition [31]. Previous studies have shown that chemotherapeutics such as cladribine induce ATR-dependent phosphorylation of H2AX, a biomarker for DNA double-strand breaks, and the p53 suppressor protein [32, 33]. In response to DNA damage, ATR phosphorylates CHK1 protein, which in turn mediates CDC25A-C phosphorylation, leading to the blocking of CDK1 and CDK2 (thus preventing cell cycle progression). CHK1 can stabilize the replisome, possibly by targeting replication proteins (e.g. CDC6, minichromosome maintenance proteins 2–7 (MCM2-7)), and after resolving the replication problems can restart stalled replication forks. Functional changeability of the ATM/ATR–CHK2/CHK1–CDC25/CDK axis underlies the molecular foundation of the intra-S-phase checkpoint [34].

In response to replication stress, replication protein A (RPA) is the first to be loaded onto the unstable single stranded DNA (ssDNA), and the long stretches of RPA-

coated ssDNA adjacent to the double-stranded DNA (dsDNA) act as a platform to trigger the ATR/CHK1 [35]. ATR combines with ATR-interacting protein (ATRIP), and their complexes are located in the cell nucleus at the sites of DNA damage [36]. The RAD9–RAD1–hUS1 (9-1-1 complex) is required for the recruitment of DNA topoisomerase 2-binding protein 1 (TopBP1) [37]. The activators of ATR–ATRIP complexes are the TopBP1 and two other factors: replication factor C (RFC) and proliferating cell nuclear antigen (PCNA). During replication, RFC recognizes the sites of primer junctions of RNA with template DNA and assembles around them a toroidal protein homotrimer, PCNA, commonly named as sliding clamp, which determines the movement of DNA polymerases associated with it [38]. The first stage of the signaling pathway is the placement of cell cycle checkpoint protein Rad17 and ATR–ATRIP complexes in the damaged sections; the second is Rad17-dependent assembly of PCNA-type complexes around the DNA. The PCNA-type complexes support the activation of ATR molecules and, consequently, the phosphorylation of its substrates located within the chromatin, such as Rad17 and Rad9 [39]. When DNA errors and damage which are caused during the genetic material replication are not removed in time, the stalled replication forks are susceptible to fork collapse, leading to highly lethal DSBs (Fig. 2).

The disappearance of the function of the internal phase S control point, caused for example by the mutation of ATR, means that cells with damaged genetic material are blocked and are unable to enter mitosis despite the occurrence of non-replicated sections. Induction of DNA damage and activation of cellular responses, i.e. cascades of DNA damage signalling pathways, by a number of anticancer drugs result in cell cycle arrest at the G1/S and G2/M phases. When the amount of DNA damage is too high to allow the cell to survive, it is most often redirected to apoptosis [40]. Hence, DNA repair has emerged as a new area for anticancer drug development [41]. Numerous drugs are currently being tested in clinical trials; some of them are presented in Table 1. Most HGSOs have mutations in TP53 and other genetic alterations associated with increased replication stress. Inhibitors of ATR and CHK1 are therefore promising drugs for ovarian cancer treatment.

DNA repair checkpoint inhibitors

PARP

Inhibition of a DNA repair pathway sensitizes tumor cells with the BRCA 1/2 mutation to the DNA-damaging results of other chemotherapeutics. Given this, patients with BRCA^{mut} can respond more effectively to chemotherapy [8]. Therefore, the analysis of BRCA mutational status is crucial for therapeutic decisions [9]. An

enhanced risk of ovarian cancer is related to DNA damage. Poly (ADP-ribose) polymerase (PARP) repairs ssDNA breaks. When these breaks are not repaired efficiently, which is the situation when PARP is blocked by the inhibitor, DSBs occur. DSBs are mainly repaired through two pathways: the HR pathway and the non-homologous end joining (NHEJ) pathway, although other mechanisms also exist. BRCA1 and BRCA2 participate in the DNA damage response, the network of interacting pathways that is essential for repair of genetic material. Both proteins are involved in the error-free repair of DSBs by HR in the S phase. BRCA1 signals DNA damage and ensures cell cycle regulation, while BRCA2 interacts and facilitates the loading and formation of RAD51 filaments on the damaged DNA strand. Tumors with impaired HR pathways lack an alternative DNA repair pathway [42, 43]. Mutation in BRCA1 or BRCA2 in HR-deficient cancer cells will lead to the repair of DSBs via error-prone repair pathways, accumulation of mutations and eventually cell death [44].

Ovarian cancer cell lines with BRCA1 mutated and impaired HR (UWB1.289, SNU-251, OVCAR8) exhibit higher sensitivity towards PARPi, when compared with cells with wild-type or restored BRCA1 (SKOV3, A2780PAR and A2780CR) [45]. One group of compounds that have drawn intense research interest are PARPi inhibitors. In BRCA mutated cancer cells, PARP inhibition leads to tumor cell death, as a result of synthetic lethality. According to this assumption, PARPi blocks the base excision repair (BER) through F-Box DNA helicase 1 (Fbh1)-dependent Rad51 regulation [46]. Combination of olaparib with anticancer agents that disrupt HR repair represents an effective strategy to sensitize ovarian cancer cells. Synthetic lethality was defined classically in 1946 to describe a functional gene–gene relationship in *Drosophila*, in which two genes are nonlethal (viable) when inactivated alone but become lethal when inactivated together. Synthetic lethality is a consequence of the tendency of organisms to maintain buffering schemes that allow phenotypic stability despite genetic variation [47, 48]. Another mechanism of PARPi action involves PARPi binding to and trapping the PARP1 enzyme on chromatin (Fig. 3). Talazoparib, a PARPi, enhances trapping of PARP1 in DSBs, leading to decreased NHEJ and leukemia cell death [49, 50]. This agent is currently under clinical evaluation in patients with deleterious BRCA 1/2 mutation-associated ovarian cancer who have had prior PARP inhibitor treatment (NCT02326844). Moreover, DSBs can be resected by the microhomology-mediated end joining (MMEJ) pathway (also known as alternative non-homologous end-joining, Alt-NHEJ). MMEJ is independent from classical NHEJ and does not rely on NHEJ core factors such as Ku protein, DNA-dependent protein kinase (DNA-PK), or

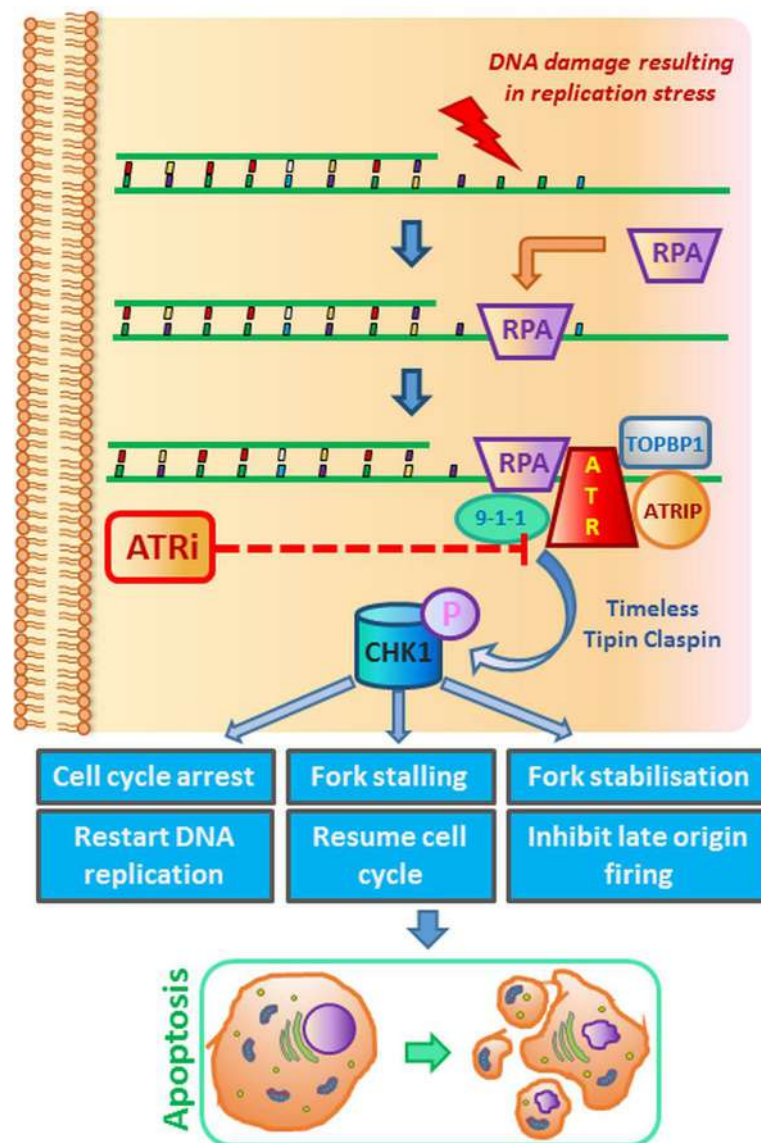


Fig. 2 DNA damage and replication checkpoints. Anticancer drugs induce replication disorders. Replication stress is the effect of the slowing or stalling of replication fork progression. DNA synthesis inhibition or damage induces checkpoint responses controlled by the ATR-CHK1 pathway. DNA lesions delay entry to S-phase (G1 checkpoint), slow the replication of damaged DNA or prevent entry to mitosis (G2 checkpoint). Given that both PARP and checkpoint proteins prevent fork collapse, their corresponding inhibitors may increase the level of replication stress, genome instability and, in consequence, cell death

ligase IV. DNA polymerase θ (POLQ) plays an important role in this pathway. Efficient recruitment of POLQ depends on PARP1 [51, 52].

The first Food and Drug Administration (FDA)-approved PARP inhibitor was olaparib (Lynparza). In 2005, the first two publications demonstrating the substantial sensitivity of BRCA-deficient cell lines to inhibition of PARP led to an unprecedented and swift implementation of PARP inhibitors in clinical practice [53]. Several PARP inhibitors, including olaparib, niraparib, veliparib, rucaparib and talazoparib, are being tested in clinical

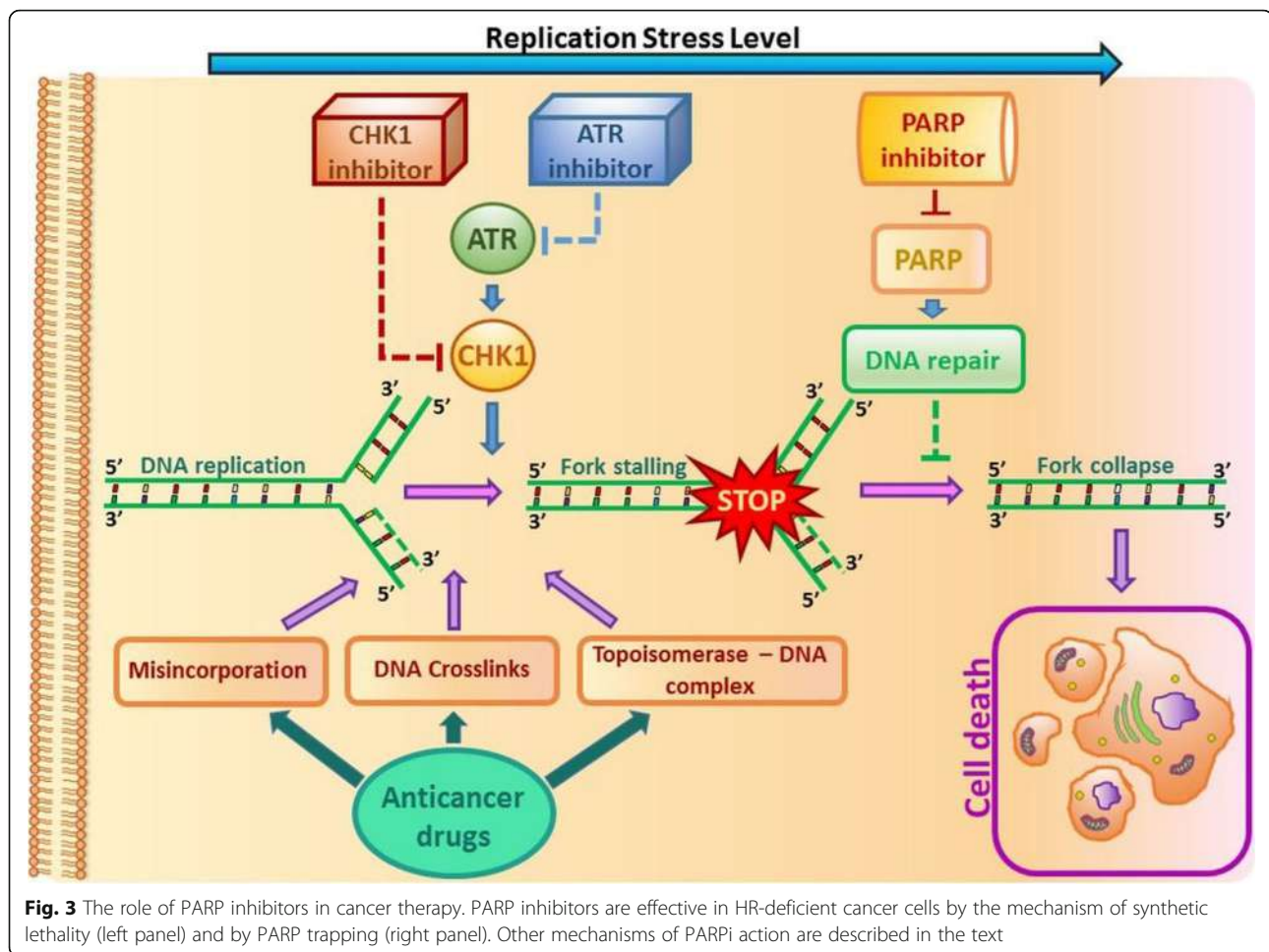
trials, and olaparib, niraparib and rucaparib (NCT03522246) have been registered for use in a clinical setting. In 2014, olaparib gained European Medicines Agency (EMA) approval to treat advanced EOC in monotherapy of patients with germline BRCA^{mut} who had received and did not respond to at least three lines of chemotherapy [54]. A phase II clinical trial revealed that olaparib significantly increased the effectiveness of standard treatment with a combination of carboplatin and paclitaxel. Progression-free survival was longer by around 3 months in the olaparib with chemotherapy

Table 1 Clinical trials with chemotherapeutic agents causing replication stress used in ovarian cancer treatment. [clinicaltrials.gov] *not applicable

Target	Name of drug/ drugs	Objective of trial	Clinical trial phase	Clinical trial identifier
PARP	BMN 673 (talazoparib)	Patients with deleterious BRCA 1/2 mutation-associated ovarian cancer who have had prior PARP inhibitor treatment	2	NCT02326844
PARP	BSI-201 (iniparib) Carboplatin/ gemcitabine	Patients with platinum-resistant recurrent ovarian cancer	2	NCT01033292
PARP	AZD2281 (olaparib)	Study to assess the efficacy and safety of a PARP inhibitor for the treatment of BRCA-positive advanced ovarian cancer	2	NCT00494442
PARP	Cediranib Olaparib	Patients with ovarian cancer whose cancer worsened despite previously receiving a PARP inhibitor (such as olaparib)	*	NCT02681237
PARP	Rucaparib Nivolumab	Treatment following response to frontline treatment in newly diagnosed ovarian cancer patient	3	NCT03522246
ATR PARP	AZD6738 Olaparib	ATARI trial test: ATR inhibitor drug AZD6738 and a PARP inhibitor drug olaparib in patients with relapsed gynaecological cancers with an abnormality in ARID1A gene	2	NCT04065269
WEE1	MK-1775 Carboplatin	Patients with p53 mutated epithelial ovarian cancer that have been treated with first line treatment (paclitaxel-carboplatin combination therapy) and that have shown early relapse (within 3 months)	2	NCT01164995
ATR PARP	AZD6738 Olaparib	Combination ATR and PARP inhibitor (CAPRI) trial with AZD 6738 and olaparib in recurrent ovarian cancer	2	NCT03462342
ATR	AZD6738 Paclitaxel	Refractory cancer patients who have failed to standard-of-care chemotherapy	1	NCT02630199
ATR	M6620 Avelumab Carboplatin	In participants with PARP-resistant, recurrent, platinum-sensitive ovarian, primary peritoneal or fallopian tube cancer	2	NCT03704467
ATR	M6620 Gemcitabine	Patients with recurrent ovarian, primary peritoneal or fallopian tube cancer	2	NCT02595892
ATR	M6620 Topotecan	In small cell cancers and extrapulmonary small cell cancers	2	NCT02487095
ATR	M6620 Carboplatin, gemcitabine	Adult women with platinum-sensitive, recurrent high-grade serous or high-grade endometrioid ovarian, primary peritoneal or fallopian tube cancer	2	NCT02627443
ATR	M6620 Avelumab Nedisertib	DDR-deficient metastatic or unresectable solid tumors	1	NCT04266912
ATR	M6620 Carboplatin Gemcitabine	Patients with recurrent and metastatic ovarian, primary peritoneal or fallopian tube cancer	2	NCT02627443
ATR	BAY 1895344	Patients with advanced solid tumors and lymphomas	1	NCT03188965
ATR PARP	BAY 1895344 Niraparib	Advanced solid tumors and ovarian cancer	1	NCT04267939
ATR	VX-803 (M4344)	Women with recurrent ovarian cancer that has progressed while on a PARP inhibitor	1	NCT02278250

Table 1 Clinical trials with chemotherapeutic agents causing replication stress used in ovarian cancer treatment: [clinicaltrials.gov] *not applicable (Continued)

Target	Name of drug/ drugs	Objective of trial	Clinical trial phase	Clinical trial identifier
ATR PARP	VX-803 (M4344) Niraparib	Women with recurrent ovarian cancer that has progressed while on a PARP inhibitor	1	NCT04149145
ATR PARP	AZD 6738 Olaparib	HR-deficient patients with/without additional mutations in ATM, CHK-2, MRN (MRE11/NBS1/RAD50), CDKN2A/B and APOBEC	2	NCT02576444
CHK1 PARP	Prexasertib (LY2606368) Olaparib	Solid tumors	1	NCT03057145
CHK1	Prexasertib (LY2606368)	BRCA1/2 mutation-associated breast or ovarian cancer, triple negative breast cancer and HGSOc	2	NCT02203513
CHK1	Prexasertib (LY2606368)	Patients with platinum-resistant or refractory ovarian cancer	2	NCT03414047



group compared with chemotherapy alone. In the USA in 2018, the FDA-approved olaparib for the maintenance treatment of patients with BRCA^{mut} advanced EOC who are in complete or partial response to first-line platinum-based chemotherapy [55]. Two more PARP inhibitors, rucaparib (Rubraca) and niraparib (Zejula), approved by the FDA, are a promising class of agents for targeted EOC therapy [56]. Research is ongoing into the use of iniparib in combination with carboplatin and gemcitabine in the treatment of patients with platinum-resistant recurrent ovarian cancer (NCT01033292). PARP inhibitors are usually combined with other drugs to increase the therapeutic effect. A combination of two investigational drugs, cediranib and olaparib, was evaluated in patients with ovarian cancer whose cancer worsened despite previously receiving a PARP inhibitor such as olaparib (NCT02681237).

Clinical trials have shown PARPi response rates of around 40% in women who carry a mutation in the BRCA1/2 genes (NCT00494442). However, PARPi is responsible for tumor suppression, but not for complete tumor regression [57]. Although olaparib is a step

forward in the treatment of BRCA1/2-deficient tumors, resistance to PARP inhibitors is unfortunately a common phenomenon. Rare complete responses are seen with PARPi monotherapy in clinical practice [58]. BRCA1/2-deficient tumor cells can become resistant to PARP inhibitors by restoring HR repair and/or by stabilizing replication forks. PARPi-induced drug resistance mechanisms have focused also on heat shock protein 90 (HSP90)-mediated stabilization of BRCA1^{mut}, RAD51 upregulation, loss of REV7 or promotion of alternative error-prone NHEJ DNA repair [59, 60]. Furthermore, a BRCA2-mutated ovarian cancer cell line, with sensitivity to both platinum and PARPi, regained the BRCA2 function by secondary mutation after treatment with cisplatin and PARPi [61]. In addition, an acquired low level of expression of PARP1 may be a cause of resistance to PARPi in patient-derived tumor xenograft models [62]. Moreover, as a result of PARP1 inhibition, cancer cells may upregulate the HR repair pathway and increase RAD51 expression to maintain cell viability [63]. The formation of RAD51 foci was observed together with PARPi resistance in patient-derived xenograft models, as

well as patient-derived samples carrying the BRCA^{mut} [64]. On the other hand, increased expression of the ATP-binding cassette sub-family B member 1 (ABCB1) (also known as multidrug resistance protein 1 [MDR1]), which encodes the membrane drug transporter P-glycoprotein, is a well-described mechanism of resistance to doxorubicin, paclitaxel and related taxane drugs. ABCB1-mediated resistance to PARPi is a novel finding in ovarian cancer [65]. Nonetheless, loss of BRCA1/2 factors determines PARPi sensitivity. MiR-493-5p may induce platinum and PARPi resistance, specifically in the cells with BRCA2 mutation [66]. Hence, there is an urgent need to develop new, more effective strategies.

All drugs, including olaparib, have potential side effects. Most side effects of olaparib were of low grade, with anaemia and neutropenia being the most common, in the SOLO1 trial [67]. On the other hand, cardiac adverse effects are the leading cause of discontinuation of clinical trials and withdrawal of drugs from the market. There are reports suggesting that olaparib is a cardioprotective agent against doxorubicin-induced cardiomyopathy [68] and that it protects cardiomyocytes against oxidative stress [69].

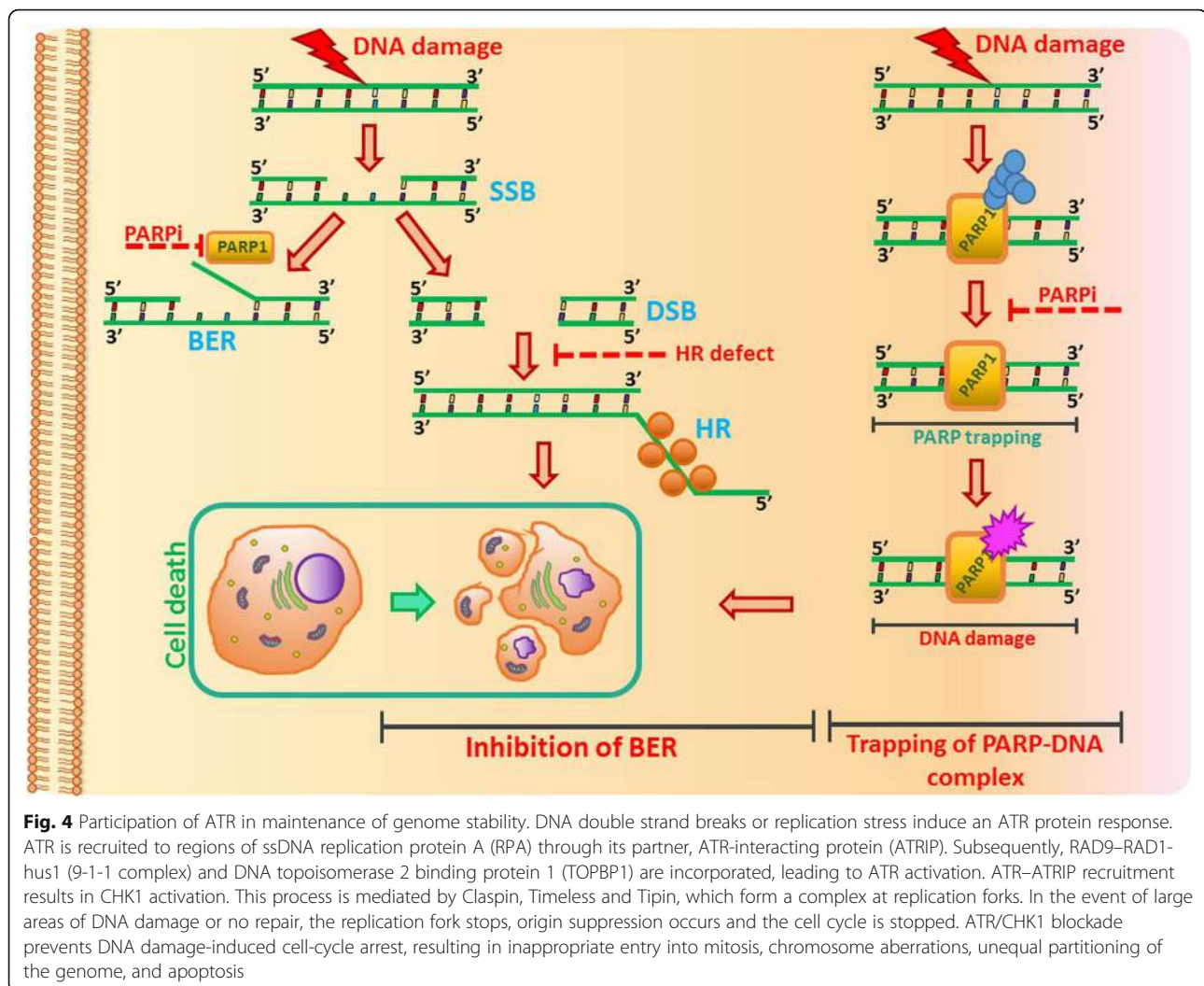
ATR

ATM and ATR kinases are two master regulators of DNA damage responses. ATR, a serine/threonine-protein kinase belonging to the phosphatidylinositol 3-kinase-related kinase (PIKK) family of proteins, is a key regulator of the DNA replication stress response (RSR) and DNA-damage activated checkpoints [70]. As ATR is a master regulator of the DDR, this finding underscores the relevance of DDR as a new therapeutic target in ovarian cancer therapy. ATR is activated in response to a broad spectrum of DNA damage, such as single- and double-stranded DNA, and also adducts, cross-links and inhibits DNA polymerase, while ATM is primarily activated in response to DNA double-strand breaks [71–73]. Moreover, ATM is responsible for the phosphorylation of checkpoint kinase 2 (CHK2) and ATR phosphorylates checkpoint kinase 1 (CHK1) [74]. CHK1 activation is mediated by Claspin (CLSPN), Timeless and Tipin [75]. The ATR lies upstream of CHK1 and phosphorylates numerous factors including Werner syndrome ATP-dependent helicase (WRN), SWI/SNF-related matrix-associated actin-dependent regulator of chromatin sub-family A-like protein 1 (SMARCA1), and Fanconi anaemia complementation group I (FANCI), which may help preserve replication fork stability and control cell-cycle progression [76–78]. The direct substrates of ATR include RPA, MCM2, p53 and many other factors that play roles in replication fork progression, DNA repair and control of the cell cycle

[79, 80]. Additionally, ATR substrates control protein modification, transcriptional regulation and developmental processes [81]. ATR has a crucial role in stabilizing genomic integrity throughout the cell cycle and is therefore essential for cell survival [82] (Fig. 4). ATR controls cell cycle arrest from S to G2 phases [83]. Furthermore, ATR plays a role in the G2/M phase checkpoint [84]. In cells with TP53 mutation, it leads to checkpoint-defective cells, and the inhibition of ATR is lethal [85, 86]. Dysregulation of ATR disrupts a broad range of cellular processes [16]. Recent reports suggest that cells with impaired HR activities due to mutations in TP53 gene or specific DNA repair proteins are specifically sensitive to ATR inhibitors [86–89]. However, the underlying mechanisms of ATR inhibition monotherapy on ATM status remain unclear [84].

ATR inhibitors have the potential to show preferential cell killing of tumor cells where ATM is defective or where replicative stress is high. In recent years, ATR inhibitors with far greater potency and selectivity have been developed as drug-like agents. Many ATR inhibitors, such as NU6027, ETP-46464 and VX-970, also inhibit CDK2, mTOR, ATM and PIK3 kinases [90, 91]. VX-970/M6620 is an analogue of VE-821 from the aminopyrazine series with a marked increase in ATR enzyme cytotoxicity ($IC_{50} = 0.019 \mu\text{M}$) in HCT116 cells. VX-970 is selective versus DNA-PK, mTOR, PI3K γ and 50 unrelated protein kinases [92]. One of the most promising is AZD6738, which is a potent and selective sulfoximine morpholinopyrimidine ATR inhibitor.

AZD6738 is currently used as a monotherapy and in combination with gemcitabine (NCT02595892), gemcitabine and carboplatin (NCT02627443), avelumab and nedisertib (NCT04266912), paclitaxel (NCT02630199) and radiotherapy (NCT02223923). VE-821, another identified ATR inhibitor, sensitized OVCAR-8, SKOV-3 and PEO1 ovarian cancer cell lines to cisplatin, topotecan and veliparib [93, 94]. Additionally, cisplatin or topotecan, combined with MK-877 (CHK1i) or VE-821, reduced the G2/M phase accumulations [94]. Currently, clinical trials are ongoing on M6620 in combination with gemcitabine, avelumab (NCT03704467), topotecan (NCT02487095) and carboplatin (NCT02627443) in ovarian cancer. On the other hand, VX-970 is the most effective in combination with platinum agents or melphalan [95]. BAY 1895344 is a new potent ATR inhibitor developed by Bayer. BAY 1895344 is being studied in cancers with DNA repair deficiency. The in vivo antitumor efficacy of BAY 1895344 in combination with carboplatin was investigated in the IGROV-1 ovarian cancer model [96]. BAY 1895344 is currently under clinical investigation in patients with advanced solid tumors and lymphomas (NCT03188965). VX-803 (M4344), on



the other hand, is now in clinical trials as a monotherapy or in combination with carboplatin for advanced solid tumors (NCT02278250), and in combination with niraparib against ovarian cancer (NCT04149145).

CHK1

CHK1 is a serine/threonine kinase, which responds to DNA damage and replication stress and therefore regulates mitotic progression. ATR and CHK1 share the same pathway; it is possible that the antitumor properties of ATR inhibitors may not differ significantly from those of CHK1 inhibitors currently tested in clinical trials. Moreover, ATR controls many other proteins, not only CHK1, as described in the previous section, suggesting that it is responsible for controlling additional cell responses. Nonetheless, CHK1 can be autophosphorylated and thus activated, independently of ATR [97].

Activation of CHK1 and its downstream effectors leads to an array of coordinated activities that include reduced

new origin firing, delay of cell cycle progression and restoration of the stalled replication forks. The phosphorylation of CHK1 at Ser317 and Ser345 after checkpoint signaling is regulated by ATR, and thus, phosphorylation at Ser345 fosters relocalization or retention of the protein in the nucleus [98]. Translocation of the protein from the cytoplasm to the nucleus causes the activation of the G2/M checkpoint and regulates cell cycle progression [99] by inactivating CDC25 phosphatases (CDC25A and CDC25C), which would otherwise activate the CDKs, responsible for the G2/M transition [100]. Cancer cells with p53 mutation cannot activate the G1/S checkpoint and relies only on the S and G2/M checkpoints, both controlled by CHK1 [101]. This suggests that patients with p53-mutated tumors could benefit from the treatment based on CHK1 inhibition [102]. CHK1 also phosphorylates BRCA2 and RAD51 proteins [103]. Therefore, CHK1 inhibition renders the cells to be more sensitive to DNA damage [93]. As previously mentioned, CHK1 may also be autophosphorylated at Ser296 [104];

thus, once activated, it may restrain replication catastrophe in S-phase, even in the presence of an ATRi [97].

Several CHK1 inhibitors are known, including compounds in research phase I (AZD7762, PF-477736, GDC-0425 and GDC-0575) or in phase II (LY2603618 and LY2606368) of trials in combination with gemcitabine, irinotecan, pemetrexed and cytarabine [105, 106]. V158411 inhibited CHK1 and CHK2 and abolished DNA damage-induced S- and G2-phase checkpoints. The *in vitro* cytotoxicity of gemcitabine, cisplatin, SN38 and camptothecin was potentiated by V158411 in TP53-deficient, but not in TP53-proficient, human tumor cell lines [107]. Research has also been conducted on Prexasertib (LY2606368), which is a small ATP-competitive selective inhibitor of CHK1 and CHK2. Prexasertib blocks the autophosphorylation of and subsequently activates the CHK proteins, which regulate the activity of phase-M inducer cyclin-dependent kinases and phosphatases [108]. Prexasertib is currently in phase 1 and 2 clinical trials and was tested either as a single agent (NCT02203513, NCT03414047) or in combination with olaparib in 14 clinically annotated and molecularly characterized luciferized HGSOC patient-derived xenograft (PDX) models, and in a panel of ovarian cancer cell lines. The ability of prexasertib to impair HR repair and replication fork stability was assessed. Thirteen models were resistant to olaparib monotherapy, including four carrying a BRCA1 mutation [102]. Another example is MK-8776 (formerly, SCH900776, a pyrazolopyrimidine derivative), a highly selective CHK1 inhibitor [79]. MK-8776 is approximately 500 times more selective for CHK1 than for CHK2. MK-8776 and LY 2603618 sensitized cells only to gemcitabine [93, 94]. UCN-01, another CHK1 inhibitor, also exhibits a radiosensitivity effect; however, MK-8776 demonstrated more pronounced effects with lower cytotoxicity [80]. Even in the absence of DNA damage caused by external agents, CHK1/2 inhibition yielded DNA damage and mitotic catastrophe preclinically in tumors with DNA repair dysfunction [109]. Moreover, in cells lacking BRCA1, CHK1 is necessary for the repair of endogenous DNA damage; therefore, inhibition of this protein had an anti-proliferative effect on the cells [102]. Several potential mechanisms for sensitization by CHK1 inhibition have been proposed, including inhibition of repair systems for DSBs, spindle assembly checkpoint (SAC) activation, promotion of premature mitosis, and mitotic catastrophe (MC). However, it remains unclear how CHK1 inhibition triggers sensitization in ovarian cancer cells.

Synergy in cell killing based on ATR/CHK1 and PARP inhibitors

BRCA1/2 proteins play an important role in the protection of stalled replication forks. This is controlled

by the ATR/CHK1 checkpoint kinase pathway. Impaired ATM kinase function activates ATR. This system of mutual taking of functions in the cell has been used to fight cancer. By binding to reversed forks, the BRCA1/2 proteins play a critical role in protecting the cell from genomic instability. On the other hand, ATR/CHK1 blockade prevents DNA damage-induced cell-cycle arrest, resulting in inappropriate entry into mitosis, chromosome aberrations, unequal partitioning of the genome, and apoptosis [93]. The ATR/CHK1 pathway stabilizes replication forks and prevents their collapse into DNA double-strand breaks. Thus, inhibition of ATR/CHK1 is expected to increase reliance on HR to reorganize the replication fork structure and complete replication. ATR inhibition is lethal with numerous cancer-associated changes, including oncogenic stress (oncogenic RAS mutations, MYC and G1/S-specific cyclin-E1 (CCNE1) overexpression), deficiencies in DNA repair (TP53, BRCA1/2, partner and localizer of BRCA2 (PALB2) and ATM loss) and other defects [110]. Several studies have shown that some tumors are even more sensitive to combinations of ATR inhibitors with inhibitors of other repair proteins such as PARP and CHK1. Inhibiting these proteins alone may be insufficient to cause cell death, so it may be necessary to apply PARPi and cell cycle checkpoint inhibitors as combination therapies [57].

Clinical trials are currently underway using the combination of AZD6738 and olaparib in recurrent ovarian cancer (NCT03462342) and in gynaecological cancers with ARID1A loss or no loss (NCT04065269). An extensive signal-searching study is being conducted. HR-deficient patients with/without additional mutations in ATM, CHK-2, MRN (MRE11/NBS1/RAD50), CDKN2A/B and APOBEC will be treated with olaparib or olaparib and AZD6738 (NCT02576444). Moreover, patients with advanced solid tumors and ovarian cancer will be treated with BAY1895344 in combination with niraparib (NCT04267939). The investigators are combining LY2606368 (CHK1i) with olaparib (NCT03057145) in patients with solid tumors. Moreover, NU6027 (CHK1i) in combination with a PARP inhibitor was shown to attenuate G2/M arrest and was synthetically lethal in the MCF7 cell line [87].

New platforms for optimizing ovarian cancer therapy under replication stress

New models for preclinical ovarian cancer have been sought for a long time. The resolve to achieve this was strengthened with the decision by the National Cancer Institute (NCI) to retire the NCI-60, a panel of 60 human cancer cell lines grown in culture, from its drug screening programme [111]. Cell lines and cell-line-

derived xenografts (CDXs) are still the most commonly used basic research models in ovarian cancer. Recently, scientific interest has increasingly focused on the cancer microenvironment. Given this, preclinical modelling of individual cancers should be included in the framework of personalized medicine. Currently, attention is focused on promising new research models including patient-derived xenografts (PDX) and organoids.

PDX maintain the characteristics of the patient's original tumor, including histology, mutational status and gene expression, through multiple passages in mice. PDX also exhibit a similar response to standard chemotherapy to that demonstrated in the patient. They are a copy of the xenograft model in which fresh tumor tissue is obtained directly from patients and implanted into an immunodeficient mice lacking a human immune system [57]. Different types of mice (e.g. NCG, NOD-Prkdc^{em26Cd52} IL2rg^{em26Cd22}/Gp t; NSG, NOD-SCID IL2Rγ^{-/-}) have been used in PDX models of ovarian cancer. Olaparib, MK8776 or AZD6738 were used to treat ovarian tumors with BRCA2^{mut} obtained with PDX [112]. Moreover, PDX has been applied to study the olaparib response predicted on the basis of HR gene analysis. The homogenate was injected subcutaneously into the lower dorsal flank or axilla of the NCG mice and DDR mutation analysis of PDX cases was carried out [113]. A PDX model (NSG mice) was also derived from BRCA-mutant HGSOCs exhibiting solid, pseudoendometrioid and transitional cell carcinomas. It exhibited higher levels of phosphorylated CHK1 than BRCA-intact HGSOC. Using PET imaging, studies have shown that PARP inhibitor treatment results in tumor suppression but not complete tumor regression, similar to the response observed in clinical settings [57]. The response of 12 HGSOCs (PDX; NSG mice) to the PARPi rucaparib was measured, with dose-dependent responses observed in chemo-naïve BRCA1/2-mutated PDX and no responses in PDX lacking DNA repair pathway defects. Among BRCA1-methylated PDX, silencing of all BRCA1 copies predicted the rucaparib response, whereas heterozygous methylation was correlated with resistance (ARIEL2 part 1 trial) [114].

Until now, PDX models could only be established in immunocompromised mouse strains. Currently, to assess immunotherapy, research is being carried out on PDX to which autologous transfer of patient-specific tumor infiltrating lymphocytes (TILs) has been performed [115].

Another approach in personalized medicine involves organoid cultures of patient-derived tumors. These are three-dimensional (3D) constructs that represent an excellent preclinical model for human tumors that has cancer homology and has been gradually applied to gene analysis, drug screening and other types of research; they facilitate

the translation from basic cancer research to clinical practice [116]. Researchers have also begun to apply organoids in studies of ovarian cancer. Several teams have confirmed that patient-derived organoids closely resemble the original gynecologic tumors, and thereby may serve as a promising resource for preclinical studies [117, 118]. Hans Clevers' team collected 56 organoids from 32 patients, representing all the main subtypes of OC, and confirmed that homologous recombinant (HR) defective cells are sensitive to PARP inhibitors, which are also present in the ovarian cancer organoid [117]. Another team developed a HGSOC organoid and used it for functional analysis of DNA repair and prediction of patients' clinical response to DNA repair inhibitors [118]. By studying the HR and cross-protection defects of 33 HGS-like organoids in 22 patients, it was confirmed that the functional defects of HR in the organoid are related to the sensitivity of PARP inhibitors regardless of the mutation status of DNA repair genes. In addition, the functional defects in cross-protection of replication are related to the sensitivity to carboplatin, CHK1, and ATR inhibitors. These findings indicate that genome analysis and organ-like function testing can identify targeted DNA damage and repair defects. The OC organoid can be used for DNA repair analysis and therapeutic sensitivity testing, which can immediately evaluate target defects in maternal tumors and provide appropriate treatment options [118].

Western blot analysis of 33 organoid cultures showed that prexasertib increases DNA damage, indicated by increased expression of γH2AX, and increased replication stress, as indicated by increased phosphorylated RPA (pRPA). Prexasertib activates the ATR pathway in both fork-unstable and fork-stable lines, as shown by the increased phosphorylation of the ATR targets KAP1 (pKAP1) and CHK1 (pCHK1) [119]. The elevated pCHK1 level is a pharmacodynamic marker of CHK1 inhibition by prexasertib. Prexasertib stimulates a tumor in terms of sensitivity to other DNA repair agents, blocking the ATR/CHK1 pathway, thereby increasing replication stress [120]. In addition, other factors that increase replication stress may interact with prexasertib and promote fork instability and cancer cell death. For example, regardless of the genetic status, a stalled fork protection defect was present in 61% of the organoid lines tested, and this defect was associated with carboplatin, prexasertib, and VE-822 sensitivity. In contrast, only 6% of organoid lines tested had a functional HR defect and PARPi sensitivity. Overall, this suggests that stalled fork protection defects are more common than HR defects and have a larger array of specific therapies [118].

Conclusions

The first generation of ATR and CHK1 inhibitors has been shown to sensitize ovarian tumors to DNA-

damaging agents that primarily induce replicative stress as their mechanism of action. The analysis of BRCA mutational status is still the first step in designing individualized strategies for the management of patients with ovarian cancer. Inhibition of ATR or CHK1 as a monotherapy or in combination with DNA-damaging chemotherapy drugs or PARP inhibitors is being tested in early-phase clinical trials in gynaecological cancers. ATR inhibitors, such as M6620 and AZD6738, give a very good prognosis. Phase 2 combination trials are ongoing. In turn, two of the best studied CHK1 inhibitors are MK-8776 and prexasertib. Preclinical observations indicate that the synthetic lethality of ATR or CHK1 inhibitors in ATM-deficient cancers may be a new opportunity for effective ovarian cancer therapy.

We also need to understand the long-term tolerability of the various PARP inhibitors and the mechanisms leading to the development of multidrug resistance. Moreover, mutations and damage in ATM or p53 genes are therapeutic opportunities for inhibitors involved in replication stress. Despite learning about a dozen or so genes that lead to synthetic lethality with PARP, new ones are still being sought. The development of new in vivo model systems such as PDX and organoids will facilitate the optimization of ovarian cancer therapy. Clustered regularly interspaced short palindromic repeats (CRISPR)-directed Cas9-mediated endonuclease activity disrupts specific genetic sequences in the genome and is a new tool for finding therapeutic goals. In this way, the sequence of C12orf5 was identified, which is a gene that encodes a metabolic regulator, TP53-induced glycolysis and apoptosis regulator (TIGAR). Downregulation of TIGAR results in enhanced cytotoxic effects of olaparib [121]. Only further deepening of the knowledge about genes involved in DNA repair and blocking all restoration options in the pathway can lead to definitive ovarian cancer cell death.

Abbreviations

ABC1: ATP-binding cassette sub-family B member 1; ATM: Ataxia telangiectasia mutated protein; ATR: Ataxia telangiectasia and Rad3-related protein; ATRIP: ATR-interacting protein; BER: Base excision repair; BRCA: Breast cancer gene; CDK: Cyclin-dependent kinases; CHK1: Checkpoint kinase 1; DDR: DNA damage response; DNA-PK: DNA-dependent protein kinase; EOC: Epithelial ovarian cancer; HGSOCs: High-grade serous ovarian carcinomas; HR: Homologous recombination; MMEJ: Microhomology-mediated end joining; NHEJ: Non-homologous end joining; PARP: Poly (ADP-ribose) polymerase; PCNA: Proliferating cell nuclear antigen; PI3Ks: Phosphatidylinositol 3-kinase-related kinases; POLQ: DNA polymerase θ ; RPA: Replication protein A; RSR: Replication stress response; TopBP1: DNA topoisomerase 2-binding protein 1; WEE1: Tyrosine kinase

Acknowledgements

Not applicable.

Authors' contributions

PG, AG, AM and AR wrote this review, in order of contribution. All authors read and approved the final manuscript.

Funding

This research was funded by the Polish National Science Centre, project grant number: Sonata Bis 2019/34/E/NZ7/00056

Availability of data and materials

All data and materials supporting the conclusions of this study have been included within the article.

Ethics approval and consent to participate

Not applicable.

Consent for publication

Not applicable.

Competing interests

The authors declare that they have no competing interests.

Received: 10 December 2019 Accepted: 8 April 2020

Published online: 21 April 2020

References

- Momenivahed Z, Tiznobaik A, Taheri S, Salehiniya H. Ovarian cancer in the world: epidemiology and risk factors. *Int J Womens Health*. 2019;11:287–99.
- Budiana ING, Angelina M, Pemayun TGA. Ovarian cancer: pathogenesis and current recommendations for prophylactic surgery. *J Turk Ger Gynecol Assoc*. 2019;20(1):47–54.
- McGee J, Peart TM, Foley N, Bertrand M, Prefontaine M, Sugimoto A, et al. Direct genetics referral pathway for high-grade serous ovarian cancer patients: the "opt-out" process. *J Oncol*. 2019;2019:6029097.
- Siegel RL, Miller KD, Jemal A. Cancer statistics, 2019. *CA Cancer J Clin*. 2019; 69(1):7–34.
- Koshiyama M, Matsumura N, Konishi I. Recent concepts of ovarian carcinogenesis: type I and type II. *Biomol Res Int*. 2014;2014:934261.
- Cancer Genome Atlas Research N. Integrated genomic analyses of ovarian carcinoma. *Nature*. 2011;474(7353):609–15.
- Konstantinopoulos PA, Ceccaldi R, Shapiro GI, D'Andrea AD. Homologous recombination deficiency: exploiting the fundamental vulnerability of ovarian cancer. *Cancer Discov*. 2015;5(11):1137–54.
- Huang YW. Association of BRCA1/2 mutations with ovarian cancer prognosis: an updated meta-analysis. *Medicine (Baltimore)*. 2018;97(2):e9380.
- Gadducci A, Guarneri V, Peccatori FA, Ronzino G, Scandurra G, Zamagni C, et al. Current strategies for the targeted treatment of high-grade serous epithelial ovarian cancer and relevance of BRCA mutational status. *J Ovarian Res*. 2019;12(1):9.
- Dasari S, Tchounwou PB. Cisplatin in cancer therapy: molecular mechanisms of action. *Eur J Pharmacol*. 2014;740:364–78.
- Komiyama S, Nagashima M, Taniguchi T, Rikitake T, Morita M. Bevacizumab plus direct oral anticoagulant therapy in ovarian cancer patients with distal deep vein thrombosis. *Clin Drug Investig*. 2019.
- Park GB, Ko HS, Kim D. Sorafenib controls the epithelial-mesenchymal transition of ovarian cancer cells via EGF and the CD44HA signaling pathway in a cell type-dependent manner. *Mol Med Rep*. 2017;16(2):1826–36.
- DeVorkin L, Hattersley M, Kim P, Ries J, Spowart J, Anglesio MS, et al. Autophagy inhibition enhances sunitinib efficacy in clear cell ovarian carcinoma. *Mol Cancer Res*. 2017;15(3):250–8.
- Lokadasan R, James FV, Narayanan G, Prabhakaran PK. Targeted agents in epithelial ovarian cancer: review on emerging therapies and future developments. *Ecancermedscience*. 2016;10:626.
- Liu R, Guo H, Lu S. MiR-335-5p restores cisplatin sensitivity in ovarian cancer cells through targeting BCL2L2. *Cancer Med*. 2018;7(9):4598–609.
- Wang J, He J, Su F, Ding N, Hu W, Yao B, et al. Repression of ATR pathway by miR-185 enhances radiation-induced apoptosis and proliferation inhibition. *Cell Death Dis*. 2013;4:e699.
- Rybackek D. Hydroxyurea-induced replication stress causes poly (ADP-ribose) polymerase-2 accumulation and changes its intranuclear location in root meristems of *Vicia faba*. *J Plant Physiol*. 2016;198:89–102.
- Murai J. Targeting DNA repair and replication stress in the treatment of ovarian cancer. *Int J Clin Oncol*. 2017;22(4):619–28.

19. Beggs R, Yang ES. Targeting DNA repair in precision medicine. *Adv Protein Chem Struct Biol.* 2019;115:135–55.
20. Harrington KJ. Chemotherapy and targeted agents. *Maxillofacial Surgery.* 2017;339–54.
21. Potapova TA, Daum JR, Byrd KS, Gorbsky GJ. Fine tuning the cell cycle: activation of the Cdk1 inhibitory phosphorylation pathway during mitotic exit. *Mol Biol Cell.* 2009;20(6):1737–48.
22. Perry JA, Kornbluth S. Cdc25 and Wee1: analogous opposites? *Cell Div.* 2007;2:12.
23. Brandsma I, Fleuren EDG, Williamson CT, Lord CJ. Directing the use of DDR kinase inhibitors in cancer treatment. *Expert Opin Investig Drugs.* 2017; 26(12):1341–55.
24. Schmid BC, Oehler MK. New perspectives in ovarian cancer treatment. *Maturitas.* 2014;77(2):128–36.
25. Westin SN, Sood AK, Coleman RL. Targeted therapy and molecular genetics. *Clin Gynecol Oncol.* 2018;470–92.
26. Moiseeva TN, Qian C, Sugitani N, Osmanbeyoglu HU, Bakkenist CJ. WEE1 kinase inhibitor AZD1775 induces CDK1 kinase-dependent origin firing in unperturbed G1- and S-phase cells. *Proc Natl Acad Sci U S A.* 2019;116(48):23891–3.
27. Azenha D, Lopes MC, Martins TC. Claspin: from replication stress and DNA damage responses to cancer therapy. *Adv Protein Chem Struct Biol.* 2019; 115:203–46.
28. Leijen S, van Geel RM, Sonke GS, de Jong D, Rosenberg EH, Marchetti S, et al. Phase II study of WEE1 inhibitor AZD1775 plus carboplatin in patients with TP53-mutated ovarian cancer refractory or resistant to first-line therapy within 3 months. *J Clin Oncol.* 2016;34(36):4354–61.
29. Ivy SP, Kunos CA, Arnaldez FI, Kohn EC. Defining and targeting wild-type BRCA high-grade serous ovarian cancer: DNA repair and cell cycle checkpoints. *Expert Opin Investig Drugs.* 2019;28(9):771–85.
30. Marechal A, Zou L. DNA damage sensing by the ATM and ATR kinases. *Cold Spring Harb Perspect Biol.* 2013;5(9).
31. Roos WP, Kaina B. DNA damage-induced cell death: from specific DNA lesions to the DNA damage response and apoptosis. *Cancer Lett.* 2013; 332(2):237–48.
32. Sun XL, Jiang H, Han DX, Fu Y, Liu JB, Gao Y, et al. The activated DNA double-strand break repair pathway in cumulus cells from ageing patients may be used as a convincing predictor of poor outcomes after in vitro fertilization-embryo transfer treatment. *PLoS One.* 2018;13(9):e0204524.
33. Beyaert M, Starczewska E, Perez ACG, Vanlangendonck N, Saussoy P, Tilman G, et al. Reevaluation of ATR signaling in primary resting chronic lymphocytic leukemia cells: evidence for pro-survival or pro-apoptotic function. *Oncotarget.* 2017;8(34):56906–20.
34. Rybaczek D, Kowalewicz-Kulbat M. Premature chromosome condensation induced by caffeine, 2-aminopurine, staurosporine and sodium metavanadate in S-phase arrested HeLa cells is associated with a decrease in Chk1 phosphorylation, formation of phospho-H2AX and minor cytoskeletal rearrangements. *Histochem Cell Biol.* 2011;135(3):263–80.
35. Bian X, Lin W. Targeting DNA replication stress and DNA double-strand break repair for optimizing SCLC treatment. *Cancers (Basel).* 2019;11(9).
36. Nie Y, Lang T. The interaction between ATRIP and MCM complex is essential for ATRIP chromatin loading and its phosphorylation in mantle cell lymphoma cells. *Pharmazie.* 2017;72(11):670–3.
37. Fukumoto Y, Takahashi K, Suzuki N, Ogra Y, Nakayama Y, Yamaguchi N. Casein kinase 2 promotes interaction between Rad17 and the 9-1-1 complex through constitutive phosphorylation of the C-terminal tail of human Rad17. *Biochem Biophys Res Commun.* 2018;504(2):380–6.
38. Chen Y, Li J, Cao F, Lam J, Cheng CC, Yu CH, et al. Nucleolar residence of the seckel syndrome protein TRAP1 is coupled to ribosomal DNA transcription. *Nucleic Acids Res.* 2018;46(19):10119–31.
39. Post SM, Tomkinson AE, Lee EY. The human checkpoint Rad protein Rad17 is chromatin-associated throughout the cell cycle, localizes to DNA replication sites, and interacts with DNA polymerase epsilon. *Nucleic Acids Res.* 2003;31(19):5568–75.
40. Abraham RT. Cell cycle checkpoint signaling through the ATM and ATR kinases. *Genes Dev.* 2001;15(17):2177–96.
41. Abbotts R, Thompson N, Madhusudan S. DNA repair in cancer: emerging targets for personalized therapy. *Cancer Manag Res.* 2014;6:77–92.
42. Lord CJ, Ashworth A. Mechanisms of resistance to therapies targeting BRCA-mutant cancers. *Nat Med.* 2013;19(11):1381–8.
43. Pitroda SP, Pashtan IM, Logan HL, Budke B, Darga TE, Weichselbaum RR, et al. DNA repair pathway gene expression score correlates with repair proficiency and tumor sensitivity to chemotherapy. *Sci Transl Med.* 2014; 6(229):229ra42.
44. Rajawat J, Shukla N, Mishra DP. Therapeutic targeting of poly(ADP-ribose) polymerase-1 (PARP1) in cancer: current developments, therapeutic strategies, and future opportunities. *Med Res Rev.* 2017;37(6):1461–91.
45. Baloch T, Lopez-Ozuna VM, Wang Q, Matanis E, Kessous R, Kogan L, et al. Sequential therapeutic targeting of ovarian cancer harboring dysfunctional BRCA1. *BMC Cancer.* 2019;19(1):44.
46. Ronson GE, Piberger AL, Higgs MR, Olsen AL, Stewart GS, McHugh PJ, et al. PARP1 and PARP2 stabilise replication forks at base excision repair intermediates through Fbh1-dependent Rad51 regulation. *Nat Commun.* 2018;9(1):746.
47. Bryant HE, Schultz N, Thomas HD, Parker KM, Flower D, Lopez E, et al. Specific killing of BRCA2-deficient tumours with inhibitors of poly(ADP-ribose) polymerase. *Nature.* 2005;434(7035):913–7.
48. Farmer H, McCabe N, Lord CJ, Tutt AN, Johnson DA, Richardson TB, et al. Targeting the DNA repair defect in BRCA mutant cells as a therapeutic strategy. *Nature.* 2005;434(7035):917–21.
49. Valdez BC, Li Y, Murray D, Liu Y, Nieto Y, Champlin RE, et al. Combination of a hypomethylating agent and inhibitors of PARP and HDAC traps PARP1 and DNMT1 to chromatin, acetylates DNA repair proteins, down-regulates NuRD and induces apoptosis in human leukemia and lymphoma cells. *Oncotarget.* 2018;9(3):3908–21.
50. Robert C, Nagaria PK, Pawar N, Adewuyi A, Gojo I, Meyers DJ, et al. Histone deacetylase inhibitors decrease NHEJ both by acetylation of repair factors and trapping of PARP1 at DNA double-strand breaks in chromatin. *Leuk Res.* 2016;45:14–23.
51. Gourley C, Balmana J, Ledermann JA, Serra V, Dent R, Loibl S, et al. Moving from poly (ADP-Ribose) polymerase inhibition to targeting DNA repair and DNA damage response in cancer therapy. *J Clin Oncol.* 2019;37(25):2257–69.
52. Dai CH, Chen P, Li J, Lan T, Chen YC, Qian H, et al. Co-inhibition of pol theta and HR genes efficiently synergize with cisplatin to suppress cisplatin-resistant lung cancer cells survival. *Oncotarget.* 2016;7(40):65157–70.
53. McCabe N, Turner NC, Lord CJ, Kluzek K, Bialkowska A, Swift S, et al. Deficiency in the repair of DNA damage by homologous recombination and sensitivity to poly(ADP-ribose) polymerase inhibition. *Cancer Res.* 2006; 66(16):8109–15.
54. Kim G, Ison G, McKee AE, Zhang H, Tang S, Gwise T, et al. FDA approval summary: olaparib monotherapy in patients with deleterious germline BRCA-mutated advanced ovarian cancer treated with three or more lines of chemotherapy. *Clin Cancer Res.* 2015;21(19):4257–61.
55. Pujade-Lauraine E, Ledermann JA, Selle F, Gebski V, Penson RT, Oza AM, et al. Olaparib tablets as maintenance therapy in patients with platinum-sensitive, relapsed ovarian cancer and a BRCA1/2 mutation (SOLO2/ENGOT-Ov21): a double-blind, randomised, placebo-controlled, phase 3 trial. *Lancet Oncol.* 2017;18(9):1274–84.
56. Lin ZP, Zhu YL, Lo YC, Moscarelli J, Xiong A, Korayem Y, et al. Combination of triapine, olaparib, and cediranib suppresses progression of BRCA-wild type and PARP inhibitor-resistant epithelial ovarian cancer. *PLoS One.* 2018; 13(11):e0207399.
57. George E, Kim H, Krepler C, Wenz B, Makvandi M, Tanyi JL, et al. A patient-derived-xenograft platform to study BRCA-deficient ovarian cancers. *JCI Insight.* 2017;2(1):e89760.
58. Morgan RD, Clamp AR, Evans DGR, Edmondson RJ, Jayson GC. PARP inhibitors in platinum-sensitive high-grade serous ovarian cancer. *Cancer Chemother Pharmacol.* 2018;81(4):647–58.
59. D'Andrea AD. Mechanisms of PARP inhibitor sensitivity and resistance. *DNA Repair (Amst).* 2018;71:172–6.
60. Bitler BG, Watson ZL, Wheeler LJ, Behbakht K. PARP inhibitors: clinical utility and possibilities of overcoming resistance. *Gynecol Oncol.* 2017;147(3):695–704.
61. Sakai W, Swisher EM, Jacquemont C, Chandramohan KV, Couch FJ, Langdon SP, et al. Functional restoration of BRCA2 protein by secondary BRCA2 mutations in BRCA2-mutated ovarian carcinoma. *Cancer Res.* 2009;69(16): 6381–6.
62. Makvandi M, Pantel A, Schwartz L, Schubert E, Xu K, Hsieh CJ, et al. A PET imaging agent for evaluating PARP-1 expression in ovarian cancer. *J Clin Invest.* 2018;128(5):2116–26.
63. Jiang X, Li X, Li W, Bai H, Zhang Z. PARP inhibitors in ovarian cancer: sensitivity prediction and resistance mechanisms. *J Cell Mol Med.* 2019;23(4): 2303–13.

64. Liu X, Han EK, Anderson M, Shi Y, Semizarov D, Wang G, et al. Acquired resistance to combination treatment with temozolomide and ABT-888 is mediated by both base excision repair and homologous recombination DNA repair pathways. *Mol Cancer Res*. 2009;7(10):1686–92.
65. Francica P, Rottenberg S. Mechanisms of PARP inhibitor resistance in cancer and insights into the DNA damage response. *Genome Med*. 2018;10(1):101.
66. Meghani K, Fuchs W, Detappe A, Drane P, Gogola E, Rottenberg S, et al. Multifaceted impact of microRNA 493-5p on genome-stabilizing pathways induces platinum and PARP inhibitor resistance in BRCA2-mutated carcinomas. *Cell Rep*. 2018;23(1):100–11.
67. Moore K, Colombo N, Scambia G, Kim BG, Oaknin A, Friedlander M, et al. Maintenance olaparib in patients with newly diagnosed advanced ovarian cancer. *N Engl J Med*. 2018;379(26):2495–505.
68. Li S, Wang W, Niu T, Wang H, Li B, Shao L, et al. Nrf2 deficiency exaggerates doxorubicin-induced cardiotoxicity and cardiac dysfunction. *Oxid Med Cell Longev*. 2014;2014:748524.
69. Korkmaz-Icoz S, Szczesny B, Marcatti M, Li S, Ruppert M, Lasitschka F, et al. Olaparib protects cardiomyocytes against oxidative stress and improves graft contractility during the early phase after heart transplantation in rats. *Br J Pharmacol*. 2018;175(2):246–61.
70. Block WD, Yu Y, Lees-Miller SP. Phosphatidyl inositol 3-kinase-like serine/threonine protein kinases (PIKKs) are required for DNA damage-induced phosphorylation of the 32 kDa subunit of replication protein A at threonine 21. *Nucleic Acids Res*. 2004;32(3):997–1005.
71. Zou L. Single- and double-stranded DNA: building a trigger of ATR-mediated DNA damage response. *Genes Dev*. 2007;21(8):879–85.
72. Cimprich KA, Cortez D. ATR: an essential regulator of genome integrity. *Nat Rev Mol Cell Biol*. 2008;9(8):616–27.
73. Adams BR, Golding SE, Rao RR, Valerie K. Dynamic dependence on ATR and ATM for double-strand break repair in human embryonic stem cells and neural descendants. *PLoS One*. 2010;5(4):e10001.
74. Matsuoka S, Rotman G, Ogawa A, Shiloh Y, Tamai K, Elledge SJ. Ataxia telangiectasia-mutated phosphorylates Chk2 *in vivo* and *in vitro*. *Proc Natl Acad Sci U S A*. 2000;97(19):10389–94.
75. Bianco JN, Bergoglio V, Lin YL, Pillaire MJ, Schmitz AL, Gilhodes J, et al. Overexpression of Claspin and Timeless protects cancer cells from replication stress in a checkpoint-independent manner. *Nat Commun*. 2019;10(1):910.
76. Zhang X, Lu X, Akhter S, Georgescu MM, Legerski RJ. FANCI is a negative regulator of Akt activation. *Cell Cycle*. 2016;15(8):1134–43.
77. Pugliese GM, Salaris F, Palermo V, Marabitti V, Morina N, Rosa A, et al. Inducible SMARCAL1 knockdown in iPSC reveals a link between replication stress and altered expression of master differentiation genes. *Dis Model Mech*. 2019.
78. Yeom G, Kim J, Park CJ. Investigation of the core binding regions of human Werner syndrome and Fanconi anemia group J helicases on replication protein A. *Sci Rep*. 2019;9(1):14016.
79. Zhou ZR, Yang ZZ, Wang SJ, Zhang L, Luo JR, Feng Y, et al. The Chk1 inhibitor MK-8776 increases the radiosensitivity of human triple-negative breast cancer by inhibiting autophagy. *Acta Pharmacol Sin*. 2017;38(4):513–23.
80. Suzuki M, Yamamori T, Bo T, Sakai Y, Inanami O. MK-8776, a novel Chk1 inhibitor, exhibits an improved radiosensitizing effect compared to UCN-01 by exacerbating radiation-induced aberrant mitosis. *Transl Oncol*. 2017;10(4):491–500.
81. Kim HJ, Min A, Im SA, Jang H, Lee KH, Lau A, et al. Anti-tumor activity of the ATR inhibitor AZD6738 in HER2 positive breast cancer cells. *Int J Cancer*. 2017;140(1):109–19.
82. Gamper AM, Rofougaran R, Watkins SC, Greenberger JS, Beumer JH, Bakkenist CJ. ATR kinase activation in G1 phase facilitates the repair of ionizing radiation-induced DNA damage. *Nucleic Acids Res*. 2013;41(22):10334–44.
83. Reinhardt HC, Yaffe MB. Kinases that control the cell cycle in response to DNA damage: Chk1, Chk2, and MK2. *Curr Opin Cell Biol*. 2009;21(2):245–55.
84. Min A, Im SA, Jang H, Kim S, Lee M, Kim DK, et al. AZD6738, a novel oral inhibitor of ATR, induces synthetic lethality with ATM deficiency in gastric cancer cells. *Mol Cancer Ther*. 2017;16(4):566–77.
85. Pabla N, Huang S, Mi QS, Daniel R, Dong Z. ATR-Chk2 signaling in p53 activation and DNA damage response during cisplatin-induced apoptosis. *J Biol Chem*. 2008;283(10):6572–83.
86. Reaper PM, Griffiths MR, Long JM, Charrier JD, McCormick S, Charlton PA, et al. Selective killing of ATM- or p53-deficient cancer cells through inhibition of ATR. *Nat Chem Biol*. 2011;7(7):428–30.
87. Peasland A, Wang LZ, Rowling E, Kyle S, Chen T, Hopkins A, et al. Identification and evaluation of a potent novel ATR inhibitor, NU6027, in breast and ovarian cancer cell lines. *Br J Cancer*. 2011;105(3):372–81.
88. Toledo LI, Murga M, Zur R, Soria R, Rodriguez A, Martinez S, et al. A cell-based screen identifies ATR inhibitors with synthetic lethal properties for cancer-associated mutations. *Nat Struct Mol Biol*. 2011;18(6):721–7.
89. Mohni KN, Kavanaugh GM, Cortez D. ATR pathway inhibition is synthetically lethal in cancer cells with ERCC1 deficiency. *Cancer Res*. 2014;74(10):2835–45.
90. Weber AM, Ryan AJ. ATM and ATR as therapeutic targets in cancer. *Pharmacol Ther*. 2015;149:124–38.
91. Foote KM, Lau A, Nissink JW. Drugging ATR: progress in the development of specific inhibitors for the treatment of cancer. *Future Med Chem*. 2015;7(7):873–91.
92. Knegtel R, Charrier JD, Durrant S, Davis C, O'Donnell M, Storck P, et al. Rational design of 5-(4-(isopropylsulfonyl)phenyl)-3-(3-(4-((methylamino)methyl)phenyl)isoxazol-5-yl)pyrazin-2-amine (VX-970, M6620): optimization of intra- and intermolecular polar interactions of a new ataxia telangiectasia mutated and Rad3-Related (ATR) kinase inhibitor. *J Med Chem*. 2019;62(11):5547–61.
93. Engelke CG, Parsels LA, Qian Y, Zhang Q, Karnak D, Robertson JR, et al. Sensitization of pancreatic cancer to chemoradiation by the Chk1 inhibitor MK8776. *Clin Cancer Res*. 2013;19(16):4412–21.
94. Huntoon CJ, Flatten KS, Wahner Hendrickson AE, Huehls AM, Sutor SL, Kaufmann SH, et al. ATR inhibition broadly sensitizes ovarian cancer cells to chemotherapy independent of BRCA status. *Cancer Res*. 2013;73(12):3683–91.
95. Kurmasheva RT, Kurmashev D, Reynolds CP, Kang M, Wu J, Houghton PJ, et al. Initial testing (stage 1) of M6620 (formerly VX-970), a novel ATR inhibitor, alone and combined with cisplatin and melphalan, by the Pediatric Preclinical Testing Program. *Pediatr Blood Cancer*. 2018;65(2).
96. Wengner AM, Siemeister G, Lucking U, Lefranc J, Wortmann L, Lienau P, et al. The novel ATR inhibitor BAY 1895344 is efficacious as monotherapy and combined with DNA damage-inducing or repair-compromising therapies in preclinical cancer models. *Mol Cancer Ther*. 2020;19(1):26–38.
97. Buisson R, Boisvert JL, Benes CH, Zou L. distinct but concerted roles of ATR, DNA-PK, and Chk1 in countering replication stress during S phase. *Mol Cell*. 2015;59(6):1011–24.
98. Jiang K, Pereira E, Maxfield M, Russell B, Goudelock DM, Sanchez Y. Regulation of Chk1 includes chromatin association and 14-3-3 binding following phosphorylation on Ser-345. *J Biol Chem*. 2003;278(27):25207–17.
99. Niida H, Katsuno Y, Banerjee B, Hande MP, Nakanishi M. Specific role of Chk1 phosphorylations in cell survival and checkpoint activation. *Mol Cell Biol*. 2007;27(7):2572–81.
100. Guzi TJ, Paruch K, Dwyer MP, Labroli M, Shanahan F, Davis N, et al. Targeting the replication checkpoint using SCH 900776, a potent and functionally selective CHK1 inhibitor identified via high content screening. *Mol Cancer Ther*. 2011;10(4):591–602.
101. Ronco C, Martin AR, Demange L, Benhida R. ATM, ATR, CHK1, CHK2 and WEE1 inhibitors in cancer and cancer stem cells. *Medchemcomm*. 2017;8(2):295–319.
102. Paculova H, Kramara J, Simeckova S, Fedr R, Soucek K, Hylse O, et al. BRCA1 or CDK12 loss sensitizes cells to CHK1 inhibitors. *Tumour Biol*. 2017;39(10):1010428317727479.
103. Bahassi EM, Ovesen JL, Riesenberger AL, Bernstein WZ, Hasty PE, Stambrook PJ. The checkpoint kinases Chk1 and Chk2 regulate the functional associations between hBRCA2 and Rad51 in response to DNA damage. *Oncogene*. 2008;27(28):3977–85.
104. Yang XH, Shiotani B, Classon M, Zou L. Chk1 and Claspin potentiate PCNA ubiquitination. *Genes Dev*. 2008;22(9):1147–52.
105. Blasina A, Hallin J, Chen E, Arango ME, Kraynov E, Register J, et al. Breaching the DNA damage checkpoint via PF-00477736, a novel small-molecule inhibitor of checkpoint kinase 1. *Mol Cancer Ther*. 2008;7(8):2394–404.
106. King C, Diaz H, Barnard D, Barda D, Clawson D, Blosser W, et al. Characterization and preclinical development of LY2603618: a selective and potent Chk1 inhibitor. *Invest New Drugs*. 2014;32(2):213–26.
107. Massey AJ, Stokes S, Browne H, Foloppe N, Fiumana A, Scrase S, et al. Identification of novel, *in vivo* active Chk1 inhibitors utilizing structure guided drug design. *Oncotarget*. 2015;6(34):35797–812.
108. Angius G, Tomao S, Stati V, Vici P, Bianco V, Tomao F. Prexasertib, a checkpoint kinase inhibitor: from preclinical data to clinical development. *Cancer Chemother Pharmacol*. 2019.

109. Syljuasen RG, Sorensen CS, Hansen LT, Fugger K, Lundin C, Johansson F, et al. Inhibition of human Chk1 causes increased initiation of DNA replication, phosphorylation of ATR targets, and DNA breakage. *Mol Cell Biol*. 2005;25(9):3553–62.
110. Kawahara N, Ogawa K, Nagayasu M, Kimura M, Sasaki Y, Kobayashi H. Candidate synthetic lethality partners to PARP inhibitors in the treatment of ovarian clear cell cancer. *Biomed Rep*. 2017;7(5):391–9.
111. Ledford H. US cancer institute to overhaul tumour cell lines. *Nature*. 2016; 530(7591):391.
112. Kim H, George E, Ragland R, Rafail S, Zhang R, Krepler C, et al. Targeting the ATR/CHK1 axis with PARP inhibition results in tumor regression in BRCA-mutant ovarian cancer models. *Clin Cancer Res*. 2017;23(12):3097–108.
113. Sun C, Cao W, Qiu C, Li C, Dongol S, Zhang Z, et al. MiR-509-3 augments the synthetic lethality of PARPi by regulating HR repair in PDX model of HGSOc. *J Hematol Oncol*. 2020;13(1):9.
114. Kondrashova O, Topp M, Nestic K, Lieschke E, Ho GY, Harrell MI, et al. Methylation of all BRCA1 copies predicts response to the PARP inhibitor rucaparib in ovarian carcinoma. *Nat Commun*. 2018;9(1):3970.
115. Gitto SB, Kim H, Rafail S, Omran DK, Medvedev S, Kinose Y, et al. An autologous humanized patient-derived-xenograft platform to evaluate immunotherapy in ovarian cancer. *Gynecol Oncol*. 2020;156(1):222–32.
116. Liu HD, Xia BR, Jin MZ, Lou G. Organoid of ovarian cancer: genomic analysis and drug screening. *Clin Transl Oncol*. 2020.
117. Kopper O, de Witte CJ, Lohmussaar K, Valle-Inclan JE, Hami N, Kester L, et al. An organoid platform for ovarian cancer captures intra- and interpatient heterogeneity. *Nat Med*. 2019;25(5):838–49.
118. Hill SJ, Decker B, Roberts EA, Horowitz NS, Muto MG, Worley MJ Jr, et al. Prediction of DNA repair inhibitor response in short-term patient-derived ovarian cancer organoids. *Cancer Discov*. 2018;8(11):1404–21.
119. Saldivar JC, Cortez D, Cimprich KA. The essential kinase ATR: ensuring faithful duplication of a challenging genome. *Nat Rev Mol Cell Biol*. 2017; 18(10):622–36.
120. Yazinski SA, Comaills V, Buisson R, Genois MM, Nguyen HD, Ho CK, et al. ATR inhibition disrupts rewired homologous recombination and fork protection pathways in PARP inhibitor-resistant BRCA-deficient cancer cells. *Genes Dev*. 2017;31(3):318–32.
121. Fang P, De Souza C, Minn K, Chien J. Genome-scale CRISPR knockout screen identifies TIGAR as a modifier of PARP inhibitor sensitivity. *Commun Biol*. 2019;2:335.

Publisher's Note

Springer Nature remains neutral with regard to jurisdictional claims in published maps and institutional affiliations.

Ready to submit your research? Choose BMC and benefit from:

- fast, convenient online submission
- thorough peer review by experienced researchers in your field
- rapid publication on acceptance
- support for research data, including large and complex data types
- gold Open Access which fosters wider collaboration and increased citations
- maximum visibility for your research: over 100M website views per year

At BMC, research is always in progress.

Learn more biomedcentral.com/submissions





Article

PARP Inhibition Increases the Reliance on ATR/CHK1 Checkpoint Signaling Leading to Synthetic Lethality—An Alternative Treatment Strategy for Epithelial Ovarian Cancer Cells Independent from HR Effectiveness

Patrycja Gralewska ¹, Arkadiusz Gajek ¹, Agnieszka Marczak ¹, Michał Mikula ², Jerzy Ostrowski ^{2,3}, Agnieszka Śliwińska ⁴ and Aneta Rogalska ^{1,*}

¹ Department of Medical Biophysics, Faculty of Biology and Environmental Protection, Institute of Biophysics, University of Lodz, 90-236 Lodz, Poland; patrycja.gralewska@edu.uni.lodz.pl (P.G.); arkadiusz.gajek@biol.uni.lodz.pl (A.G.); agnieszka.marczak@biol.uni.lodz.pl (A.M.)

² Department of Genetics, Maria Skłodowska-Curie National Research Institute of Oncology, 02-781 Warsaw, Poland; michal.mikula@pib-nio.pl (M.M.); jerzy.ostrowski@pib-nio.pl (J.O.)

³ Department of Gastroenterology, Hepatology and Clinical Oncology, Centre of Postgraduate Medical Education, 01-813 Warsaw, Poland

⁴ Department of Nucleic Acid Biochemistry, Medical University of Lodz, 92-213 Lodz, Poland; agnieszka.sliwinska@umed.lodz.pl

* Correspondence: aneta.rogalska@biol.uni.lodz.pl; Tel.: +48-42-635-44-77

Received: 4 November 2020; Accepted: 16 December 2020; Published: 19 December 2020



Abstract: Poly (ADP-ribose) polymerase inhibitor (PARPi, olaparib) impairs the repair of DNA single-strand breaks (SSBs), resulting in double-strand breaks (DSBs) that cannot be repaired efficiently in homologous recombination repair (HRR)-deficient cancers such as BRCA1/2-mutant cancers, leading to synthetic lethality. Despite the efficacy of olaparib in the treatment of BRCA1/2 deficient tumors, PARPi resistance is common. We hypothesized that the combination of olaparib with anticancer agents that disrupt HRR by targeting ataxia telangiectasia and Rad3-related protein (ATR) or checkpoint kinase 1 (CHK1) may be an effective strategy to reverse ovarian cancer resistance to olaparib. Here, we evaluated the effect of olaparib, the ATR inhibitor AZD6738, and the CHK1 inhibitor MK8776 alone and in combination on cell survival, colony formation, replication stress response (RSR) protein expression, DNA damage, and apoptotic changes in BRCA2 mutated (PEO-1) and HRR-proficient BRCA wild-type (SKOV-3 and OV-90) cells. Combined treatment caused the accumulation of DNA DSBs. PARP expression was associated with sensitivity to olaparib or inhibitors of RSR. Synergistic effects were weaker when olaparib was combined with CHK1i and occurred regardless of the BRCA2 status of tumor cells. Because PARPi increases the reliance on ATR/CHK1 for genome stability, the combination of PARPi with ATR inhibition suppressed ovarian cancer cell growth independently of the efficacy of HRR. The present results were obtained at sub-lethal doses, suggesting the potential of these inhibitors as monotherapy as well as in combination with olaparib.

Keywords: ATR inhibitor; CHK1 inhibitor; ovarian cancer; PARP inhibitor; targeted therapy

1. Introduction

Ovarian cancer is the most common cause of death among gynecological cancers, which is partly attributed to the fact that epithelial ovarian cancer (EOC) is often diagnosed at an advanced stage. The risk of ovarian cancer is associated with DNA damage [1]. Most type II ovarian carcinomas (96%)

have TP53 mutation [2,3] and approximately 50% of germline high-grade serous ovarian cancers (HGSOCs) carry an alteration in homologous recombination (HR) pathway genes, most commonly in breast cancer (BRCA) gene 1/2 [4]. Moreover, DNA damage repair genes are mutated in 40.3% of patients with HGSOC, and the rate of somatic BRCA mutations in the absence of germline mutation is 8.5% [5]. Therefore, targeting DNA repair-associated proteins is increasingly becoming an applicable approach to cancer treatment. Single-strand breaks (SSBs) can be accurately repaired using the other strand as a template, and this process involves the poly (ADP-ribose) polymerase (PARP) enzyme [6]. DNA double-strand breaks (DSBs) are repaired through two pathways: the HR pathway and non-homologous end joining, although other mechanisms also exist [7]. BRCA1 and BRCA2 are involved in the DNA damage response; they are important members of the network of interacting DNA repair pathways responsible for the maintenance of genome stability. Both proteins are related to the error-free repair of DSBs by HR [8]. BRCA1 signals DNA damage and ensures cell cycle regulation, whereas BRCA2 interacts with RAD51 and facilitates the loading and formation of RAD51 filaments on the damaged DNA strand [9]. HR-deficient cancer cells with mutations in BRCA1 or BRCA2 are associated with DSB repair via error-prone repair pathways, the accumulation of mutations, and cell death [10]. PARP inhibitors (PARPi) impair SSB repair, thereby causing DSBs that cannot be repaired efficiently in BRCA1/2-mutant cancers, leading to synthetic lethality [11]. The first FDA-approved PARPi was olaparib (Lynparza). In 2014, olaparib gained European Medicines Agency approval for the treatment of advanced EOC in patients with germline BRCA^{MUT} who did not respond to at least three lines of chemotherapy [12]. Olaparib is currently the only FDA-approved PARPi for first-line maintenance therapy in BRCA^{MUT} patients [13]. Despite the efficacy of olaparib in the treatment of BRCA1/2 deficient tumors, the development of resistance to PARPi is common. It is known that PARP1 is altered in 1.12% of high-grade ovarian serous adenocarcinoma patients and in 1.05% of ovarian carcinoma patients [14]. Mutations of the PARP1 DNA-binding zinc-finger (ZnF) domains cause PARPi resistance and can alter PARP1 trapping [15]. Although olaparib treatment increases the survival rate of patients with stage IV disease, the 5-year survival rate of patients with advanced stage cancer remains below 30% [16].

ATR/CHK1 blockade prevents DNA damage-induced cell cycle arrest, resulting in inappropriate entry into mitosis, chromosome aberrations, unequal partitioning of the genome, and cell apoptosis [17]. The ATR/CHK1 pathway stabilizes replication forks and prevents their collapse into DNA DSBs. Phosphorylation of ATR at Thr1989 occurs in response to DNA damage and is important for the activation of the ATR/CHK1 pathway. Replication protein A (RPA), ATR-interacting protein (ATRIP), and ATR kinase are involved in Thr1989 phosphorylation [18]. Replication blocks and genotoxic stress induce CHK1 phosphorylation at Ser317 and Ser345. Combination treatment with olaparib and anticancer agents that disrupt HR repair such as ATR inhibitors (ATRi) or CHK1 inhibitors (CHK1i) may therefore represent an effective strategy to sensitize ovarian cancer cells to olaparib. Thus, the inhibition of ATR/CHK1 is expected to increase reliance on HR to reorganize the replication fork structure and complete the replication. ATR is a key regulator of DNA replication stress response (RSR) and DNA damage-activated checkpoints. Together with CHK1, ATR plays a role in M-phase inducer phosphatase (CDC25) phosphorylation and inactivation [19]. The ATR kinase lies upstream of its effector protein, CHK1 [20], and phosphorylates numerous factors, including Werner syndrome ATP-dependent helicase (WRN), SWI/SNF-related matrix-associated actin-dependent regulator of chromatin subfamily A-like protein 1 (SMARCA1), and Fanconi anemia complementation group I (FANCI), which may help preserve replication fork stability and control cell cycle progression [21–23]. Additionally, replication protein A (RPA), DNA replication licensing factor (MCM2), and p53 are the direct substrates of ATR [24]. Thus, ATR is essential for cell survival, as it has a crucial role in stabilizing genomic integrity [25].

ATR inhibition is lethal in numerous ovarian cancer cell lines associated with changes in TP53 (OV-90) or BRCA1/2 (PEO-1, BRCA2^{MUT}) [26,27]. Oncogene expression (oncogenic RAS protein mutations and MYC proto-oncogene protein and G1/S-specific cyclin-E1 overexpression) and other

defects such as deficiencies in DNA repair (PALB2 and the ataxia telangiectasia mutated (ATM) loss) can cause DNA replication stress and increased reliance on the ATR [28]. The activation of CHK1 and its downstream effectors leads to coordinated activities, including reduced new origin firing, delay of cell cycle progression, and restoration of the stalled replication forks [29]. CHK1 is an important molecular target for sensitizing cancer cells to DNA-damaging agents. In response to DNA damage, CHK1 inhibits the Cdc25 phosphatase, resulting in cyclin-dependent kinase (Cdk) inhibition and cell cycle arrest in the G2 phase mainly in p53 mutant tumor cells. Therefore, CHK1 inhibition renders cells more sensitive to DNA damage and programmed cell death [17].

Herein, we showed that PARPi treatment increased ATR and CHK1 phosphorylation, a molecular step crucial for the activation of the ATR/CHK1 fork protection pathway. We also investigated the efficacy of the combination of PARPi with ATRi or CHK1i in BRCA^{MUT} ovarian cancer cells, as well as in serous ovarian cancers without BRCA1/2 mutation.

2. Results

2.1. PARP Inhibition Is Not Sufficient to Kill Ovarian Cancer Cells, but Acts Synergistically with CHK1 or ATR Inhibition

The antiproliferative activity of the compounds was assessed using the 3-(4,5-dimethylthiazol-2-yl)-2,5-diphenyltetrazolium bromide (MTT) assay. Olaparib (AZD2281) had a dose-dependent effect and was more cytotoxic in BRCA^{MUT} cells (PEO-1) than in HR-proficient cells (OV-90 and SKOV-3 cells, BRCA^{WT}), as indicated by the IC₅₀ values (Figure 1A). PARPi did not cause complete cell death in SKOV-3 cells (48% of viable cells) or in OV-90 cells (60% of viable cells), which was also observed in BRCA^{MUT} cells (29% of the cells still viable) after 5 days of incubation. We therefore examined the effect of PARPi on the ATR/CHK-1 pathway. The CHK1i MK8776 was added in increasing concentrations and was more cytotoxic in HR-proficient cells (OV-90, SKOV-3) than in BRCA^{MUT} cells (PEO-1) after 5 days of treatment. The ATRi AZD6738 caused a dose-dependent decrease in cell viability in all cell lines, although its effect was stronger in BRCA^{MUT} (PEO-1) than in BRCA^{WT} (OV-90, SKOV-3) cell lines. The IC₅₀ values for ATRi in SKOV-3, OV-90, and PEO-1 were 3.59, 2.77, and 0.21 μ M, respectively (Figure 1A).

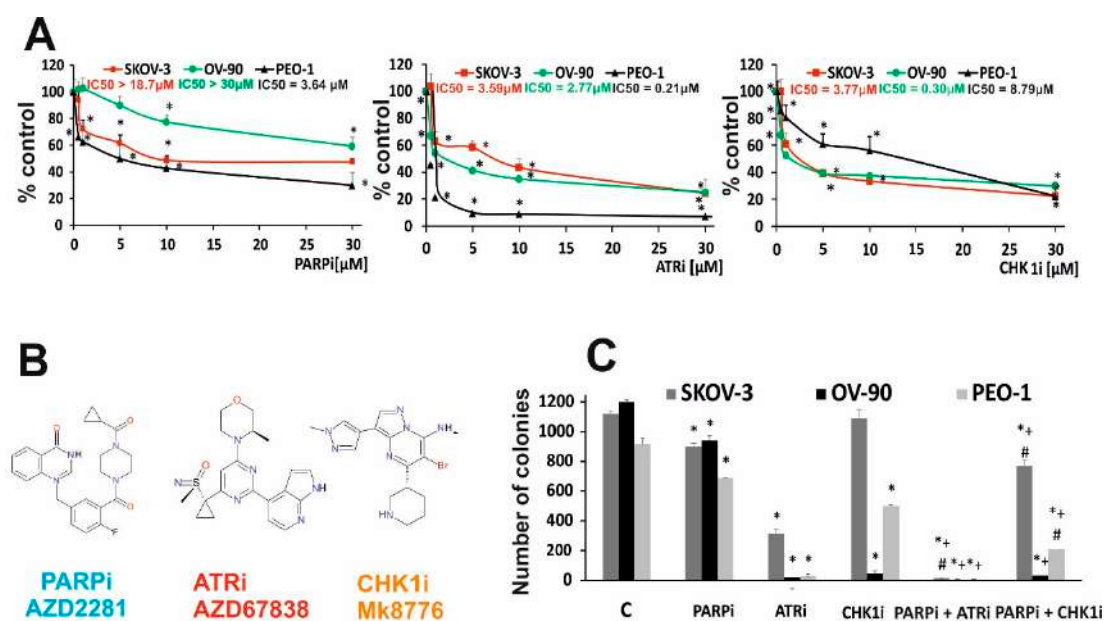


Figure 1. Cont.

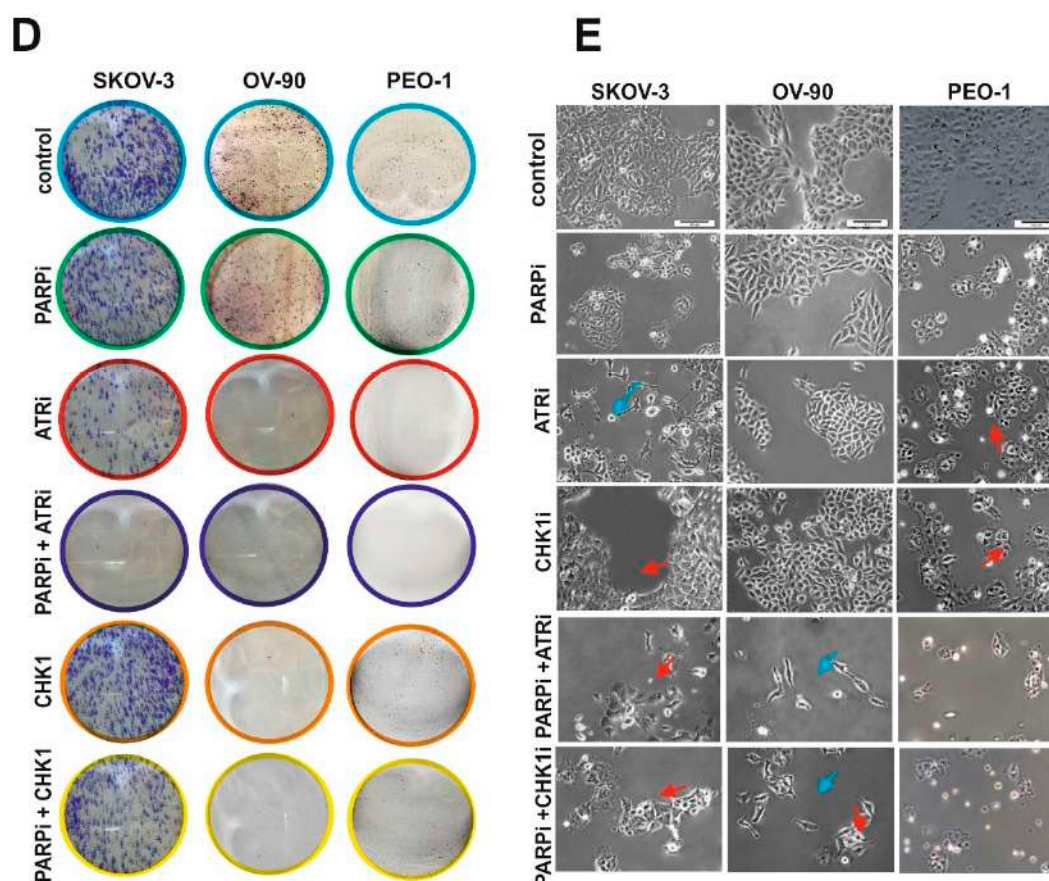


Figure 1. PARPi in combination with CHK1i or ATRi decreased viability more effectively than PARPi monotherapy. (A) Cell viability after treatment with PARPi (AZD2281), CHK1i (MK8776), and ATRi (AZD6738) in HR-deficient (PEO-1, BRCA2^{MUT}) and HR-proficient (OV-90, SKOV-3, BRCA^{WT}) cells at increasing concentrations for 5 days was assessed by the MTT assay. (B) Structural formulas of PARPi, ATRi, CHK1i. (C,D) Colony formation assay. Colony formation was evaluated after treatment with PARPi at 0.5 μ M in SKOV-3, OV-90, and PEO-1 cells. Cells (200 cells/well) were seeded into six-well plates and incubated with the indicated drug concentrations for 14 days. Colony numbers were counted manually (* $p < 0.05$). For each sample, the results from three replicates were averaged. PARPi and CHK1i decreased viability to 80.17% and 97.28%, respectively, compared with the control SKOV-3 cells; to 78.33% and 3.63%, respectively, in OV-90; and to 75.35% and 0.25%, respectively, in PEO-1 cells. Combination therapy with PARPi and CHK1i decreased colony formation to 68% in SKOV-3, 2.5% in OV-90, and 22.82% in PEO-1 cells. In all cell lines, drugs used in combination had a synergistic effect compared with single drug administration (SKOV-3, CDI = 0.07; OV-90, CDI = 0.07; PEO-1, CDI = 0.06). Combined PARPi and ATRi treatment decreased colony formation to <1% compared with PARPi alone and ATRi alone. In all cell lines, the combination of PARPi/ATRi had a synergistic effect compared with single compounds (SKOV-3, CDI = 0.004; OV-90, CDI = 0.03; PEO-1, CDI = 0.01). All data correspond to three biological assays and were graphed as means \pm SD. (E) The morphology of SKOV-3, OV-90, and PEO-1 cells treated for 24 h with ATRi, CHK1i, and their combination with olaparib (0.5 μ M concentration of each single drug) was examined under an inverted microscope (Olympus IX70, Japan) (scale bar = 100 μ m). The cells were elongated and thin (blue arrows) or enlarged (red arrows). * Statistically significant changes between samples incubated with the compound compared with control cells ($p < 0.05$). + Statistically significant changes between samples incubated with PARPi and combination treatments (PARPi/ATRi; PARPi/CHK1i) ($p < 0.05$). # Statistically significant differences between samples incubated with ATRi or CHK1i and their combination (PARPi/ATRi; PARPi/CHK1i) ($p < 0.05$).

The in vitro effect of single drug or combined treatment with PARPi and ATRi or CHK1i on ovarian cancer cell lines was evaluated by colony formation assay, a reliable test for measuring cell survival based on the ability of a cell to grow into a colony. Treatment with 0.5 μM PARPi decreased the colony-forming ability to a greater extent in BRCA^{MUT} cells than in HR-proficient cells (Figure 1B,C). ATRi completely suppressed colony formation in HGSOCS (PEO-1 and OV-90) and significantly decreased colony numbers in SKOV-3 cells (up to 28%) (Figure 2B,C). An extended incubation period of 14 days with the tested compounds showed that cell lines with mutated BRCA2 (PEO-1) and those with mutated p53 (OV-90) were CHK1i-sensitive. Combined therapy with PARPi and CHK1i decreased colony formation to 74.55% in SKOV-3 (coefficient of drug interaction (CDI) = 0.79), to 46.06% in OV-90 (CDI = 0.67), and to 45.41% in PEO-1 cells (CDI = 0.74). Combined PARPi and ATRi treatment decreased cell viability to 66.22% in SKOV-3, 56.29% in OV-90, and 11.06% in PEO-1 cells compared with the effect of PARPi alone and ATRi alone ($p < 0.05$) (Figure 2B).

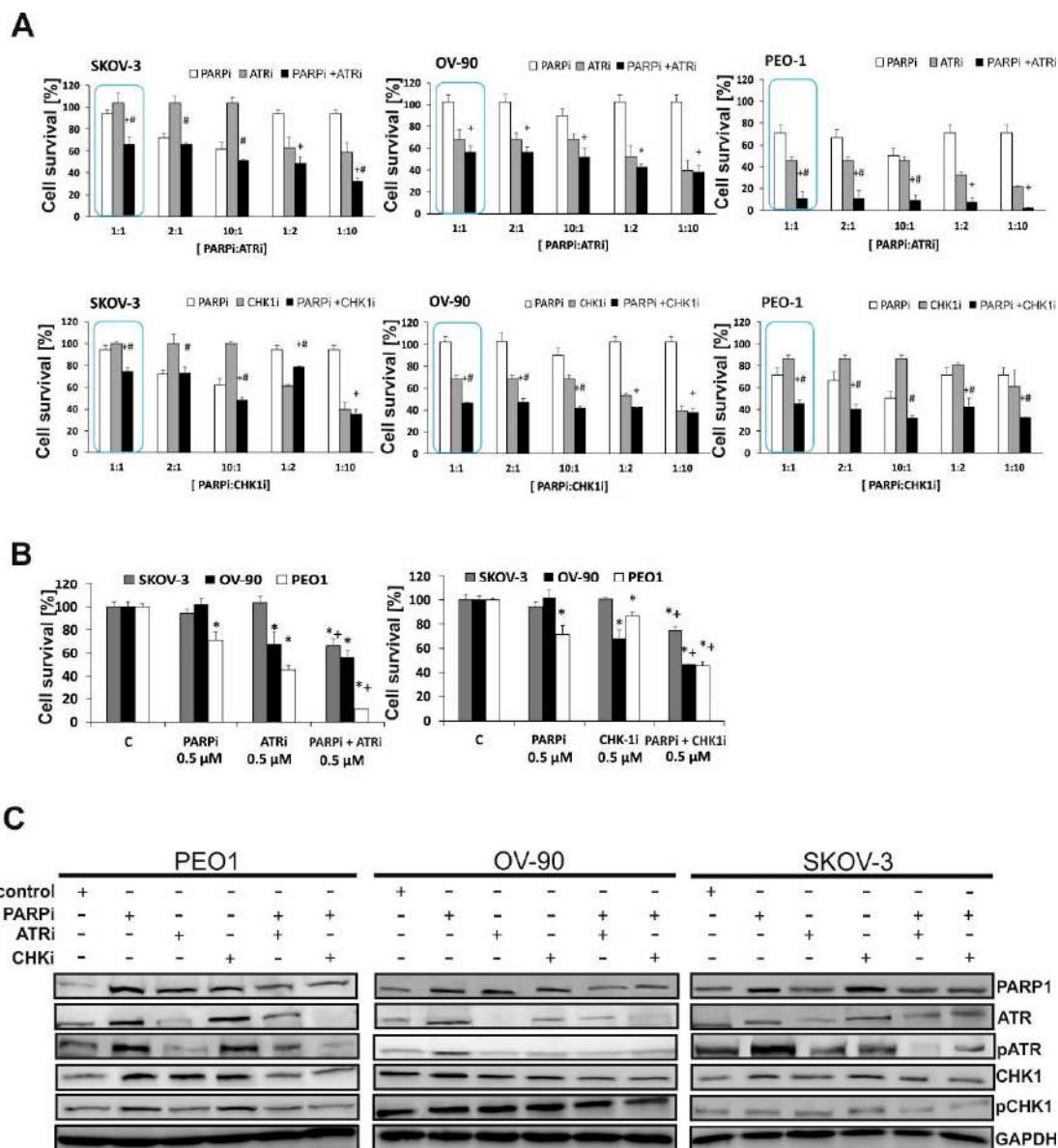


Figure 2. PARPi in combination with CHK1i or ATRi has a synergistic effect in ovarian cancer cells. (A) The effect of combination treatment with ATRi or CHK1i and PARPi at different ratios was evaluated by the MTT assay. In all cell lines, the combination of ATRi/PARPi had a synergistic effect compared with either drug alone (SKOV-3, CDI = 0.69; OV-90, CDI = 0.82; and PEO-1, CDI = 0.34). Similar effects were obtained with the combination of CHK1i/PARPi compared with either drug alone (SKOV-3, CDI = 0.79;

OV-90, CDI = 0.66; and PEO-1, CDI = 0.74). (B) The combination effect of PARPi/ATRi and PARPi/CHK1i at 0.5 μ M was evaluated by the MTT assay. * Statistically significant differences between samples incubated with the compound compared with control cells ($p < 0.05$). + Statistically significant changes between samples incubated with PARPi and combination treatment (PARPi/ATRi; PARPi/CHK1i) ($p < 0.05$). # Statistically significant differences between the samples incubated with ATRi or CHK1i and combination treatment (PARPi/ATRi; PARPi/CHK1i) ($p < 0.05$). (C) BRCA2^{MUT} (PEO-1) and HR-proficient (SKOV-3 and OV-90) cells were treated with PARPi, ATRi, CHK1i, and the combination of PARPi/ATRi or PARPi/CHK1i at 0.5 μ M, and lysates were collected at 24 h. Western blot analysis of phosphorylated and total proteins was performed. PARP increased with PARPi by 4.9-fold in PEO-1 cells, 2.52-fold in OV-90 cells, and 2.3-fold in SKOV-3 cells. PARPi with ATRi decreased PARP by 1.43-fold in PEO-1 cells, 1.3-fold in OV-90 cells, and 1.1-fold in SKOV-3 cells. PARPi with CHK1i decreased PARP by 1.7-fold in PEO-1 cells, 1.6-fold in OV-90 cells, and 1.1-fold in SKOV-3 cells. ATRi treatment decreased pATR 1.4-fold in PEO-1 cells, 1.34-fold in OV-90 cells, and 2.36-fold in SKOV-3 cells. PARPi increased pATR, whereas the combination of PARPi/ATRi decreased pATR by 2-fold in PEO-1 and OV-90 cells and 1.8-fold in SKOV-3 cells. With CHK1i, pCHK1 increased by 1.36-fold in PEO-1 cells, 1.34-fold in OV-90 cells, and 1.17-fold in SKOV-3 cells. PARPi with ATRi decreased pCHK1 by 1.8-fold in PEO-1 cells and 1.18-fold in SKOV-3 cells compared with PARPi alone. PARPi with CHK1i decreased pCHK1 by 2.95-fold in PEO-1 cells, 1.5-fold in OV-90 cells, and 1.25-fold in SKOV-3 cells compared with PARPi alone.

Among ovarian cancer cells treated with PARPi, ATRi, or CHK1i for 24 h (Figure 1D), a small percentage of cells exhibited morphological changes such as elongation and thinning. Exposure of HR-deficient and HR-proficient cells to the combined action of PARPi/ATRi or PARPi/CHK1i significantly increased the number of deteriorated, elongated cells. PARPi/ATRi- and PARPi/CHK1i-treated cells showed an increase in volume, which is characteristic of a defective cell division arrest [30]. In addition, exposure to combinations of compounds led to cell disintegration and detachment of cells from the culture well surface.

To determine the most effective ratio of PARPi to ATRi or CHK1i, the effect of multiple-dose combinations was examined as displayed in Figure 2A,B. The 1:1 (0.5 μ M: 0.5 μ M) combination was the most effective among those tested. Subtoxic concentrations of PARPi had a smaller effect on cell viability in SKOV-3 and OV-90 cells than in PEO-1 cells (71.15 % of control). CHK1i caused a significant loss of viability (68%) in OV-90 cells and resulted in 86% of viable PEO-1 cells.

The effect of PARP inhibition on activating the ATR/CHK1 pathway was demonstrated by Western blotting as shown in Figure 2C. PARPi treatment at 0.5 μ M upregulated phospho-ATR (pATR) and phospho-CHK1 (pCHK1) in both BRCA^{MUT} (PEO-1) and HR-proficient cells (OV-90) within 24 h, although it was more effective in BRCA^{MUT} cells, suggesting the activation of ATR/CHK1 for survival. PARPi did not significantly affect the level of pATR and pCHK1 in the SKOV-3 line (HR-proficient cells), whereas it caused a 2.36-fold increase of pATR in PEO-1 and 1.3-fold increase in OV-90. In PEO-1 and OV-90 cells, pCHK1 increased 1.5- and 1.21-fold, respectively, compared with the controls after 24 h (Figure 2C). In all cell lines, PARPi in combination with ATRi or CHK1i decreased the PARPi-induced upregulation of pATR and pCHK1. CHK1i treatment upregulated pCHK1 in PEO-1 and OV-90 cells.

Despite the dose-dependent cytotoxic effects of olaparib on all ovarian cancer cell lines tested, its activity was not sufficient to significantly reduce cancer cell populations at the concentration range used. Combination treatment with two compounds, PARPi and CHK1i, had a significantly greater cytotoxic effect, decreasing colony formation ability to a greater extent than either drug alone in BRCA2^{MUT} cells compared with BRCA^{WT}. ATRi in combination with PARPi was equally cytotoxic in both BRCA2-deficient and wild-type cells. The PARPi/ATRi combination demonstrated synergy in all the tested cell lines, whereas the PARPi/CHK1i combination showed synergism only in BRCA^{MUT} cells.

2.2. PARPi in Combination with CHK1i or ATRi Increases DNA Damage in BRCA^{MUT} and BRCA^{WT} Ovarian Cells

We hypothesized that treatment with the ATRi/CHK1i and PARPi combination may result in DNA damage. Alkali-labile sites, SSBs, and DSBs were analyzed by the comet assay, and the data are presented in Figure 3. The alkaline comet assay was performed after exposure to 0.5 μ M of each drug for 2, 24, and 48 h. DNA damage in comet tails was detected as early as 2 h after treatment. The results of the comet assay showed that PARPi, ATRi, or CHK1i alone induced DNA damage in a time-dependent manner. The level of DNA damage was associated with cytotoxicity, measured by the MTT assay. DNA damage increased after PARPi treatment in BRCA^{MUT} and HR-proficient lines, and it increased markedly in HR-deficient cells (by approximately 1.8-fold). After 48 h of treatment, the level of DNA damage differed among the cell lines in response to ATRi (SKOV-3: 0.5%, OV-90: 33%, and PEO-1: 54.4%) or CHK1i (SKOV-3: 21%, OV-90: 30%, and PEO-1: 51%). Combination treatment with PARPi and ATRi increased the level of DNA damage in all cell lines after 24 h of incubation and the effect was not dependent on HR proficiency. Treatment with the combination of PARPi and ATRi caused a steady increase in DNA damage in comet tails that reached 38.9% in SKOV-3 cells, 48.2% in OV-90 cells, and 70.13% in PEO-1 cells after 48 h. In the OV-90 and PEO-1 cell lines, the effect of combination treatment on the level of DNA damage differed from that of PARPi alone by >15%.

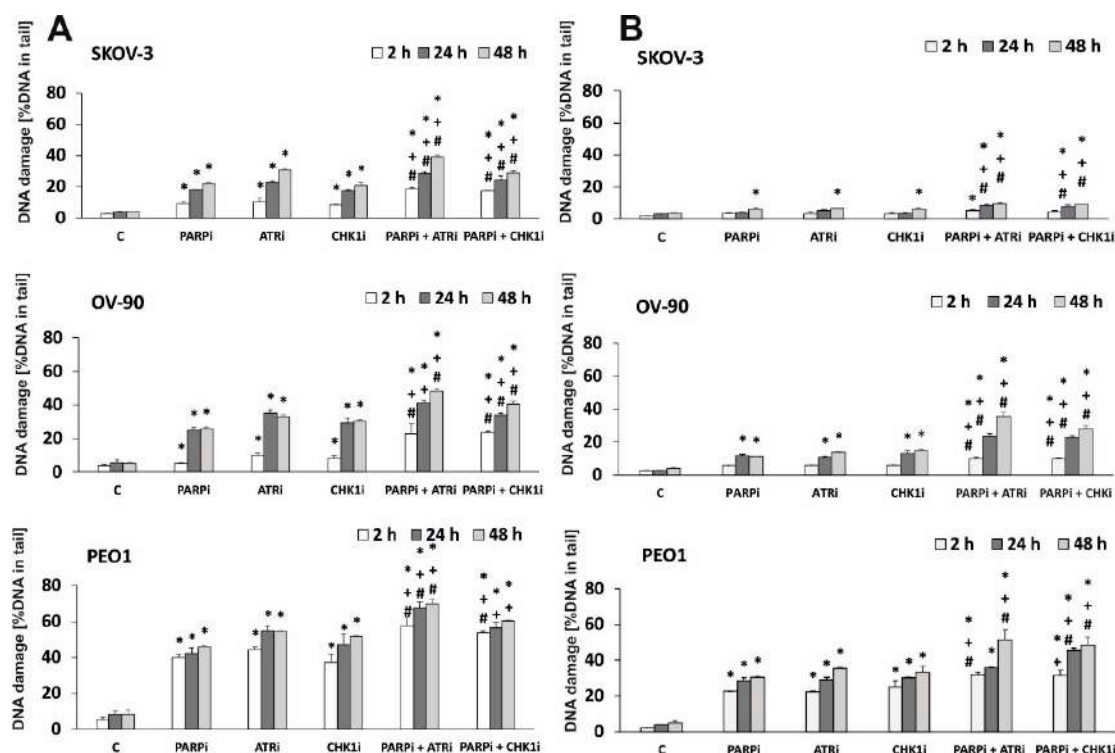


Figure 3. CHK1i and ATRi have a synergistic effect with PARPi on inducing DNA damage. The level of DNA damage in EOC cell lines treated with PARPi, ATRi, and CHK1i alone and in combination, measured as a percentage of the DNA in the comet tail. (A) The alkaline version, (B) the neutral version of the comet assay. Samples were treated for 2, 24, and 48 h. Error bars denote SD, * indicates statistically significant differences between the samples incubated with the drugs compared with control cells ($p < 0.05$). + Statistically significant differences between samples incubated with PARPi and combination treatment (PARPi/ATRi; PARPi/CHK1i) ($p < 0.05$). # Statistically significant differences between the samples incubated with ATRi or CHK1i and combination treatment (PARPi/ATRi; PARPi/CHK1i) ($p < 0.05$). Statistical analysis was performed using the ANOVA test with the Tukey's post-hoc test for multiple comparisons.

We also tested the level of DNA damage using the neutral comet assay, which directly measures DNA DBSs. PARPi/ATRi and PARPi/CHK1i significantly increased DNA damage compared with each drug alone in a time-dependent manner (Figure 3B). Taken together, these results are consistent with the synergy observed in the antiproliferative studies. The representative images of comets are shown in Supplementary Figure S1.

2.3. Combined Treatment Induces Higher Levels of Apoptosis than Monotherapy in EOC Cells

We showed that PARPi combined with ATRi and CHK1i increased DNA damage in EOC cell lines to a greater extent than PARPi, ATRi, and CHK1i alone. Because DNA damage induces apoptosis, we investigated the effect of the compounds on the caspase 3/7 ratio, a marker of apoptosis. The results are presented in Figure 4. Changes in the level of caspase 3/7 were time-dependent. Combination treatment induced apoptosis even in HR-proficient cells (SKOV-3 and OV-90 cells). PARPi, ATRi, or CHK1i alone at sub-lethal doses increased apoptosis only slightly. In all cell lines, the most significant changes in caspase activation were observed after 48 h of treatment. The PEO-1 cell line showed the highest levels of caspase 3/7 and was also the most sensitive cell line. After 48 h of treatment, ATRi combined with PARPi caused the highest increase in caspase 3/7 activity in all cell lines. For the CHK1i and PARPi combination, prolonged treatment time also caused a significant increase in caspase 3/7 activity. These results indicate that the major mechanism by which olaparib and ATRi/CHKi induced death of EOC cells may be apoptosis since we observed significant elevation of the caspase 3/7 activity. However, further studies are required to finally determine which processes are responsible for cell death.

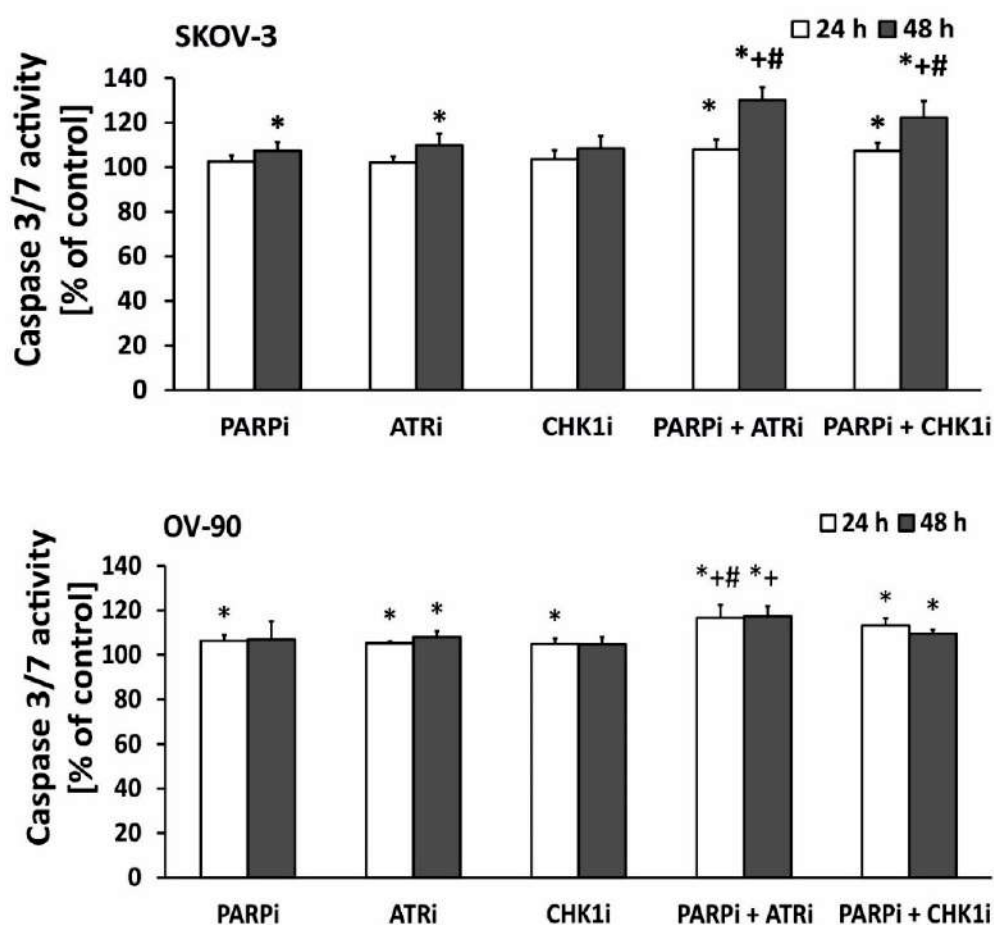


Figure 4. Cont.

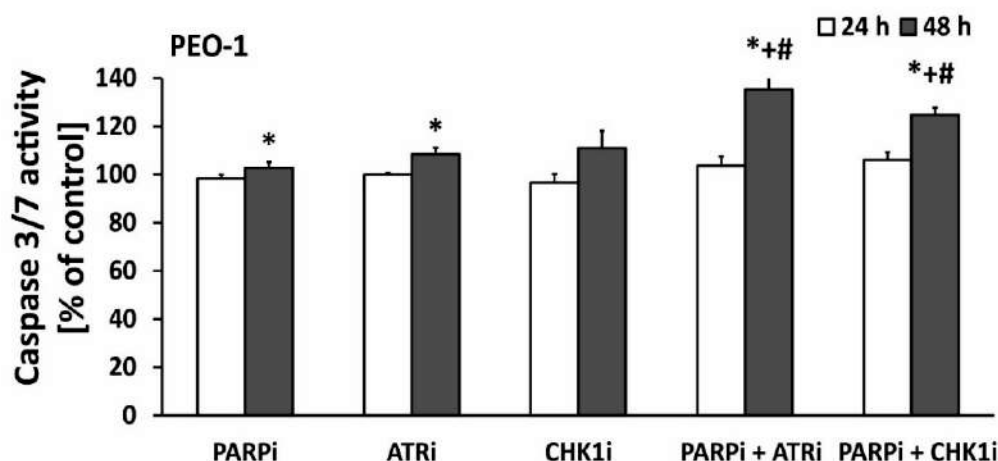


Figure 4. ATRi/CHK1i combined with PARPi increases apoptosis. Caspase 3/7 expression was used as an indicator of apoptosis in EOC cell lines exposed to 0.5 $\mu\text{mol/L}$ PARPi, 0.5 $\mu\text{mol/L}$ CHK1i, and 0.5 $\mu\text{mol/L}$ ATRi for 24 and 48 h. Untreated cells were used as controls and considered 100%. In SKOV-3 cells, apoptosis was increased by both ATRi in combination with PARPi (30%) and CHK1 combination with PARPi (22%) after 48 h of treatment. In OV-90 (p53MUT) cells, apoptosis was increased after 24 and 48 h of incubation with ATRi in combination with PARPi (16% and 17%, respectively) and CHK1 in combination with PARPi (13% and 9% respectively). In PEO-1 (BRCA2^{MUT}) cells, apoptosis was increased by ATRi in combination with PARPi (35%) and CHK1 in combination with PARPi (24%) after 48 h of treatment. Error bars denote standard deviation, * indicates statistically significant differences between the samples incubated with the drugs compared with control cells ($p < 0.05$). + Statistically significant differences between the samples incubated with PARPi and combination treatment (PARPi/ATRi; PARPi/CHK1i) ($p < 0.05$). # Statistically significant differences between samples incubated with ATRi or CHK1i and combination treatment (PARPi/ATRi; PARPi/CHK1i). Statistical analysis was performed using the ANOVA test with the Tukey's post-hoc test for multiple comparisons.

3. Discussion

First-line chemotherapy for ovarian cancer, which is usually based on a platinum drug, has little impact on the overall survival of patients. Combination treatment with carboplatin and a taxane leads to a better overall clinical response than anthracyclines in patients with ovarian cancer [31,32]. However, the slight improvement in survival is associated with a significant increase in adverse effects, underscoring the need to identify and design novel therapeutic strategies.

The discovery of drugs that induce replication stress has emerged as a new research area to identify therapies against resistant tumors or tumors with poor prognosis. Olaparib, which is the most extensively studied PARPi, constitutes a significant step forward in ovarian cancer treatment. Phase II clinical trials revealed that it increases efficacy of the standard treatment when combined with carboplatin and paclitaxel. Progression-free survival was approximately 3 months longer in the olaparib with additional chemotherapy group than in the monotherapy group. Two additional PARP inhibitors have been approved by the FDA: rucaparib (Rubraca) and niraparib (Zejula), which are a promising class of agents for targeted EOC therapy [33]. The SOLO-1 Phase III trial demonstrated that olaparib therapy reduces the risk of disease progression or death by 70% in patients with newly diagnosed advanced BRCA-mutated ovarian cancer [13]. As a result, olaparib was approved as first-line maintenance therapy for BRCA^{MUT} advanced ovarian cancer. However, a small percentage (~15%) of EOC cases are BRCA-mutated. Most patients with high-grade serous EOC exhibit a phenotype of defective HR without BRCA mutations known as BRCAness [33]. One approach to overcome the limitations of olaparib is the use of cediranib, a vascular endothelial growth factor inhibitor. Cediranib suppresses pro-survival and anti-apoptotic signaling, thereby enhancing the efficacy of olaparib against BRCA^{WT} EOC cells [34]. Despite the contribution of olaparib to modern ovarian cancer therapy, the response rate in women is not satisfactory [35]. Identifying novel and effective treatments

is extremely important. Therefore, the purpose of this study was to show that the efficacy of PARP inhibition can be increased by targeting critical cell cycle checkpoints, which may cause a significant reduction in the survival of EOC lines. Because the ATR/CHK1 pathway stabilizes replication forks and prevents DSBs [36], inhibition of ATR/CHK1 is expected to increase dependence on HR to complete replication. The combination of olaparib with anticancer agents that disrupt HR repair, namely, ATRi or CHK1i, represents a novel strategy to effectively sensitize ovarian cancer cells to olaparib.

We started our research by establishing cytotoxicity of drugs in a wide range of concentrations (0.1–30 μ M) after 120 h of continuous incubation in order to make preliminary findings on their potential efficacy in cancer therapy. We showed that PARPi, ATRi, and CHK1i are cytotoxic in all the investigated ovarian cancer cell lines (SKOV-3, resistant, among others, to doxorubicin and cisplatin, grade 1/2, serous type (S); OV-90, human ovarian papillary serous adenocarcinoma, grade 3, high-grade serous (HGS); PEO-1, (BRCA2^{MUT}; c.C4965G) grade 3). The results obtained by George et al. [37] are similar to our observations. They demonstrated that olaparib at 1 μ M was significantly more cytotoxic to BRCA^{MUT} cell lines (PEO-1, JHOS4) than to the BRCA^{REV} (BRCA reverse) platinum-resistant PEO-4 cell line. Similar to PARPi, CHK1i was significantly more cytotoxic in BRCA2^{MUT} cells than in BRCA^{WT} ovarian cancer cells. On the other hand, ATRi (AZD6738) was cytotoxic to both BRCA^{MUT} and BRCA^{WT} cells [37]. In another study, it was shown that olaparib, after 5 days of treatment in the 0.1–1 μ M range of concentration, was more cytotoxic in BRCA^{MUT} cells (PEO-1, JHOS4) compared with HR-proficient cells (PEO4^{REV}, WO-20 ATR/CHK1 primary tumor cultures, BRCA^{WT}). The authors also demonstrated that CHK1i (0.1–10 μ M) was more effective in BRCA^{MUT} cells than in BRCA^{WT} cells as compared to ATRi (0.1–5 μ M), which was equally active in all the tested cell lines [38].

We showed that ATRi and CHK1i increased the effect of olaparib in all the investigated ovarian cancer cell lines. To confirm the toxicity of the tested compounds and their combination, we performed a long-term survival assay (colony formation assay). The results were particularly significant in HR-deficient PEO-1 cells, in which combination therapy with ATRi decreased cell viability most effectively compared with olaparib alone. In HR-proficient lines (OV-90, SKOV-3), both combinations of inhibitors were also highly effective. Our results are in accordance with the study by Kim et al. [38] who revealed that the colony-forming ability after treatment with ATRi in combination with PARPi had been decreased. This observation confirmed a significantly higher cytotoxicity of the combination of ATRi and PARPi than the cytotoxicity of either drug alone in both BRCA2-deficient and wild-type cells [38]. The same group of authors extended cytotoxicity determination with multiple cell lines. Using Kuramochi (BRCA2^{MUT}), FUOV1 (CCNE1-amplified; CCNE1^{AMP}, Cyclin E gene amplification), OVKATE (BRCA^{WT} and CCNE1 copy normal), COV318 (CCNE1^{AMP}), and OVCAR3 (CCNE1^{AMP}), they reported findings similar to their previous study [39]. Moreover, ATR/CHK1 and DNA repair pathways were confirmed to be significantly altered in PARPi-resistant cells (PEO1-PR). ATRi alone was insufficient to overcome PARPi resistance in comparison to ATRi combined with PARPi [39]. Another study showed that the combination of PARPi with ATRi or CHK1i is as cytotoxic as the standard chemotherapy (carboplatin/paclitaxel) in BRCA^{MUT} cells (PEO-1, JHOS4) [37]. The combination of olaparib with both ATRi and CHK1i drastically decreases the viability of UWB-BRCA1^{MUT} ovarian cancer cells and UWB1-resistant cells compared with single agent administration [40]. Moreover, olaparib acts synergistically with ATRi (AZD6738) in ATM deficient cancer cells [41]. Combined treatment with ATRi and PARPi caused 84% cell death of ATM deficient cancer cells in contrast to only 37% growth inhibition in ATM-proficient wild-type cells [42]. The ATRi VE-821 sensitizes OVCAR-8, SKOV-3, and PEO-1 ovarian cancer cells to common chemotherapeutics, such as cisplatin, topotecan, and veliparib [26]. Furthermore, prexasertib (CHK1i) and olaparib monotherapy decrease cell viability in a dose-dependent manner in both BRCA^{WT} and BRCA^{MUT} ovarian cancer cells (OVCAR-3, OV-90, PEO-1, and PEO-4). Synergism was assessed at the lowest doses of prexasertib/olaparib (5 nM/5 μ M) [43].

PARP1 coordinates and increases the speed of DNA repair, probably by detecting DNA lesions. The enzyme is essential not only for SSB repair binding, but also for DSBs, and is involved in the restart of stalled forks after release from replication blocks [44]. Small molecule inhibitors of PARP

inhibit PARP activity, thereby preventing the dissociation of PARP from DNA damage sites on chromatin [45]. We detected a significant increase in PARP1 expression in all cell lines after exposure to olaparib. The combined action of the inhibitors led to a decrease in PARP expression in all cell lines. Osoegawa et al. showed that the basal level of PARP activity is positively correlated with PARP abundance in solid tumor cells [46], which is consistent with results of the present study. Other studies showed that PARP expression increases after exposure to 1.5 μ M olaparib for 24 or 48 h. Studies on cervical cancer found a direct correlation between the abundance of PARP, its activity, and sensitivity to olaparib treatment. Cell lines with higher PARP expression are more sensitive to olaparib [47].

This study confirmed the link between PARP expression and the sensitivity to PARPi or inhibitors of replication stress proteins. DSBs and SSBs may result from the inactivation of tumor suppressor genes, activation of oncogenes, and alterations in the structure of mutator genes [48]. Aberrant products of ATR/CHK1 pathway genes may contribute to the induction, promotion, and progression of cancer transformation. DNA repair is the main cellular response to DNA damage. If cellular repair systems are ineffective against DNA damage, the repair time may be prolonged to allow for checkpoint activation [49]. PARPi increases ATR/CHK1 signaling and causes replication fork collapse into DSBs through different mechanisms. Thus, the combination of ATRi or CHK1i with PARPi would be more effective to diminish cancer cell survival. In the present study, we assessed the overall level of DNA damage, including SSBs and DSBs, using the alkaline and neutral variants of the comet assay. The results showed that ATRi and CHK1i had a marked effect on DNA strand breaks, inducing damage in all cell lines. Recently, the presence of DSBs was monitored by measuring the DSB marker γ H2AX in BRCA2^{MUT} cells. The level of γ H2AX increases in BRCA2^{MUT} cells relative to wild-type cells in the S-phase. The study suggests that fork destabilization or defects during the S-phase might be a source of DNA damage and leads to elevated sensitivity to combined action of PARPi and ATRi [38]. Prexasertib (CHK1i) predisposes cells to DSBs and allows cells to die [50]. ATR and CHK1 are pro-survival proteins playing a critical role in maintaining genome integrity against DNA damage. Synthetic lethality is a cellular phenomenon, indicating that simultaneous inactivation of two or more genes, which are nonlethal when inactivated alone, become lethal when inactivated together. Moreover, it is a consequence of the tendency to maintain genome stability despite various alterations occurring in the cell. Although BRCA^{MUT} tumors are selectively sensitive to PARPi [51], even a small number of persistent DSBs may be dangerous for the cancer cell. Simultaneous administration of ATRi/CHK1i and PARPi induced a higher level of DSBs than both compounds administered as single agents. Previously, it was described that PARPi/ATRi treatment exerts its dominant effects on replication by slowing fork progression and increasing fork asymmetry that leads to DSBs [39].

The highest level of DNA damage occurred in the BRCA^{MUT} cell line (PEO-1), although DNA damage was also observed in HR-proficient lines, such as SKOV-3 and OV-90 (HGSOCs) cells with p53^{MUT}. The synergistic effect observed in our study was the result of high accumulation of DSBs after combination treatment with ATRi or CHK1i and olaparib in HR-deficient and HR-proficient cell lines. The increased genotoxic effect of the combined action of inhibitors may be related to a mutation in the p53 gene in the OV-90 line. The tumor suppressor p53 plays a crucial role in the DNA damage response. Mutation or loss of p53 occurs in approximately 50% of cancers [52]. However, whether p53 is a useful biomarker of the effect of RSR inhibitor treatment remains unclear. In this study, the OV-90 line was more sensitive to inhibitor treatment than the SKOV-3 line. Previous studies showed that checkpoint inhibitors synergize with genotoxins more effectively in cells with defects in the p53 pathway than in p53-proficient cells, which may be related to the increased replication stress caused by a relaxed S-phase entry [27,53]. Olaparib therapy combined with CHK1i selectively radiosensitizes p53 mutant pancreatic cancer cells, suggesting that inhibition of HR by CHK1i is a useful strategy for selective induction of a BRCA1 “deficient-like” phenotype in p53 mutant tumor cells sparing normal tissue [54].

The present results showing the effectiveness of the synergistic action of olaparib with the standard drug therapy or RSR modulators are consistent with previous studies. CDK4/6 inhibition by palbociclib has a synthetic lethal effect in combination with PARP inhibition by olaparib by inducing HR deficiency

in a MYC-dependent manner in HGSOCs [55]. Combination treatment with BKM120 (phosphoinositide 3-kinase, PI3K, inhibitor) and olaparib is more effective than single agent treatment for inducing DNA damage in OVCAR-433, OVCAR-5, and OVCAR-8 cells, as indicated by the production of large numbers of DNA DSBs as a result of dual inhibition of PI3K and PARP. The combination of BKM120 and olaparib is effective in ovarian cancers with a broader spectrum of cancer-associated genetic alterations, but not limited to those with mutant PI3KCA or BRCA genes [56]. Exposure of cells to PARPi PJ34 blocks CHK1i-induced PARP1 activation and PARP1 adenosine diphosphate (ADP) ribosylation [57]. Suppression of ATR by VE-821 (ATRi) can affect HR repair in ovarian cancer cells, leading to accumulation of DNA DSBs in cell nuclei, thereby increasing the sensitivity of ovarian cancer SKOV-3 cells to cisplatin [58]. Therefore, inhibition of ATR/CHK1 and PARP together increases DSB generation from fork collapse and diminished alternative DNA repair mechanisms.

Cells treated with replication stress inhibitors die through two major pathways: apoptosis (the predominant type of programmed cell death) or necrosis. Both processes differ biochemically and morphologically. Cell destruction through the apoptotic pathway is the most effective way to eradicate cancer cells because it does not cause inflammation in adjacent healthy tissues. Programmed cell death ensures removal of mutated, infected, or damaged cells and maintains normal tissue homeostasis, regulating the balance between cell division and a “silent disappearance” of cells. The proliferation and colony formation assays used in this study did not clarify whether the toxic effects of the investigated drugs resulted from the activation of the apoptotic cell death machinery. PARPi, as well as ATRi and CHK1i, also cause necrotic cell death. Therefore, we examined the type of cell death induced by the drugs and the role of apoptosis in their cytotoxic and antiproliferative activities. Members of the caspase family are crucial mediators of the complex biochemical events associated with apoptosis. Caspase 3, a key effector in the apoptotic pathway, amplifies the signal from initiator caspases leading to full commitment to cellular disassembly. It was demonstrated that PARPi/ATRi combination treatment significantly increased apoptosis compared with monotherapy in HR-deficient and HR-proficient ovarian cancer cells. Our results are in agreement with the study performed on BRCA^{MUT} PEO-1 and BRCA^{REV} PEO-4 cell lines. Cleaved caspase 3 after 48 h of treatment with 1 μ M CHK1i and 1 μ M ATRi was significantly increased as compared with untreated control cells. However, contrary to our results, the combination of PARPi/ATRi and PARPi/CHK1i did not substantially increase caspase 3 in relation to each agent alone [38]. Interestingly, the combination of drugs led to worse apoptosis than monotherapy in the olaparib and carboplatin-resistant cell lines (PEO1-PR, JHOS4-PR, PEO1-CR, OVCAR-3) [39]. Additional studies are necessary to confirm whether apoptosis is a leading process responsible for cytotoxicity of tested inhibitors' combinations.

The presented results indicate that ovarian cells harboring loss-of-function mutations other than BRCA may also benefit from novel treatments. In addition, most EOC patients are BRCA^{WT}, underscoring the importance of these results. We also showed that the combination of ATRi and PARPi is more cytotoxic than that of CHK1i and PARPi. Thus, ATR may stabilize replication forks independently from CHK1 [59]. Our observation can also be explained by the action of MRE11 that mediates PARPi sensitivity of BRCA1-deficient cells. ATRi disrupts BRCA1-independent RAD51 leading to DSBs and stalled forks in PARPi-resistant BRCA1-deficient cells. Thus, ATRi enables MRE11-mediated fork degradation [60]. Another study also confirmed that ATR plays the main role in avoiding replication catastrophe. Two- to ten-fold reduction in fork speed led to global chromatin recruitment of sensors and mediators of the ATR pathway without substantial activation of CHK1, ATM, or p53. Analysis of the cell phenotypes depleted of ATR or CHK1 and their exposure to moderate levels of stress shows that ATR, but not CHK1, is crucial for common fragile site (CFS) integrity. Moreover, in ATR-deficient cells, single stranded DNA (ssDNA) foci result from the MRE11-dependent resection of collapsed forks, suggesting that long stretches of ssDNA are a consequence rather than a cause of CFS instability [61]. It is also known that RPA protein (replication protein A) binds to single-stranded DNA generated in the replication forks. The study by Toledo et al. confirmed that if replication is blocked, ssDNA is formed, linked to RPA, and led to the recruitment of the ATR kinase. Although ATR

requires the RPA-coated ssDNA for its own activation, the endpoint of ATR signaling to protect forks against fatal breakage also feeds back on the level of RPA. Partial reduction in RPA enhanced fork breakage and forced elevation of RPA was sufficient to delay such replication catastrophe even in the absence of ATR activity. ATR inhibition increases ssDNA break generation up to the point where it would deplete all available RPA [62]. The research by Mengwasser et al. also points to the extremely important role of ATR kinases. They found that BRCA2^{MUT} cells (colonic DLD-1 BRCA2^{MUT} cell line and PEO-1 BRCA2^{MUT}) are dependent on ATR activation; that was confirmed by using VE-821 as ATRi. Ape2 (Apurinic/aprimidinic endonuclease) depletion led to a more prominent phosphorylation of CHK1 and RPA32 in the BRCA2^{MUT} cell line than in the BRCA2^{WT} cell line (C4-2 clone that contains BRCA^{REV} selected for cisplatin resistance), suggesting increased ATR activation [63].

Although the efficacy of the PARPi/ATRi and PARPi/CHK1i combinations differed, each of these combinations was significantly more effective than single agent treatment in ovarian cancer cells.

4. Materials and Methods

4.1. Reagents

Culture media (RPMI 1640, DMEM) were obtained from Gibco (Thermo Fisher Scientific, Waltham, MA, USA), and fetal bovine serum (FBS) was from Capricorn Scientific GmbH (Ebsdorfergrund, Germany); trypsin–EDTA, penicillin, and streptomycin were acquired from Sigma-Aldrich (St. Louis, MO, USA). CellEvent™ Caspase-3/7 Green Detection Reagent was from Thermo Fisher Scientific, Waltham, MA, USA (cat # C10423). PARPi (AZD2281), ATRi (AZD6738), and CHK1i (MK8776) were purchased from Selleckchem (Munich, Germany). Other chemicals and solvents were of high analytical grade and were obtained from Sigma-Aldrich or Avantor Performance Materials Poland S.A. (Gliwice, Poland).

4.2. Cell Culture and Drug Administration

The human OV-90 (human malignant papillary serous carcinoma, American Type Culture Collection (ATCC) CRL-11732™) and SKOV-3 (human ovarian adenocarcinoma, ATCC HTB-77) cell lines were bought from ATCC (Rockville, MD, USA), and PEO-1 cells (human ovarian cancer; estrogen rec, 10032308) for preliminary research were donated by Dr. Gallo (Fondazione Policlinico Universitario A. Gemelli, IRCCS, Rome, Italy), and then bought from the European Collection of Authenticated Cell Cultures. The newly received cells were expanded and aliquots of less than 10 passages were stored in liquid nitrogen. All cell lines were kept at low passage, returning to original frozen stocks every 6 months. During the course of the study, cells were thawed and passaged within 2 months in each experiment. The cells were cultured in DMEM and RPMI with 10% FBS, penicillin (10 U/mL), and streptomycin (50 µg/mL) and regularly checked for mycoplasma contamination. The cells were cultured in an atmosphere of 5% CO₂ and 95% air at 37 °C.

4.3. MTT Assay

To select the most effective PARPi/ATRi and PARPi/CHK1i ratios, several concentration ratios of the compounds (1:1; 2:1; 10:1; 1:2; 1:10) were tested at the lowest effective concentration based on the survival curve (0.5 µM). To analyze the drug interaction between ATRi and CHK1i and PARPi combined with either agent, the coefficient of drug interaction (CDI) was calculated [64]. The CDI is defined by the following formula: $CDI = AB/(A \times B)$. According to the absorbance of each group, AB is the ratio of the two-drug combination group to the untreated control group, and A or B is the ratio of the single drug group to the control group. A CDI < 1 indicates synergism, CDI < 0.7—significant synergism, CDI = 1—additivity, and CDI > 1—antagonism.

4.4. Clonogenic Assay

The effect of PARPi, CHK1i, and ATRi on cell growth was assessed using a clonogenic assay. For this analysis, 200 cells were plated onto six-well plates in a growth medium, and after overnight

attachment, cells were exposed to the test compounds for 5 days. The cells were washed with a fresh medium and allowed to grow for 10–14 days under drug-free conditions. Then, the cell colonies were fixed with methanol mixed with acetic acid (7:1) for 10 min and stained with 0.5% crystal violet for 20 min. The plates were rinsed with water, air-dried, photographed, and evaluated for colony estimation. Colonies containing more than 50 cells were counted. For each sample, the results from three replicates were averaged.

4.5. Morphological Assessment

SKOV-3, OV-90, and PEO-1 cells were treated with olaparib, ATRi, CHK1i, and a combination of PARPi with ATRi or PARPi with CHK1i, each at a concentration of 0.5 μ M, for 24 h and then examined under an inverted optical microscope (Olympus IX70, Tokyo, Japan).

4.6. Western Blot Analysis

The cells were lysed in a cell extraction buffer (Invitrogen™, Waltham, MA, USA) containing a protease inhibitor cocktail and phenylmethylsulfonyl fluoride (PMSF) (Roche, Mannheim, Germany) in accordance with the manufacturer's protocol. The protein concentration was determined using the Bradford method. SDS polyacrylamide gel electrophoresis and the wet transfer of proteins (35 μ g per lane) onto 0.45 μ m polyvinylidene difluoride (PVDF) membranes were performed using standard procedures. To confirm equal loading and transfer, Precision Plus Protein™ WesternC™ Blotting Standards were used. After blocking nonspecific sites using 5% bovine serum albumin (BSA) (Sigma-Aldrich) or 5% non-fat dry milk, membranes were incubated with the rabbit monoclonal antibody against PARP at a dilution of 1/1000 (cat. # 9532), phospho-ATR (Thr1989) (cat. # 30632), total ATR (cat. # 13934), phospho-CHK1 (Ser345) (cat. # 2348), and glyceraldehyde 3-phosphate dehydrogenase (GAPDH) (cat. #2118), all from Cell Signaling Technology, Inc. (Danvers, MA, USA), and the rabbit anti-CHK1 polyclonal antibody (cat. # STJ92269, St John's Laboratory). The membranes were then exposed to the anti-rabbit IgG horseradish peroxidase-conjugated secondary antibody (cat. # 7074, Cell Signaling Technology), followed by detection using a chemiluminescent substrate (Thermo Fisher Scientific, Waltham, MA, USA). Immunoreactive bands were visualized using a DNR MicroChemi system. Band intensities were quantified using the ImageJ software (NIH, Bethesda, MD, USA). The integrated optical density of the bands was measured in a digitized image. Relative expression was expressed as the ratio of the densitometric volume of the test band to that of the respective GAPDH band.

4.7. Comet Assay

The alkaline version of single cell gel electrophoresis (comet assay) was used to detect alkali-labile sites, single-strand breaks (SSBs), and DSBs caused by exposure to the tested compounds. Each experiment was repeated three times. In the neutral versions, the tail DNA percentage is positively correlated with DSBs. The cells were plated on 12-well plates (105 cells/well) and treated with PARPi, ATRi, CHK1i, and their combination at the 0.5 μ M dose for 2, 24, and 48 h at 37 °C. Next, the cells were collected into Eppendorf tubes and rinsed with PBS. The cells were then suspended in 0.75% low melting point agarose dissolved in PBS (pH 7.4) and placed on microscope slides precoated with 0.5% normal melting point agarose. Subsequently, the slides were treated with a cooled lysis buffer (2.5 M NaCl, 100 mM EDTA, 10 mM Tris, 1% Triton X-100, pH 9.0) for 1–24 h at 4 °C. Then, slides were placed in the developing buffer (300 mM NaOH, 1 mM EDTA) for 20 min. Electrophoresis was performed in a buffer composed of 30 mM NaOH and 1 mM EDTA at 0.73 V/cm and 290 mA for 20 min. In the neutral version of the comet assay, electrophoresis was run in a buffer consisting of 100 mM Tris and 300 mM sodium acetate, with the pH adjusted to 9.0 using glacial acetic acid. Electrophoresis was performed for 60 min after a 20 min equilibrium period at an electric field strength of 0.41 V/cm and 50 mA at 4 °C.

The samples were stained with 4,6-diamidino-2-phenylindole (DAPI) (1 g/mL). The slides were stored in a wet chamber at 4 °C and analyzed under a fluorescence microscope. Fifty randomly selected

cells from each slide were measured using an image analysis system (Nikon, Japan) attached to a COHU 4910 video camera, which was equipped with a UV-1 filter block consisting of an excitation filter (359 nm) and a barrier filter (461 nm) connected to the image analysis system Lucia-Comet v. 4.51 (Laboratory Imaging, Prague, Czech Republic) [30].

4.8. Caspase 3/7 Assay

The activities of caspases 3 and 7 were estimated with CellEvent™ Caspase-3/7 Green Detection Reagent (Thermo Fisher Scientific, Waltham, MA, USA) according to the manufacturer's protocol. The cells were seeded on 96-well plates (15 × 103/well) and after 24 h they were incubated with the appropriate drugs for 24 h or 48 h. The cells were fixed by adding a final concentration of 4% paraformaldehyde solution (10 min, room temperature). Cells were labeled with CellEvent™ Caspase-3/7 Green Detection Reagent (5 μM) diluted in PBS with 5% FBS to avoid fluorescence background. After activation of caspase 3/7 in apoptotic cells, the four amino acid (Asp-Glu-Val-Asp, DEVD) peptide was cleaved, enabling the dye to bind to DNA, which produced a bright fluorogenic response with absorption/emission maxima of 502/530 nm according to the manufacturer's protocol. Fluorescence intensity was measured using a Fluoroskan Ascent FL plate reader (Labsystem, Stockholm, Sweden). Cysteine protease activity was expressed as a ratio of the fluorescence of drug-treated samples to that of the corresponding untreated controls (taken as 100%).

4.9. Statistical Analysis

The data are presented as means ± SD of at least three independent experiments. Statistical analyses were performed with the Student's t-test and ANOVA with the Tukey's post-hoc test for multiple comparisons as appropriate (StatSoft, Tulsa, OK, USA) [30]. *p*-values < 0.05 were considered statistically significant.

5. Conclusions

ATR and CHK1 suppressed DNA break formation and induced DSB repair to remove DNA damage (Figure 5). PARPi increased the dependence on ATR/CHK1 for maintaining genome stability. Combination treatment with PARPi and ATRi completely suppressed ovarian cell growth independently from HR effectiveness. Inhibition of ATR or CHK1 concomitant with PARP inhibition increased DSB generation, resulting in apoptosis induction. The present results were obtained at sub-lethal doses, underscoring the high potential of the inhibitors tested. The effect of PARPi/ATRi and PARPi/CHK1i was dependent on the genetics of the tumor. The present results confirmed the sensitivity of ovarian cancer cells to CHK1i and especially to ATRi. The simultaneous use of olaparib with inhibitors of RSR proteins leads to synthetic lethality and sensitizes cells to olaparib therapy by blocking DNA repair. Thus, the present data may provide new prospects for the treatment of ovarian cancer patients and establish a basis for further research.

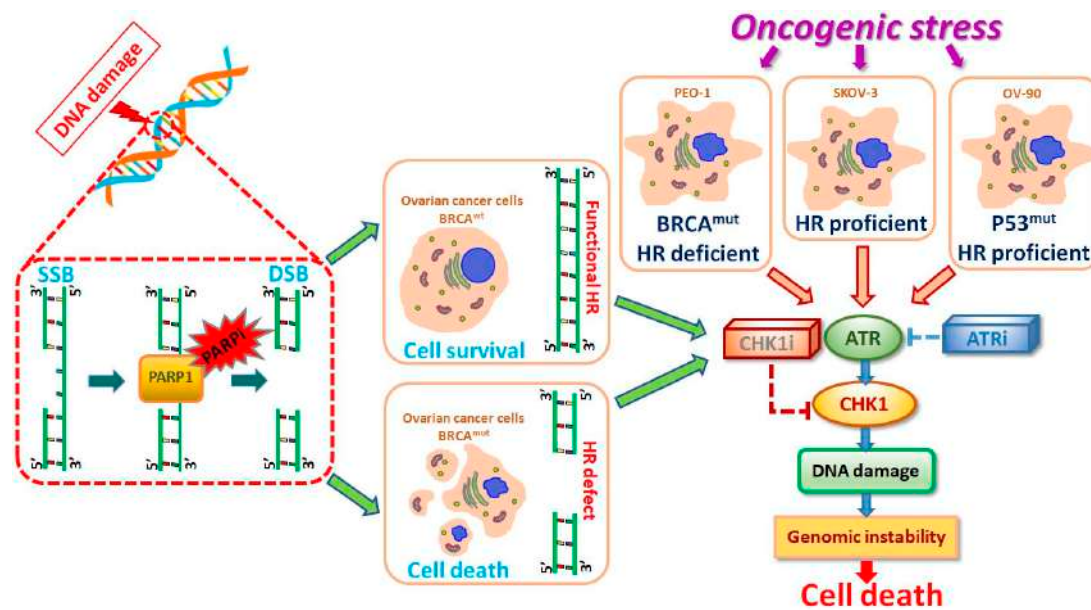


Figure 5. Proposed model of the molecular and cellular responses to new replication stress inhibitors. ATR/CHK1 stabilizes replication forks and prevents their collapse into DSBs. SSBs can be accurately repaired using the undamaged strand as a template, a process involving the PARP enzyme. SSBs are mainly repaired through the homologous recombination (HR) pathway. BRCA is related to the error-free repair of DSBs by HR. ATRi or CHK1i in monotherapy and in combined treatment with PARPi cause genome instability and leads to the synthetic lethality of ovarian cancer cells.

Supplementary Materials: The following are available online at <http://www.mdpi.com/1422-0067/21/24/9715/s1>.

Author Contributions: Conceptualization, P.G., A.G., A.M., and A.R.; data curation, P.G., A.G., and A.R.; formal analysis, P.G., A.G., and A.R.; funding acquisition, A.M. and A.R.; methodology, P.G., A.G., and A.R.; writing—original draft, P.G., A.G., and A.R.; writing—review and editing, P.G., A.G., A.M., M.M., J.O., A.S., and A.R. All authors have read and agreed to the published version of the manuscript.

Funding: This research was funded by the Polish National Science Centre (project grant number Sonata Bis 2019/34/E/NZ7/00056; grant approval date: 18.02.2020) and supported by a statutory research grant for the Department of Medical Biophysics of the University of Lodz No. B181100000190.01.

Acknowledgments: The authors would like to thank Daniela Gallo (Fondazione Policlinico Universitario A. Gemelli, IRCCS, 00168, Rome, Italy), Marta De Donato (Fondazione Policlinico Universitario A. Gemelli, IRCCS, 00168, Rome, Italy), and Maria Cristina De Rosa (Institute of Chemical Sciences and Technologies “Giulio Natta” (SCITEC)-CNR, 00168, Rome, Italy) for donating the PEO-1 cell line for preliminary research.

Conflicts of Interest: The authors declare no conflict of interest.

Abbreviations

ADP	Adenosine diphosphate
ATM	Ataxia telangiectasia mutated protein
ATR	Ataxia telangiectasia and Rad3-related protein
ATRi	Ataxia telangiectasia and Rad3-related protein inhibitor
BSA	Bovine serum albumin
CDI	Coefficient of drug interaction
CHK1	Checkpoint kinase 1
CHK1i	Checkpoint kinase 1 inhibitor
DAPI	4,6-diamidino-2-phenylindole
DSB	Double-strand break
FANCI	Fanconi anemia complementation group I
GAPDH	Glyceraldehyde 3-phosphate dehydrogenase
HRR	Homologous recombination repair
MCM2	DNA replication licensing factor
MTT	3-(4,5-Dimethylthiazol-2-yl)-2,5-Diphenyltetrazolium Bromide

PARP	Poly (ADP-ribose) polymerase
PARPi	Poly (ADP-ribose) polymerase inhibitor
PMSF	Phenylmethylsulfonyl fluoride
PVDF	Polyvinylidene difluoride
RPA	Replication protein A
SMARCAL1	SWI/SNF-related matrix-associated actin-dependent regulator of chromatin subfamily A-like protein 1
SSB	Single-strand break
ssDNA	single stranded DNA
WRN	Werner syndrome ATP-dependent helicase

References

1. He, S.; Zhang, C.; Liu, L.; Li, L.; Duan, Y.; Liu, J.; Shao, F. Efficacy and safety of PARP inhibitors as the maintenance therapy in ovarian cancer: A meta-analysis of nine randomized controlled trials. *Biosci. Rep.* **2020**, *40*. [[CrossRef](#)]
2. Integrated genomic analyses of ovarian carcinoma. *Nature* **2011**, *474*, 609–615. [[CrossRef](#)] [[PubMed](#)]
3. Buttarelli, M.; De Donato, M.; Raspaglio, G.; Babini, G.; Ciucci, A.; Martinelli, E.; Baccaro, P.; Pasciuto, T.; Fagotti, A.; Scambia, G.; et al. Clinical Value of lncRNA MEG3 in High-Grade Serous Ovarian Cancer. *Cancers* **2020**, *12*, 966. [[CrossRef](#)] [[PubMed](#)]
4. Konstantinopoulos, P.A.; Ceccaldi, R.; Shapiro, G.I.; D'Andrea, A.D. Homologous Recombination Deficiency: Exploiting the Fundamental Vulnerability of Ovarian Cancer. *Cancer Discov.* **2015**, *5*, 1137–1154. [[CrossRef](#)] [[PubMed](#)]
5. Choi, M.C.; Hwang, S.; Kim, S.; Jung, S.G.; Park, H.; Joo, W.D.; Song, S.H.; Lee, C.; Kim, T.-H.; Kang, H.; et al. Clinical Impact of Somatic Variants in Homologous Recombination Repair-Related Genes in Ovarian High-Grade Serous Carcinoma. *Cancer Res. Treat.* **2020**, *52*, 634–644. [[CrossRef](#)] [[PubMed](#)]
6. Martí, J.M.; Fernández-Cortés, M.; Serrano-Sáenz, S.; Zamudio-Martinez, E.; Delgado-Bellido, D.; Garcia-Diaz, A.; Oliver, F.J. The Multifactorial Role of PARP-1 in Tumor Microenvironment. *Cancers* **2020**, *12*, 739. [[CrossRef](#)]
7. Bohrer, R.C.; Dicks, N.; Gutierrez, K.; Duggavathi, R.; Bordignon, V. Double-strand DNA breaks are mainly repaired by the homologous recombination pathway in early developing swine embryos. *FASEB J.* **2018**, *32*, 1818–1829. [[CrossRef](#)]
8. Spriggs, D.R.; Longo, D.L. Progress in BRCA-Mutated Ovarian Cancer. *N. Engl. J. Med.* **2018**, *379*, 2567–2568. [[CrossRef](#)]
9. Sánchez, H.; Paul, M.W.; Grosbart, M.; Van Rossum-Fikkert, S.E.; Lebbink, J.H.G.; Kanaar, R.; Houtsmuller, A.B.; Wyman, C. Architectural plasticity of human BRCA2–RAD51 complexes in DNA break repair. *Nucleic Acids Res.* **2017**, *45*, 4507–4518. [[CrossRef](#)]
10. Rajawat, J.; Shukla, N.; Mishra, D.P. Therapeutic Targeting of Poly(ADP-Ribose) Polymerase-1 (PARP1) in Cancer: Current Developments, Therapeutic Strategies, and Future Opportunities. *Med. Res. Rev.* **2017**, *37*, 1461–1491. [[CrossRef](#)]
11. Tinker, A.V.; Gelmon, K. The role of PARP inhibitors in the treatment of ovarian carcinomas. *Curr. Pharm. Des.* **2012**, *18*, 3770–3774. [[CrossRef](#)] [[PubMed](#)]
12. Kim, G.; Ison, G.; McKee, A.E.; Zhang, H.; Tang, S.; Gwise, T.; Sridhara, R.; Lee, E.; Tzou, A.; Philip, R.; et al. FDA Approval Summary: Olaparib Monotherapy in Patients with Deleterious Germline BRCA-Mutated Advanced Ovarian Cancer Treated with Three or More Lines of Chemotherapy. *Clin. Cancer Res.* **2015**, *21*, 4257–4261. [[CrossRef](#)] [[PubMed](#)]
13. Moore, K.; Colombo, N.; Scambia, G.; Kim, B.-G.; Oaknin, A.; Friedlander, M.; Lisyanskaya, A.; Floquet, A.; Leary, A.; Sonke, G.S.; et al. Maintenance Olaparib in Patients with Newly Diagnosed Advanced Ovarian Cancer. *N. Engl. J. Med.* **2018**, *379*, 2495–2505. [[CrossRef](#)] [[PubMed](#)]
14. Consortium, A.P.G. AACR Project GENIE: Powering Precision Medicine through an International Consortium. *Cancer Discov.* **2017**, *7*, 818–831. [[CrossRef](#)] [[PubMed](#)]
15. Pettitt, S.J.; Krastev, D.B.; Brandsma, I.; Drean, A.; Song, F.; Aleksandrov, R.; Harrell, M.I.; Menon, M.; Brough, R.; Campbell, J.; et al. Genome-wide and high-density CRISPR-Cas9 screens identify point mutations in PARP1 causing PARP inhibitor resistance. *Nat. Commun.* **2018**, *9*, 1849. [[CrossRef](#)]
16. Montemorano, L.; Lightfoot, M.; Bixel, K. Role of Olaparib as Maintenance Treatment for Ovarian Cancer: The Evidence to Date. *OncoTargets Ther.* **2019**, *12*, 11497–11506. [[CrossRef](#)]

17. Engelke, C.G.; Parsels, L.A.; Qian, Y.; Zhang, Q.; Karnak, D.; Robertson, J.R.; Tanska, D.M.; Wei, D.; Davis, M.A.; Parsels, J.D.; et al. Sensitization of Pancreatic Cancer to Chemoradiation by the Chk1 Inhibitor MK8776. *Clin. Cancer Res.* **2013**, *19*, 4412–4421. [[CrossRef](#)]
18. Gupta, D.; Lin, B.; Cowan, A.; Heinen, C.D. ATR-Chk1 activation mitigates replication stress caused by mismatch repair-dependent processing of DNA damage. *Proc. Natl. Acad. Sci. USA* **2018**, *115*, 1523–1528. [[CrossRef](#)]
19. Menolfi, D.; Zha, S. ATM, ATR and DNA-PKcs kinases—The lessons from the mouse models: Inhibition ≠ deletion. *Cell Biosci.* **2020**, *10*. [[CrossRef](#)]
20. Saldivar, J.C.; Cortez, D.; Cimprich, K.A. The essential kinase ATR: Ensuring faithful duplication of a challenging genome. *Nat. Rev. Mol. Cell Biol.* **2017**, *18*, 622–636. [[CrossRef](#)]
21. Zhang, X.; Lu, X.; Akhter, S.; Georgescu, M.-M.; Legerski, R.J. FANCI is a negative regulator of Akt activation. *Cell Cycle* **2016**, *15*, 1134–1143. [[CrossRef](#)] [[PubMed](#)]
22. Yeom, G.; Kim, J.; Park, C.-J. Investigation of the core binding regions of human Werner syndrome and Fanconi anemia group J helicases on replication protein A. *Sci. Rep.* **2019**, *9*. [[CrossRef](#)]
23. Pugliese, G.M.; Salaris, F.; Palermo, V.; Marabitti, V.; Morina, N.; Rosa, A.; Franchitto, A.; Pichierri, P. Inducible SMARCAL1 knockdown in iPSC reveals a link between replication stress and altered expression of master differentiation genes. *Dis. Models Mech.* **2019**, *12*. [[CrossRef](#)] [[PubMed](#)]
24. Kim, H.-J.; Min, A.; Im, S.-A.; Jang, H.; Lee, K.H.; Lau, A.; Lee, M.; Kim, S.; Yang, Y.; Kim, J.; et al. Anti-tumor activity of the ATR inhibitor AZD6738 in HER2 positive breast cancer cells. *Int. J. Cancer* **2017**, *140*, 109–119. [[CrossRef](#)] [[PubMed](#)]
25. Gamper, A.M.; Rofougaran, R.; Watkins, S.C.; Greenberger, J.S.; Beumer, J.H.; Bakkenist, C.J. ATR kinase activation in G1 phase facilitates the repair of ionizing radiation-induced DNA damage. *Nucleic Acids Res.* **2013**, *41*, 10334–10344. [[CrossRef](#)] [[PubMed](#)]
26. Huntoon, C.J.; Flatten, K.S.; Wahner Hendrickson, A.E.; Huehls, A.M.; Sutor, S.L.; Kaufmann, S.H.; Karnitz, L.M. ATR Inhibition Broadly Sensitizes Ovarian Cancer Cells to Chemotherapy Independent of BRCA Status. *Cancer Res.* **2013**, *73*, 3683–3691. [[CrossRef](#)] [[PubMed](#)]
27. Reaper, P.M.; Griffiths, M.R.; Long, J.M.; Charrier, J.-D.; MacCormick, S.; Charlton, P.A.; Golec, J.M.C.; Pollard, J.R. Selective killing of ATM- or p53-deficient cancer cells through inhibition of ATR. *Nat. Chem. Biol.* **2011**, *7*, 428–430. [[CrossRef](#)]
28. Kawahara, N.; Ogawa, K.; Nagayasu, M.; Kimura, M.; Sasaki, Y.; Kobayashi, H. Candidate synthetic lethality partners to PARP inhibitors in the treatment of ovarian clear cell cancer. *Biomed. Rep.* **2017**, *7*, 391–399. [[CrossRef](#)]
29. Ciardo, D.; Goldar, A.; Marheineke, K. On the Interplay of the DNA Replication Program and the Intra-S Phase Checkpoint Pathway. *Genes* **2019**, *10*, 94. [[CrossRef](#)]
30. Rogalska, A.; Gajek, A.; Marczak, A. Epothilone B induces extrinsic pathway of apoptosis in human SKOV-3 ovarian cancer cells. *Toxicol. Vitro.* **2014**, *28*, 675–683. [[CrossRef](#)]
31. Kampan, N.C.; Madondo, M.T.; McNally, O.M.; Quinn, M.; Plebanski, M. Paclitaxel and Its Evolving Role in the Management of Ovarian Cancer. *BioMed Res. Int.* **2015**, *2015*, 1–21. [[CrossRef](#)] [[PubMed](#)]
32. De Donato, M.; Righino, B.; Filippetti, F.; Battaglia, A.; Petrillo, M.; Pirolli, D.; Scambia, G.; De Rosa, M.C.; Gallo, D. Identification and antitumor activity of a novel inhibitor of the NIMA-related kinase NEK6. *Sci. Rep.* **2018**, *8*. [[CrossRef](#)] [[PubMed](#)]
33. Ahmad, A.; Lin, Z.P.; Zhu, Y.-L.; Lo, Y.-C.; Moscarelli, J.; Xiong, A.; Korayem, Y.; Huang, P.H.; Giri, S.; LoRusso, P.; et al. Combination of triapine, olaparib, and cediranib suppresses progression of BRCA-wild type and PARP inhibitor-resistant epithelial ovarian cancer. *PLoS ONE* **2018**, *13*. [[CrossRef](#)]
34. Hjortkjær, M.; Malik Aagaard Jørgensen, M.; Waldstrøm, M.; Ørnskov, D.; Søgaard-Andersen, E.; Jakobsen, A.; Dahl-Steffensen, K. The clinical importance of BRCAness in a population-based cohort of Danish epithelial ovarian cancer. *Int. J. Gynecol. Cancer* **2019**, *29*, 166–173. [[CrossRef](#)]
35. Baloch, T.; López-Ozuna, V.M.; Wang, Q.; Matanis, E.; Kessous, R.; Kogan, L.; Yasmeen, A.; Gotlieb, W.H. Sequential therapeutic targeting of ovarian Cancer harboring dysfunctional BRCA1. *BMC Cancer* **2019**, *19*. [[CrossRef](#)]
36. Kim, W.; Zhao, F.; Wu, R.; Qin, S.; Nowsheen, S.; Huang, J.; Zhou, Q.; Chen, Y.; Deng, M.; Guo, G.; et al. ZFP161 regulates replication fork stability and maintenance of genomic stability by recruiting the ATR/ATRIP complex. *Nat. Commun.* **2019**, *10*. [[CrossRef](#)]

37. George, E.; Kim, H.; Krepler, C.; Wenz, B.; Makvandi, M.; Tanyi, J.L.; Brown, E.; Zhang, R.; Brafford, P.; Jean, S.; et al. A patient-derived-xenograft platform to study BRCA-deficient ovarian cancers. *JCI Insight* **2017**, *2*. [[CrossRef](#)]
38. Kim, H.; George, E.; Ragland, R.L.; Rafail, S.; Zhang, R.; Krepler, C.; Morgan, M.A.; Herlyn, M.; Brown, E.J.; Simpkins, F. Targeting the ATR/CHK1 Axis with PARP Inhibition Results in Tumor Regression in BRCA-Mutant Ovarian Cancer Models. *Clin. Cancer Res.* **2017**, *23*, 3097–3108. [[CrossRef](#)]
39. Kim, H.; Xu, H.; George, E.; Hallberg, D.; Kumar, S.; Jagannathan, V.; Medvedev, S.; Kinose, Y.; Devins, K.; Verma, P.; et al. Combining PARP with ATR inhibition overcomes PARP inhibitor and platinum resistance in ovarian cancer models. *Nat. Commun.* **2020**, *11*. [[CrossRef](#)]
40. Burgess, B.T.; Anderson, A.M.; McCorkle, J.R.; Wu, J.; Ueland, F.R.; Kolesar, J.M. Olaparib Combined with an ATR or Chk1 Inhibitor as a Treatment Strategy for Acquired Olaparib-Resistant BRCA1 Mutant Ovarian Cells. *Diagnostics* **2020**, *10*, 121. [[CrossRef](#)]
41. Jette, N.R.; Kumar, M.; Radhamani, S.; Arthur, G.; Goutam, S.; Yip, S.; Kolinsky, M.; Williams, G.J.; Bose, P.; Lees-Miller, S.P. ATM-Deficient Cancers Provide New Opportunities for Precision Oncology. *Cancers* **2020**, *12*, 687. [[CrossRef](#)] [[PubMed](#)]
42. Lloyd, R.; Falenta, K.; Wijnhoven, P.W.; Chabbert, C.; Stott, J.; Yates, J.; Lau, A.Y.; Young, L.A.; Hollingsworth, S.J. Abstract 337: The PARP inhibitor olaparib is synergistic with the ATR inhibitor AZD6738 in ATM deficient cancer cells. In Proceedings of the Molecular and Cellular Biology/Genetics, American Association for Cancer Research (AACR), Chicago, IL, USA, 14–18 April 2018; Volume 78, p. 337.
43. Brill, E.; Yokoyama, T.; Nair, J.; Yu, M.; Ahn, Y.-R.; Lee, J.-M. Prexasertib, a cell cycle checkpoint kinases 1 and 2 inhibitor, increases in vitro toxicity of PARP inhibition by preventing Rad51 foci formation in BRCA wild type high-grade serous ovarian cancer. *Oncotarget* **2017**, *8*, 111026–111040. [[CrossRef](#)] [[PubMed](#)]
44. Ray Chaudhuri, A.; Nussenzweig, A. The multifaceted roles of PARP1 in DNA repair and chromatin remodelling. *Nat. Rev. Mol. Cell Biol.* **2017**, *18*, 610–621. [[CrossRef](#)] [[PubMed](#)]
45. Parsels, L.A.; Karnak, D.; Parsels, J.D.; Zhang, Q.; Vélez-Padilla, J.; Reichert, Z.R.; Wahl, D.R.; Maybaum, J.; O'Connor, M.J.; Lawrence, T.S.; et al. PARP1 Trapping and DNA Replication Stress Enhance Radiosensitization with Combined WEE1 and PARP Inhibitors. *Mol. Cancer Res.* **2018**, *16*, 222–232. [[CrossRef](#)]
46. Osoegawa, A.; Gills, J.J.; Kawabata, S.; Dennis, P.A. Rapamycin sensitizes cancer cells to growth inhibition by the PARP inhibitor olaparib. *Oncotarget* **2017**, *8*, 87044–87053. [[CrossRef](#)]
47. Bianchi, A.; Lopez, S.; Altwerger, G.; Bellone, S.; Bonazzoli, E.; Zammataro, L.; Manzano, A.; Manara, P.; Perrone, E.; Zeybek, B.; et al. PARP-1 activity (PAR) determines the sensitivity of cervical cancer to olaparib. *Gynecol. Oncol.* **2019**, *155*, 144–150. [[CrossRef](#)]
48. Parmar, K.; Kochupurakkal, B.S.; Lazaro, J.-B.; Wang, Z.C.; Palakurthi, S.; Kirschmeier, P.T.; Yang, C.; Sambel, L.A.; Färkkilä, A.; Reznichenko, E.; et al. The CHK1 Inhibitor Prexasertib Exhibits Monotherapy Activity in High-Grade Serous Ovarian Cancer Models and Sensitizes to PARP Inhibition. *Clin. Cancer Res.* **2019**, *25*, 6127–6140. [[CrossRef](#)]
49. Szczepanska, J.; Poplawski, T.; Synowiec, E.; Pawlowska, E.; Chojnacki, C.J.; Chojnacki, J.; Blasiak, J. 2-Hydroxyethyl methacrylate (HEMA), a tooth restoration component, exerts its genotoxic effects in human gingival fibroblasts through methacrylic acid, an immediate product of its degradation. *Mol. Biol. Rep.* **2011**, *39*, 1561–1574. [[CrossRef](#)]
50. Angius, G.; Tomao, S.; Stati, V.; Vici, P.; Bianco, V.; Tomao, F. Prexasertib, a checkpoint kinase inhibitor: From preclinical data to clinical development. *Cancer Chemother. Pharmacol.* **2019**, *85*, 9–20. [[CrossRef](#)]
51. Liu, Y.; Burness, M.L.; Martin-Trevino, R.; Guy, J.; Bai, S.; Harouaka, R.; Brooks, M.D.; Shang, L.; Fox, A.; Luther, T.K.; et al. RAD51 Mediates Resistance of Cancer Stem Cells to PARP Inhibition in Triple-Negative Breast Cancer. *Clin. Cancer Res.* **2017**, *23*, 514–522. [[CrossRef](#)]
52. Baugh, E.H.; Ke, H.; Levine, A.J.; Bonneau, R.A.; Chan, C.S. Why are there hotspot mutations in the TP53 gene in human cancers? *Cell Death Differ.* **2017**, *25*, 154–160. [[CrossRef](#)] [[PubMed](#)]
53. Karnitz, L.M.; Zou, L. Molecular Pathways: Targeting ATR in Cancer Therapy. *Clin. Cancer Res.* **2015**, *21*, 4780–4785. [[CrossRef](#)] [[PubMed](#)]
54. Vance, S.; Liu, E.; Zhao, L.; Parsels, J.D.; Parsels, L.A.; Brown, J.L.; Maybaum, J.; Lawrence, T.S.; Morgan, M.A. Selective radiosensitization of p53 mutant pancreatic cancer cells by combined inhibition of Chk1 and PARP1. *Cell Cycle* **2014**, *10*, 4321–4329. [[CrossRef](#)] [[PubMed](#)]

55. Yi, J.; Liu, C.; Tao, Z.; Wang, M.; Jia, Y.; Sang, X.; Shen, L.; Xue, Y.; Jiang, K.; Luo, F.; et al. MYC status as a determinant of synergistic response to Olaparib and Palbociclib in ovarian cancer. *EBioMedicine* **2019**, *43*, 225–237. [[CrossRef](#)]
56. Wang, D.; Li, C.; Zhang, Y.; Wang, M.; Jiang, N.; Xiang, L.; Li, T.; Roberts, T.M.; Zhao, J.J.; Cheng, H.; et al. Combined inhibition of PI3K and PARP is effective in the treatment of ovarian cancer cells with wild-type PIK3CA genes. *Gynecol. Oncol.* **2016**, *142*, 548–556. [[CrossRef](#)]
57. Mitchell, C.; Park, M.; Eulitt, P.; Yang, C.; Yacoub, A.; Dent, P. Poly(ADP-Ribose) Polymerase 1 Modulates the Lethality of CHK1 Inhibitors in Carcinoma Cells. *Mol. Pharmacol.* **2010**, *78*, 909–917. [[CrossRef](#)]
58. Zhou, J.; Yang, F.; Zhou, L.; Wang, J.-g.; Wen, P.; Luo, H.; Li, W.; Song, Z.; Sharman, E.H.; Bondy, S.C. Dietary melatonin attenuates age-related changes in morphology and in levels of key proteins in globus pallidus of mouse brain. *Brain Res.* **2014**, *1546*, 1–8. [[CrossRef](#)]
59. Stingele, J.; Bellelli, R.; Alte, F.; Hewitt, G.; Sarek, G.; Maslen, S.L.; Tsutakawa, S.E.; Borg, A.; Kjær, S.; Tainer, J.A.; et al. Mechanism and Regulation of DNA-Protein Crosslink Repair by the DNA-Dependent Metalloprotease SPRTN. *Mol. Cell* **2016**, *64*, 688–703. [[CrossRef](#)]
60. Yazinski, S.A.; Comaills, V.; Buisson, R.; Genois, M.M.; Nguyen, H.D.; Ho, C.K.; Todorova Kwan, T.; Morris, R.; Lauffer, S.; Nussenzweig, A.; et al. ATR inhibition disrupts rewired homologous recombination and fork protection pathways in PARP inhibitor-resistant BRCA-deficient cancer cells. *Genes Dev.* **2017**, *31*, 318–332. [[CrossRef](#)]
61. Koundrioukoff, S.; Carignon, S.; Techer, H.; Letessier, A.; Brison, O.; Debatisse, M. Stepwise activation of the ATR signaling pathway upon increasing replication stress impacts fragile site integrity. *PLoS Genet.* **2013**, *9*, e1003643. [[CrossRef](#)]
62. Toledo, L.I.; Altmeyer, M.; Rask, M.B.; Lukas, C.; Larsen, D.H.; Povlsen, L.K.; Bekker-Jensen, S.; Mailand, N.; Bartek, J.; Lukas, J. ATR prohibits replication catastrophe by preventing global exhaustion of RPA. *Cell* **2013**, *155*, 1088–1103. [[CrossRef](#)] [[PubMed](#)]
63. Mengwasser, K.E.; Adeyemi, R.O.; Leng, Y.; Choi, M.Y.; Clairmont, C.; D’Andrea, A.D.; Elledge, S.J. Genetic Screens Reveal FEN1 and APEX2 as BRCA2 Synthetic Lethal Targets. *Mol. Cell* **2019**, *73*, 885–899.e6. [[CrossRef](#)] [[PubMed](#)]
64. Lopez-Acevedo, M.; Grace, L.; Teoh, D.; Whitaker, R.; Adams, D.J.; Jia, J.; Nixon, A.B.; Secord, A.A. Dasatinib (BMS-35482) potentiates the activity of gemcitabine and docetaxel in uterine leiomyosarcoma cell lines. *Gynecol. Oncol. Res. Pract.* **2014**, *1*. [[CrossRef](#)] [[PubMed](#)]

Publisher’s Note: MDPI stays neutral with regard to jurisdictional claims in published maps and institutional affiliations.



© 2020 by the authors. Licensee MDPI, Basel, Switzerland. This article is an open access article distributed under the terms and conditions of the Creative Commons Attribution (CC BY) license (<http://creativecommons.org/licenses/by/4.0/>).

Article

PARP Inhibition Increases the Reliance on ATR/CHK1 Checkpoint Signaling Leading to Synthetic Lethality—an Alternative Treatment Strategy for Epithelial Ovarian Cancer Cells Independent from HR Effectiveness

Patrycja Gralewska ¹, Arkadiusz Gajek ¹, Agnieszka Marczak ¹, Michał Mikuła ²,

Jerzy Ostrowski ^{2,3}, Agnieszka Śliwińska ⁴ and Aneta Rogalska ^{1,*}

¹ Department of Medical Biophysics, Institute of Biophysics, Faculty of Biology and Environmental Protection, University of Lodz, 90-236 Lodz, Poland; patrycja.gralewska@edu.uni.lodz.pl (P.G.); arkadiusz.gajek@biol.uni.lodz.pl (A.G.); agnieszka.marczak@biol.uni.lodz.pl (A.M.)

² Department of Genetics, Maria Skłodowska-Curie National Research Institute of Oncology, 02-781 Warsaw, Poland; michal.mikula@pib-nio.pl (M.M.); jerzy.ostrowski@pib-nio.pl (J.O.)

³ Department of Gastroenterology, Hepatology and Clinical Oncology, Centre of Postgraduate Medical Education, 01-813 Warsaw, Poland

⁴ Department of Nucleic Acid Biochemistry, Medical University of Lodz, 92-213 Lodz, Poland; agnieszka.sliwinska@umed.lodz.pl

* Correspondence: aneta.rogalska@biol.uni.lodz.pl; Tel.: +48-42-635-44-77

Received: 4 November 2020; Accepted: 16 December 2020; Published: 20 December 2020

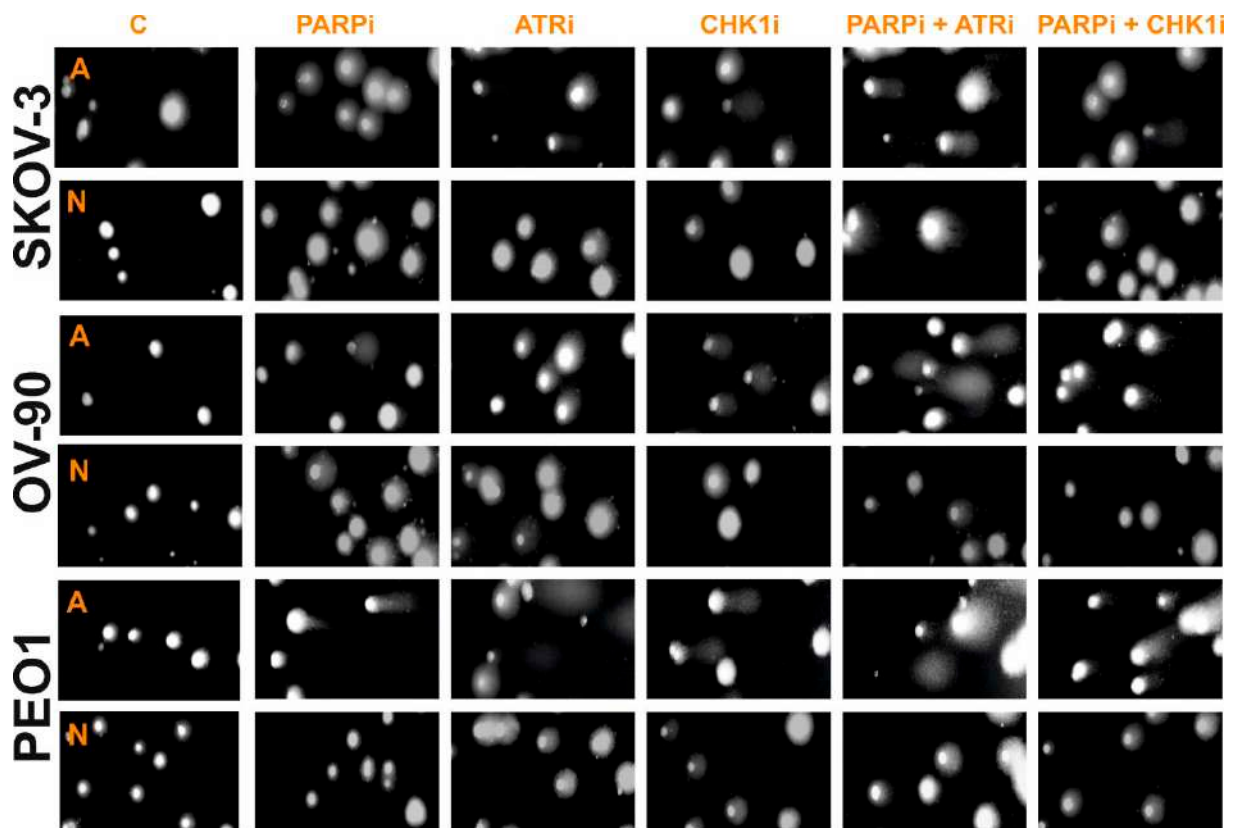


Figure S1. Representative images of the DNA damage in EOC cell lines treated with PARPi, ATRi and CHK1i alone and in combination, measured as a percentage of the DNA in the comet tail. Comets were visualized under a fluorescence microscope after staining with DAPI. The letter A indicates the alkaline version and N the neutral version of the comet assay. Comet assay: exponentially growing cells were treated the same as in Figure 3 for 48 h and processed for comet assay as described under Materials and Methods. Comet image were obtained by analysis system Lucia-Comet v. 4.51.

Article

The Influence of PARP, ATR, CHK1 Inhibitors on Premature Mitotic Entry and Genomic Instability in High-Grade Serous $BRCA^{MUT}$ and $BRCA^{WT}$ Ovarian Cancer Cells

Patrycja Gralewska ¹, Arkadiusz Gajek ¹, Dorota Rybaczek ², Agnieszka Marczak ¹
and Aneta Rogalska ^{1,*}

¹ Department of Medical Biophysics, Institute of Biophysics, Faculty of Biology and Environmental Protection, University of Lodz, Pomorska 141/143, 90-236 Lodz, Poland; patrycja.gralewska@edu.uni.lodz.pl (P.G.); arkadiusz.gajek@biol.uni.lodz.pl (A.G.); agnieszka.marczak@biol.uni.lodz.pl (A.M.)

² Department of Cytophysiology, Faculty of Biology and Environmental Protection, University of Lodz, Pomorska 141/143, 90-236 Lodz, Poland; dorota.rybaczek@biol.uni.lodz.pl

* Correspondence: aneta.rogalska@biol.uni.lodz.pl; Tel.: +48-42-635-44-77

Abstract: Olaparib is a poly (ADP-ribose) polymerase inhibitor (PARPi) that inhibits PARP1/2, leading to replication-induced DNA damage that requires homologous recombination repair. Olaparib is often insufficient to treat $BRCA$ -mutated ($BRCA^{MUT}$) and $BRCA$ wild-type ($BRCA^{WT}$) high-grade serous ovarian carcinomas (HGSOCs). We examined the short-term (up to 48 h) efficacy of PARPi treatment on a DNA damage response pathway mediated by ATR and CHK1 kinases in $BRCA^{MUT}$ (PEO-1) and $BRCA^{WT}$ (SKOV-3 and OV-90) cells. The combination of ATRi/CHK1i with PARPi was not more cytotoxic than ATR and CHK1 monotherapy. The combination of olaparib with inhibitors of the ATR/CHK1 pathway generated chromosomal abnormalities, independent on $BRCA^{MUT}$ status of cells and formed of micronuclei (MN). However, the beneficial effect of the PARPi:ATRi combination on MN was seen only in the PEO1 $BRCA^{MUT}$ line. Monotherapy with ATR/CHK1 inhibitors reduced BrdU incorporation due to a slower rate of DNA synthesis, which resulted from elevated levels of replication stress, while simultaneous blockade of PARP and ATR caused beneficial effects only in OV-90 cells. Inhibition of ATR/CHK1 increased the formation of double-strand breaks as measured by increased γ H2AX expression at collapsed replication forks, resulting in increased levels of apoptosis. Our findings indicate that ATR and CHK1 inhibitors provoke premature mitotic entry, leading to genomic instability and ultimately cell death.

Keywords: ATR inhibitor; CHK1 inhibitor; ovarian cancer; PARP inhibitor; replication stress; targeted therapy



Citation: Gralewska, P.; Gajek, A.; Rybaczek, D.; Marczak, A.; Rogalska, A. The Influence of PARP, ATR, CHK1 Inhibitors on Premature Mitotic Entry and Genomic Instability in High-Grade Serous $BRCA^{MUT}$ and $BRCA^{WT}$ Ovarian Cancer Cells. *Cells* **2022**, *11*, 1889. <https://doi.org/10.3390/cells11121889>

Academic Editors: Valentina De Falco and Zhixiang Wang

Received: 21 April 2022

Accepted: 8 June 2022

Published: 10 June 2022

Publisher's Note: MDPI stays neutral with regard to jurisdictional claims in published maps and institutional affiliations.



Copyright: © 2022 by the authors. Licensee MDPI, Basel, Switzerland. This article is an open access article distributed under the terms and conditions of the Creative Commons Attribution (CC BY) license (<https://creativecommons.org/licenses/by/4.0/>).

1. Introduction

Ovarian cancer is the leading cause of death from gynecological malignancies [1]. High-grade serous ovarian carcinoma (HGSOC) accounts for approximately 50% of ovarian cancers and is characterized by $TP53$ mutations (96%), homologous recombination (HR) DNA repair defects (50%), cyclin E1 (CCNE1) amplification and genomic instability [2]. The cells often carry $BRCA1$ or $BRCA2$ ($BRCA1/2$) mutations, germline or somatic mutations in ataxia telangiectasia and Rad3-related protein (ATR) or checkpoint kinase 1 (CHK1), as well as mutations in genes associated with the HR pathway [3]. Due to $TP53$ mutations, HGSOCs lose their G1 checkpoint control, resulting in increased dependence on S and G2 checkpoints [4].

It is estimated that about 10,000 single-strand breaks (SSBs) of DNA occur daily in a mammalian cell. DNA damage induced by olaparib treatment has been shown to significantly increase genetic instability [5]. Olaparib and veliparib, poly (ADP-ribose) polymerase inhibitors (PARPi), induce genomic instability, resulting in a marked increase

in sister chromatid exchange (SCE) frequencies and chromatid-type aberrations. Olaparib induces chromatid-type aberrations, including gaps, breaks, radial chromosomes and telomere associations [6]. Genomic instability in olaparib-treated cells manifests as the extensive accumulation of gaps, breaks, radial chromosomes, and micronuclei (MN) in response to aberrant double strand break (DSB) repair [7]. In addition, PARP1 inhibition in cancer cells may lead to the upregulation of the HR repair pathway to maintain cell viability [8]. Although PARPi can delay cancer progression, they do not improve overall survival [9]; thus, there is an urgent need to develop new, more successful therapies. One effective strategy to potentiate PARP cytotoxicity in ovarian cancer cells would be to target cell cycle checkpoints and force mitotic entry with DSBs, thereby inducing cell death.

Our previous study confirmed that the inactivation of cell cycle checkpoint kinases such as ATR or CHK1 may increase the cytotoxicity of PARPi after 5 days of treatment [10]. In response to DNA damage, ATR phosphorylates CHK1 protein, which in turn mediates CDC25A-C phosphorylation, leading to the inhibition of CDK1 and CDK2 (thus preventing cell cycle progression) [11,12]. DSB lesions lead to the activation of the G2/M cell cycle checkpoint, which blocks entry into mitosis [13]. Progression through mitosis has previously been shown to promote PARPi cytotoxicity in HR-deficient cells [14].

The effect of ATR and CHK1 kinases in response to PARPi treatment on cell cycle disorders and its consequences in ovarian cancer cells remain unclear. Genetic predisposition (*BRCA1/2* mutations) or phenotypic characteristics (platinum resistance) are not sufficient to predict patient response to olaparib treatment [15]. Whether DNA damage from replication stress (RS) produces an efficient G2/M checkpoint response in ovarian cancer is not known. Thus, in this study, we investigated the role of ATR and CHK1 inhibition at the early stage of olaparib response in *BRCA2^{MUT}* (PEO-1) and *BRCA^{WT}* (OV-90 and SKOV-3) ovarian cancer cells and sought to further elucidate the mechanisms leading to ovarian cancer cell death. Here, we report that PARPi has a cytostatic effect, while its cytotoxic effects and diminished DNA repair are caused by ATRi and CHK1i monotherapy. The combination of olaparib with inhibitors of the ATR/CHK1 pathway generated chromosomal abnormalities, independent on *BRCA^{MUT}* status of cells and formed of micronuclei. ATR and CHK1 inhibitors provoke premature mitotic entry and provide genomic instability to ovarian cancer cells.

2. Materials and Methods

2.1. Reagents

Culture media (RPMI 1640, DMEM) and fetal bovine serum (FBS) were obtained from Gibco (Thermo Fisher Scientific, Waltham, MA, USA). Trypsin-EDTA was acquired from Sigma-Aldrich (St. Louis, MO, USA). Violet Chromatin Condensation/Dead Cell Apoptosis Kit (Cat no: A35135) and CLICK EDU (Cat no: C10337) were from Thermo Fisher Scientific. The FITC BrdU Flow Kit was purchased from BD Biosciences (Franklin Lakes, NJ, USA). PARPi (AZD2281), ATRi (AZD6738), and CHK1i (MK8776) were purchased from Selleckchem (Houston, TX, USA). Other chemicals and solvents were of high analytical grade and were obtained from Sigma-Aldrich or Avantor Performance Materials Poland S.A. (Gliwice, Poland).

2.2. Cell Culture and Drug Administration

The human OV-90 cell line with mutated *TP53* gene (human malignant papillary serous carcinoma, American Type Culture Collection (ATCC) CRL-11732™) and SKOV-3 cell line with loss of *TP53* function (*TP53* null) (human ovarian adenocarcinoma, ATCC HTB-77) were purchased from ATCC (Rockville, MD, USA). *BRCA^{MUT}* PEO-1 cells (human ovarian cancer; estrogen rec, 10032308) were obtained from the European Collection of Authenticated Cell Cultures. The newly acquired cells were expanded, and aliquots of less than 10 passages were stored in liquid nitrogen. All cell lines were kept at a low passage, returning to original frozen stocks every 6 months. During the course of the study, cells were thawed and passaged within 2 months of each experiment. Cells were cultured in

DMEM and RPMI with 10% FBS and regularly checked for mycoplasma contamination. Cells were cultured in an atmosphere of 5% CO₂ and 95% air at 37 °C.

2.3. MTT Assay

Logarithmically growing cells (1×10^4) were seeded into 96-well plates and treated with the indicated doses of PARPi (AZD2281), CHK1i (MK8776), and ATRi (AZD6738) for 24 and 48 h. After treatment, cells were washed twice with PBS, and incubated with 50 µL MTT (at a final concentration of 0.5 mg/mL) (Sigma Aldrich, St. Louis, MO, USA) for 4 h. The medium in each well was aspirated and violet formazan crystals that formed as a result of MTT reduction within metabolically viable cells were dissolved in 100 µL DMSO per well. Absorbance was measured at 570 nm with a microplate reader (Awareness Technology Inc., Palm City, FL, USA) [16]. To analyze the drug interactions between olaparib combined with ATRi and CHK1i, the coefficient of drug interaction (CDI) was calculated as described previously [17].

2.4. Metaphase Spread

Cells were treated with the inhibitors for 24 h, then harvested for chromosome preparations using colcemid (50 ng/mL) for 90 min, followed by incubation with 0.075 mol/L potassium chloride (KCl) for 18 min at 37 °C. Following drop wise addition of Carnoy fixative (3:1 methanol:acetic acid), samples were incubated in the fixative for one hour, pelleted at 1000 g, and incubated in fresh fixative at 4 °C overnight. After replenishing the fixative again, the fixed cells were placed onto uncoated microscope slides and dried for at least 24 h at room temperature. Slides were stained in Giemsa staining solution (Aqua-med, Łódź, Poland) for 4 min, then analyzed for total gaps and breaks using a 100× objective and a Nikon ECLIPSE E600W (Nikon, Warsaw, Poland) fluorescent microscope. Fifty metaphases were scored for each sample in two independent experiments. An index of aberrations (M-phase aberrant cells) was calculated as the percent ratio between the number of cells showing chromosomal aberrations and all mitotic cells. Quantification of the number of aberrant M-phase cells (AI: aberration index) and nuclear phenotypes in cells was determined by counterstaining with Giemsa and DAPI (0.1 mg/mL; 4',6-diamidino-2-phenylindole; Sigma Aldrich, Saint Quentin, France) for 5 min at room temperature. PEO-1, OV-90 and SKOV-3 cells were observed using an AxioImagerA1 fluorescence microscope (ZEISS, Jena, Germany) equipped with an UV-2A filter (UV-light; $\lambda = 518$ nm). All images were recorded at exactly the same time of integration with an AxioCam MRc5 CCD camera (ZEISS, Jena, Germany).

2.5. Micronucleus Assay

Cells (2×10^6) were seeded onto 100 mm Petri dishes and cultured for 24 h before treatment with olaparib, ATRi, CHK1i, and a combination of PARPi with ATRi or PARPi with CHK1i, each at a concentration of 4 µM. After 48 h of exposure, cells were washed twice with PBS, collected and incubated in a chilled hypotonic solution of KCl (75 mM) for 30 min. Samples were then centrifuged at $200 \times g$ for 5 min at 25 °C and fixed with Carnoy's fixative (3:1 ratio of methanol:glacial acetic acid) for 5 min. After centrifugation at $200 \times g$ for 5 min, cells were resuspended in fresh Carnoy's fixative. This step was repeated twice. Finally, cells were placed on microscopic slides, fixed with methanol for 15 min, air dried and stained with acridine orange for 2 min (10 µg/mL in PBS). Micronuclei (MN) were examined under an Optiphot-2 fluorescence microscope (Nikon) equipped with a B-2A filter (blue light; $\lambda = 495$ nm). The MN images presented were visualized by fluorescence microscopy (Olympus IX70, Tokyo, Japan; magnification 400×).

2.6. Determination of Proliferation Rate

To determine the OV-90, SKOV-3 and PEO-1 cell proliferation rates, we employed the trypan blue exclusion method [18]. Cells, seeded at a density of 2×10^5 , were treated with the drugs and counted 24–168 h after treatment. Briefly, 4% trypan blue solution

was mixed with the cell suspension in a ratio of 1:1, transferred to a Thoma chamber and viable/nonviable cells were counted under an optical microscope. Based on the number of cells at the beginning and at each studied time point, we calculated the doubling time using the following formula $t_d = t / \log_2 (N_t / N_0)$, where t_d is the time required for duplication of cell number, t is the time interval between the initial and final calculation of cell number, and N_0 and N_t are the number of cells at the beginning and end of the experiment, respectively [19,20].

2.7. Cell-Cycle Analysis

Cell cycle distribution was quantified using a FITC-BrdU Flow Kit (BD Biosciences, San Jose, CA, USA) according to the manufacturer's protocol. Briefly, cells (1×10^6) were plated onto 100 mm Petri dishes and once attached were treated with drugs for 24 h. Ten μM of bromodeoxyuridine (BrdU) was added to the culture medium and incubated for 2 h. Cells were harvested, fixed and incubated with FITC-conjugated anti-BrdU and 7-AAD solution for 15 min at room temperature, then analyzed immediately in a flow cytometer (LSR II, Becton Dickinson, San Jose, CA, USA). The mitotic index was calculated as the percent ratio between the number of dividing cells and the entire cell population by labeling cells with FITC-conjugated anti-BrdU and 7-AAD. The population of cells at specific phases of the cell cycle were quantified from a standard count of 10,000 cells using FlowJo software v7.6 (Ashland, OR, USA).

2.8. Immunofluorescence and Immunocytochemistry Staining

Cells (1.5×10^4 cells/well) were cultured for 24 h on ten-chambered glass slides (Greiner Bio-One, Frickenhausen, Germany), then treated with the compounds for 48 h. Next, the cells were fixed with paraformaldehyde (4% *w/v* in PBS), incubated with blocking buffer for 60 min (PBS/5% normal goat serum/0.3% Triton X-100), followed by incubation with primary antibodies against caspase-3 (cat.: 9664, at 1:400) and phospho-histone H2AX (Ser139) (cat.: 9718, at 1:400) prepared in Antibody Dilution Buffer (PB/1% BSA/0.3% Triton X-100). The secondary antibodies used were anti-rabbit IgG (H+L), F(ab')₂ fragment (Alexa Fluor 555 conjugate, at 1:1000) to detect caspase-3, and anti-rabbit IgG (H+L), F(ab')₂ fragment (Alexa Fluor 488 conjugate, at 1:2000) to detect phospho-histone H2AX. Nuclei were stained with DAPI (Vectashield mounting medium, cat no.: H-1200, Vector Laboratories, Newark, CA, USA) and 3,3'-dihexyloxycarbocyanine iodide (DiOC₆, cat no: 318426, Sigma Aldrich, Steinheim am Albuch, Germany; 1 μM) was used to visualize cells with caspase-3. For visualization of membranes stained with DiOC₆, a supercontinuum laser with 485 nm excitation and emission at 538–595 nm was applied. For nuclei stained with DAPI, the excitation and emission parameters used were 405 nm and 460–480 nm, respectively. Immunofluorescence images were acquired using a confocal laser scanning microscope (SP8, Leica Microsystems AG, Wetzlar, Germany) equipped with a 63 \times oil immersion objective [21].

2.9. Measurement of Chromatin Condensation

The Violet Chromatin Condensation/Dead Cell Apoptosis Kit with Vybrant[®] DyeCycle[™] Violet and SYTOX[®] AADvanced[™] was used to examine chromatin condensation during apoptosis (cat. no. A35135; Molecular probes[®], Invitrogen[™], Waltham, MA, USA). Briefly, 1×10^6 control and drug-treated cells were washed and resuspended in 1 mL Hank's Balanced Salt Solution buffer (HBSS) containing Vybrant[®] DyeCycle[™] Violet and SYTOX[®] AADvanced[™] dyes, according to the manufacturer's protocol. After 30 min of incubation (protected from light), stained cells were analyzed immediately without washing by flow cytometry (LSR II, Becton Dickinson, Franklin Lakes, NJ, USA) using ~405/488 nm dual excitation, while measuring the fluorescence emission at ~440/660 nm [22].

2.10. Detection of S-Phase Progression Using 5-Ethynyl-2'-deoxyuridine (EdU) Incorporation with Click-iT Chemistry

Cells were labeled for 30 min with 100 μ M EdU (Life Technologies, Invitrogen, Paisley, Renfrewshire, UK), then fixed in 4% (*w/v*) paraformaldehyde (Merc, St. Louis, MO, USA) for 45 min and permeabilized with 1% Triton X-100 (Merc, St. Louis, MO, USA) for 20 min. For EdU staining, the Click-iT Alexa Fluor 488 Imaging Kit was used according to the manufacturer's instructions, with some minor modifications. Briefly, cells were rinsed twice with 1% bovine serum albumin (BSA; Merc, St. Louis, MO, USA) and incubated for 30 min at 20 °C with 250 μ L EdU Click-iT reaction cocktail per well. After removing the reaction cocktail, each well was washed once with 1% BSA. Cells were visualized using a fluorescence microscope (Zeiss, Jena, Germany) equipped with GFP and DAPI filters. Analysis was performed with AxioVision software (Zeiss, Jena, Germany). All images were recorded at exactly the same exposure time on an AxioCam MRc5 CCD camera (Zeiss, Jena, Germany).

2.11. Measurement of Phosphatidylserine Externalization

Double staining of cells with annexin V and propidium iodide was used to assess the first stage of apoptosis. This method is a useful tool for distinguishing viable cells (unstained with either fluorochrome) from apoptotic cells (stained with annexin V) and necrotic (dead) cells (stained with PI). Visualization of cells stained with annexin V- Alexa Fluor™ 488 and PI was applied according to the protocol of the manufacturer (cat: V13245, Invitrogen, Thermo Fisher Scientific, Waltham, MA, USA). Briefly, 4×10^5 control and drug treated cells after 24 and 48 h were washed with cold PBS and resuspended in 140 μ L binding buffer (delivered from producer) that contained 3 μ L of annexin V-Alexa Fluor™ 488, 1 μ L 100 μ g/mL of PI and stained for 15 min on ice. Finally, at least 10^4 cells were analyzed for Alexa Fluor™ 488 and PI fluorescence (Ex ~488 nm; Em ~530 nm) using a flow cytometer (LSR II, Becton Dickinson, Franklin Lakes, NJ, USA). With the use of the annexin V- Alexa Fluor™ 488 and propidium iodide (PI) double staining regime, three populations of cells were distinguishable in a two color flow cytometry: normal cells: annexin V- Alexa Fluor™ 488 negative, PI negative; apoptotic cells: annexin V-Alexa Fluor™ 488 positive, PI negative; dead cells: annexin V-Alexa Fluor™ 488 positive and PI positive; annexin V-Alexa Fluor™ 488 negative and PI positive. The populations of cells were quantified from a standard count of 10^4 cells using FlowJo software v7.6 (Ashland, OR, USA).

2.12. Morphological Assessment of Apoptosis and Necrosis: Double Staining with Hoechst 33258 and Propidium Iodide (PI)

To determine the ratio between live, apoptotic, and necrotic cellular fractions, simultaneous cell staining with Hoechst 33258 and PI was performed as described previously [23]. These fluorescent dyes vary in their spectral characteristics and ability to penetrate cells. Analysis was performed with the Olympus IX70 fluorescence microscope. Cells were cultured with the drugs for 48 h, trypsinized, centrifuged, and resuspended in PBS to a final concentration of 1×10^6 cells/mL. One μ L of Hoechst 33258 (0.13 mM) and 1 μ L of PI (0.23 mM) were added to 100 μ L of the cell suspension. At least 100 cells were counted under a microscope on each slide and each experiment was performed in triplicate. Cells were classified as live, apoptotic or necrotic on the basis of their morphological and staining characteristics, and the percentage of specific cellular fractions was determined from the total number of cells. Cells were classified as live (bright blue fluorescence), early apoptotic cells (cells showing intensive blue fluorescence), late apoptotic cells (blue–violet stained cells with concomitant apoptotic morphology), and necrotic cells (red fluorescence) [24].

2.13. Western Blot Analysis

Drug-treated cells were lysed in cell extraction buffer (Invitrogen™) containing a protease inhibitor cocktail and PMSF (Sigma-Aldrich) in accordance with the manufacturer's protocol. The protein concentration was determined using the Bradford method.

Proteins (70 µg per lane) were separated by SDS polyacrylamide gel electrophoresis and transferred onto 0.45 µm PVDF membranes using semi-dry transfer with the Trans-Blot Turbo Transfer System (Bio-Rad). After blocking nonspecific sites with 5% non-fat dry milk, membranes were incubated with rabbit monoclonal antibodies (1/1000) against caspase-3 (cat no.: #9664) and phospho-histone H2AX (Ser139) (cat.no.: #9718) from Cell Signaling Technology, Inc. (Danvers, MA, USA), and mouse monoclonal anti-β-actin antibodies (cat. A1878, Sigma-Aldrich). Membranes were then incubated with anti-rabbit IgG horseradish peroxidase-conjugated (cat.: 7074, Cell Signaling Technology) or anti-mouse IgG HRP-conjugated (cat: A28177, Invitrogen, Thermo Fisher Scientific, Waltham, MA, USA) secondary antibodies, followed by incubation with a chemiluminescent substrate (SuperSignal™ West Pico PLUS Chemiluminescent Substrate or SuperSignal™ West Atto Ultimate Sensitivity Substrate, Thermo Fisher Scientific, Waltham, MA, USA). Immunoreactive bands were visualized using a c300 imaging system (Azure Biosystems, Dublin, CA, USA). Band intensities were quantified using ImageJ software v1.5 (NIH, Bethesda, MD, USA). The integrated optical density of the bands was measured in a digitized image. Relative protein levels were expressed as the ratio of the densitometric volume of the tested band to that of the respective β-actin band [10].

2.14. Statistical Analysis

Data are presented as the mean ± SD of at least three independent experiments. Statistical analyses were performed with the Student's *t*-test and one-way ANOVA, with the Tukey post hoc test for multiple comparisons, as appropriate (StatSoft, Tulsa, OK, USA). *p*-values of <0.05 were considered statistically significant.

3. Results

3.1. CHK1 or ATR Inhibition Is Cytotoxic to Ovarian Cancer Cells

In our previous study, we demonstrated that using PARPi:ATRi and PARPi:CHK1i at a concentration ratio of 1:1 was the most effective combination [10]. Thus, in the present study, cells were incubated with the test compounds at a ratio of 1:1 for 24 and 48 h at a concentration of 4 µM.

The tested combinations, as well as olaparib or CHK1i monotherapy, did not significantly affect the cell survival rate after 24 h (Figure 1A). After 48 h of incubation, ATRi was more cytotoxic in the *BRCA*^{MUT} cell line (PEO-1), reducing the cell viability to 44% compared to approximately 60% in the *BRCA*^{WT} cell lines (SKOV-3 and OV-90). In contrast, CHK1i monotherapy was slightly more cytotoxic in the *BRCA*^{WT} cell lines (72%) compared to the *BRCA*^{MUT} cells (PEO-1, 77% viable cells). PARPi:ATRi combination treatment was the most cytotoxic in PEO-1 cells, decreasing cell viability to 45% compared to 61% in OV-90 and SKOV-3 cells. The combinations treatment did not significantly affect the cytotoxicity compared to ATRi or CHK1i monotherapy, although it was more cytotoxic than PARPi treatment. Treatment with the PARPi:CHK1i combination was less cytotoxic than PARPi:ATRi, reducing the cell viability to 68% in ovarian cancer cells; however, the beneficial effect of PARPi:CHK1i combination at the selected concentrations after 48 h was more visible, as calculated by the coefficient of drug interaction (CDI) (PARPi:CHK1i: SKOV-3, CDI = 0.97; OV-90, CDI = 0.97; PEO-1, CDI = 0.87). As shown in the growth curves in Figure 1B, the average doubling time of the untreated cells was 54.3 h in OV-90 cells, 57.6 h in SKOV-3 cells and 59.9 h in PEO-1 cells.

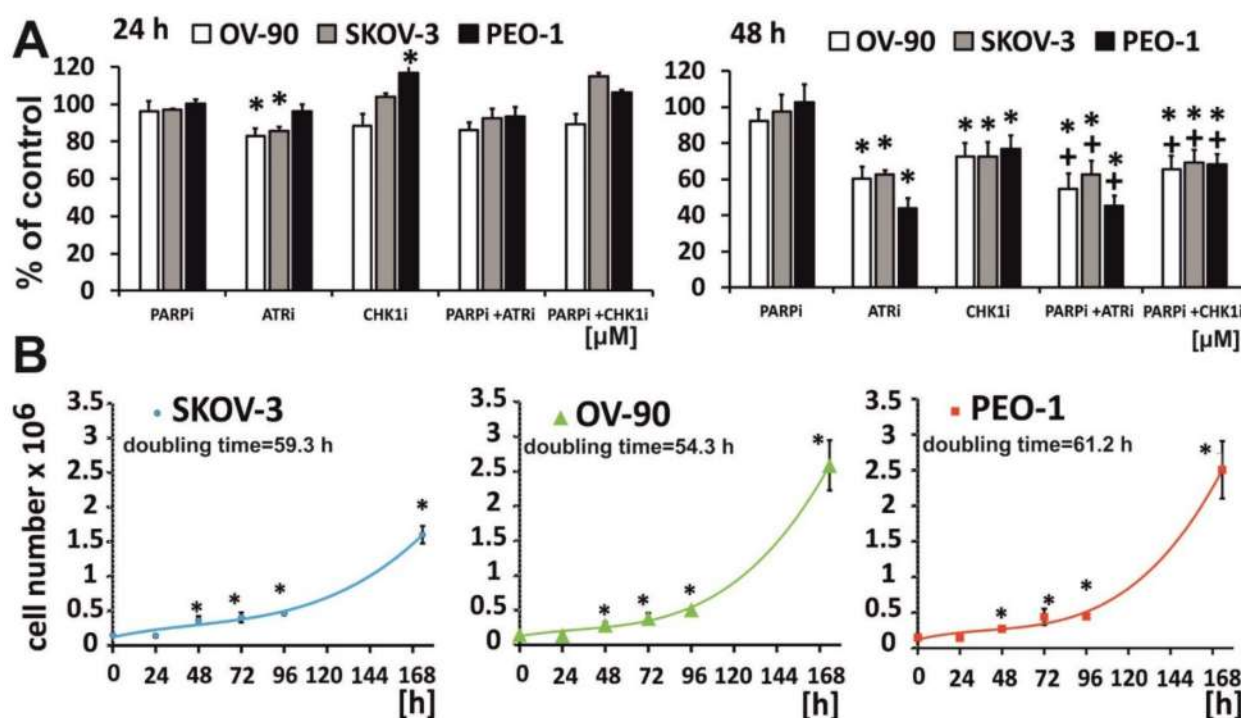


Figure 1. CHK1i or ATRi decreased cell (A) Cell viability after treatment with PARPi, CHK1i, and ATRi in *BRCA*^{MUT} (PEO-1) and *BRCA*^{WT} (OV-90, SKOV-3) cells at a concentration of 4 μ M for 24 and 48 h was assessed by the MTT assay; (B) Cell doubling time was calculated from the cell growth curve during the exponential growth phase using the formula, $T_d = t / \log_2 (N_t / N_0)$. * indicates statistically significant differences between samples incubated with the compound compared with control cells ($p < 0.05$); + indicates statistically significant differences between samples incubated with PARPi alone and the combination treatments (PARPi:ATRi; PARPi:CHK1i) ($p < 0.05$).

3.2. ATRi and CHK1i monotherapy Increases Apoptosis and DNA Damage

Morphological changes induced by the inhibitors were assessed by Hoechst 33258/PI double staining (Figure 2 and Supplementary Figure S1). The greatest apoptotic changes were observed in the *BRCA*^{MUT} cell line (PEO-1). Olaparib monotherapy did not significantly increase the frequency of apoptotic cells, whereas ATRi monotherapy was the most potent in terms of apoptosis induction, leading to increases in the frequency of early apoptotic cells of 40% in PEO-1 cells and 36% in OV-90 cells, but only 19% in SKOV-3 cells. Combination treatment of PARPi with ATRi caused an almost 2-fold increase in early and late apoptotic cellular fractions compared to treatment with PARPi alone in all tested cell lines (PARPi:ATRi: SKOV-3, 40%; OV-90, 45%; PEO-1, 48% compared to PARPi alone: SKOV-3, 22%; OV-90, 22%; PEO-1, 27%) (Figure 2). PARPi:CHK1i combination treatment also led to significant changes in the apoptotic cellular fractions compared to PARPi treatment in OV-90 and PEO-1 cell lines. Nevertheless, no differences were observed between the performance of the combination treatment compared with ATRi or CHK1i.

The exposure of phospholipid phosphatidylserine (PS) on the cell membrane represents a major characteristic of the caspase-dependent apoptosis process. Thus, annexin V, which is a PS-binding protein, is used to detect PS externalization. In order to distinguish between apoptotic and nonapoptotic cells, annexin V was combined with cell impermeable dye, propidium iodide (PI). Olaparib monotherapy was not sufficient to induce apoptosis within the tested time range and concentration (Figure 3 and Supplementary Figure S2). ATRi monotherapy effect was the most prominent in PEO-1 cells, where after 48 h of drug treatment the apoptotic cell fraction equaled 25%. CHK1i monotherapy was the most effective in OV-90 cell line, where the apoptotic cell fraction reached 20%. PARPi:ATRi combination increased apoptosis in OV-90 and PEO-1; however, PARPi:ATRi mediated

apoptotic changes were the most visible in PEO-1 cells compared to olaparib monotherapy. PARPi:CHK1i combination effect was more pronounced in SKOV-3 and OV-90 cell lines. Despite the upward trends, no statistically significant differences were noted between the effect of the combination of PARPi:ATRi and PARPi:CHK1i compared to monotherapy with ATRi or CHK1i in the studied time range.

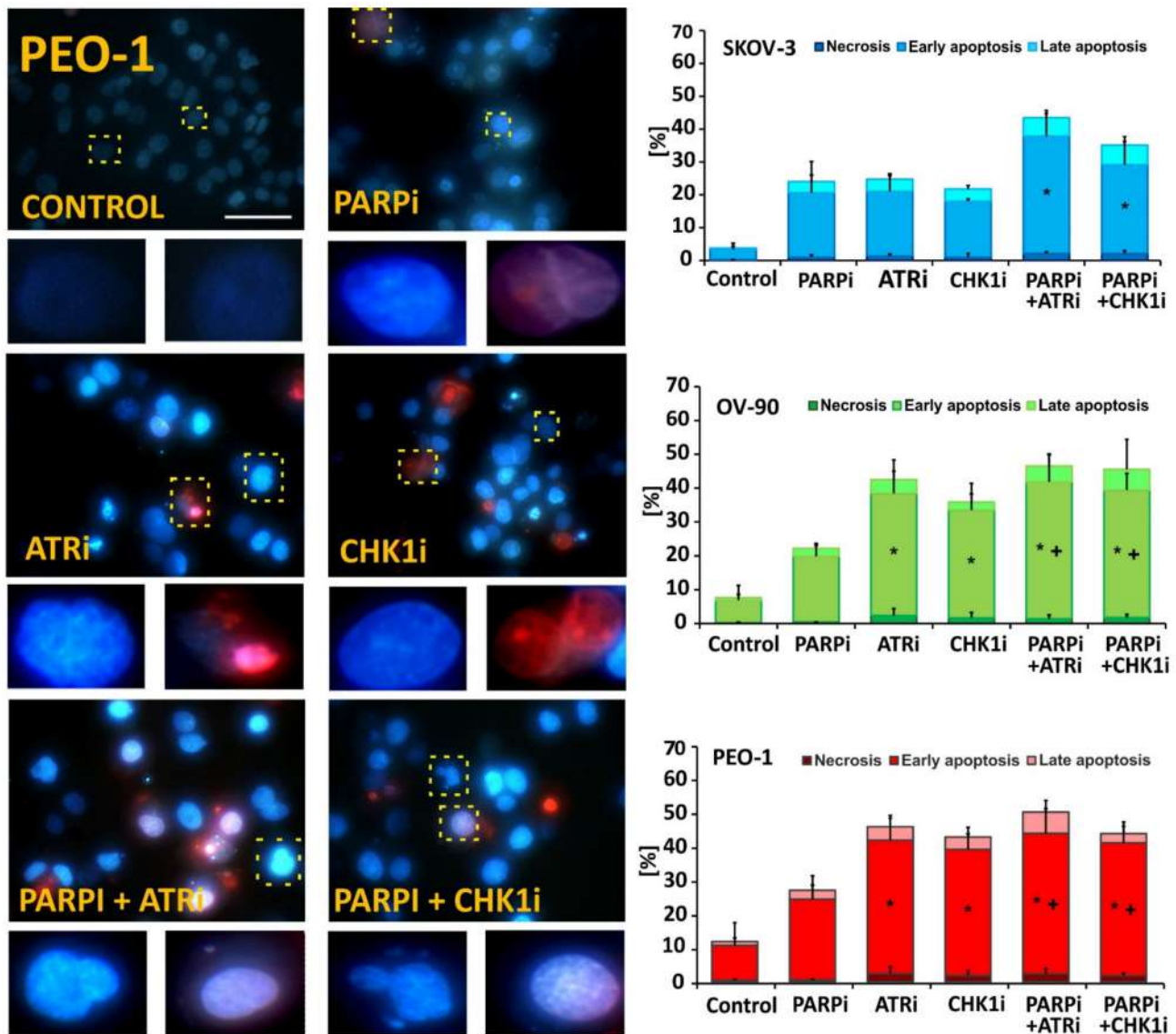


Figure 2. ATRi/CHK1i monotherapy and combination treatment caused cell death. Representative fluorescence images of the apoptotic and necrotic changes caused by the compounds in PEO-1 cells. Representative images in SKOV-3 and OV-90 cells are shown in Supplementary Figure S1. Apoptotic and necrotic changes were visualized after double staining with Hoechst 33258/PI under a fluorescence microscope (Olympus IX70; scale bar 50 μ m, magnification 400 \times). Representative cells are marked with a dashed line and enlarged. The cells were divided into four categories as follows: live cells (dark blue fluorescence), early apoptotic (bright blue fluorescence), late-apoptotic (pink-violet fluorescence), and necrotic cells (red fluorescence). Data are from three independent assays and are presented as the mean \pm SD. * indicates statistically significant differences between treated samples and control cells ($p < 0.05$); + indicates statistically significant differences between samples incubated with PARPi alone and the combination treatments (PARPi:ATRi; PARPi:CHK1i) ($p < 0.05$).

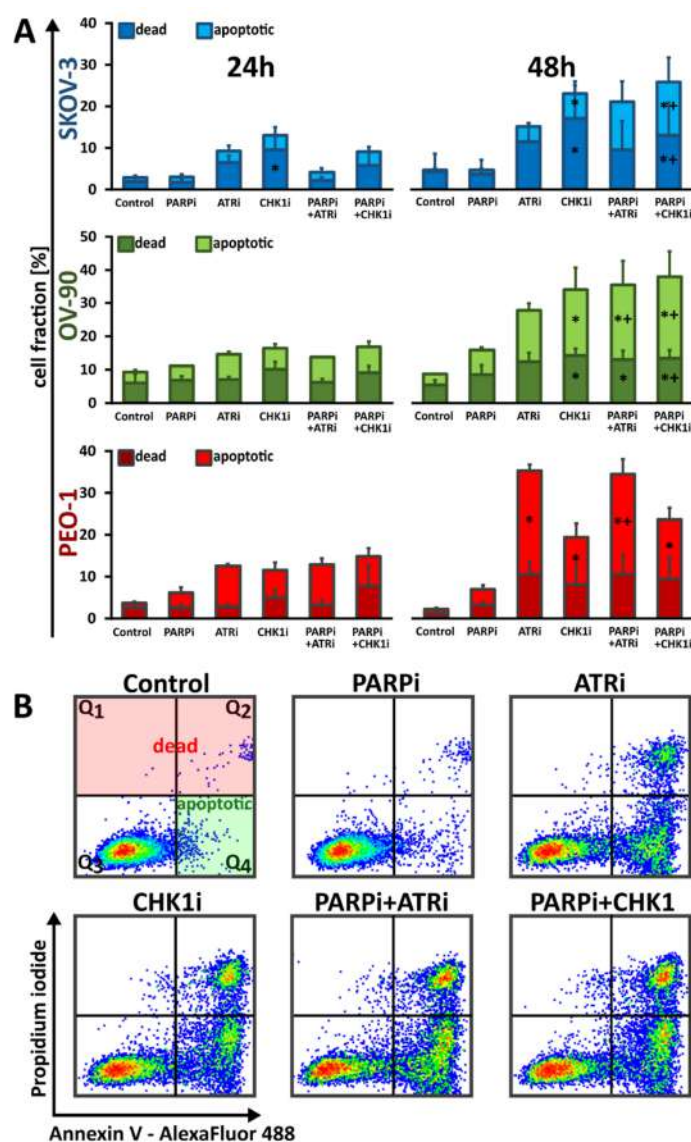


Figure 3. ATRi/CHK1i monotherapy and combination treatment caused phosphatidylserine externalization. (A) Percentage of apoptotic and dead SKOV-3, PEO-1 and OV-90 cells after 24 and 48 h treatment with PARPi (4 μ M), ATRi (4 μ M) or CHK1i (4 μ M) alone or in combination. Data are presented as mean \pm SD of 3 independent experiments. * indicates statistically significant differences between samples incubated with the compound compared with control cells ($p < 0.05$); + indicates statistically significant differences between samples incubated with PARPi alone and the combination treatments (PARPi:ATRi; PARPi:CHK1i) ($p < 0.05$). (B) Representative dot plots showing induction of apoptosis and fraction of dead PEO-1 cells after 48 h treatment with PARPi (4 μ M), ATRi (4 μ M) or CHK1i (4 μ M) alone and in combination. Data for SKOV-3 and OV-90 cells are shown in Supplementary Figure S2. Individual samples are presented as data points. The population of apoptotic cells was calculated according to the presented gating strategy.

Caspases are key mediators of DNA fragmentation. Caspase-3, a protein activated in both extrinsic and intrinsic apoptosis pathways, was used as a marker of apoptosis. We found that cleaved caspase-3 expression, as well as the accumulation of the DNA damage marker γ H2AX, was not significantly increased following PARPi monotherapy in *BRCA^{MUT}* and HR-proficient cells. Treatment with ATRi or CHK1i increased cleaved caspase-3 levels (SKOV-3, 5.2-fold (ATRi) and 6.12-fold (CHK1i); OV-90, 2.6-fold (ATRi) and 2.9-fold (CHK1i); PEO-1, 4.2-fold (ATRi) and 3.2-fold (CHK1i)) compared to control cells (Figure 4B). Each combination treatment was found to be more effective than treatment

with PARPi alone. Although cleaved caspase-3 expression levels were not significantly increased in combination treatments compared to ATRi or CHK1i monotherapy, we did find that compared to PARPi treatment alone, cleaved caspase-3 levels were increased 6-fold, 3.5-fold and 4.2-fold in SKOV-3, OV-90 and PEO-1 cells, respectively, after PARPi:ATRi and PARPi:CHK1i combination treatments.

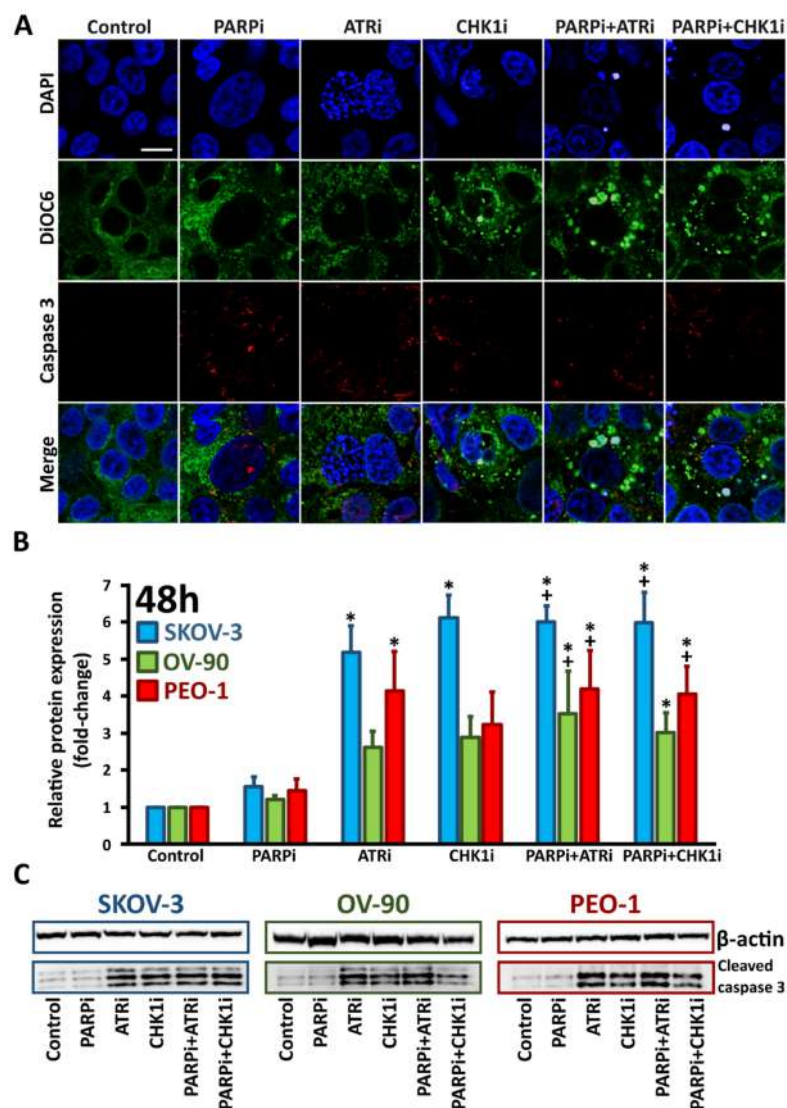


Figure 4. ATRi/CHK1i treatment increases caspase-3 expression. (A) For immunofluorescence staining, PEO-1 cells were incubated with PARPi, ATRi or CHK1i alone, or the combination of PARPi:ATRi or PARPi:CHK1i at 4 μ M for 48 h and labeled with antibodies against caspase-3 (red colour). Representative images for SKOV-3 and OV-90 cell lines are shown in Supplementary Figure S3. Images were acquired using a confocal laser scanning microscope (scale bar 20 μ m, magnification 63 \times); (B) Relative expression of cleaved caspase-3 in the cells. * indicates statistically significant differences between samples incubated with the compound compared with control cells ($p < 0.05$); + indicates statistically significant differences between samples incubated with PARPi alone and the combination treatments (PARPi:ATRi; PARPi:CHK1i) ($p < 0.05$); (C) Representative Western blot images.

An increase in γ H2AX expression was observed after treatment with ATRi or CHK1i (SKOV-3, 28.8-fold (ATRi) and 44.1-fold (CHKi); OV-90, 4.9-fold (ATRi) and 5.5-fold (CHKi); PEO-1, 2.1-fold (ATRi) and 1.8-fold (CHKi)). PARPi in combination with CHK1i increased γ H2AX phosphorylation compared with PARPi alone by 32.2-fold in SKOV-3 cells, 6.3-fold in OV-90 cells and 2.1-fold in PEO-1 cells. Similarly, PARPi treatment in combination with

ATRi increased γ H2AX expression compared with PARPi alone by 28.4-fold in SKOV-3 cells, 5.6-fold in OV-90 cells and 2.2-fold in PEO-1 cells. The combination treatment did not significantly increase γ H2AX expression compared to ATRi or CHK1i monotherapy. Although the largest changes in protein expression levels were found in *BRCA*^{WT} SKOV-3 cells, this cell line was found to have the lowest protein expression levels in the control cells (Supplementary Figure S5).

In situ confocal laser scanning immunofluorescence (Figures 4A and 5A and Supplementary Figures S3 and S4) were consistent with the Western blot data for cleaved caspase-3 and γ H2AX expression.

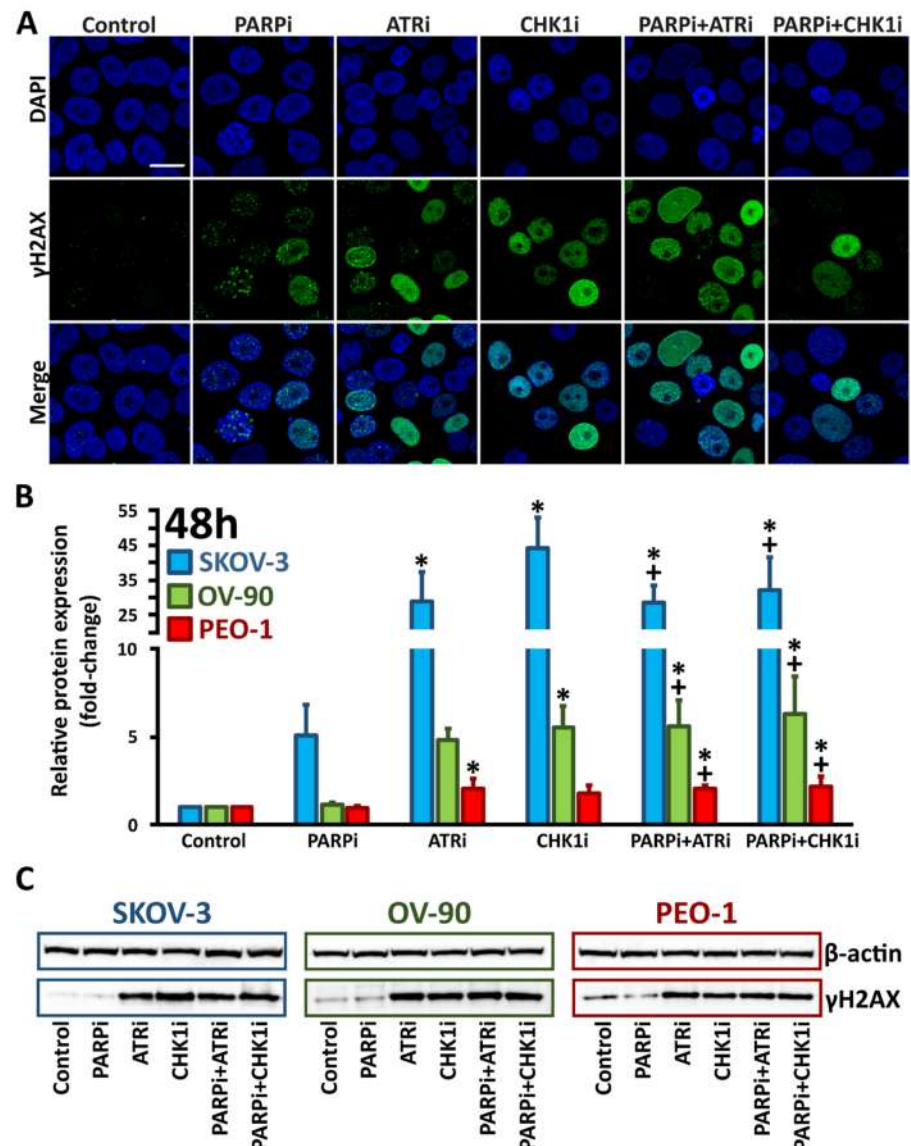


Figure 5. ATRi/CHK1i increases γ H2AX expression. (A) For immunofluorescence staining, PEO-1 cells were treated with PARPi, ATRi or CHK1i, or a combination of PARPi:ATRi or PARPi:CHK1i at 4 μ M for 48 h and labeled with antibodies against γ H2AX (green colour). Representative images in SKOV-3 and OV-90 cells are shown in Supplementary Figure S4. Images were acquired using a confocal laser scanning microscope (scale bar 20 μ m, magnification 63 \times); (B) Relative expression of γ H2AX. * indicates statistically significant differences between samples incubated with the compound compared with control cells ($p < 0.05$); + indicates statistically significant differences between samples incubated with PARPi alone and the combination treatments (PARPi:ATRi; PARPi:CHK1i) ($p < 0.05$); (C) Representative Western blot images.

3.3. Monotherapy with ATRi/CHK1i and Combination Treatment with PARPi Activates DNA Damage Response Signaling through Chromatin Condensation and Progression through the G2/M Checkpoint

In contrast to SKOV-3 and PEO-1 cells, OV-90 cells were slightly more susceptible to chromatin condensation after exposure to the drugs. In SKOV-3 cells, changes in the apoptotic cellular fraction did not exceed 7%, regardless of whether the cells were exposed to monotherapy or co-treatment. Similarly, in the *BRCA^{MUT}* cell line (PEO-1), the increase in the apoptotic cellular fraction after PARPi:CHK1i co-treatment was negligible (~13%) compared to olaparib monotherapy (~10%) (Figure 6A,C and Supplementary Figure S6).

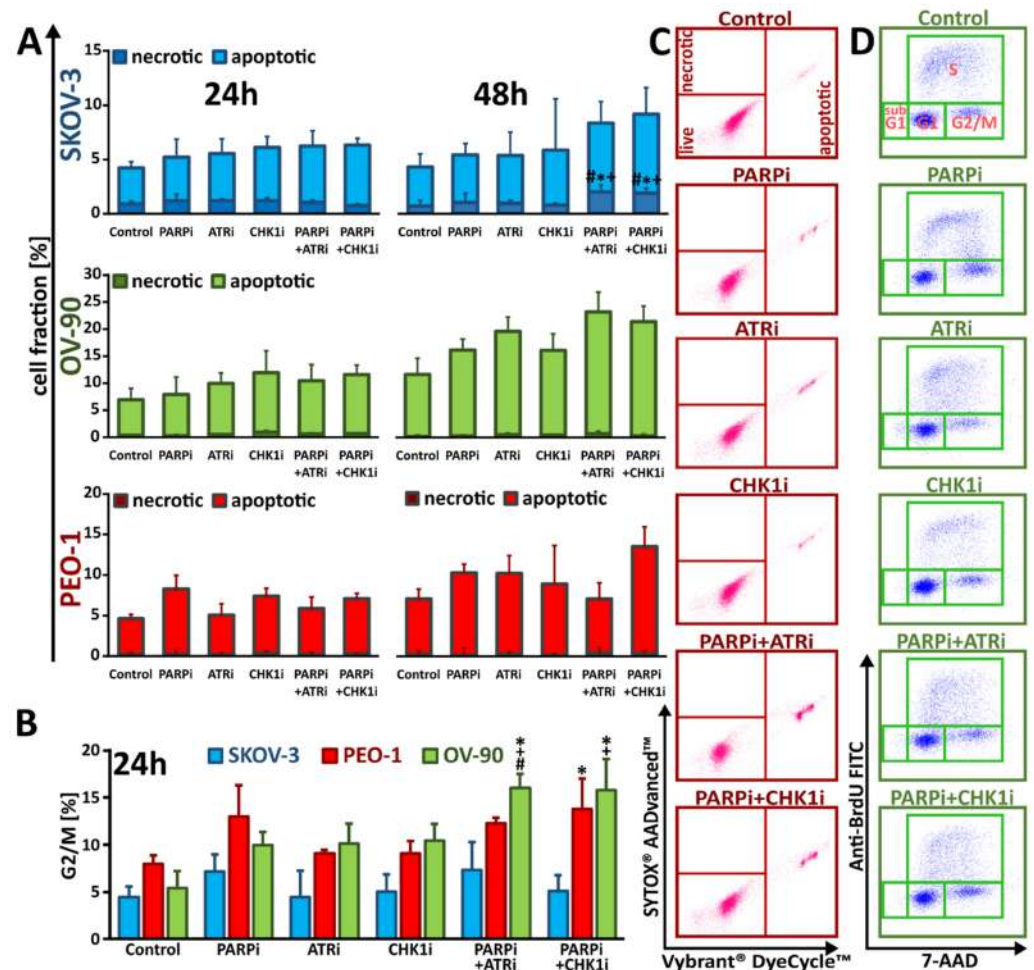


Figure 6. Treatment with PARPi in combination with ATR/CHK1 pathway inhibitors bypasses the cell cycle checkpoint due to an early signal of cell death. (A) Percentage of apoptotic and necrotic SKOV-3, PEO-1 and OV-90 cells after 24 and 48 h treatment with PARPi (4 μ M), ATRi (4 μ M) or CHK1i (4 μ M) alone or in combination; (B) G2/M phase distribution of PEO-1 treated for 24 h. Data are presented as mean \pm SD of 3 independent experiments. * $p < 0.05$ vs. control cells. * indicates statistically significant differences between samples incubated with the compound compared with control cells ($p < 0.05$); + indicates statistically significant differences between samples incubated with PARPi alone and the combination treatments (PARPi:ATRi; PARPi:CHK1i) ($p < 0.05$); # denotes statistically significant differences between samples incubated with ATRi or CHK1i alone and their corresponding combination treatments (PARPi:ATRi; PARPi:CHK1i) ($p < 0.05$); (C) Representative dot plots showing induction of apoptosis and necrosis in PEO-1 cells after 48 h treatment with PARPi (4 μ M), ATRi (4 μ M) or CHK1i (4 μ M) alone and in combination. Data for SKOV-3 and OV-90 cells are shown in Supplementary Figure S6. Individual samples are presented as data points. The population of apoptotic cells was calculated according to the presented gating strategy; (D) Representative dot

plots demonstrating the distribution of cell cycle phases in PEO-1 cells after 24 h treatment alone and in combination. Representative dot plots for SKOV-3 and OV-90 cells are shown in Supplementary Figure S7. Individual samples are presented as data points. The population of cells in each phase of the cell cycle was calculated according to the presented gating strategy.

The largest changes were observed in OV-90 cells, where simultaneous treatment with ATRi enhanced the effect of olaparib on the apoptotic cellular fraction from ~16% to ~23%. Similar results were found after co-treatment with CHK1i and PARPi, where an increase in the frequency of apoptosis to ~21% was observed. It should also be noted that after 48 h of treatment, only OV-90 cells were found to have significantly increased apoptosis compared to the 24 h time point. In summary, our data suggest that biochemical changes were associated with apoptotic cell death and not necrosis.

We previously confirmed that PARPi treatment activated the ATR/CHK1 pathway [10], which in turn affected cell cycle progression in the context of PARPi-induced DNA damage (Figure 6B,D and Supplementary Figure S7). Thus, we evaluated the effect of PARPi, ATRi, and CHK1i alone or in combination on cell cycle phase distribution, paying particular attention to G2/M, since cells with damaged DNA are arrested at the G2/M checkpoint prior to mitosis. We did not observe a significant change in the distribution of the G2/M phase of the cell cycle after treatment with PARPi in combination with ATRi or CHK1i in both SKOV-3 and PEO-1 cells. Furthermore, we found that PARPi treatment alone increased the frequency of G2/M cells to only 7% in SKOV-3 cells and 15% in PEO-1 cells. In both cell lines, ATRi and CHK1i alone did not increase the frequency of cells in G2/M compared to PARPi alone, with levels similar to those observed in untreated cells.

Interestingly, only OV-90 cells were more sensitive to treatment with a combination of drugs compared to monotherapy. ATRi and CHK1i administered with olaparib significantly induced G2/M arrest. Simultaneous treatment with ATRi enhanced the effect of olaparib alone (~10%) and significantly increased the frequency of G2/M cells (~16%). A similar effect, resulting in an ~15% increase in G2/M arrest, was observed when olaparib was co-administered with the CHK1 inhibitor. Cells treated with PARPi in combination with ATRi/CHK1i-induced DNA damage. Inhibition of the ATR–CHK1 pathway resulted in some cells passing through the G2/M checkpoint, leading to chromosomal damage, genomic instability, and cell death.

3.4. Treatment with ATRi/CHK1i Induces Aberrant Cell Cycle Progression and Increases RS Levels

To investigate the effects of kinase inhibitors in combination with olaparib on cell proliferation, we used BrdU and EdU incorporation to monitor S-phase progression. BrdU-positive cells were gated into early mid or mid-late S-phase populations. An increase in the abundance of early S-phase cells was observed in PEO-1 cells (Figure 7A), indicating the slower progression of cells through the S-phase, a sign of RS. S-phase extension was also observed in OV-90 cells after PARPi:ATRi treatment, although these changes were not statistically significant. Interestingly, treatment with ATRi and CHK1i alone or in combination with olaparib decreased BrdU intensity in S-phase, consistent with slower DNA synthesis and higher RS in OV-90 and PEO-1 cells (Figure 7B). BrdU incorporation into S-phase PEO-1 cells was more diminished after combination treatment than after treatment with olaparib alone. The combination treatment did not significantly change cell proliferation compared to ATRi or CHK1i monotherapy.

Next, we used EdU incorporation to examine the effects of the inhibitors on the three distinct S-phase stages [25–27]. In control cells, we observed characteristic labeling of normal S-phase: low homogeneous labeling, typical of the early S-phase (with uniform fluorescence throughout the nucleus); strong homogeneous labeling, specific to middle S-phase, and heterogeneous labeling (Figure 7C) [28]. Thus, ATR and CHK1 are critical in the early S-phase to limit replication origin firing and to suppress the formation of ssDNA.

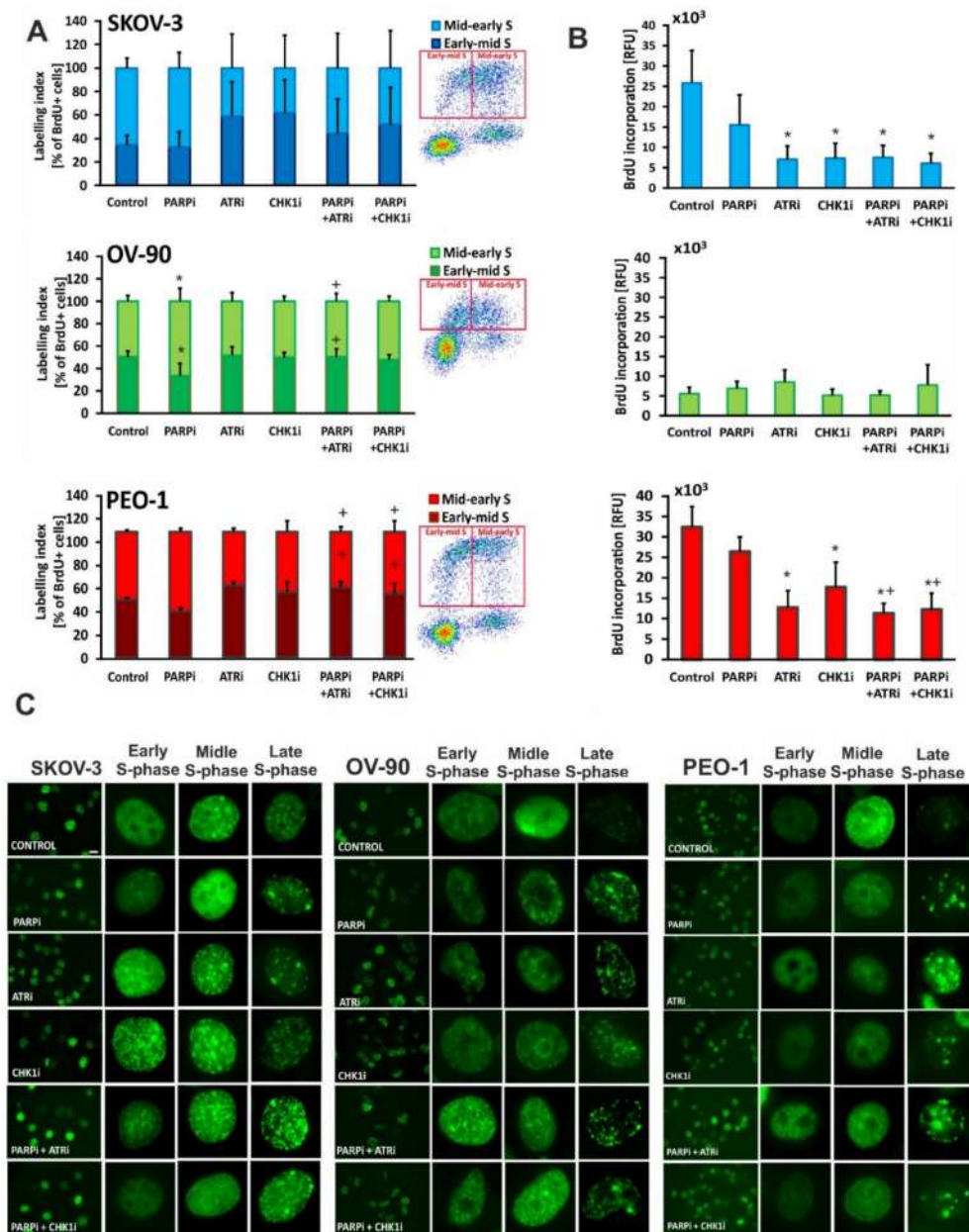


Figure 7. The effects of PARPi, ATRi or CHK1i alone and in combination on the S-phase of the cell cycle. (A) BrdU-positive heterochromatin labelling (labelling index) was used to examine the S-phase of the cell cycle after 24 h treatment with PARPi (4 μ M), ATRi (4 μ M) or CHK1i (4 μ M) alone and in combination. The cells were gated into early mid or mid-late S-phase populations based on DNA content; (B) Incorporation of BrdU. Data are presented as mean \pm SD of 3 independent experiments. * indicates statistically significant differences between samples incubated with the compound compared with control cells ($p < 0.05$), + indicates statistically significant differences between samples incubated with PARPi alone and the combination treatments (PARPi:ATRi; PARPi:CHK1i) ($p < 0.05$); (C) Fluorescence images of EdU incorporation. Based on differences in the pattern of DNA replication (EdU), cells were identified as progressing through early, mid, and late stages of the S-phase (magnification 40 \times , scale bar 20 μ m). Enlarged fragments of photos are presented in the columns on the right side of each individual cell line panel.

3.5. Treatment with ATRi/CHK1i in Combination with PARPi Increases Chromosomal Abnormalities

Combination treatment using olaparib with ATRi or CHK1i can lead to a temporary latency in DNA damage, since inhibition of these kinases allows cells to pass through the

G2/M checkpoint. Flow cytometry analysis of the cell cycle showed a slight decrease in the mitotic index after PARPi:CHK1i treatment in SKOV-3 cells (Figure 8A). A decrease in mitotic levels was also observed in OV-90 cells following treatment with ATRi or CHK1i, either alone or in combination with olaparib. Treatment with these inhibitors did not significantly affect the mitotic index of the PEO-1 cell line.

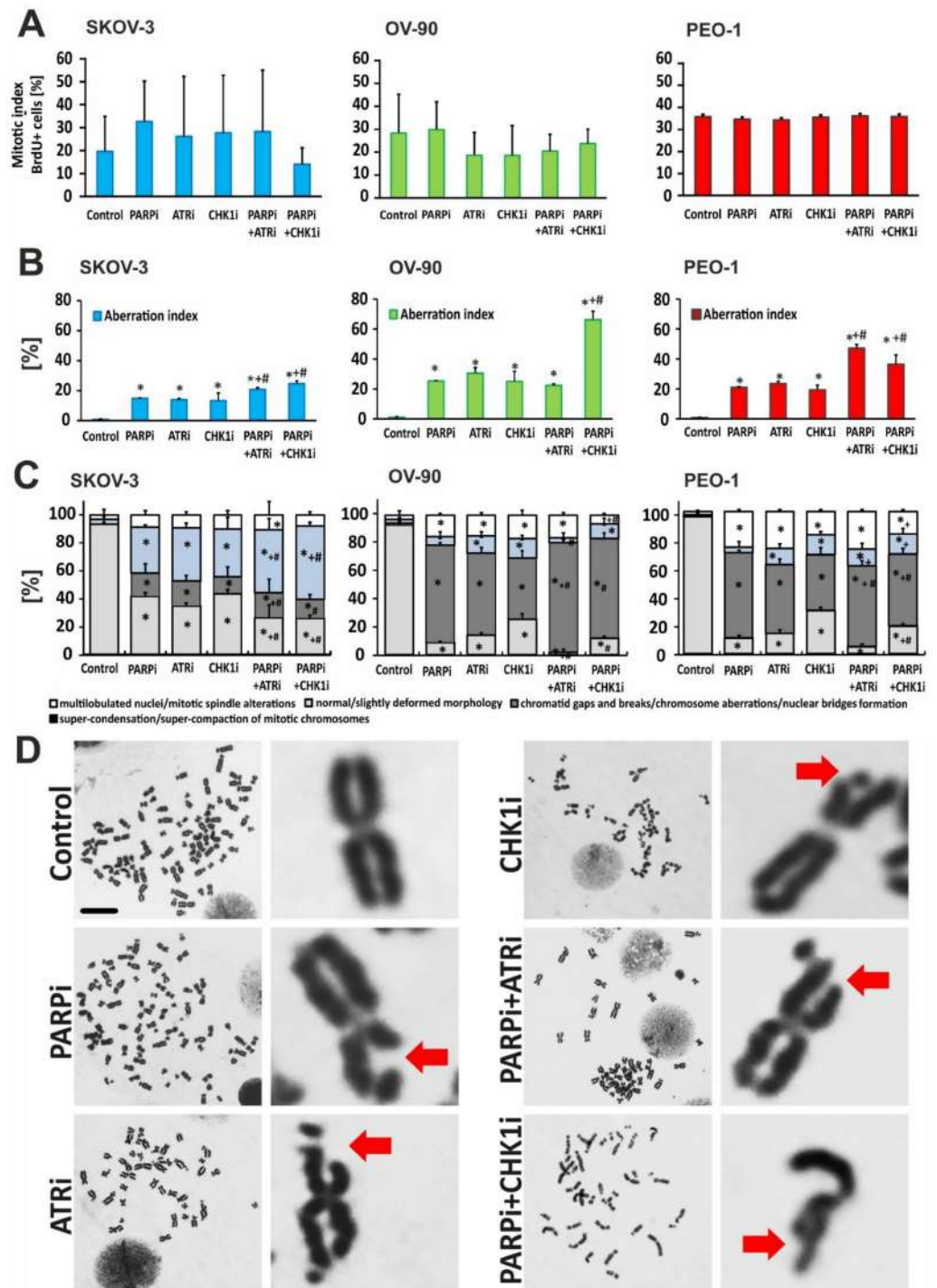


Figure 8. PARPi treatment in combination with CHK1i and ATRi causes chromosome aberrations. DNA damage effects were measured by metaphase chromosome spread. (A) The mitotic index was calculated as the percent ratio between the number of dividing cells and the entire cell population.

The quantification was determined by BrdU incorporation; (B) Aberration index (M-phase aberrant cells) was calculated as the percent ratio between the number of cells showing chromosome aberrations and all mitotic cells; (C) Nuclear phenotypes in PEO-1/OV-90/SKOV-3 cells were determined by Giemsa and by counterstaining with DAPI (0.1 mg/mL). Types of chromosomal aberrations were counted under the microscope (Zeiss, Jena, Germany). * indicates statistically significant differences between samples incubated with the compound compared with control cells ($p < 0.05$); + indicates statistically significant differences between samples incubated with PARPi and the corresponding combination treatments (PARPi:ATRi; PARPi:CHK1i) ($p < 0.05$); # denotes statistically significant differences between samples incubated with ATRi or CHK1i and their corresponding combination treatments (PARPi:ATRi; PARPi:CHK1i) ($p < 0.05$); (D) Replication stress inhibitors synergize with PARPi and cause chromosomal aberrations in PEO-1 cells. Representative images of OV-90 and SKOV-3 cells are shown in Supplementary Figure S8. Red arrows show damaged chromosomes. Stained slides were analyzed using a 100 \times objective (scale bar 20 μ m) and a Nikon ECLIPSE E600W microscope (Nikon, Warsaw, Poland).

Despite slight changes in the mitotic index, premature initiation of mitosis follows an aberration course, because the nonreplicated regions of the genome are expressed in the form of losses or breaks in the chromosomes. Aberrant M-phase cells (included in the aberration index) showed chromosomal abnormalities. In the SKOV-3 and PEO-1 cell lines, a combination of PARPi:CHK1i and PARPi:ATRi treatment led to an increase in chromosomal aberrations compared to monotherapy (Figure 8B). However, the level of damage was 2-fold higher in the PEO-1 $BRCA^{MUT}$ cell line than in the SKOV-3 $BRCA^{WT}$ cell line.

Next, we distinguished between the specific types of chromosomal aberrations (Figure 8C). The frequency of normal cells decreased significantly after treatment with PARPi to 11.1% in PEO-1 ($BRCA^{MUT}$) cells and 8.7% in OV-90 ($p53^{MUT}$) cells compared to controls. Similarly, after ATRi treatment, the frequency of normal cells was 14.4% in the PEO-1 cell line and 14.2% in the OV-90 cell line compared to the controls. Less significant changes were observed after treatment with CHK1i alone (~30%). Virtually no normal cells were observed after treatment with the PARPi:ATRi combination (Figure 8D). Although the PARPi:CHK1i combination had a weaker effect than PARPi:ATRi (PEO-1, 19.4% normal cells; OV-90, 12.1% normal cells), this effect was still larger than that observed after treatment with CHK1i alone. The drugs had virtually no effect on the SKOV-3 line at each dose tested. In contrast, in the OV-90 cell line, both combinations led to an increase in chromosomal aberrations (chromatid gaps and breaks, nuclear bridge formation) compared to monotherapy. Furthermore, although an increased number of aberrations was observed in the PEO-1 cell line, no differences between the combination treatment and monotherapy were found. With respect to the subcategory comprising multilobulated nuclei and mitotic spindle alterations, the greatest changes occurred in the PEO-1 cell line (26%), followed by the OV-90 (16%) and SKOV-3 (8–10%) cell lines. Noted gaps and breaks or abnormal morphology means that unrepaired DSBs enter the M-phase. Thus, blocking checkpoints with ATR or CHK1 inhibitors results in genomic instability and may lead to mitotic catastrophe (MC). Here, we found that PARPi:ATRi-treated cells that progressed into mitosis after a transient cell cycle arrest failed to separate, resulting in MC.

3.6. ATR Inhibition Intensifies PARPi-Induced Formation of MN in $BRCA^{MUT}$ Cells

MN are pieces of chromosomes or entire chromosomes that are formed during cell division. MN are not incorporated into one of the two main daughter nuclei [29]. After the telophase, they form a rounded body inside the cytoplasm, which is separate from the main nuclei [30]. Here, we found that a mitosis-dependent type of MN formation, identified as a typical consequence of lost or lagging chromosomal fragments during the anaphase–telophase transition (Figure 9). Following 24 h treatment, ATRi induced a statistically significant increase in the frequency of cells with MN (44.7% vs. control) in OV-90 cells. Combination treatment with PARPi and ATRi, as well as PARPi and CHK1i,

induced similar frequencies of MN (43.3% and 37.4%, respectively). In the SKOV-3 and OV-90 lines, no beneficial effect of the combination was observed. Monotherapy with either PARPi or CHK1i did not significantly affect the number of cells with MN. However, in SKOV-2 cells, elevated levels of MN were only detected after treatment with a combination of PARPi and ATRi (38%) or PARPi and CHK1i (32.7%). In PEO-1 cells, ATRi synergized with PARPi to increase the frequency of MN to 48% in contrast to treatment with PARPi or ATRi alone.

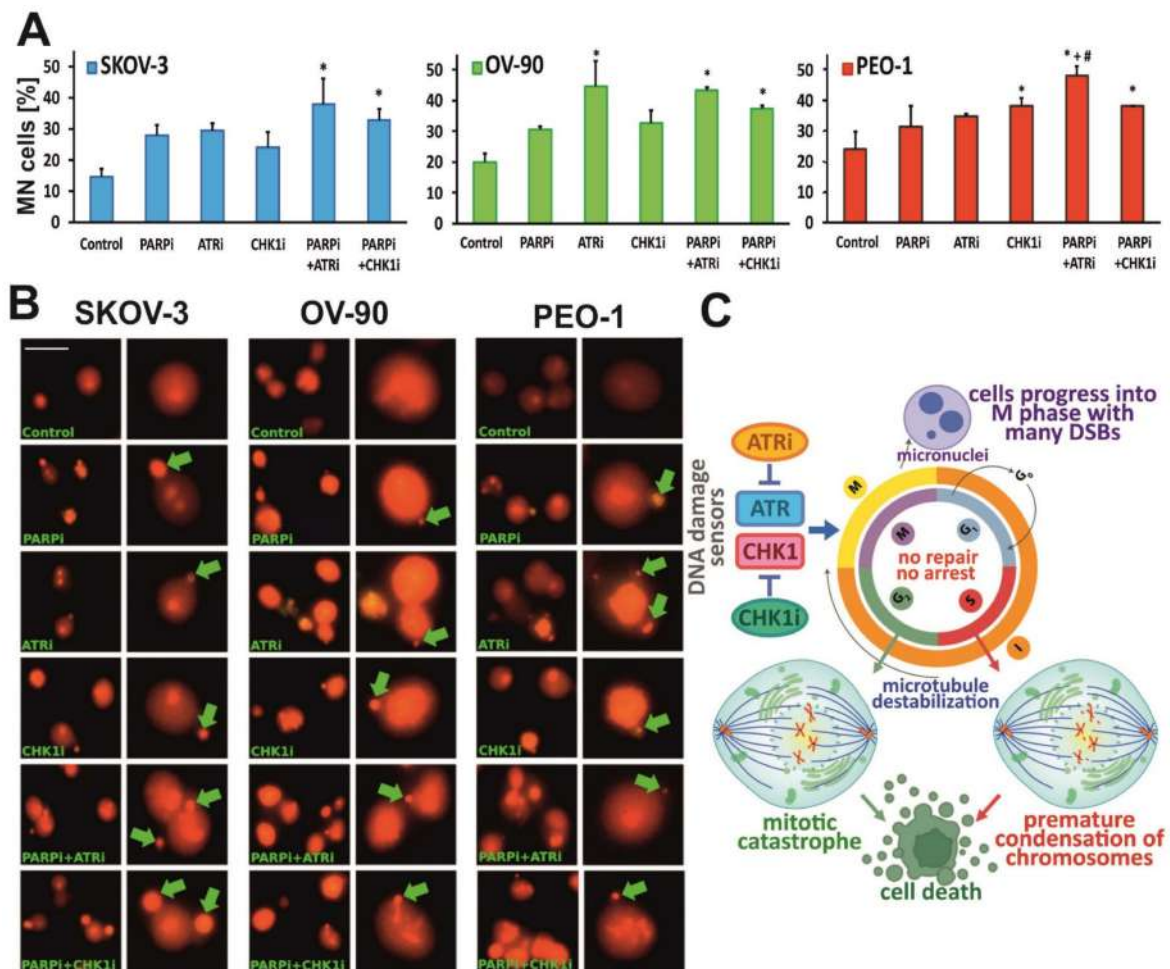


Figure 9. PARPi treatment in combination with ATRi/CHK1i elevates the number of cells with MN. (A) Number of cells with MN in OV-90, SKOV-3 and PEO-1 cell lines after 24 h treatment with PARPi (4 μ M), ATRi (4 μ M) or CHK1i (4 μ M) alone and in combination. * indicates statistically significant differences between samples incubated with the compound compared with control cells ($p < 0.05$); + indicates statistically significant differences between samples incubated with PARPi alone and the combination treatments (PARPi:ATRi; PARPi:CHK1i) ($p < 0.05$); # denotes statistically significant differences between samples incubated with ATRi or CHK1i and their corresponding combination treatments (PARPi:ATRi; PARPi:CHK1i) ($p < 0.05$); (B) Morphological changes after 24 h treatment with compounds related to the formation of MN. Extranuclear bodies of the damaged part of chromosome are marked by green arrows. Enlarged fragments of photos are presented in the columns on the right side of each individual cell line panel. The cells were stained with acridine orange and visualized by fluorescence microscopy (Olympus IX70, Japan; scale bar 50 μ m, magnification 400 \times); (C) Ovarian cancer cells with ATR/CHK1 deficiencies progress to M phase without G2/M checkpoint arrest. ATRi/CHK1i induces premature chromosome condensation (PCC) by bypassing the internal S-phase checkpoint mechanism. The failure of G2/M checkpoint arrest causes severe DNA fragmentation such as unrepaired double-strand breaks (DSBs) during M phase, which result in multiple MN. Cells with multiple nuclear fragmentations undergoing MC.

4. Discussion

Ovarian cancer remains a highly lethal disease [31]. PARP inhibitors are now used as a maintenance therapy for patients with *BRCA*^{MUT} epithelial ovarian cancer and as a treatment of relapsed *BRCA*^{MUT} ovarian cancer in patients who have been treated with two or more chemotherapies before [32,33]. Despite their effectiveness, resistance to PARP inhibitors has been clinically reported [34–36]. Thus, it is critical to determine the mechanism of action of PARPi, as well as other inhibitors that compromise genomic stability linked to cell cycle disruption. There is a strong connection between genomic instability acquired during the S-phase and chromosomal instability following mitotic progression. The purpose of our study was to examine the short-term (up to 48 h) efficacy of PARPi together with DDR-targeting agents. We investigated whether premature mitotic entry induced by ATR/CHK1 inhibition increases genomic instability in *BRCA*^{MUT} and *BRCA*^{WT} HGSOC. We demonstrated that a combination of inhibitors was not more cytotoxic than monotherapy. However, despite the weak cytostatic activity of PARP, treatment with CHK1i or ATRi in combination with PARPi results in an increase in replication disorders due to a lack of checkpoint control by CHK1/ATR and PARP. ATR and CHK1 kinase inhibitors disrupt the cell cycle and as a result, cells with high levels of DSBs enter mitosis prematurely in the presence of unrepaired DNA. The combination of olaparib with inhibitors of the ATR/CHK1 pathway generated chromosomal abnormalities, independent of the *BRCA*^{MUT} status of the cells, and formed micronuclei. Our data suggest that DNA DSB lesions do not immediately lead to cell death, but can progress into mitosis, resulting in chromatin aberrations. Chromosome instability might cause cell death by MC. Abrogation of the ATR-initiated checkpoint cascade mediated through CHK1 has previously been shown to direct cells into MC [37].

DDR is controlled not only by the concentration and persistence of DNA lesions, but also by the proliferative status of the damaged cell. Previously, we examined the effect of prolonged PARPi, ATRi and CHK1i treatment and confirmed a differential drug response profile, which was dependent on *BRCA* status [10]. In this study, abnormalities in the proliferation process were initially observed 24 h after combined treatment with PARPi and ATRi, with a significantly stronger effect seen after 48 h. Changes in the proliferation machinery were manifested as a decrease in the mitotic index and an increase in heterochromatin formation. Our studies showed that the combination of ATRi/CHK1i with PARPi is no more cytotoxic than monotherapy with ATRi and CHK1. This may indicate that at the selected time and dose, olaparib in the tested lines has a cytostatic effect. Combining olaparib with ATRi was cytotoxic in ATM-deficient cells and cytostatic in ATM^{WT} cells [38]. Cytotoxic and cytostatic effects of olaparib and IR were induced in a PTEN (phosphatase and tensin homolog) independent manner in the endometrial HEC-6 cells [39]. Cell survival variance of triple-negative breast cancers were impacted at 40% by the time of olaparib exposure, at 39% by radiotherapy, at 14% by the olaparib concentration, and at 9% by the type of cell line [40]. In our study, the cytostatic effect of olaparib may require prolonged dosing for therapeutic effect [41]. Although the PEO-1 *BRCA*^{MUT} cell line was the most sensitive to treatment with RS kinase inhibitors, we found that the ATRi and CHK1i were cytotoxic and genotoxic to *BRCA*^{WT} cells. Loss of the integral HR pathway components in cancers with non-*BRCA* HR defects due to germline or somatic mutations in *PALB2*, *RAD51B*, *RAD51C*, or *RAD51D*, or their inactivation through promoter methylation, might be the cause of olaparib susceptibility [42].

Next, we examined chromatin condensation as an early marker of repaired DNA damage after treatment with the tested inhibitors. Our data showed slight changes in chromatin condensation in all cell lines. Significant differences were observed in the SKOV-3 line after treatment with both drug combinations. Previous studies have demonstrated that chromatin needs to be dynamically reorganized to properly orchestrate DDR [43]. Moreover, chromatin compaction may provide the structural and molecular environment to mimic the DDR amplification step, and therefore trigger ATM and ATR signaling independent of the DNA lesions [43,44]. PARP1 selectively binds to transcriptionally active chromatin and

controls the fidelity of gene transcription [45,46]. Inactive forms of PARP1 may contribute to the formation of condensed chromatin structures [47]. On the other hand, histone eviction and local chromatin decondensation have been observed in the presence of DSBs, which is then followed by chromatin compaction [48] and acceleration of DDR downstream pathways, including signaling through the CHK1 and CHK2 kinases [43,49].

ATR and CHK1 inhibitors result in the accumulation of DNA damage in mitosis, including MN formation and thus cell death. The beneficial effect of the PARPi:ATRi combination on MN was seen only in the PEO-1 *BRCA^{MUT}* cell line. Lagging chromosomes and MN are elevated upon PARP1/2 depletion or inhibition, following the accumulation of unrepaired or inappropriately repaired DNA lesions during the S-phase that progress into mitosis [14]. Olaparib was shown to induce MN formation and anaphase chromatin bridges, which are hallmarks of chromosome missegregation [50]. ATRi was found to promote the generation of acentric dysfunctional MN and abrogate radiation-induced G2 cell-cycle checkpoint arrest due to aberrant mitosis and MC [51]. ATRi extended mitotic duration, associated with lagging chromosomes, anaphase bridges and MN formation upon completion of mitosis. Combined PARPi and ATRi treatment resulted in severely extended mitotic duration, eventually leading to genome disintegration and catastrophic damage [52]. Treatment with PARPi and ATRi in combination were also found to be effective in ATM-deficient tumors, elevating the number of MN to a greater extent than olaparib monotherapy [38]. Our findings are partly consistent with a study by Schoonen et al., where increased mitotic defects and elevated numbers of MN in *BRCA2*-defective cells were observed after PARP inhibition, while the number of MN increased upon ATR inhibition [53].

One of the consequences associated with the presence of MN is cell death. In DDR, MC is induced when chromatin condensation and spindle assembly occur on incompletely replicated DNA to cause chromosome fragmentation [54]. PARP plays a crucial role in the maintenance of chromosomal stability to avoid an increase in cells with structural chromosomal aberrations. A higher frequency of chromatid breaks, anaphase bridges and MN have been found following PARP1 inhibition, particularly in response to genotoxic stress [55]. Another study confirmed that olaparib-treated cells might die by MC [14]. In the unperturbed S-phase, ATR is activated at a low level during the early S-phase, and its activity declines at the end of the S-phase. ATR inhibition leads to the premature accumulation of cyclin B through the expression of forkhead box protein M1 (FOXO1) in S-phase cells [56]. We demonstrate that ATRi and CHK1i alone impact replication throughout the S-phase as a result of raising the RS. Previously, we reported that the activation of the S-phase checkpoint in response to DNA damage might be associated with CHK1 phosphorylation in PARPi-treated cells [10]. It is known that the basal levels of CHK1 protein during the S-phase inhibit mitotic entry. Inhibiting CHK1 has the opposite effect and has been found to increase the initiation of DNA synthesis, as well as DNA damage [57]. However, despite olaparib-induced checkpoint activation, cancer cells still progress into mitosis. Extensive DNA damage in mitosis causes metaphase arrest due to defective kinetochore attachment and activation of the spindle-assembly checkpoint (SAC) [58].

Metaphase arrest due to DNA damage leads to MC, whereby cells die by apoptosis or by avoiding mitotic arrest [59]. Here, apoptosis was found to be significantly increased with the ATRi/CHK1i monotherapy in both *BRCA^{MUT}* and HR-proficient cell models. ATRi and CHK1i-treated cells that underwent apoptosis had DNA content consistent with the early S-phase, suggesting that cells carrying DNA lesions into the S-phase, in the absence of functional ATR, are predisposed to higher levels of RS and intensified cell death [60]. Treatment with olaparib alone was unable to increase the expression of cleaved caspase-3, an apoptosis marker, in the SKOV-3 cell line [61]. Here, the apoptotic cellular fractions assessed by double staining with Hoechst 33258/PI and by the externalization of phosphatidylserine did not significantly increase after olaparib monotherapy, similar to changes in caspase-3 levels, suggesting that olaparib alone was insufficient to induce cell death by apoptosis in the tested time range. ATRi and CHK1i monotherapies were more efficient in apoptosis

induction, elevating cleaved caspase-3 levels and the frequency of apoptotic cells in the OV-90 and *BRCA*^{MUT} PEO-1 cell lines. Previously, we assessed the overall level of DNA damage, including SSBs and DSBs, using the alkaline and neutral variants of the comet assay, and found that ATRi and CHK1i had a marked effect on DNA strand breaks [10]. In the current study, DSBs were monitored using the DSB marker, γ H2AX. PIKK-mediated phosphorylation of histone H2AX generates γ H2AX, which functions as a chromatin marker for the assembly of repair and signaling complexes [54]. Chromatin regulatory mechanisms are engaged during DDR to promote lesion recognition, repair, and signal transduction [54]. Unresolved replication lesions do not necessarily block mitotic entry, but progress into mitosis, leading to chromosome instability. In our study, weak expression of γ H2AX was observed after PARPi treatment in all cell lines tested. Our findings are similar to a study by Fleury et al., which demonstrated that olaparib treatment alone was not effective enough to increase the number of γ H2AX foci and even MN in HGSOV cell lines [62]. Here, we confirmed the presence of γ H2AX after the ATRi monotherapy, PARPi:ATRi and PARPi:CHK1i combined therapy in PEO-1 cells. Our findings are consistent with previous studies [53,63]. Furthermore, consistent with a study by Huntoon et al., we found that γ H2AX levels were increased after ATRi and CHK1i treatment alone or in combination with PARPi in *BRCA*^{MUT} and *BRCA*^{WT} cells [64]. Interestingly, we observed high γ H2AX levels in the SKOV-3 (*BRCA*^{WT}) line. However, when comparing the control values of the tested cell lines, it is worth noting that the SKOV-3 cells had lower levels of γ H2AX than PEO-1 cells. Our data are consistent with other studies. Phosphorylated histone H2AX was observed following PARPi treatment to the same extent in wild-type and *BRCA1/2*-deficient cell lines, suggesting that DSBs occur independent of *BRCA* function [65].

Inhibition of PARP1/2 during mitosis does not lead to the same mitotic phenotypes that arise in response to PARP1/2 inhibition during DNA replication in the S-phase. Furthermore, premature loss of cohesion occurred when olaparib was added during the S-phase (S-phase stalling), suggesting that replication fork blockage due to PARP entrapment leads to a loss of cohesion and subsequent defects in mitosis. Olaparib causes loss of sister chromatid cohesion. Loss of cohesion in interphase cells causes chromatid scattering in metaphase cells, metaphase arrest and cell death [66]. It has been shown that PARP trapping during the S-phase is required for the induction of mitotic chromosomal bridges [14]. Chromosomal aberrations in either PARPi:ATRi- or PARPi:CHK1i-treated cells imply inappropriate repair of DSBs before entry into mitosis, increased replication fork collapse and abrogation of the G2/M-phase checkpoints in PEO-1 and SKOV-3 cells. Only in OV-90 cells were ATRi or CHK1i found to enhance the olaparib effect and promote a small increase in G2/M cells (~16%). Inhibition of ATR or CHK1 led to an increase in olaparib-induced markers of RS [67]. Other studies have confirmed that a lack of G2/M activation and/or spindle checkpoints in cells suffering from DNA damage occurs due to inhibition of the ATR/CHK1 pathway [54,68].

5. Conclusions

MC is not a separate mode of cell death, but rather a process preceding cell death, which can occur through necrosis or apoptosis in ovarian cancer cells [37]. Importantly, PARPi in short incubation times show cytostatic effect rather than cytotoxic activity. Therefore, the combination of ATRi/CHK1i with PARPi is not more cytotoxic than monotherapy. Our research indicates that the cytotoxic effect of the combination is time dependent. The final outcome of cell death depends on the molecular profile of the cell and, in our study, is independent on *BRCA* status. There is undoubtedly a connection between ATR/CHK1 inhibition and DNA damage-induced cell-cycle disruption [69]. Both ATRi and CHK1i tested in this study were found to cause inappropriate entry into mitosis, leading to chromosomal aberrations, genome instability, and apoptosis. We confirmed that ATRi and CHK1i cytotoxicity was due to mitotic dysfunction. Additional research in vivo is required to further explore the effect of PARPi:ATRi and PARPi:CHK1i on genome stability and cancer cell survival, which may also depend on the genetics of the tumor.

Supplementary Materials: The following supporting information can be downloaded at: <https://www.mdpi.com/article/10.3390/cells1121889/s1>, Figure S1: ATRi/CHK1i monotherapy and combination treatment caused cell death. Fluorescence images of the apoptotic and necrotic changes caused by treatment with the compounds in SKOV-3 and OV-90 cells. Representative cells are marked with a dashed line and enlarged. The cells were divided into four categories as follows: live cells (dark blue fluorescence), early apoptotic (bright blue fluorescence), late-apoptotic (pink–violet fluorescence), and necrotic cells (red fluorescence). Apoptotic and necrotic changes were visualized after double staining with Hoechst 33258/PI under a fluorescence microscope (Olympus IX70; scale bar 50 μ m; magnification 400 \times); Figure S2: ATRi/CHK1i monotherapy and combination treatment caused phosphatidylserine externalization. Representative dot plots showing induction of apoptosis and dead SKOV-3 and OV-90 cells after 48 h treatment with PARPi (4 μ M), ATRi (4 μ M) or CHK1i (4 μ M) alone and in combination. Individual samples are presented as data points. The population of apoptotic cells was calculated according to the presented gating strategy; Figure S3: ATRi/CHK1i increases caspase-3 expression. For immunofluorescence staining, SKOV-3 and OV-90 cells were stimulated with PARPi, ATRi or CHK1i alone, or the combination of PARPi:ATRi or PARPi:CHK1i at 4 μ M and labeled with antibodies against caspase-3 (red colour). Images were acquired using a confocal laser scanning microscope (scale bar 20 μ m, magnification 63 \times); Figure S4: ATRi/CHK1i increases γ H2AX expression. For immunofluorescence staining, SKOV-3 and OV-90 cells were stimulated with PARPi, ATRi or CHK1i alone, or the combination of PARPi:ATRi or PARPi:CHK1i at 4 μ M and labeled with antibodies against γ H2AX (green colour). Images were acquired using a confocal laser scanning microscope (scale bar 20 μ m, magnification 63 \times); Figure S5: γ H2AX expression in SKOV-3, OV-90 and PEO-1 control cells presented as arbitrary area value; Figure S6: Representative dot plots showing induction of apoptosis and necrosis in SKOV-3 and OV-90 cells after treatment with PARPi (4 μ M), ATRi (4 μ M) or CHK1i (4 μ M) alone and in combination. Individual samples are presented as data points. Population of apoptotic [Q2 (Vybrant-positive and Sytox-positive) + Q4 (Vybrant-positive and Sytox-negative)] and necrotic cells [Q1 (Vybrant-negative and Sytox-positive)] was calculated according to the presented gating strategy; Figure S7: Representative dot plots showing the distribution of cell cycle phases in SKOV-3 and OV-90 cells after 24 h treatment with PARPi (4 μ M), ATRi (4 μ M) or CHK1i (4 μ M) alone and in combination. Individual samples are presented as data points; Figure S8: Replication stress inhibitors synergize with PARPi to induce chromosomal aberrations in (A) OV-90 and (B) SKOV-3 cells. Red arrows show damaged chromosomes, (50 metaphase spreads in each group were counted). Stained slides were analyzed using a 100 \times objective and a Nikon ECLIPSE E600W microscope (Nikon, Warsaw, Poland).

Author Contributions: Conceptualization, P.G., A.G., A.M. and A.R.; methodology, P.G., A.G., D.R. and A.R.; data curation, P.G., A.G., D.R. and A.R.; writing/original draft preparation, P.G., A.G. and A.R.; writing/review and editing, P.G., A.G., D.R., A.M. and A.R. All authors have read and agreed to the published version of the manuscript.

Funding: This research was funded by the National Science Centre, Poland (Project grant number: Sonata Bis 2019/34/E/NZ7/00056).

Institutional Review Board Statement: Not applicable.

Informed Consent Statement: Not applicable.

Data Availability Statement: The datasets presented during the current study are available from the corresponding author on reasonable request.

Acknowledgments: Research was conducted, in part, using equipment of the Laboratory of Microscopic Imaging and Specialized Biological Techniques, Faculty of Biology and Environmental Protection, University of Lodz.

Conflicts of Interest: The authors declare no conflict of interest.

References

1. Ahmed, N.; Kadife, E.; Raza, A.; Short, M.; Jubinsky, P.T.; Kannourakis, G. Ovarian Cancer, Cancer Stem Cells and Current Treatment Strategies: A Potential Role of Magmas in the Current Treatment Methods. *Cells* **2020**, *9*, 719. [[CrossRef](#)] [[PubMed](#)]
2. Beaufort, C.M.; Helmijr, J.C.; Piskorz, A.M.; Hoogstraat, M.; Ruigrok-Ritstier, K.; Besselink, N.; Murtaza, M.; Van, I.W.F.; Heine, A.A.; Smid, M.; et al. Ovarian cancer cell line panel (OCCP): Clinical importance of in vitro morphological subtypes. *PLoS ONE* **2014**, *9*, e103988. [[CrossRef](#)] [[PubMed](#)]

3. Da Cunha Colombo Bonadio, R.R.; Fogace, R.N.; Miranda, V.C.; Diz, M. Homologous recombination deficiency in ovarian cancer: A review of its epidemiology and management. *Clinics* **2018**, *73*, e450s. [[CrossRef](#)] [[PubMed](#)]
4. Konstantinopoulos, P.A.; Lheureux, S.; Moore, K.N. PARP Inhibitors for Ovarian Cancer: Current Indications, Future Combinations, and Novel Assets in Development to Target DNA Damage Repair. *Am. Soc. Clin. Oncol. Educ. Book* **2020**, *40*, e116–e131. [[CrossRef](#)]
5. Barnes, D.E.; Lindahl, T. Repair and genetic consequences of endogenous DNA base damage in mammalian cells. *Annu. Rev. Genet.* **2004**, *38*, 445–476. [[CrossRef](#)]
6. Ito, S.; Murphy, C.G.; Doubrovina, E.; Jasin, M.; Moynahan, M.E. PARP Inhibitors in Clinical Use Induce Genomic Instability in Normal Human Cells. *PLoS ONE* **2016**, *11*, e0159341. [[CrossRef](#)]
7. Paviolo, N.S.; Vega, M.B.; Pansa, M.F.; Garcia, I.A.; Calzetta, N.L.; Soria, G.; Gottifredi, V. Persistent double strand break accumulation does not precede cell death in an Olaparib-sensitive BRCA-deficient colorectal cancer cell model. *Genet. Mol. Biol. Cell Biol.* **2019**, *43*, e20190070. [[CrossRef](#)]
8. Ray Chaudhuri, A.; Nussenzweig, A. The multifaceted roles of PARP1 in DNA repair and chromatin remodelling. *Nat. Rev. Mol. Cell Biol.* **2017**, *18*, 610–621. [[CrossRef](#)]
9. Huang, X.Z.; Jia, H.; Xiao, Q.; Li, R.Z.; Wang, X.S.; Yin, H.Y.; Zhou, X. Efficacy and Prognostic Factors for PARP Inhibitors in Patients With Ovarian Cancer. *Front. Oncol.* **2020**, *10*, 958. [[CrossRef](#)]
10. Gralewska, P.; Gajek, A.; Marczak, A.; Mikula, M.; Ostrowski, J.; Sliwinska, A.; Rogalska, A. PARP Inhibition Increases the Reliance on ATR/CHK1 Checkpoint Signaling Leading to Synthetic Lethality—An Alternative Treatment Strategy for Epithelial Ovarian Cancer Cells Independent from HR Effectiveness. *Int. J. Mol. Sci.* **2020**, *21*, 9715. [[CrossRef](#)]
11. Zhao, H.; Piwnica-Worms, H. ATR-mediated checkpoint pathways regulate phosphorylation and activation of human Chk1. *Mol. Cell. Biol.* **2001**, *21*, 4129–4139. [[CrossRef](#)] [[PubMed](#)]
12. Rybaczek, D.; Kowalewicz-Kulbat, M. Premature chromosome condensation induced by caffeine, 2-aminopurine, staurosporine and sodium metavanadate in S-phase arrested HeLa cells is associated with a decrease in Chk1 phosphorylation, formation of phospho-H2AX and minor cytoskeletal rearrangements. *Histochem. Cell Biol.* **2011**, *135*, 263–280. [[CrossRef](#)] [[PubMed](#)]
13. De Gooijer, M.C.; Van den Top, A.; Bockaj, I.; Beijnen, J.H.; Wurdinger, T.; Van Tellingen, O. The G2 checkpoint—a node-based molecular switch. *FEBS Open Bio* **2017**, *7*, 439–455. [[CrossRef](#)] [[PubMed](#)]
14. Schoonen, P.M.; Talens, F.; Stok, C.; Gogola, E.; Heijink, A.M.; Bouwman, P.; Fojier, F.; Tarsounas, M.; Blatter, S.; Jonkers, J.; et al. Progression through mitosis promotes PARP inhibitor-induced cytotoxicity in homologous recombination-deficient cancer cells. *Nat. Commun.* **2017**, *8*, 15981. [[CrossRef](#)]
15. Helleday, T. Putting poly (ADP-ribose) polymerase and other DNA repair inhibitors into clinical practice. *Curr. Opin. Oncol.* **2013**, *25*, 609–614. [[CrossRef](#)]
16. Carmichael, J.; Degraff, W.G.; Gazdar, A.F.; Minna, J.D.; Mitchell, J.B. Evaluation of a Tetrazolium-Based Semiautomated Colorimetric Assay—Assessment of Radiosensitivity. *Cancer Res.* **1987**, *47*, 943–946.
17. Lopez-Acevedo, M.; Grace, L.; Teoh, D.; Whitaker, R.; Adams, D.J.; Jia, J.; Nixon, A.B.; Secord, A.A. Dasatinib (BMS-35482) potentiates the activity of gemcitabine and docetaxel in uterine leiomyosarcoma cell lines. *Gynecol. Oncol. Res. Pract.* **2014**, *1*, 2. [[CrossRef](#)]
18. Kaltenbach, J.P.; Kaltenbach, M.H.; Lyons, W.B. Nigrosin as a dye for differentiating live and dead ascites cells. *Exp. Cell Res.* **1958**, *15*, 112–117. [[CrossRef](#)]
19. Uzbekov, R.E. Analysis of the cell cycle and a method employing synchronized cells for study of protein expression at various stages of the cell cycle. *Biochemistry* **2004**, *69*, 485–496. [[CrossRef](#)]
20. Korzyńska, A.; Zychowicz, M. A method of estimation of the cell doubling time on basis of the cell culture monitoring data. *Biocybern. Biomed. Eng.* **2008**, *28*, 75–82.
21. Rogalska, A.; Gajek, A.; Marczak, A. Suppression of autophagy enhances preferential toxicity of epothilone A and epothilone B in ovarian cancer cells. *Phytomedicine* **2019**, *61*, 152847. [[CrossRef](#)]
22. Gajek, A.; Poczta, A.; Łukawska, M.; Cecuda-Adamczewska, V.; Tobiasz, J.; Marczak, A. Chemical modification of melphalan as a key to improving treatment of haematological malignancies. *Sci. Rep.* **2020**, *10*, 4479. [[CrossRef](#)]
23. Rogalska, A.; Marczak, A.; Gajek, A.; Szwed, M.; Śliwińska, A.; Drzewoski, J.; Józwiak, Z. Induction of apoptosis in human ovarian cancer cells by new anticancer compounds, epothilone A and B. *Toxicol. In Vitro.* **2013**, *27*, 239–249. [[CrossRef](#)]
24. Gralewska, P.; Gajek, A.; Marczak, A.; Rogalska, A. Metformin Affects Olaparib Sensitivity through Induction of Apoptosis in Epithelial Ovarian Cancer Cell Lines. *Int. J. Mol. Sci.* **2021**, *22*, 10557. [[CrossRef](#)]
25. Olins, A.L.; Olins, D.E. Spheroid chromatin units (v bodies). *Science* **1974**, *183*, 330–332. [[CrossRef](#)]
26. Thoma, F.; Koller, T.; Klug, A. Involvement of histone H1 in the organization of the nucleosome and of the salt-dependent superstructures of chromatin. *J. Cell Biol.* **1979**, *83*, 403–427. [[CrossRef](#)]
27. Gotoh, E. Visualizing the dynamics of chromosome structure formation coupled with DNA replication. *Chromosoma* **2007**, *116*, 453–462. [[CrossRef](#)]
28. Balcerzyk, A.; Rybaczek, D.; Wojtala, M.; Pirola, L.; Okabe, J.; El-Osta, A. Pharmacological inhibition of arginine and lysine methyltransferases induces nuclear abnormalities and suppresses angiogenesis in human endothelial cells. *Biochem. Pharmacol.* **2016**, *121*, 18–32. [[CrossRef](#)]

29. Luzhna, L.; Kathiria, P.; Kovalchuk, O. Micronuclei in genotoxicity assessment: From genetics to epigenetics and beyond. *Front. Genet.* **2013**, *4*, 131. [[CrossRef](#)]
30. Fenech, M. Cytokinesis-block micronucleus cytome assay. *Nat. Protoc.* **2007**, *2*, 1084–1104. [[CrossRef](#)]
31. Xu, Q.; Li, Z. Update on Poly ADP-Ribose Polymerase Inhibitors in Ovarian Cancer with Non-BRCA Mutations. *Front. Pharmacol.* **2021**, *12*, 743073. [[CrossRef](#)]
32. FDA. FDA Approved Olaparib (LYNPARZA, AstraZeneca Pharmaceuticals LP) for the Maintenance Treatment of Adult Patients with Deleterious or Suspected Deleterious Germline or Somatic BRCA-Mutated (gBRCAm or sBRCAm) Advanced Epithelial Ovarian, Fallopian Tube or Primary Peritoneal Cancer Who Are in Complete or Partial Response to First-Line Platinum-Based. Available online: <https://www.fda.gov/drugs/fda-approved-olaparib-lynpa-azena-pharmaceuticals-lp-maintenance-treatment-adult-patients> (accessed on 2 June 2022).
33. Balasubramaniam, S.; Beaver, J.A.; Horton, S.; Fernandes, L.L.; Tang, S.; Horne, H.N.; Liu, J.; Liu, C.; Schrieber, S.J.; Yu, J.; et al. FDA Approval Summary: Rucaparib for the Treatment of Patients with Deleterious BRCA Mutation–Associated Advanced Ovarian Cancer. *Clin. Cancer Res.* **2017**, *23*, 7165–7170. [[CrossRef](#)]
34. Do, K.T.; Hill, S.J.; Kochupurakkal, B.; Supko, J.G.; Gannon, C.; Anderson, A.; Muzikansky, A.; Wolanski, A.; Hedglin, J.; Parmar, K.; et al. Abstract CT232: Phase I combination study of the CHK1 inhibitor prexasertib (LY2606368) and olaparib in patients with high-grade serous ovarian cancer and other advanced solid tumors. *Cancer Res.* **2019**, *79*, CT232. [[CrossRef](#)]
35. Gomez, M.K.; Illuzzi, G.; Colomer, C.; Churchman, M.; Hollis, R.L.; O'Connor, M.J.; Gourley, C.; Leo, E.; Melton, D.W. Identifying and Overcoming Mechanisms of PARP Inhibitor Resistance in Homologous Recombination Repair-Deficient and Repair-Proficient High Grade Serous Ovarian Cancer Cells. *Cancers* **2020**, *12*, 1503. [[CrossRef](#)]
36. Paik, J. Olaparib: A Review as First-Line Maintenance Therapy in Advanced Ovarian Cancer. *Target Oncol.* **2021**, *16*, 847–856. [[CrossRef](#)]
37. Vakifahmetoglu, H.; Olsson, M.; Zhivotovsky, B. Death through a tragedy: Mitotic catastrophe. *Cell Death Differ.* **2008**, *15*, 1153–1162. [[CrossRef](#)]
38. Lloyd, R.L.; Wijnhoven, P.W.G.; Ramos-Montoya, A.; Wilson, Z.; Illuzzi, G.; Falenta, K.; Jones, G.N.; James, N.; Chabbert, C.D.; Stott, J.; et al. Combined PARP and ATR inhibition potentiates genome instability and cell death in ATM-deficient cancer cells. *Oncogene* **2020**, *39*, 4869–4883. [[CrossRef](#)]
39. Miyasaka, A.; Oda, K.; Ikeda, Y.; Wada-Hiraike, O.; Kashiyama, T.; Enomoto, A.; Hosoya, N.; Koso, T.; Fukuda, T.; Inaba, K.; et al. Anti-tumor activity of olaparib, a poly (ADP-ribose) polymerase (PARP) inhibitor, in cultured endometrial carcinoma cells. *BMC Cancer* **2014**, *14*, 179. [[CrossRef](#)]
40. Dubois, C.; Martin, F.; Hassel, C.; Magnier, F.; Daumar, P.; Aubeil, C.; Guerder, S.; Mounetou, E.; Penault-Lorca, F.; Bamdad, M. Low-Dose and Long-Term Olaparib Treatment Sensitizes MDA-MB-231 and SUM1315 Triple-Negative Breast Cancers Spheroids to Fractionated Radiotherapy. *J. Clin. Med.* **2019**, *9*, 64. [[CrossRef](#)]
41. Kummar, S.; Gutierrez, M.; Doroshow, J.H.; Murgo, A.J. Drug development in oncology: Classical cytotoxics and molecularly targeted agents. *Br. J. Clin. Pharmacol.* **2006**, *62*, 15–26. [[CrossRef](#)]
42. Poti, A.; Gyergyak, H.; Nemeth, E.; Ruzs, O.; Toth, S.; Kovacshazi, C.; Chen, D.; Szikriszt, B.; Spisak, S.; Takeda, S.; et al. Correlation of homologous recombination deficiency induced mutational signatures with sensitivity to PARP inhibitors and cytotoxic agents. *Genome Biol.* **2019**, *20*, 240. [[CrossRef](#)] [[PubMed](#)]
43. Burgess, R.C.; Burman, B.; Kruhlak, M.J.; Misteli, T. Activation of DNA damage response signaling by condensed chromatin. *Cell Rep.* **2014**, *9*, 1703–1717. [[CrossRef](#)]
44. Soutoglou, E.; Misteli, T. Activation of the cellular DNA damage response in the absence of DNA lesions. *Science* **2008**, *320*, 1507–1510. [[CrossRef](#)] [[PubMed](#)]
45. Nalabothula, N.; Al-jumaily, T.; Eteleeb, A.M.; Flight, R.M.; Xiaorong, S.; Moseley, H.; Rouchka, E.C.; Fondufe-Mittendorf, Y.N. Genome-Wide Profiling of PARP1 Reveals an Interplay with Gene Regulatory Regions and DNA Methylation. *PLoS ONE* **2015**, *10*, e0135410. [[CrossRef](#)]
46. Andronikou, C.; Rottenberg, S. Studying PAR-Dependent Chromatin Remodeling to Tackle PARPi Resistance. *Trends Mol. Med.* **2021**, *27*, 630–642. [[CrossRef](#)] [[PubMed](#)]
47. Ji, Y.; Tulin, A.V. The roles of PARP1 in gene control and cell differentiation. *Curr. Opin. Genet. Dev.* **2010**, *20*, 512–518. [[CrossRef](#)] [[PubMed](#)]
48. Khurana, S.; Kruhlak, M.J.; Kim, J.; Tran, A.D.; Liu, J.; Nyswaner, K.; Shi, L.; Jailwala, P.; Sung, M.H.; Hakim, O.; et al. A macrohistone variant links dynamic chromatin compaction to BRCA1-dependent genome maintenance. *Cell Rep.* **2014**, *8*, 1049–1062. [[CrossRef](#)]
49. Smeenk, G.; Wiegant, W.W.; Vrolijk, H.; Solari, A.P.; Pastink, A.; Van Attikum, H. The NuRD chromatin-remodeling complex regulates signaling and repair of DNA damage. *J. Cell Biol.* **2010**, *190*, 741–749. [[CrossRef](#)]
50. Colicchia, V.; Petroni, M.; Guarguaglini, G.; Sardina, F.; Sahún-Roncero, M.; Carbonari, M.; Ricci, B.; Heil, C.; Capalbo, C.; Belardinelli, F.; et al. PARP inhibitors enhance replication stress and cause mitotic catastrophe in MYCN-dependent neuroblastoma. *Oncogene* **2017**, *36*, 4682–4691. [[CrossRef](#)]
51. Dillon, M.T.; Barker, H.E.; Pedersen, M.; Hafsi, H.; Bhide, S.A.; Newbold, K.L.; Nutting, C.M.; McLaughlin, M.; Harrington, K.J. Radiosensitization by the ATR Inhibitor AZD6738 through Generation of Acentric Micronuclei. *Mol. Cancer Ther.* **2017**, *16*, 25–34. [[CrossRef](#)]

52. Michelena, J.; Lezaja, A.; Teloni, F.; Schmid, T.; Imhof, R.; Altmeyer, M. Analysis of PARP inhibitor toxicity by multidimensional fluorescence microscopy reveals mechanisms of sensitivity and resistance. *Nat. Commun.* **2018**, *9*, 2678. [[CrossRef](#)]
53. Schoonen, P.M.; Kok, Y.P.; Wierenga, E.; Bakker, B.; Foijer, F.; Spierings, D.C.J.; Van Vugt, M. Premature mitotic entry induced by ATR inhibition potentiates olaparib inhibition-mediated genomic instability, inflammatory signaling, and cytotoxicity in BRCA2-deficient cancer cells. *Mol. Oncol.* **2019**, *13*, 2422–2440. [[CrossRef](#)]
54. Wang, J.Y.J. Cell Death Response to DNA Damage. *Yale J. Biol. Med.* **2019**, *92*, 771–779.
55. Gravells, P.; Neale, J.; Grant, E.; Nathubhai, A.; Smith, K.M.; James, D.I.; Bryant, H.E. Radiosensitization with an inhibitor of poly(ADP-ribose) glycohydrolase: A comparison with the PARP1/2/3 inhibitor olaparib. *DNA Repair* **2018**, *61*, 25–36. [[CrossRef](#)]
56. Saldivar, J.C.; Hamperl, S.; Bocek, M.J.; Chung, M.; Bass, T.E.; Cisneros-Soberanis, F.; Samejima, K.; Xie, L.; Paulson, J.R.; Earnshaw, W.C.; et al. An intrinsic S/G2 checkpoint enforced by ATR. *Science* **2018**, *361*, 806–810. [[CrossRef](#)]
57. Patil, M.; Pabla, N.; Dong, Z. Checkpoint kinase 1 in DNA damage response and cell cycle regulation. *Cell Mol. Life Sci.* **2013**, *70*, 4009–4021. [[CrossRef](#)]
58. Mikhailov, A.; Cole, R.W.; Rieder, C.L. DNA damage during mitosis in human cells delays the metaphase/anaphase transition via the spindle-assembly checkpoint. *Curr. Biol.* **2002**, *12*, 1797–1806. [[CrossRef](#)]
59. Slade, D. Mitotic functions of poly(ADP-ribose) polymerases. *Biochem. Pharmacol.* **2019**, *167*, 33–43. [[CrossRef](#)]
60. Young, L.A.; O'Connor, L.O.; De Renty, C.; Veldman-Jones, M.H.; Dorval, T.; Wilson, Z.; Jones, D.R.; Lawson, D.; Odedra, R.; Maya-Mendoza, A.; et al. Differential Activity of ATR and WEE1 Inhibitors in a Highly Sensitive Subpopulation of DLBCL Linked to Replication Stress. *Cancer Res.* **2019**, *79*, 3762–3775. [[CrossRef](#)]
61. Vescarelli, E.; Gerini, G.; Megiorni, F.; Anastasiadou, E.; Pontecorvi, P.; Solito, L.; De Vitis, C.; Camero, S.; Marchetti, C.; Mancini, R.; et al. MiR-200c sensitizes Olaparib-resistant ovarian cancer cells by targeting Neuropilin 1. *J. Exp. Clin. Cancer Res.* **2020**, *39*, 3. [[CrossRef](#)]
62. Fleury, H.; Malaquin, N.; Tu, V.; Gilbert, S.; Martinez, A.; Olivier, M.-A.; Sauriol, A.; Communal, L.; Leclerc-Desaulniers, K.; Carmona, E.; et al. Exploiting interconnected synthetic lethal interactions between PARP inhibition and cancer cell reversible senescence. *Nat. Commun.* **2019**, *10*, 2556. [[CrossRef](#)] [[PubMed](#)]
63. Sule, A.; Van Doorn, J.; Sundaram, R.K.; Ganesa, S.; Vasquez, J.C.; Bindra, R.S. Targeting IDH1/2 mutant cancers with combinations of ATR and PARP inhibitors. *NAR Cancer* **2021**, *3*, zcab018. [[CrossRef](#)]
64. Huntoon, C.J.; Flatten, K.S.; Wahner Hendrickson, A.E.; Huehls, A.M.; Sutor, S.L.; Kaufmann, S.H.; Karnitz, L.M. ATR Inhibition Broadly Sensitizes Ovarian Cancer Cells to Chemotherapy Independent of BRCA Status. *Cancer Res.* **2013**, *73*, 3683–3691. [[CrossRef](#)] [[PubMed](#)]
65. Fong, P.C.; Boss, D.S.; Yap, T.A.; Tutt, A.; Wu, P.; Mergui-Roelvink, M.; Mortimer, P.; Swaisland, H.; Lau, A.; O'Connor, M.J.; et al. Inhibition of poly(ADP-ribose) polymerase in tumors from BRCA mutation carriers. *N. Engl. J. Med.* **2009**, *361*, 123–134. [[CrossRef](#)] [[PubMed](#)]
66. Kukolj, E.; Kaufmann, T.; Dick, A.E.; Zeillinger, R.; Gerlich, D.W.; Slade, D. PARP inhibition causes premature loss of cohesion in cancer cells. *Oncotarget* **2017**, *8*, 103931–103951. [[CrossRef](#)] [[PubMed](#)]
67. Southgate, H.E.D.; Chen, L.; Tweddle, D.A.; Curtin, N.J. ATR Inhibition Potentiates PARP Inhibitor Cytotoxicity in High Risk Neuroblastoma Cell Lines by Multiple Mechanisms. *Cancers* **2020**, *12*, 1095. [[CrossRef](#)] [[PubMed](#)]
68. Kim, H.; George, E.; Ragland, R.L.; Rafail, S.; Zhang, R.; Krepler, C.; Morgan, M.A.; Herlyn, M.; Brown, E.J.; Simpkins, F. Targeting the ATR/CHK1 Axis with PARP Inhibition Results in Tumor Regression in BRCA-Mutant Ovarian Cancer Models. *Clin. Cancer Res.* **2017**, *23*, 3097–3108. [[CrossRef](#)] [[PubMed](#)]
69. Engelke, C.G.; Parsels, L.A.; Qian, Y.; Zhang, Q.; Karnak, D.; Robertson, J.R.; Tanska, D.M.; Wei, D.; Davis, M.A.; Parsels, J.D.; et al. Sensitization of pancreatic cancer to chemoradiation by the Chk1 inhibitor MK8776. *Clin. Cancer Res.* **2013**, *19*, 4412–4421. [[CrossRef](#)]

Article

The Influence of PARP, ATR, CHK1 Inhibitors on Premature Mitotic Entry and Genomic Instability in High-Grade Serous *BRCA^{MUT}* and *BRCA^{WT}* Ovarian Cancer Cells

Patrycja Gralewska ¹, Arkadiusz Gajek ¹, Dorota Rybaczek ², Agnieszka Marczak ¹, and Aneta Rogalska ^{1,*}

¹ Department of Medical Biophysics, Institute of Biophysics, Faculty of Biology and Environmental Protection, University of Lodz, Pomorska 141/143, 90-236, Lodz, Poland; patrycja.gralewska@edu.uni.lodz.pl (P.G.); arkadiusz.gajek@biol.uni.lodz.pl (A.G.); agnieszka.marczak@biol.uni.lodz.pl (A.M.)

² Department of Cytophysiology, Faculty of Biology and Environmental Protection, University of Lodz, Pomorska 141/143, 90-236, Lodz, Poland; dorota.rybaczek@biol.uni.lodz.pl

* Correspondence: aneta.rogalska@biol.uni.lodz.pl; Tel.: +48 42 635-44-77

Supplementary files

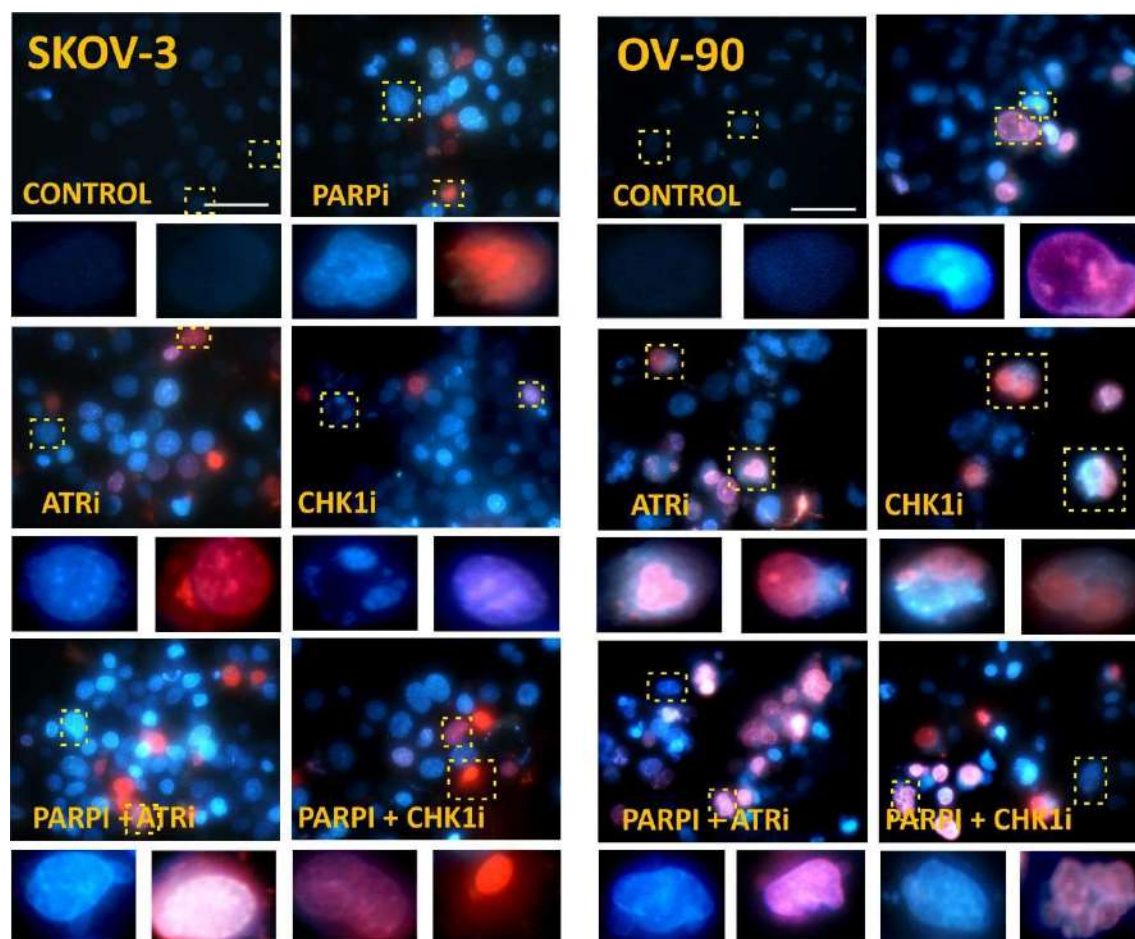


Figure S1. ATRi/CHK1i monotherapy and combination treatment caused cell death. Fluorescence images of the apoptotic and necrotic changes caused by treatment with the compounds in SKOV-3 and OV-90 cells. Representative cells are marked with a dashed line and enlarged. The cells were divided into four categories as follows: live cells (dark blue fluorescence), early-apoptotic (bright blue fluorescence), late-apoptotic (pink-violet fluorescence), and necrotic cells (red fluorescence). Apoptotic and necrotic changes were visualized after double staining with Hoechst 33258/PI under a fluorescence microscope (Olympus IX70; scale bar 50 μm ; magnification 400 \times).

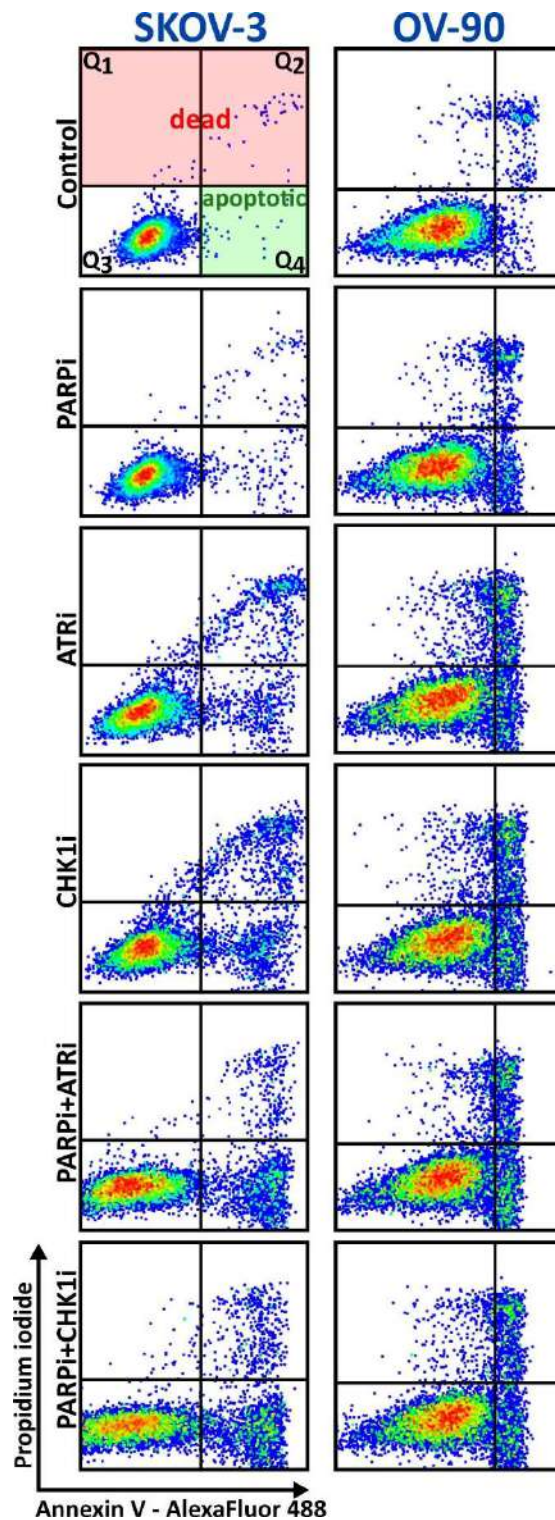


Figure S2. ATRi/CHK1i monotherapy and combination treatment caused phosphatidylserine externalization. Representative dot plots showing induction of apoptosis and dead SKOV-3 and OV-90 cells after 48h treatment with PARPi (4 μ M), ATRi (4 μ M) or CHK1i (4 μ M) alone and in combination. Individual samples are presented as data points. The population of apoptotic cells was calculated according to the presented gating strategy.

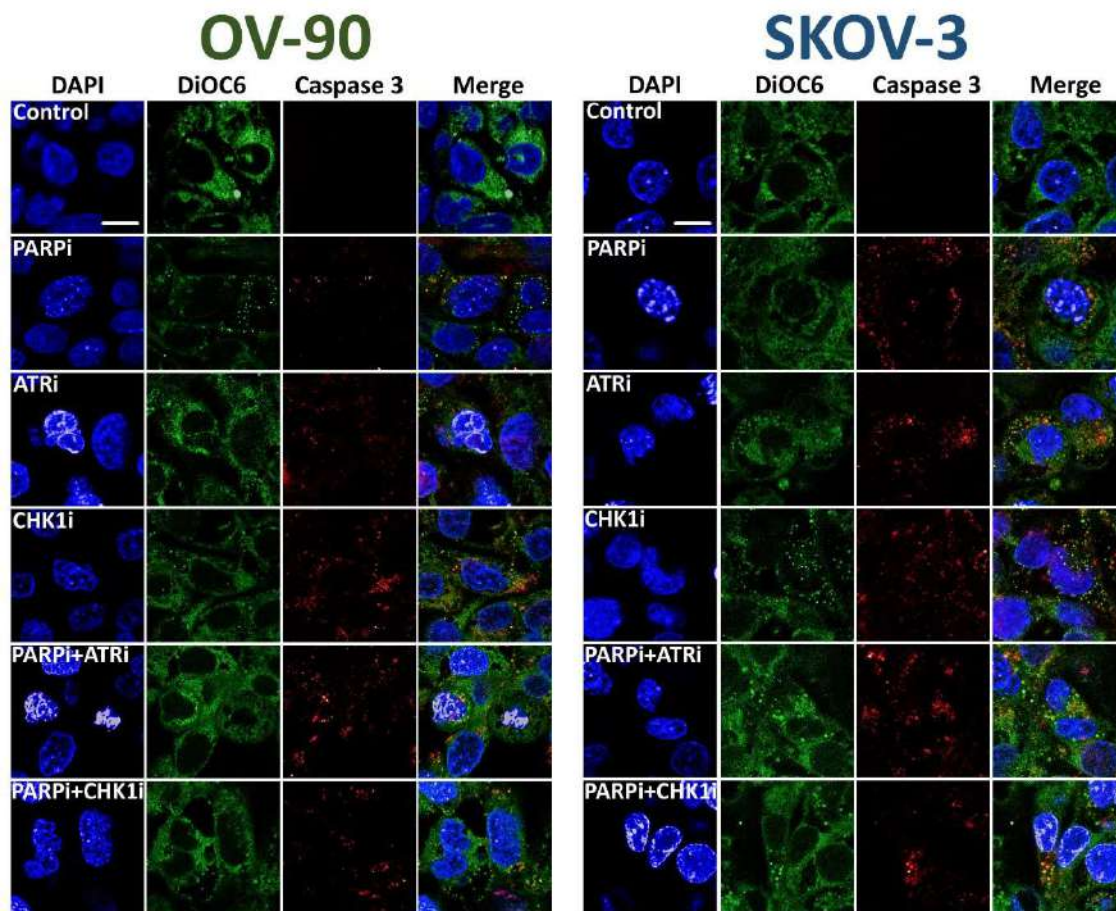


Figure S3. ATRi/CHK1i increases caspase-3 expression. For immunofluorescence staining, SKOV-3 and OV-90 cells were stimulated with PARPi, ATRi or CHK1i alone, or the combination of PARPi:ATRi or PARPi:CHK1i at 4 μ M and labeled with antibodies against caspase-3 (red colour). Images were acquired using a confocal laser scanning microscope (scale bar 20 μ m, magnification 63 \times).

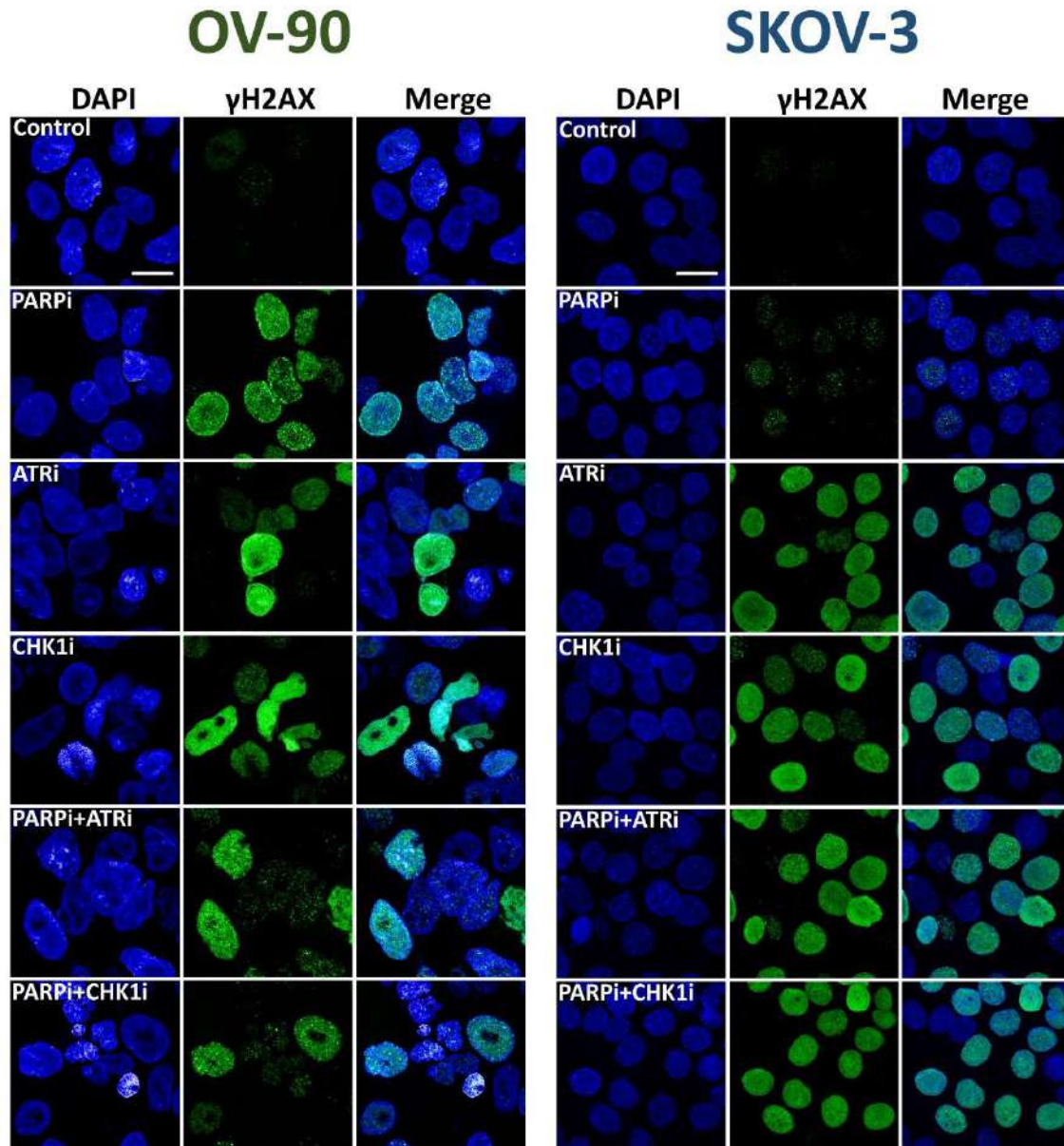


Figure S4. ATRi/CHK1i increases γ H2AX expression. For immunofluorescence staining, SKOV-3 and OV-90 cells were stimulated with PARPi, ATRi or CHK1i alone, or the combination of PARPi:ATRi or PARPi:CHK1i at 4 μ M and labeled with antibodies against γ H2AX (green colour). Images were acquired using a confocal laser scanning microscope (scale bar 20 μ m, magnification 63 \times).

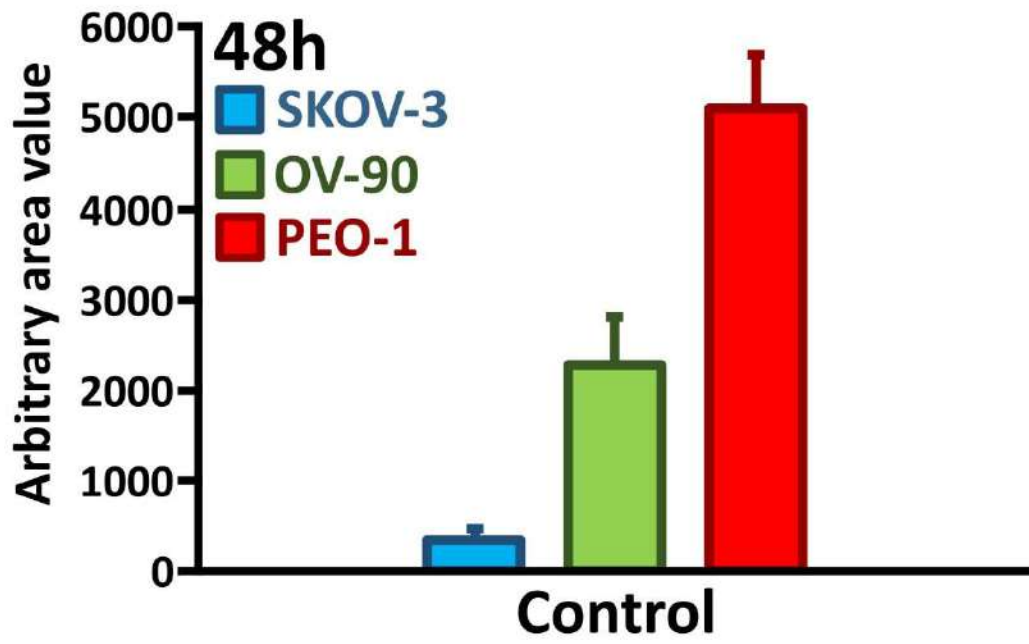


Figure S5. γ H2AX expression in SKOV-3, OV-90 and PEO-1 control cells presented as arbitrary area value.

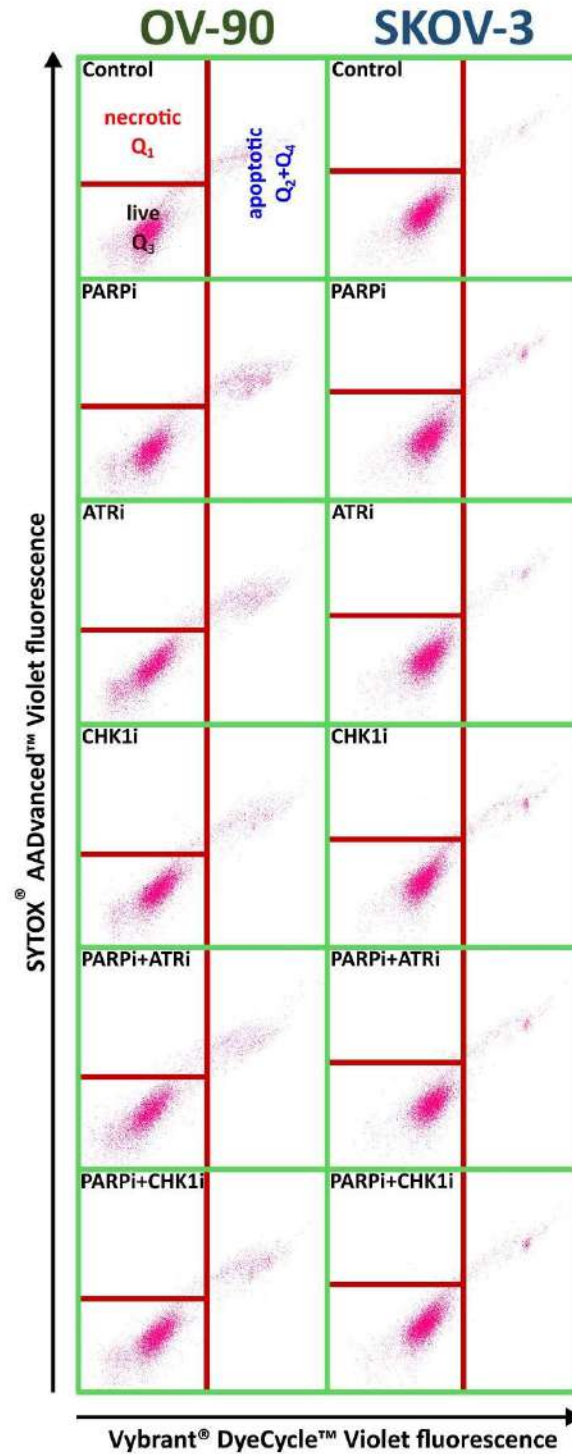


Figure S6. Representative dot plots showing induction of apoptosis and necrosis in SKOV-3 and OV-90 cells after treatment with PARPi (4 μ M), ATRi (4 μ M) or CHK1i (4 μ M) alone and in combination. Individual samples are presented as data points. Population of apoptotic [Q2 (Vybrant-positive and Sytox-positive) + Q4 (Vybrant-positive and Sytox-negative)] and necrotic cells [Q1 (Vybrant-negative and Sytox-positive)] was calculated according to the presented gating strategy.

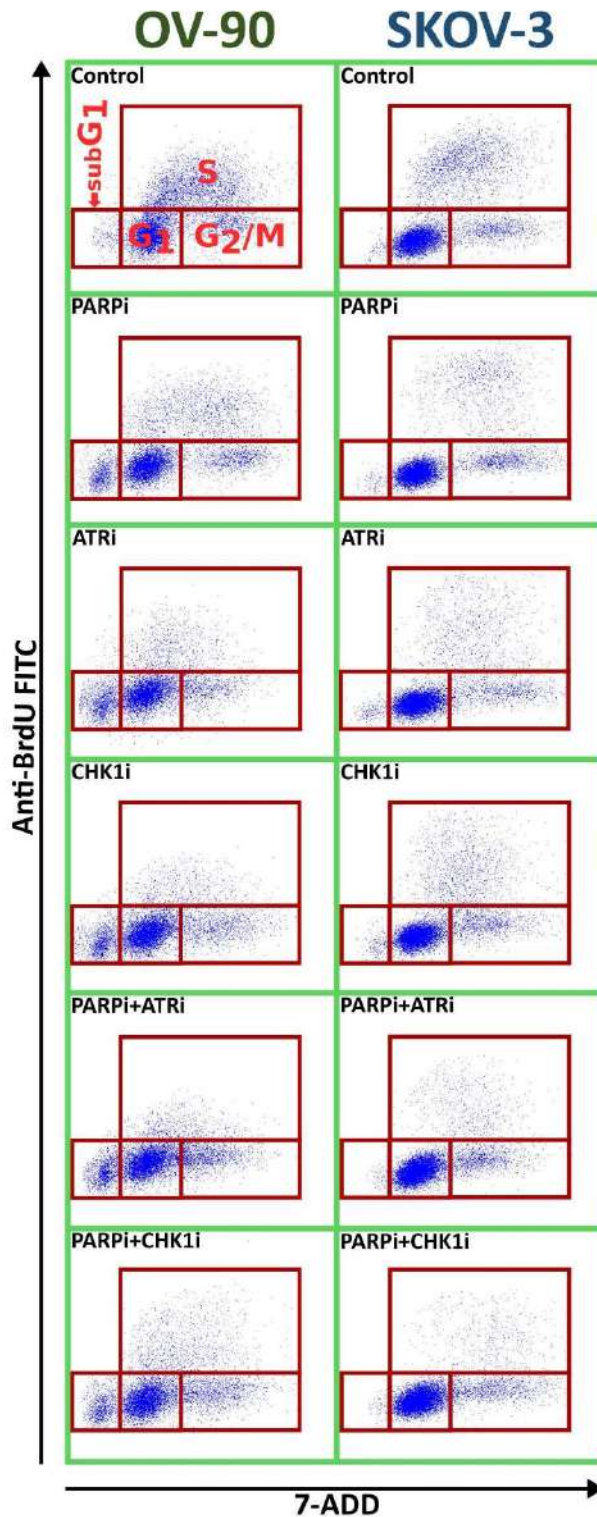


Figure S7. Representative dot plots showing the distribution of cell cycle phases in SKOV-3 and OV-90 cells after 24 h treatment with PARPi (4 μ M), ATRi (4 μ M) or CHK1i (4 μ M) alone and in combination. Individual samples are presented as data points.

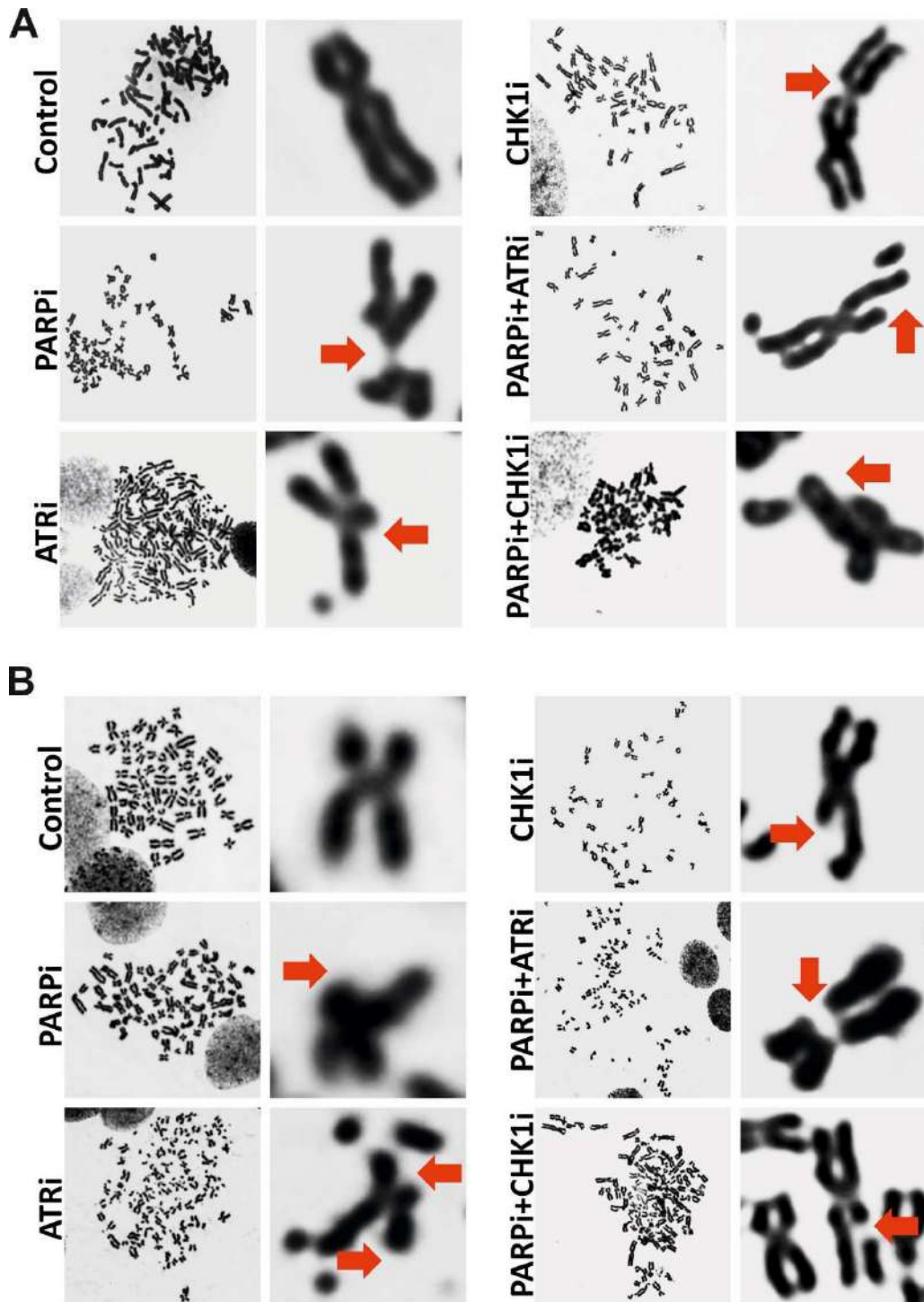


Figure S8. Replication stress inhibitors synergize with PARPi to induce chromosomal aberrations in (A) OV-90 and (B) SKOV-3 cells. Red arrows show damaged chromosomes, (50 metaphase spreads in each group were counted). Stained slides were analyzed using a 100× objective and a Nikon ECLIPSE E600W microscope (Nikon, Warsaw, Poland).

**OŚWIADCZENIA WSPÓLAUTORÓW PUBLIKACJI WCHODZĄCYCH W SKŁAD
ROZPRAWY DOKTORSKIEJ**

Łódź, 21 listopada 2022 r.

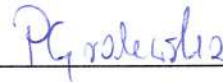
mgr inż. Patrycja Gralewska
Katedra Biofizyki Medycznej
Uniwersytet Łódzki

OŚWIADCZENIE WSPÓŁAUTORA

Dotyczy publikacji:

Gralewska P., Gajek A., Marczak A., Rogalska A. *Participation of the ATR/CHK1 pathway in replicative stress targeted therapy of high-grade ovarian cancer. J Hematol Oncol* 13, 39 (2020). <https://doi.org/10.1186/s13045-020-00874-6>

Oświadczam, że mój wkład w powstanie powyższej pracy polegał na głównym udziale w napisaniu i zredagowaniu pracy oraz odpowiedzi na recenzje. Mój udział procentowy oceniam na 50 %.

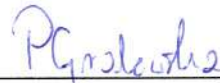


mgr inż. Patrycja Gralewska

Dotyczy publikacji:

Gralewska P., Gajek A., Marczak A., Miłkuła M., Ostrowski J., Śliwińska A., Rogalska A. *PARP inhibition increases the reliance on ATR/CHK1 checkpoint signaling leading to synthetic lethality-an alternative treatment strategy for epithelial ovarian cancer cells independent from HR effectiveness. Int. J. Mol. Sci.* 2020, 21(24), 9715; <https://doi.org/10.3390/ijms21249715>

Oświadczam, że mój wkład w powstanie powyższej pracy polegał na współudziale w stworzeniu koncepcji, udziale w wykonaniu części doświadczeń – testu MTT, testu wzrostu klonalnego, metody western blot oraz testu kometowego, opracowaniu wyników oraz ich interpretacji, wykonaniu analizy statystycznej oraz współtworzeniu manuskryptu, a także odpowiedzi na recenzje. Uczestniczyłam także w wykonaniu metody oznaczającej aktywność kaspazy 3/7. Mój udział procentowy oceniam na 50 %.

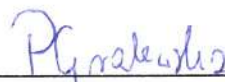


mgr inż. Patrycja Gralewska

Dotyczy publikacji:

Gralewska P., Gajek A., Rybaczek D., Marczak A., Rogalska A. *The Influence of PARP, ATR, CHK1 Inhibitors on Premature Mitotic Entry and Genomic Instability in High-Grade Serous BRCA^{MUT} and BRCA^{WT} Ovarian Cancer Cells. Cells.* 2022, 11, 1889; <https://doi.org/10.3390/cells11121889>

Oświadczam, że mój wkład w powstanie powyższej pracy polegał na współudziale w stworzeniu koncepcji, udziale w wykonaniu części doświadczeń – testu MTT, określeniu proliferacji komórek, testu mikrojądrowego, określeniu eksternalizacji fosfatydylseryny, podwójnego barwienia (Hoechst/PI), metody western blot, opracowaniu oraz interpretacji uzyskanych wyników, wykonaniu analizy statystycznej. Uczestniczyłam także w wykonaniu metody płytki metafazowej, cyklu komórkowego, zmierzeniu kondensacji chromatyny. Współtworzyłam manuskrypt i brałam udział w odpowiedzi na recenzje. Mój udział procentowy oceniam na 50%.



mgr inż. Patrycja Gralewska

Łódź, 16 listopada 2022 r.

dr hab. Aneta Rogalska, prof. UŁ
Katedra Biofizyki Medycznej
Uniwersytet Łódzki

OŚWIADCZENIE WSPÓŁAUTORA

Dotyczy publikacji:

Gralewska P., Gajek A., Marczak A., **Rogalska A.** *Participation of the ATR/CHK1 pathway in replicative stress targeted therapy of high-grade ovarian cancer. J Hematol Oncol 13, 39 (2020).* <https://doi.org/10.1186/s13045-020-00874-6>

Oświadczam, że mój wkład w powstanie powyższej pracy polegał na współudziale w stworzeniu koncepcji, współtworzeniu manuskryptu i nadaniu ostatecznego kształtu pracy oraz udziale w przygotowaniu korekty. Autor korespondencyjny. Mój udział procentowy oceniam na 15 %.



dr hab. Aneta Rogalska, prof. UŁ

Dotyczy publikacji:

Gralewska P., Gajek A., Marczak A., Mikuła M., Ostrowski J., Śliwińska A., **Rogalska A.** *PARP inhibition increases the reliance on ATR/CHK1 checkpoint signaling leading to synthetic lethality-an alternative treatment strategy for epithelial ovarian cancer cells independent from HR effectiveness.* *Int. J. Mol. Sci.* **2020**, 21(24), 9715; <https://doi.org/10.3390/ijms21249715>

Oświadczam, że mój wkład w powstanie powyższej pracy polegał na kierowaniu projektem obejmującym badania, współudziale w stworzeniu koncepcji, wykonaniu części doświadczeń, współtworzeniu manuskryptu i nadaniu ostatecznego kształtu pracy oraz udziale w przygotowaniu korekty. Autor korespondencyjny. Mój udział procentowy oceniam na 10 %.



dr hab. Aneta Rogalska, prof. UŁ

Dotyczy publikacji:

Gralewska P., Gajek A., Rybaczek D., Marczak A., **Rogalska A.** *The Influence of PARP, ATR, CHK1 Inhibitors on Premature Mitotic Entry and Genomic Instability in High-Grade Serous BRCA^{MUT} and BRCA^{WT} Ovarian Cancer Cells.* *Cells.* **2022**, 11, 1889; <https://doi.org/10.3390/cells11121889>

Oświadczam, że mój wkład w powstanie powyższej pracy polegał na kierowaniu projektem obejmującym badania, współudziale w stworzeniu koncepcji, wykonaniu części doświadczeń, opracowaniu wyników, współtworzeniu manuskryptu oraz udziale w przygotowaniu korekty. Autor korespondencyjny. Mój udział procentowy oceniam na 10 %.



dr hab. Aneta Rogalska, prof. UŁ

Łódź, 21 listopada 2022 r.

dr Arkadiusz Gajek
Katedra Biofizyki Medycznej
Uniwersytet Łódzki

OŚWIADCZENIA WSPÓŁAUTORA

Dotyczy publikacji:

Gralewska P, **Gajek A**, Marczak A, Rogalska A. *Participation of the ATR/CHK1 pathway in replicative stress targeted therapy of high-grade ovarian cancer. J Hematol Oncol.* 2020 Apr 21;13(1):39. doi: 10.1186/s13045-020-00874-6. PMID: 32316968; PMCID: PMC7175546.

Oświadczam, że mój wkład w powstanie powyższej pracy polegał na współudziale w stworzeniu koncepcji artykułu, współtworzeniu manuskryptu i nadaniu ostatecznego kształtu pracy oraz udziale w przygotowaniu korekty. Mój udział procentowy oceniam na 25%.



dr Arkadiusz Gajek

Dotyczy publikacji:

Gralewska P, **Gajek A**, Marczak A, Mikuła M, Ostrowski J, Śliwińska A, Rogalska A. *PARP Inhibition Increases the Reliance on ATR/CHK1 Checkpoint Signaling Leading to Synthetic Lethality-An Alternative Treatment Strategy for Epithelial Ovarian Cancer Cells Independent from HR Effectiveness.* Int J Mol Sci. 2020 Dec 19;21(24):9715. doi: 10.3390/ijms21249715. PMID: 33352723; PMCID: PMC7766831.

Oświadczam, że mój wkład w powstanie powyższej pracy polegał na współudziale w stworzeniu koncepcji artykułu, wykonaniu części doświadczeń związanych z oznaczeniem cytotoksyczności badanych związków, określeniem współczynnika oddziaływania leków, stopnia aktywacji kaspaz wykonawczych, współtworzeniu manuskryptu i nadaniu ostatecznego kształtu pracy oraz udziale w przygotowaniu korekty. Mój udział procentowy oceniam na 20%.



dr Arkadiusz Gajek

Dotyczy publikacji:

Gralewska P, **Gajek A**, Rybaczek D, Marczak A, Rogalska A. *The Influence of PARP, ATR, CHK1 Inhibitors on Premature Mitotic Entry and Genomic Instability in High-Grade Serous BRCAMUT and BRCAWT Ovarian Cancer Cells.* Cells. 2022 Jun 10;11(12):1889. doi: 10.3390/cells11121889. PMID: 35741017; PMCID: PMC9221516.

Oświadczam, że mój wkład w powstanie powyższej pracy polegał na współudziale w stworzeniu koncepcji pracy, wykonaniu części doświadczeń związanych z oznaczeniem stopnia eksternalizacji fosfatydoseryny, kondensacji chromatyny, analizą rozkładu faz cyklu komórkowego z równoczesną oceną stopnia inkorporacji BrdU, immunofluorescencyjną wizualizacją ekspresji kaspazy 3 oraz fosforylowanego histonu H2AX, wizualizacją płytki metafazowej oraz mikrojąder, współtworzeniu manuskryptu i nadaniu ostatecznego kształtu pracy oraz udziale w przygotowaniu korekty. Mój udział procentowy oceniam na 25%.



dr Arkadiusz Gajek

Łódź, 21 listopada 2022 r.

Prof. dr hab. Agnieszka Marczak
Katedra Biofizyki Medycznej
Uniwersytet Łódzki

OŚWIADCZENIE WSPÓŁAUTORA

Dotyczy publikacji:

Galewska P., Gajek A., **Marczak A.**, Rogalska A. *Participation of the ATR/CHK1 pathway in replicative stress targeted therapy of high-grade ovarian cancer. J Hematol Oncol 13, 39 (2020).*
<https://doi.org/10.1186/s13045-020-00874-6>

Oświadczam, że mój wkład w powstanie tej pracy polegał na współudziale w tworzeniu koncepcji pracy oraz przygotowaniu ostatecznej jej formy, a także uczestniczeniu w odpowiedziach na recenzje. Mój udział procentowy oceniam na 10 %.



Prof. dr hab. Agnieszka Marczak

Dotyczy publikacji:

Galewska P., Gajek A., **Marczak A.**, Mikuła M., Ostrowski J., Śliwińska A., Rogalska A. *PARP inhibition increases the reliance on ATR/CHK1 checkpoint signaling leading to synthetic lethality-an alternative treatment strategy for epithelial ovarian cancer cells independent from HR effectiveness. Int. J. Mol. Sci. 2020, 21(24), 9715; https://doi.org/10.3390/ijms21249715*

Oświadczam, że mój wkład w powstanie tej pracy polegał na współudziale w tworzeniu koncepcji pracy oraz przygotowaniu ostatecznej jej formy, a także uczestniczeniu w odpowiedziach na recenzje. Mój udział procentowy oceniam na 5 %.



Prof. dr hab. Agnieszka Marczak

Dotyczy publikacji:

Galewska P., Gajek A., Rybaczek D., **Marczak A.**, Rogalska A. *The Influence of PARP, ATR, CHK1 Inhibitors on Premature Mitotic Entry and Genomic Instability in High-Grade Serous BRCA^{MUT} and BRCA^{WT} Ovarian Cancer Cells. Cells. 2022, 11, 1889; https://doi.org/10.3390/cells11121889*

Oświadczam, że mój wkład w powstanie powyższej pracy polegał na współudziale w stworzeniu koncepcji i współtworzeniu manuskryptu. Mój udział procentowy oceniam na 5 %.



Prof. dr hab. Agnieszka Marczak

Łódź, 23 maja 2022 r.

dr hab. n. med. Agnieszka Śliwińska
Zakład Biochemii Kwasów Nukleinowych,
Uniwersytet Medyczny w Łodzi

OŚWIADCZENIE WSPÓŁAUTORA

Dotyczy publikacji:

Gralewska P., Gajek A., Marczak M., Mikuła M., Ostrowski J., Śliwińska A., Rogalska A.
PARP inhibition increases the reliance on ATR/CHK1 checkpoint signaling leading to synthetic lethality-an alternative treatment strategy for epithelial ovarian cancer cells independent from HR effectiveness. Int. J. Mol. Sci. **2020**, 21(24), 9715; <https://doi.org/10.3390/ijms21249715>

Oświadczam, że mój wkład w powstanie powyższej pracy polegał na współudziale w stworzeniu koncepcji oraz nadaniu pracy ostatecznego kształtu. Mój udział procentowy oceniam na 5 %.



Signed by /
Podpisano przez:

Agnieszka Śliwińska
Uniwersytet
Medyczny w Łodzi

Date / Data:
2022-05-25 11:19

dr hab. n. med. Agnieszka Śliwińska

Potwierdzam zgodność
z oryginałem

GLÓWNY SPECJALISTA
w Dziekanacie
Wydziału Biologii i Ochrony Środowiska UŁ


mgr Dorota Nawrocka

Łódź, 23 maja 2022 r.

dr hab. Michał Mikula, prof. Instytutu
Zakład Genetyki,
Narodowy Instytut Onkologii im. Marii Skłodowskiej-Curie
Państwowy Instytut Badawczy

OŚWIADCZENIE WSPÓŁAUTORA

Dotyczy publikacji:

Gralewska P., Gajek A., Marczak M., Mikula M., Ostrowski J., Śliwińska A., Rogalska A.
PARP inhibition increases the reliance on ATR/CHK1 checkpoint signaling leading to synthetic lethality-an alternative treatment strategy for epithelial ovarian cancer cells independent from HR effectiveness. Int. J. Mol. Sci. **2020**, 21(24), 9715;
<https://doi.org/10.3390/ijms21249715>

Oświadczam, że mój wkład w powstanie powyższej pracy polegał na współdziałaniu w stworzeniu koncepcji oraz nadaniu pracy ostatecznego kształtu. Mój udział procentowy oceniam na 5 %.

Signed by /
Podpisano przez:



Michał Marek
Mikula

Date / Data: 2022-
05-23 12:32

dr hab. Michał Mikula, prof. Instytutu

Potwierdzam zgodność
z oryginałem

GŁÓWNY SPECJALISTA
w Dziekanacie
Wydziału Biologii i Ochrony Środowiska UŁ

mgr Dorota Nawrocka

Łódź, 23 maja 2022 r.

Prof. dr hab. n. med. Jerzy Ostrowski
Zakład Genetyki
Narodowy Instytut Onkologii im. Marii Skłodowskiej-Curie
Państwowy Instytut Badawczy

OŚWIADCZENIE WSPÓŁAUTORA

Dotyczy publikacji:

Gralewska P., Gajek A., Marczak M., Mikuła M., Ostrowski J., Śliwińska A., Rogalska A.
PARP inhibition increases the reliance on ATR/CHK1 checkpoint signaling leading to synthetic lethality-an alternative treatment strategy for epithelial ovarian cancer cells independent from HR effectiveness. Int. J. Mol. Sci. **2020**, 21(24), 9715; <https://doi.org/10.3390/ijms21249715>

Oświadczam, że mój wkład w powstanie powyższej pracy polegał na współudziale w stworzeniu koncepcji oraz nadaniu pracy ostatecznego kształtu. Mój udział procentowy oceniam na 5 %.

Prof. dr hab. n. med. Jerzy Ostrowski



Signed by /
Podpisano przez:

Jerzy Zygmunt
Ostrowski

Date / Data:
2022-05-23 12:55

Potwierdzam zgodność
z oryginałem

GŁÓWNY SPECJALISTA
w Dziekanacie
Wydziału Biologii i Ochrony Środowiska UL


mgr Dorota Nawrocka

Łódź, 21 listopada 2022 r.

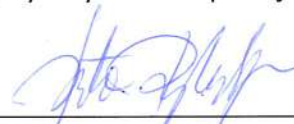
dr hab. Dorota Rybaczek, prof. UŁ
Katedra Cytofizjologii
Uniwersytet Łódzki

OŚWIADCZENIE WSPÓŁAUTORA

Dotyczy publikacji:

Gralewska P., Gajek A., **Rybaczek D.**, Marczak A., Rogalska A. *The Influence of PARP, ATR, CHK1 Inhibitors on Premature Mitotic Entry and Genomic Instability in High-Grade Serous BRCA^{MUT} and BRCA^{WT} Ovarian Cancer Cells.* Cells. **2022**, 11, 1889; <https://doi.org/10.3390/cells11121889>

Oświadczam, że mój wkład w powstanie powyższej pracy polegał na współudziale w tworzeniu koncepcji pracy oraz na wykonaniu części doświadczeń – metody płytki metafazowej oraz monitorowaniu postępu fazy S cyklu komórkowego przy użyciu inkorporacji EdU. Mój udział procentowy oceniam na 10 %.



dr hab. Dorota Rybaczek, prof. UŁ